UNIVERSIDADE D COIMBRA

Ana Margarida da Silva Figueiredo

INHIBITION OF PROTEIN TYROSINE PHOSPHATASE 1B
AS A NOVEL THERAPY FOR CHRONIC DIABETIC FOOT ULCERATION

Setembro de 2019

Departamento de Ciências da Vida

INHIBITION OF TYROSINE PHOSPHATASE 1B AS A NOVEL THERAPY FOR CHRONIC DIABETIC FOOT ULCERATION

Ana Margarida da Silva Figueiredo

Tese no âmbito do Mestrado em Biologia Celular e Molecular orientada pela Doutora Eugénia Maria Lourenço Carvalho e coorientada pela Professora Doutora Emília da Conceição Pedrosa Duarte e apresentada ao Departamento de Ciências da Vida da Faculdade de Ciências e Tecnologia da Universidade de Coimbra

Setembro de 2019

1 2 9 0

UNIVERSIDADE Ð
COIMBRA

This master thesis project entitled: "Inhibition of tyrosine phosphatase 1B as a novel therapy for chronic diabetic foot ulceration", was performed in Obesity, Diabetes and Complications group, at the Center for Neuroscience and Cell Biology, University of Coimbra, under scientific guidance of Doctor Eugénia Carvalho and Doctor Ermelindo Leal.

Agradecimentos

Abstract

Diabetes prevalence has been rapidly increasing and it is estimated that more than 400 million people suffer from diabetes worldwide. In Portugal, the prevalence of diabetes is one of the highest in Europe. The persistent hyperglycaemia leads to the development of peripheral neuropathy, peripheral arterial disease and reduced blood flow that, together with infections, are the main causes for the development of diabetic foot ulcers (DFUs). Approximately 15-25% of diabetic patients develop DFUs. Classic treatments are not sufficient to treat these ulcers from which 10-15% become chronic non-healing ulcers with 24% chance of future amputation.

Normal wound healing comprises four phases: haemostasis, inflammation, proliferation and maturation. Macrophages have an important role in all wound healing phases. In chronic wounds, the conversion of M1 macrophages into M2 macrophages is compromised, delaying the resolution of the inflammatory phase and the wound healing process.

Protein tyrosine phosphatase 1B (PTP1B) is expressed in various tissues being a negative regulator of several metabolic pathways. Due to the role of PTP1B in the modulation of several signalling pathways and since PTP1B is overexpressed in diabetic conditions, various studies have addressed its role in wound healing.

The main hypothesis of this work is that topical inhibition of PTP1B will improve wound repair in diabetes. For that, THP-1 cells cultured under normal (NG) and high glucose (HG) conditions and human monocytes, isolated from the blood of diabetic patients with and without DFUs, as well as healthy volunteers, were differentiated into macrophages and treated with MSI-1436, a PTP1B specific inhibitor, to assess the effects of PTP1B inhibition on the release of inflammatory cytokines and wound healing mediators in these cells. In THP-1 cells, the viability was measured by MTT assay. The number of M1 and M2 macrophages was evaluated by immunocytochemistry, using the double staining of CD68 and TNF-α for M1 macrophages and the double staining of CD68 and CD163 for M2 macrophages. Moreover, the expression of pro-inflammatory cytokines was analysed by qRT-PCR. Along with oxidative stress, evaluated with the DCFH-DA assay, the levels of the enzyme heme oxygenase-1 (HO-1) were also measured by immunohistochemistry and western blot. In the human monocytes, the viability and the expression of pro-inflammatory cytokines were also analysed. To determine whether inhibition of PTP1B improves wound healing under *in vivo* diabetic conditions, MSI-1436 was applied topically (at the wound site) using the streptozotocin-induced diabetic mouse model. Mouse wounds were collected and the number of M1 and M2 macrophages was evaluated by immunocytochemistry as performed in cell culture experiments. The wound vascularisation was evaluated with the detection of endothelial cells using CD31 along with ROS levels that were evaluated by DHE assay. The HO-1 expression was also measured as well as the presence of ki-67, a cell proliferation marker.

MSI-1436 treatment did not alter the viability of THP-1 cells or isolated human monocytes. Under inflammatory conditions, THP-1 cells cultured under NG and HG and treated with MSI-1436 showed an increase in M2 macrophages and a reduction in the number of M1 macrophages, a decrease in the pro-inflammatory environment, a decrease in ROS levels and a significant increase in HO-1 expression. PTP1B inhibition on human monocyte-derived macrophages decreased the pro-inflammatory environment in diabetic conditions. In the animal experiment the dose 1 μg of MSI-1436 proved to be the most effective. PTP1B inhibition in diabetic mouse wounds led to a higher number of M2 macrophages, to a decrease of M1 macrophages and to a reduction in the pro-inflammatory environment. Furthermore, this inhibition promoted a reduction of ROS levels, an increase in vascularisation, cell proliferation and HO-1 expression at the wound site, promoting a faster wound healing.

The results showed that PTP1B inhibition at wound site promotes wound healing by inducing an increase in HO-1 expression, which in turn leads to an increase in M2 macrophage polarisation, a decrease in inflammation, a decrease in oxidative stress and an increase in angiogenesis and proliferation. These effects will promote a faster and more efficient wound healing. The local modulation of PTP1B may be beneficial in the treatment of impaired wound healing in diabetes and PTP1B inhibition is a potential therapeutic target for the treatment of chronic diabetic foot ulcers.

KEYWORDS: DFUs; macrophages; PTP1B; inflammation; wound healing

Resumo

A prevalência da diabetes tem vindo a aumentar rapidamente e estima-se que mais de 400 milhões de pessoas sofram de diabetes em todo o mundo. Em Portugal, a prevalência da diabetes é uma das mais altas da Europa. A hiperglicémia persistente leva ao desenvolvimento de neuropatia periférica, doença arterial periférica e a um fluxo sanguíneo reduzido que, juntamente com infeções, são as principais causas para o desenvolvimento de úlceras do pé diabético (DFUs). Aproximadamente 15-25% dos pacientes diabéticos desenvolvem DFUs. Os tratamentos clássicos não são suficientes para tratar estas úlceras, das quais 10-15% se tornam úlceras crónicas que não curam, com 24% de probabilidade de uma futura amputação.

A cicatrização normal de feridas compreende quatro fases: hemostase, inflamação, proliferação e maturação. Os macrófagos têm um papel importante em todas estas fases da cicatrização de feridas. Em feridas crónicas, a conversão dos macrófagos M1 em macrófagos M2 está comprometida, retardando a resolução da fase inflamatória e o processo de cicatrização da ferida.

A proteína tirosina fosfatase 1B (PTP1B) é expressa em vários tecidos, sendo um regulador negativo de várias vias metabólicas. Devido ao papel da PTP1B na modulação de várias vias de sinalização e uma vez que a PTP1B está sobre-expressa em condições diabéticas, vários estudos investigaram o seu papel na cicatrização de feridas.

A principal hipótese deste trabalho é que a inibição tópica da PTP1B irá melhorar a reparação da ferida na diabetes. Para isso, células THP-1 cultivadas em condições de glucose normal (NG) e alta glucose (HG) e monócitos humanos, isolados do sangue de pacientes diabéticos com e sem DFUs, bem como de voluntários saudáveis, foram diferenciados em macrófagos e tratados com MSI-1436, um inibidor específico da PTP1B, para avaliar os efeitos da inibição da PTP1B na libertação de citocinas inflamatórias e mediadores da cicatrização de feridas nestas células. Nas células THP-1, a viabilidade foi medida usando o ensaio de MTT. O número de macrófagos M1 e M2 foi avaliado por imunocitoquímica, usando o duplo staining CD68 e TNF-α para macrófagos M1 e o duplo staining CD68 e CD163 para macrófagos M2. Além disso, a expressão de citocinas pró-inflamatórias foi analisada por qRT-PCR. Juntamente com o stress oxidativo, avaliado com o ensaio DCFH-DA, os níveis da enzima heme oxigenase-1 (HO-1) também foram medidos por imunohistoquímica e western blot. Nos monócitos humanos, a viabilidade e a expressão de citocinas pró-inflamatórias também foram analisadas. Para determinar se a inibição da PTP1B melhora a cicatrização de feridas em condições diabéticas *in vivo*, o MSI-1436 foi aplicado topicamente (no local da ferida) utilizando um modelo animal diabético, em que a diabetes foi induzida por estreptozotocina. As feridas dos ratinhos foram recolhidas e o número de macrófagos M1 e M2 foi avaliado por imunocitoquímica como realizado nas experiências de cultura celular. A vascularização da ferida foi avaliada através da deteção de células endoteliais usando o CD31

juntamente com os níveis de ROS que foram avaliados com o ensaio de DHE. A expressão de HO-1 também foi medida, assim como a presença de ki-67, um marcador de proliferação celular.

O tratamento com MSI-1436 não alterou a viabilidade das células THP-1 nem dos monócitos humanos isolados. Em condições inflamatórias, as células THP-1 cultivadas em NG e HG e tratadas com MSI-1436 mostraram um aumento dos macrófagos M2 e uma redução no número de macrófagos M1, uma diminuição no ambiente pró-inflamatório, uma diminuição nos níveis de ROS e um aumento significativo na expressão de HO-1. A inibição da PTP1B em macrófagos derivados de monócitos humanos diminuiu o ambiente pró-inflamatório em condições diabéticas. Na experiência animal, a dose 1 μg de MSI-1436 provou ser a mais eficaz. A inibição da PTP1B em feridas de murganhos diabéticos levou a um maior número de macrófagos M2, a uma diminuição dos macrófagos M1 e a uma redução no ambiente pró-inflamatório. Além disso, esta inibição promoveu uma redução dos níveis de ROS, um aumento da vascularização, proliferação celular e expressão de HO-1 no local da ferida, promovendo uma cicatrização mais rápida da ferida.

Os resultados mostraram que a inibição da PTP1B no local da ferida promove a cicatrização induzindo um aumento na expressão de HO-1, o que leva a um aumento na polarização dos macrófagos M2, a uma diminuição da inflamação, a uma diminuição do stress oxidativo e a um aumento da angiogénese e da proliferação. Estes efeitos irão promover uma cicatrização mais rápida e eficiente. A modulação local da PTP1B pode ser benéfica para o tratamento da cicatrização anormal de feridas na diabetes e a inibição da PTP1B é um potencial alvo terapêutico para o tratamento de úlceras crónicas do pé diabético.

PALAVRAS-CHAVE: DFUs; macrófagos; PTP1B; inflamação; cicatrização de feridas

List of Abbreviations

Akt - Protein kinase B

AMP - Antimicrobial peptide

AMPKα - AMP-activated protein kinase α subunit

APC - Antigen-presenting cell

ATF6 - Activating transcription factor 6

BCA - Bicinchoninic acid

BSA - Bovine serum albumin

CA - California

CD4 - Cluster of differentiation 4

CD8 - Cluster of differentiation 8

CD14 - Cluster of differentiation 14

CD31 - Cluster of differentiation 31

CD68 - Cluster of differentiation 68

CD163 - Cluster of differentiation 163

CD206 - Cluster of differentiation 206

cDNA - Complementary DNA

COX-2 - Cyclooxygenase-2

DAPI - 4′,6-diamidino-2-phenylindole

DCF - 2′,7′- dichlorofluorescein

DCFH-DA - Dichloro-dihydro-fluorescein diacetate

DCFH2 - 2′,7′-dichlorodihydrofluorescein

DCFH2-DA - 2′,7′-dichlorodihydrofluorescein diacetate

DE - Delaware

DFU - Diabetic foot ulcer

DHE - Dihydroethidium

DN - Diabetic nephropathy

DNA - Deoxyribonucleic acid

DOC - Sodium deoxycholate

DR - Diabetic retinopathy

DTT - Dithiothreitol

ECL - Enhanced chemiluminescence

ECM - Extracellular matrix

EDTA - Ethylenediaminetetraacetic acid

EGF - Epidermal growth factor.

EGFR - EGF receptor

EGTA - Egtazic acid

ER - Endoplasmic reticulum

FBS - Fetal bovine serum

FGF - Fibroblast growth factors

FMD - Flow-mediated dilation

GAG - Glycosaminoglycan

GF - Growth factor

GLUT4 - Glucose transporters type 4

Grb-2 - Growth factor receptor-bound protein 2

HCL - Hydrochloric acid

HG - High glucose

HO-1 - Heme oxygenase 1

HRP - Horseradish peroxidase

IFN - Interferon

IGF-1 - Insulin-like growth factor 1

IL-1β - Interleukin-1β

IL-6 - Interleukin-6

IL-8 - Interleukin-8

IL-10 - Interleukin-10

IR - Insulin receptor

IRE1α - Inositol-requiring protein 1α

IRS - IR substrate protein

JAK2 - Janus kinase 2

KC - Keratinocyte

KO - Knockout

LC - Langerhans cell

LPS - Lipopolysaccharide

M1 macrophage - Pro-inflammatory macrophage

M2 macrophage - Anti-inflammatory macrophage

MA - Massachusetts

MACS - Magnetic-activated cell sorting

MAP - Mitogen activated protein

MCP-1 - Monocyte chemoattractant protein-1

MDSC - Myeloid-derived suppressor cell

MMP - Matrix metalloproteinase

MO - Missouri

mRNA - Messenger RNA

MTT - 3-(4,5-dimethylthiazol-2-yl)-2,5-diphenyltetrazolium bromide

NG - Normal glucose

NKTC - Natural killer T cell

NO - Nitric oxide

NY - New York

OCT - Optimal cutting temperature

p-AKT - Phospho-Protein kinase B;

p-AMPKα - Phospho-AMP-activated protein kinase α subunit

p-JAK2 - Phospho-Janus kinase 2

p-PKB - Phospho-Protein kinase B

PBMC - Peripheral blood mononuclear cell

PBS - Phosphate- buffered saline

PDGF - Platelet-derived growth factor

PDGFR - PDGF receptor

PERK - Protein kinase RNA-like ER kinase

PFA - Paraformaldehyde

PGI2 - Prostacyclin

PI3K - Phosphoinositide 3-kinase

PIP3 - Phosphatidylinositol (3,4,5)-trisphosphate

PKB - Protein kinase B

PMA - Phorbol 12-myristate-13-acetate

PTK - Protein tyrosine kinase

PTP - Protein tyrosine phosphatase

PTP1B - Protein tyrosine phosphatase 1B

PTP1Bi - PTP1B inhibitor

PVDF - Polyvinylidene difluoride

qRT-PCR - Real-Time quantitative polymerase chain reaction

RIPA - Radioimmunoprecipitation assay

RNA - Ribonucleic acid

RNase - Ribonuclease

ROS - Reactive oxygen species

RPMI - Roswell Park Memorial Institute

RT - Room temperature

SA-PE - Streptavidin-phycoerythrin

SDS - Sodium dodecyl sulphate

SDS-PAGE - Sodium dodecyl sulphate polyacrylamide gel electrophoresis

SEM - Standard error of the mean

Shc - Src-homology-2-containing

SOS - Son-of-sevenless

STAT3 - Signal transducer and activator of transcription 3

STZ - Streptozotocin

T1DM - Type 1 diabetes mellitus

T2DM - Type 2 diabetes mellitus

TBP - TATA binding protein

TBS - Tris-buffered saline

TGF-β - Transforming growth factor beta

TLR - Toll-like receptor

TNF - Tumour necrosis factor

TNF-α - Tumour necrosis factor alpha

UK - United Kingdom

UPR - Unfolded protein response

USA - United States of America

UV - Ultraviolet

VE - Vascular endothelial

VEGF - Vascular endothelial growth factor

VEGFR2 - VEGF type 2 receptor

WT - Wild-type

Table of Contents

xiv

List of Figures

List of Tables

List of Publications

The work developed in this dissertation has been and will be presented in different national and international scientific meetings. In addition, this work will generate a literature review that is in preparation for submission:

Figueiredo A; Leal EC; Gasiunaite G; Delibegovic M; Carvalho E. "Inhibition of protein tyrosine phosphatase 1B as a novel therapy for chronic diabetic foot ulceration". *15° Congresso Português da Diabetes, March 2019, Vilamoura, Portugal.* (Poster presentation)

Gasiunaite G; Leal EC; **Figueiredo A**; Baillie J; Wilson HM; Rajnicek A; Carvalho E, Delibegovic M. "PTP1B inhibition for improved diabetic wound healing". *Physiology 2019 conference, July 2019, Aberdeen, UK.* (Poster presentation)

Figueiredo A; Leal EC; Gasiunaite G; Delibegovic M; Carvalho E. "Protein tyrosine phosphatase 1B inhibition plays a role in the macrophage phenotype under high glucose conditions: potential therapy for diabetic wound healing" *55th Annual Meeting of the European Association for the Study of Diabetes, September 2019, Barcelona, Spain.* (Poster presentation)

Gasiunaite G; Leal EC; **Figueiredo A**; Wilson HM; Rajnicek A; Carvalho E, Delibegovic M. "Inhibition of PTP1B for improved diabetic wound healing". *55th Annual Meeting of the European Association for the Study of Diabetes, September 2019, Barcelona, Spain.* (Poster presentation)

Figueiredo A; Leal EC; Carvalho E. "The role of PTP1B inhibition in wound healing: potential therapeutic target for chronic DFUs". (Review *in preparation*)

Chapter 1: Introduction

1.1. Anatomy and physiology of the skin

The skin is a structured tissue with highly important functions. It is the largest organ of the body, working as a physical barrier against external dangerous agents and dehydration [1], [2]. Skin is composed of two main layers: epidermis and dermis (**Figure 1**). The first main layer, the most superficial layer of the skin, is the epidermis which is avascular and composed of epithelial tissue, and attached to the second main layer, the dermis. The dermis is deeper and consists of connective tissue, giving elasticity to the skin. Unlike the epidermis, the dermis is vascularised, and the epidermis is dependent on the blood vessels of the dermis. Anchored to the dermis is the subcutaneous layer or hypodermis which is composed mainly by adipose tissue and collagen. Nonetheless, this layer is not part of the skin, it is a fat storage and has blood vessels which provide nutrients to the skin. Associated with the skin, we have accessory structures like hair follicles, glands and sensory nerves [1]–[5].

The main role of hair follicles is to regulate the skin temperature avoiding heat loss; however, they can also protect the skin from harmful ultraviolet (UV) light and are involved in the sensory perception of the environment as well as in the promotion of cell growth, tissue invasion and angiogenesis [6]. There are two main types of glands in the skin: sweat and sebaceous glands. Sweat glands are mainly present on the face, palms and soles and its main role is the thermoregulation of the skin. When the skin is exposed to high temperatures, the glands produce and release sweat to the surface of the skin that evaporates and helps to reduce the body temperature [7], [8]. Sebaceous glands are present in all the skin except palms and soles. They are responsible for the production and excretion of sebum which lubricates and makes the skin hydrophobic preventing too much water from entering into it and also works as heat insulation [8]–[10]. Furthermore, sebum has also antibacterial activity protecting the skin against bacterial infections [11]. Sensory nerves are responsible for transmitting sensations from the skin to the nervous system and vice-versa.

On the skin, we can also find the cutaneous vascular complex that is responsible for supplying nutrients to the entire skin and also for the removal of waste. In addition, the cutaneous vascular complex is also involved in the thermoregulation of the skin through vasodilation and vasoconstriction. When the skin is exposed to very high temperatures, in addition to sweat production by the sweat glands, blood flow increases, and blood vessels dilate for greater heat dissipation. When the temperature is too low the opposite occurs, blood flow decreases and vessels contract to decrease heat losses [10], [12].

All the layers together with the accessory structures form the integumentary system [10].
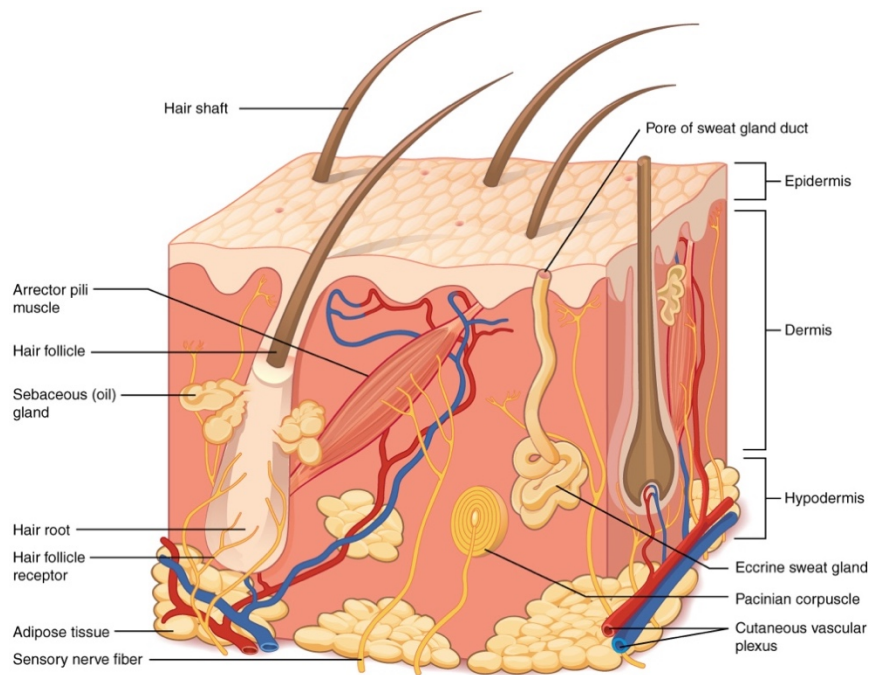
Figure 1 - Human skin anatomy. The two layers of the skin are visible: the epidermis is the most superficial and the dermis under the epidermis, followed by the hypodermis containing a layer of dermal adipocytes that are important key players in skin structure and function (Reproduced with permission from http://library.open.oregonstate.edu/aandp/chapter/5-1-layers-of-the-skin/ [4]).

1.1.1. Epidermis

The epidermis is composed mainly by four types of cells: keratinocytes, melanocytes, intraepidermal macrophages or Langerhans cells (LCs), and tactile epithelial cells or Merkel cells. Keratinocytes (KCs) make up 90% of the epidermal cells and form several layers of cells at different stages of development. KCs are responsible for the production of keratin, a protein that protects the skin against external injuries, and lamellar granules, which release a substance that controls the entry and loss of water and inhibits the entry of external substances. The second largest class of epidermal cells are melanocytes which produce melanin, a pigment responsible for skin colour and are able to absorb UV light protecting the skin from this dangerous radiation. Within the epidermis we can also find LCs, known as intraepidermal macrophages. These cells develop from dendritic cells of the immune system and are involved in immune responses against pathogens that try to penetrate into the skin. LCs phagocyte the pathogens and present the antigens to T cells. Finally, in a smaller number and in the deepest layer of the epidermis, the Merkel cells or tactile epithelial cells are responsible for the detection of touch sensations and are abundant on the surfaces of the hands and feet [3]–[5], [10].

The skin can be thin or thick. Thin skin is present in most of the body composed of epidermis with four layers: stratum corneum, stratum granulosum, stratum spinosum, and stratum basale. In the

regions that are subject to pressure and friction, like palms and soles, the epidermis has one additional layer: stratum lucidum [4], [5] (**Figure 2**).
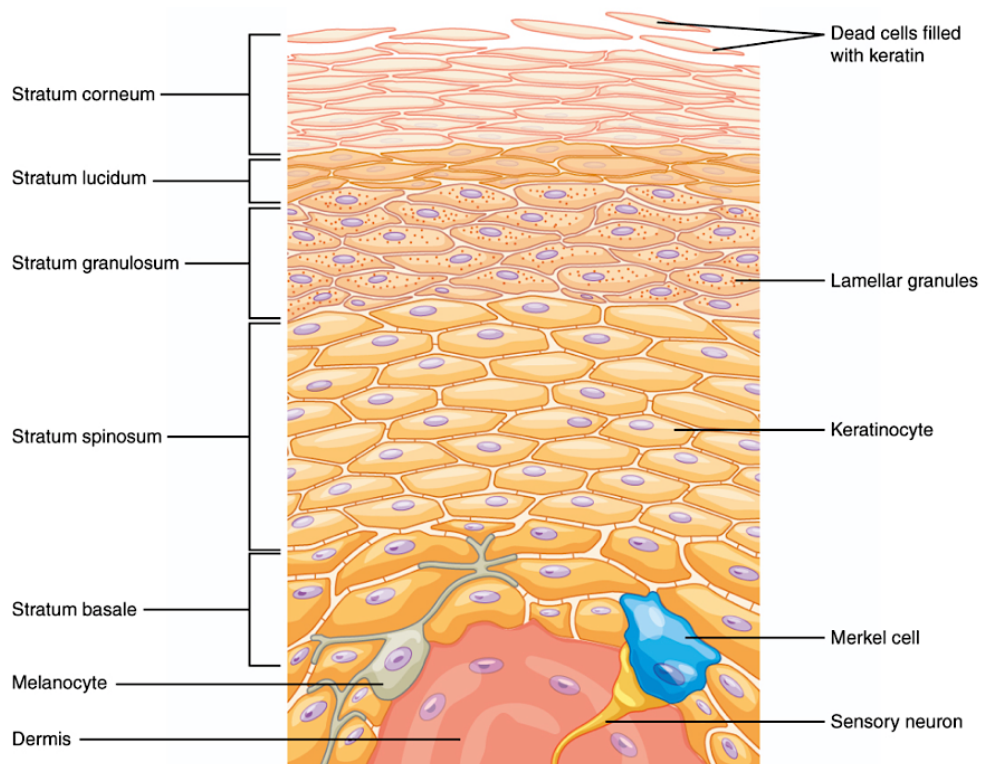
Figure 2 - Layers of the epidermis. Thick skin is composed of five layers: stratum corneum, stratum lucidum, stratum granulosum, stratum spinosum, and stratum basale. Thin skin (not shown) does not have the stratum lucidum layer (Reproduced with permission from http://library.open.oregonstate.edu/aandp/chapter/5-1-layers-of-the-skin/ [4]).

Stratum basale

The stratum basale is the deepest layer of the epidermis. This layer is composed of columnar KCs which contain keratin intermediate filaments. Moreover, it also contains some stem cells responsible for the production of new KCs and are the only cells of epidermis that can divide. When a stem cell undergoes mitosis, one of the resulting daughter cells goes to the upper layers and the other remains in the stratum basale. Thus, this layer is the source of all epidermal KCs. The KCs of this layer are held together by desmosomes. Two other cell types can be found in stratum basale: Merkel cells and Melanocytes [3], [5], [8], [10]. Merkel cells work as mechanoreceptors that detect light and pressure stimulus and transmit them to the brain. These cells are in large number in sensitive regions as fingertips [10], [12], [13]. Melanocytes produce melanin, a pigment that can be transferred to KCs, in response to UV radiation for skin protection and it is also responsible for the pigmentation of the skin [10].

Stratum spinosum

The stratum spinosum is composed of round KCs which produce keratin intermediate filaments. These cells are joined together by desmosomes which make the skin strong and flexible. In this layer, LCs are also present and some projections of melanocytes [5].

LCs are some of the first cells of the immune barrier and are essential in the early stages of wound healing, impaired in diabetes. Some diabetic patients develop foot wounds that take longer to heal than normal wound and sometimes become chronic non-healing ulcers. Studies have shown that there are more such cells in diabetic ulcers that heal when compared to non-healing ulcers, which indicates that LCs repopulate the epidermis during wound closure increasing their number, suggesting they may have an important and beneficial role in diabetic wound healing [14], [15].

Stratum granulosum

The stratum granulosum is composed of flattened KCs undergoing the process of apoptosis to give rise to the cells of the two layers above: stratum lucidum and stratum corneum. Their organelles begin to disintegrate and, since the cells are dying, they do not have any metabolic activity. KCs release keratin and keratohyalin which are its main constituents and are responsible for the layer's grainy appearance. Lamellar granules are also produced by these cells and release a substance that controls the entry and loss of water and acts as a barrier to the entry of external agents [4], [5].

Stratum lucidum

The stratum lucidum is only present in areas with thick skin, like palms and soles. It is located between the stratum corneum and stratum granulosum layers. It is constituted by several layers of dead and flat KCs with large amounts of keratin and eleidin, a protein that makes this layer waterproof [3]–[5], [8].

Stratum corneum

The stratum corneum is the superficial part of epidermis composed of several layers of dead and flat KCs which contain keratin, also known as corneocytes. This stratum provides mechanical protection to the skin and, since it is the most exposed layer to external agents, it protects the skin from pathogens and dehydration. Corneocytes' desmosomes are degraded, and the cells separate by peeling of the skin, being regularly replaced by cells coming from the deeper layer, stratum granulosum, in the case of thin skin, and stratum lucidum, in the case of thick skin. When the skin

is subjected to a lot of friction, keratin is highly produced and it leads to the formation of a callus which is the thickening of the stratum corneum [4], [5], [10].

1.1.2. Dermis

Below the epidermis is the dermis, responsible for the supply of nutrients and support to the epidermis [3]. The main compounds of dermis are extracellular matrix components like collagen, elastic tissue and reticular fibres being responsible for the elasticity of the skin [1], [12].

The dermis is composed of fibroblasts, endothelial cells, smooth muscle cells, macrophages, dendritic cells, T cells, and other immune cells (**Figure 3**) [1], [16]. These immune cells play an important role in the immunity of the skin and wound healing, and dermal macrophages play an important role in wound healing [14], [16]. Fibroblasts are responsible for the production of collagen, representing collagen 30% of the volume of the dermis [12].
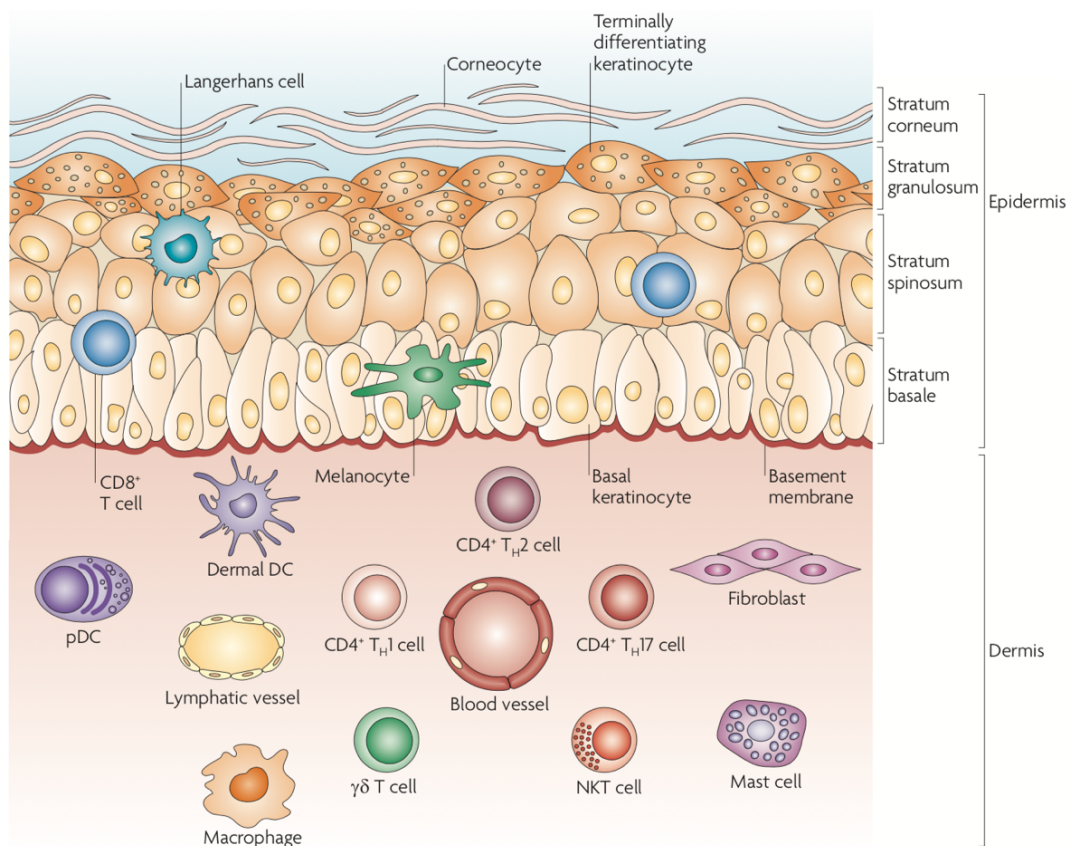
Figure 3 - Immune cells present in the dermis (Reproduced with permission from Nestle *et al*, 2009 [16], Copyright Nature Reviews Immunology).

1.1.3. Skin physical barrier function

Since the skin is the most exposed organ to the external environment, it is the body's first line of defence. The layer responsible for protecting the skin from external factors is the epidermis, more specifically the stratum corneum layer of epidermis [12], [17]. This layer is impermeable due to a lipid-rich matrix organized in a laminar form that fills the spaces between corneocytes. Lamellar granules are responsible for the production of this lipid matrix rich in ceramides, cholesterol and free fatty acids, by releasing lipid membranes for the intercellular spaces of corneocytes. Furthermore, corneocytes are bound by the cross-link between keratohyalin and involucrin proteins, which help maintain skin impermeable [12], [17], [18]. The dryness of the stratum corneum and the fact that corneocytes are always being replaced due to skin desquamation prevent the entry and growth of invasive microorganisms and possible infections [12]. When this barrier is damaged or its function disturbed, as in the case of a wound injury, the microorganism has an open path to enter and infect the skin.

However, the skin is not only a physical barrier, but it also plays key roles in immune function.

1.1.4. Skin immune function

The immune functions of the skin involve cells present in the epidermis and dermis.

In the epidermis KCs and LCs are the most important cells involved in skin immune responses [19]. KCs work like immune sentinels on the skin and are responsible for the production of antimicrobial peptides (AMPs) [16], [19], [20]. AMPs are small cationic and amphipathic molecules which are capable of killing bacteria, fungi and viruses, and are also involved in the chemoattraction of inflammatory cells to the invasion site [12], [19]. Furthermore, AMPs seem to be involved in wound healing, especially in the promotion of angiogenesis and reepithelization [21]. Other mechanism that KCs have to fight microorganisms is the production of pro-inflammatory cytokines. KCs express Toll-like receptors (TLRs) on the surface and, when a microorganism tries to penetrate into the skin, these receptors are activated and lead to the production of pro-inflammatory cytokines like interleukin-(IL)-1β, IL-8, IL-6, tumour necrosis factors (TNFs) and interferons (IFNs) [16], [19], [20]. The activation of TLRs will induce a Th1 response [16], [19]. LCs are the first members of the dendritic cells family to be in contact with the invasive pathogen and work as antigen-presenting cells (APCs) [12], [16], [22]. They collect the antigens in the epidermis and migrate to the lymph nodes where they will present the antigen to T cells and promote a Th2 response [12], [16], [19], [22]. Th1 response is a response against intracellular or phagocytable microorganisms like bacteria and viruses, whereas Th2 responses are against extracellular microorganisms that cannot be phagocytosed like helminths [23], [24]. Normally these

two responses are in balance, with the Th1 response more protective and Th2 responses involved in the resolution of inflammation [24].

Dermal dendritic cells, mast cells, macrophages and T cells are the main cells involved in dermis immunity [19]. Dermal dendritic cells have the same role of LCs but in the dermis, having the same competency to present the antigen to T cells and activate them [19], [25].

Mast cells are known to be involved in allergic reaction by the release of histamine, however they have a role in the protection against pathogens and in wound healing [19], [26]. After contact with pathogens, mast cells are able to release pro-inflammatory cytokines and AMPs that will attract other immune cells and activate different types of T cells [26], [27]. Furthermore, the interaction between mast cells, LCs and dermal dendritic cells seems to be crucial for the migration of these cells to the nodules and presentation of antigens to T cells [19].

Resident dermal macrophages live in the dermis and have antimicrobial activity, helping in the elimination of cellular debris, and can produce pro- and anti-inflammatory cytokines [16]. Macrophages can be divided into pro-inflammatory macrophages (M1 macrophages), anti-inflammatory macrophages (M2 macrophages). M1 macrophages are involved in the promotion of inflammation in the skin whereas M2 macrophages are responsible for secretion of anti-inflammatory cytokines that will contribute to the resolution of skin inflammation. Moreover, M2 macrophages can act like APCs and present antigens to lymphocytes. Wound-healing macrophages are involved in tissue repair promoting granulation tissue formation and epithelialization [28].

The number of T cells in the skin is approximately twice of the number of T cells present in the peripheral blood [19], [29]. Skin resident memory CD4$^+$ and CD8$^+$ T cells are the most common T cells found in the skin [16], [19]. When dermal dendritic cells contact with a pathogen, they will present the antigen to the skin-resident memory CD4$^+$ or CD8$^+$ T cells, activating them. The activated T-cells will release pro-inflammatory mediators promoting the inflammatory response. These cells are the first-line of defence when pathogens try to invade the skin for the second time [16]. More uncommonly, T cells are also present in the dermis, named γδ T cells, that can produce important growth factors involved in wound healing, including AMPs, and natural killer T cells (NKTCs), which produce inflammatory mediators that can contribute to the inflammatory response [16], [19].

1.2. Diabetes and complications

Diabetes is a chronic disease characterised by an increase in blood glucose levels due to defects in production and secretion and/or action of insulin. These defects lead to metabolic changes which in turn may lead to an increased risk of early death due to the appearance of various other co-morbidities and related complications in the body, such as vascular disease [30]. According to

the World Health Organization more than 400 million people suffer from diabetes in the world, with the global prevalence of diabetes among the adult population approximately 8.5%, and it is not only responsible for millions of deaths every year, but also for the very high medical costs associated [31]. In Portugal, the prevalence of this disease is approximately 9.9% in adults, one of the highest in Europe [32].

There are two main types of diabetes: type 1 (T1DM) and type 2 (T2DM) [33], with type 1 being responsible for 5-10% [34] of the cases and type 2 for about 90-95% [35]. T1DM is a consequence of the immune destruction of the β-cells in the Langerhans' islets in the pancreas. These cells are responsible for insulin production, controlling blood glucose levels [36]. Since β-cells are gradually destroyed, the body is unable to produce insulin in the required amounts, and ultimately, a complete absence of insulin production can occur. Due to this, patients require regular insulin administrations to control the level of glucose in the blood. Moreover, the cause of this type of diabetes remains unknown. T2DM is characterised by insulin resistance due to a deficient response of the insulin receptors since they are no longer sensitive to insulin. Genetic and environmental factors are the main causes of the metabolic disturbances plaguing T2DM. Both types of diabetes can be responsible for the damage of various areas of the body and can lead to several complications, such as blindness, kidney failure, heart disease and diabetic foot ulcers (DFUs) [31], [33], [37]. T1DM is more common in children and adolescents, although it may also occur in adults [31], [38]. T2DM has a higher incidence in adulthood, however, its incidence in children and adolescents has been increasing since it is associated with obesity and a lifestyle with poor diet and low physical activity which have been increasing in the global paediatric population in recent years [38]. The number of T2DM cases in adults has increased due to a dramatic increase in the incidence of obesity in the world [39].

The main complications associated with diabetes are micro- and macrovascular [40], [41]. Microvascular complications are due to damage in small blood vessels while the macrovascular complications are due to damages caused in the larger blood vessels [41]. Diabetes interferes with the microvasculature, leading to neuropathy, nephropathy, retinopathy and diabetic foot disorders [40], [41]. When diabetes affects the macrovasculature, cardiovascular diseases can surface due to lack of blood flow caused by the clogging of arteries, at least in part due to hyperglycaemia, which is also responsible for the poor blood flow in the lower limbs [41]. Diabetes can cause nerve damage leading to the onset of neuropathy, the most common complication in diabetes [41], [42]. About 50% of diabetic patients have neuropathy [42], [43]. Nerve damage can be derived from poor blood flow to the nerves due to damage of blood vessels [41]. Diabetic nephropathy (DN), which affects about 40% of diabetic patients, is due to damage in blood vessels present in the kidneys, leading to the onset of chronic kidney disease and renal failure that can lead to death [41], [44]. DN is one of the main diabetes complications responsible for most kidney transplants [41]. Diabetic retinopathy (DR) is an eye disease caused by damage to the blood vessels of the retina, which can lead to partial

loss of vision and eventually blindness [41], [45]. The global prevalence of DR among all diabetic patients is 35.4% [46]. In Portugal, there are only studies of the prevalence of DR in patients with T2DM, which is about 16.3% [47]. Diabetic foot is a complication caused essentially by the damage in blood vessels (microvascular disease) and nerves, which promotes skin changes that can lead, after injury, to the development of chronic DFUs [41].

1.2.1. Insulin signalling and resistance

Insulin is a hormone produced and released in the pancreas, more specifically in the ß-cells of the islets of Langerhans, circulating through the body in the bloodstream [48]. One of its main functions is to increase the absorption of glucose in the adipose and muscular cells [49]. When insulin binds to its receptor (IR), a tyrosine kinase receptor, the receptor undergoes autophosphorylation and tyrosine residues on IR substrates proteins (IRSs; it should be noted that also the Src-homology-2-containing (Shc) protein is also an insulin receptor substrate) are phosphorylated, which leads to the activation of these proteins [48], [50] (**Figure 4**). Shc binds to the growth factor receptor-bound protein 2 (Grb-2) and to the son-of-sevenless (SOS) protein, forming the Shc/Grb-2/SOS complex which leads to the activation of Ras and consequently the mitogen activated protein (MAP) kinase [48], [51]. The MAP kinase pathway stimulates cell growth and proliferation, differentiation and mitogenesis. Activated IRS proteins can also bind to Grb-2 and to SOS or to phosphoinositide 3-kinase (PI3K) [48]. PI3K leads to the formation of phosphatidylinositol (3,4,5)-trisphosphate (PIP3) which activates the protein kinase B (PKB or Akt), and in turn leads to the translocation of glucose transporters type 4 (GLUT4), found in vesicles, to the plasma membrane of the cell, upon stimulation with insulin, where they promote the entry of glucose used in cell metabolism [48]–[50]. Insulin is also responsible for the inhibition of the production and release of glucose in the liver in order to maintain glucose homeostasis [49].

Insulin resistance is characteristic of T2DM and occurs when the body is unable to respond to insulin, causing insulin to deficiently execute its function, ultimately leading to impaired glucose uptake by the cells [48], [52]. As the IRs are unable to respond to insulin, there is a decrease in the activity of PI3K and, consequently an impaired translocation of GLUT4 from the intracellular vesicles to the plasma membrane [49], [53], [54]. Thus, insulin resistance in muscles and fat cells causes them to be unable to uptake glucose from the bloodstream, which leads to the development of hyperglycaemia; in the liver, the inhibition of glucose production and release does not occur, which increases the blood glucose concentration and hence the development of hyperglycaemia [48], [53], and to the development of various diabetes-associated pathologies, such as cardiovascular disease and neuropathy [52]. The mechanism behind insulin resistant is not fully understood, but genetic and environmental factors seem to be involved [49], [52].
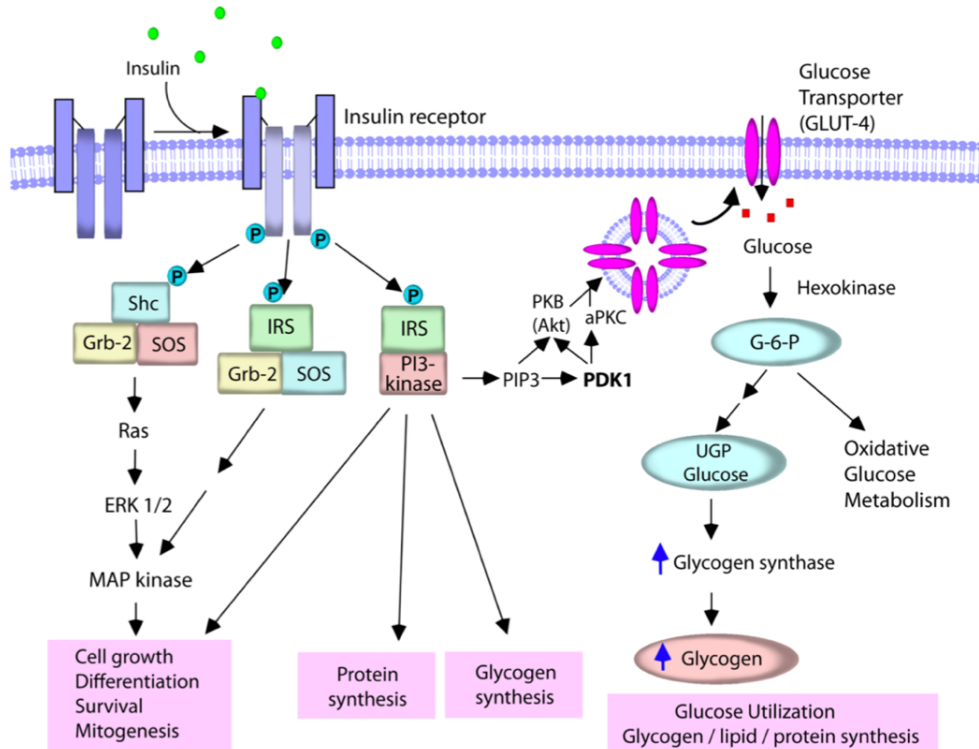
Figure 4 - Insulin signalling (Reproduced with permission from Mangmool *et al*, 2017 [48], Copyright The Korean Society of Applied Pharmacology).

1.2.2. Diabetic foot ulcers

The damages caused by diabetes in the deep tissues, blood vessels and nerves in the feet and lower limbs can result in the development of complications such as chronic ulcers, which in most cases are infected and, in the worst scenario, amputation. Chronic DFUs (also known as the diabetic foot) are the cause of 85% of the amputations in diabetic patients [31], [55], [56]. Approximately 15-25% of diabetic patients develop foot ulcers [57]. The risk of developing this pathology is higher in males, patients with T2DM and older patients. As the incidence of diabetes increased in recent years, the incidence of diabetic ulcers has also increased [55], [58]. Diabetic ulcers and amputations are responsible for high mortality rates, sometimes worse than some types of cancer [59], [60]. Furthermore, they cause enormous pain and suffering to patients.

According to the Wagner's classification system, there are six grades of diabetic foot lesions [61] (**Table 1**). Different grades require different treatment and intervention, and all grades, except for grade 5, can be treated and converted to grade 0 [61], [62].

The main causes for the development of the diabetic foot are peripheral neuropathy, peripheral arterial disease and infection [58], [63] (**Figure 5**).

Table 1 - The Wagner's classification system (Adapted with permission from Wagner Jr, 1981 [61], Copyright American Orthopaedic Foot Society. Inc; Images adapted with permission from Pinzur, 2016 [62], Copyright Springer International Publishing Switzerland 2016).

Grade	Characteristics	Diagram
0	No open lesions; may have some bony deformity	
1	Superficial ulcer however deeper layers are not affected; in most cases bony deformity is present	
2	Ulcer is deeper and affects tendons, bone or joint capsule; bony deformities and some prominence are present	
3	Deeper tissues are affected; presence of abscess, osteomyelitis or tendinitis	
4	Gangrene of some portion of the toe(s) and/or forefoot; gangrene may be wet or dry, infected or non-infected	
5	Gangrene involves the whole foot and amputation must be carried out	
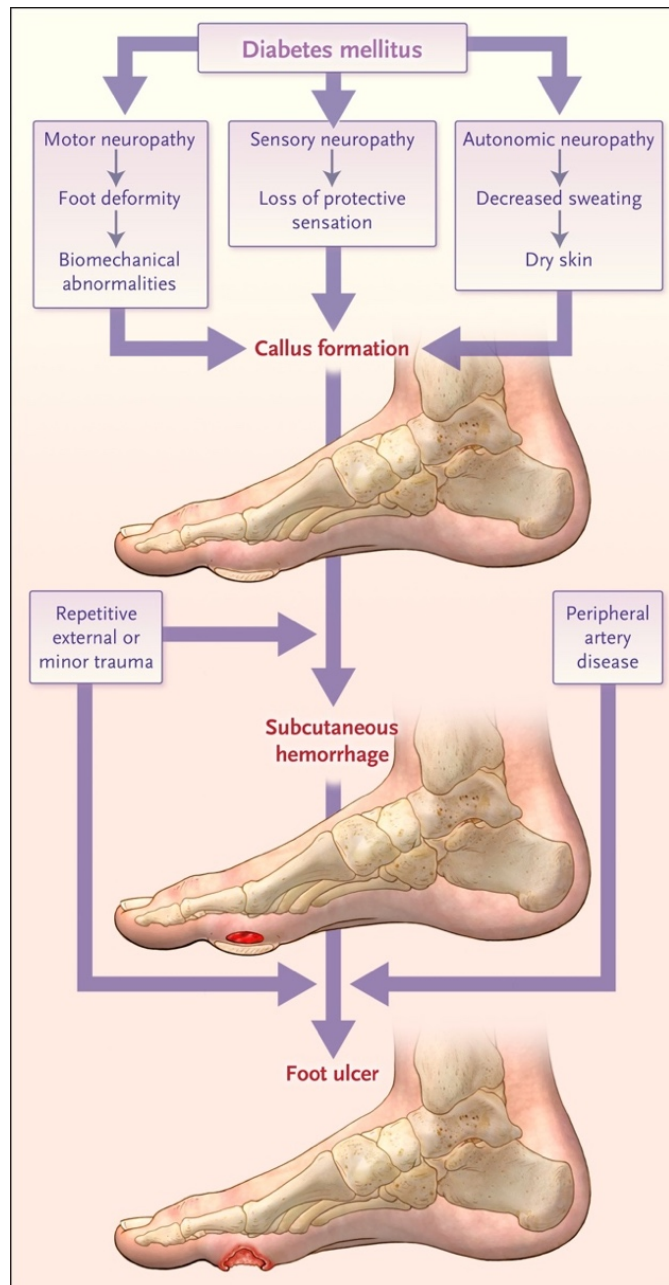
Figure 5 - Pathway of DFU formation (Reproduced with permission from Armstrong *et al*, 2017 [64], Copyright Massachusetts Medical Society).

Peripheral neuropathy is the most common form of neuropathy caused by diabetes as a result of the damage to the nerves leading to the extremities and it affects more than 50% of diabetic patients [58], [59]. Peripheral neuropathy begins in the toes and gradually increases. One result of this condition is foot innervation that leads to abnormalities in flexion and extension of the foot and anatomic deformities which will eventually lead to collapses of the skin and beginning of ulceration. The neuropathy is also responsible for lower production of sweat, the skin becomes continuously drier and start to open fissures. There is also loss of sensation of pain, pressure and heat, which is very worrying in case the patients' feet suffer an injury that can be undetected and allowed to

progress without treatment [58], [59], [63], [65]. The loss of sensitivity may be due to the damage of Merkel cells located in the epidermis [66].

In peripheral arterial disease there is atherosclerosis of lower extremity arteries which causes the blood vessels in the legs to be blocked. The main symptom is intermittent claudication, characterised by pain and/or cramping which appears during exercise and almost disappears after rest [67]. Due to this claudication, patients begin to have walking difficulties which leads to a progressive loss of limb function. Thus, ischemia (reduced blood flow) in the lower limbs and feet is the result of peripheral arterial disease and one of the causes of amputation [38]–[40].

Both peripheral neuropathy and peripheral arterial disease promote the appearance and installation of infections, hence diabetic patients have a higher risk for infections [70]. Infections are normally polymicrobial, however the main pathogens present in diabetic ulcer infections are Gram-positive aerobic cocci, mainly *Staphylococcus aureus* [71], [72].

All these factors together promote the development of ulcers that if not treated and cured will lead to amputations. Therefore, chronic foot ulcers are not a direct effect of diabetes but rather of the pathologies that develop due to this disease.

1.2.3. Treatment of diabetic foot ulceration

The classic treatments for ulcers are debridement, offloading, revascularisation and infection control [58], [73]. In debridement, the necrotic tissues are removed improving healing and decreasing the risk of infection. The purpose of offloading is to reduce the pressure on the wounds, allowing them to heal. Wheelchair or crutches are the most effective way [73]. When ischemia is present, revascularisation is a very important treatment that should be performed as soon as possible [59]. One of the most important treatments is infection control. The development of an infection may endanger patients' limbs or even their lives. Normally the infections are caused by various microbial species and virulent pathogens. The patients should be treated with antibiotics in order to kill all microorganisms and cure the infection [73], [74].

However, sometimes these treatments are inefficient to heal wounds and often these wounds come back after months of treatment. 10-15% of DFUs are non-healing from which 24% lead to future amputation [58], [75]. This failure to cure ulcers seems to be related to alterations in growth factors (GFs) and cytokine expression. It is known that the expression of GFs involved in healing is reduced in diabetic ulcers [76]. Another factor that complicates the treatment of chronic foot ulcers is the development of biofilms that are populations of microorganisms which are attached to the surface of the wound. Bacteria biofilm are highly resistant to several of the therapies used, including antibiotic therapy, once the biofilm forms a barrier that prevents antibiotics from penetrating and killing bacteria. So, when biofilms are present the most efficient therapy is the removal of the biofilm [76]–[78].

However, often these techniques are not enough to treat DFUs and it is necessary to develop new treatments capable of combating non-healing DFUs.

Recurrences are also very common, about 40% of patients have a recurrence after 1 year of treatment, nearly 60% after 3 years and 65% after 5 years [64]. New treatments have been tested but so far none have achieved excellent results in humans. Therapies using growth factors and wound healing modulators, hyperbaric oxygen and electrical stimulation, among others, were tested but with limited results [80], [81].

1.2.4. Economic impact of diabetic ulcers

Foot ulcers have a high impact on the healthcare system and health economics [82]. According to recent data in the UK in 2014-2015 the annual costs of treatment and care for foot ulcers and amputation were approximately £1 billion (1.137€ billion) [83]. In a 2014 study, estimated annual costs in the USA were between $9 – 13 billion (7.730 – 11.166€ billion) [84].

In Europe, the direct and indirect costs per patient of an amputation due to a DFU are 25,000€ and DFUs that do not cure within 12 months cost about 20,000€ [85]. Since in 2016 there were 1,037 amputation of inferior members due to diabetes in Portugal, the cost in that year only in amputations was about 26€ million [32].

Since the rate of diabetes and consequently DFUs is expected to increase in the coming years, so are the costs associated with their treatment which are going to have a significant economic impact worldwide.

1.3. Wound healing
1.3.1. Normal wound healing

As soon as the skin is injured, signalling cascades involved in pain control, infection and wound healing are activated [2]. Wound healing is a complex and dynamic process whose main objective is the restoration of skin physiology and function, and comprises four phases: haemostasis, inflammation, proliferation and maturation (**Figure 6**). Also, wound healing involves several types of cells, including: platelets, keratinocytes, immune cells and fibroblasts [2], [86], [87].
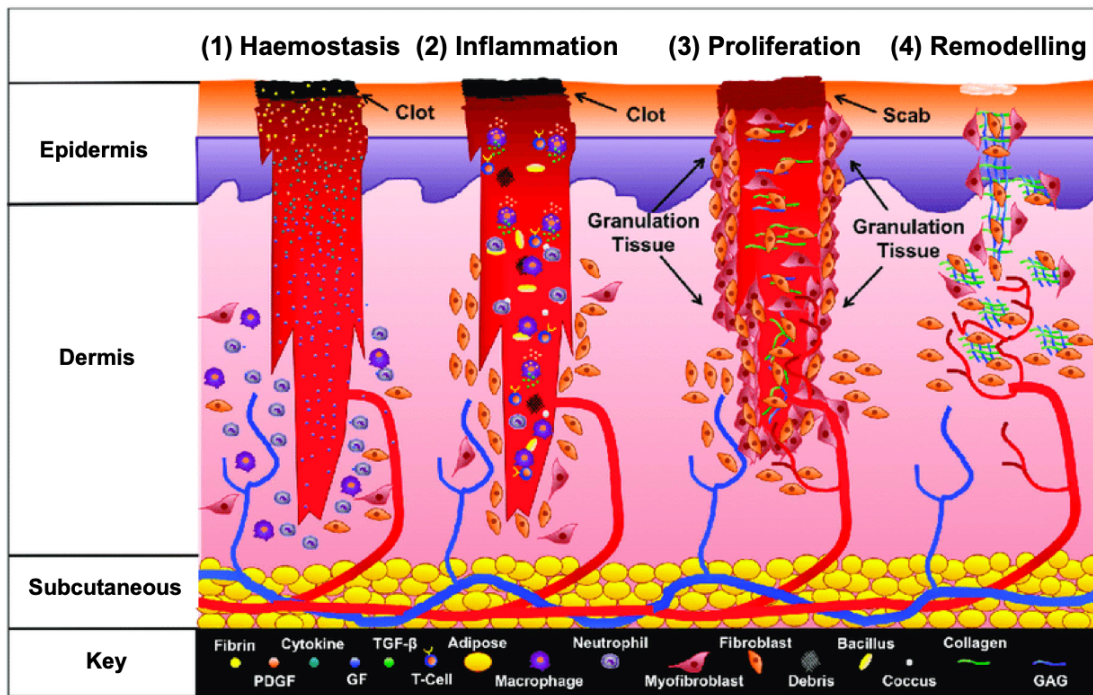
Figure 6 - The four phases of wound healing: (1) haemostasis phase, (2) inflammatory phase, (3) proliferative phase and (4) maturation phase (PDGF = Platelet-Derived Growth Factor, GF = Growth Factor, GAG = Glycosaminoglycan) (Adapted with permission from Mellott *et al*, 2016 [88], Copyright by the authors).

Haemostasis phase

The haemostasis phase starts immediately after the skin lesion and is the beginning of the healing process (**Figure 6 (1)**). The goal is to stop the bleeding, and, for this, platelets adhere to damaged blood vessels and vascular smooth muscle cells constrict vessels to reduce blood flow [86], [87], [89]. The coagulation cascade is activated, and platelets form a fibrin clot that serves as a platform for invasive cells, such as leukocytes, keratinocytes and fibroblasts, and promote the release of cytokines and GFs that recruit neutrophils and other leukocytes to the site of injury which leads to the beginning of the inflammatory phase [86], [88], [89]. Cytokines control the immune response and the GFs direct the subsequent healing events. The most important GFs are transforming growth factor β (TGF- β) and platelet-derived growth factor (PDGF) [89].

Inflammatory phase

Inflammation is the second phase of wound healing and begins immediately after injury, starting with neutrophil recruitment to the wound (**Figure 6 (2)**). Neutrophils and skin resident macrophages clean the wound, eliminating bacteria, damaged and dead cells and degrade the damaged extracellular matrix (ECM), using proteolytic enzymes. Uninjured tissue only suffers

significant damage under excessive inflammation, as it is protected by protease inhibitors. In the meantime, cytokines and GFs attract monocytes and T cells to the area, which will differentiate into effector cells (macrophages and activated T-cells). Macrophages phagocytize pathogens, tissue debris, remaining neutrophils and create the necessary conditions for angiogenesis and tissue granulation. Active macrophages attract fibroblasts and myofibroblasts that are essential for the beginning of the proliferative phase [86], [88], [89]. In addition, macrophages also release PDGF, fibroblast growth factors (FGFs), vascular endothelial growth factor (VEGF), and TGF-β, which are involved in cell migration and proliferation and matrix formation that occur in the next phase [86].

Proliferative phase (or tissue formation)

In this phase (**Figure 6 (3)**), the wound is repaired with new cells as inflammation declines and cell proliferation begins, with GFs having a very important role. The reepithelization of the epidermis begins, keratinocytes are formed from stem cells which will proliferate and migrate to the wound where they will cover it and form the various layers of the epidermis. VEGF and FGF lead to the beginning of angiogenesis. VEGF attracts endothelial cells that form new blood vessels, which supply the newly formed tissue with nutrients and oxygen. Endothelial cells also produce nitric oxide (NO) which leads to vasodilation and thus increases blood flow in the wound. The set of macrophages, fibroblasts and endothelial cells form granulation tissue that is highly vascularised. Furthermore, more fibroblasts are attracted to the wound. PDGF and tumour necrosis factor-α (TNF-α) produced by platelets and macrophages stimulate the fibroblasts to produce collagen, glycosaminoglycans and other components, which stabilize and close the wound. ECM production is stimulated by TGF-β, which also increases the production of collagen [14], [86], [88], [89].

Maturation phase (or tissue remodelling)

Maturation is the last phase (**Figure 6 (4)**). In this phase ECM is remodelled and a new organized matrix of collagen is formed. Homeostasis is reached between synthesis and degradation of collagen, there is no increase in collagen content but rather a reorganization of the collagen fibres into a more organized structure that allows wound remodelling to begin, with the remodelling of collagen from type III to type I. During this phase, the collagen deposition becomes increasingly thick, making the ECM stronger [89], [90]. In the end, an acellular and avascular scar is formed [2]. Failures during wound healing phases can result in chronic ulcers characterised by prolonged inflammation and the inability to re-epithelialize [86].

1.3.2. The role of macrophages in wound healing

Immune cells play an important role in all phases of wound healing. When skin damage occurs, platelets and damaged tissues release cytokines and other mediators which will attract immune cells to the wound [91]. The immune system may be divided into innate and adaptive. The innate response is rapid, occurring soon after the injury, whereas the adaptive response is slower and occurs later [92].

Innate immunity is the body's second line of defence, after the skin, and involves macrophages, neutrophils, mast cells and others [93]. Its main role is to respond quickly in order to avoid infection of deeper tissues [92]. If infection is not resolved quickly, the adaptive response is initiated, involving the clonal expansion of pathogen-specific cells with effector and regulatory functions [92], [94].

Macrophages have one of the most important roles in wound healing with functions at all wound healing phases [14] (**Figure 7**). Before injury, tissue-resident macrophages are in a resting state. However, when injury occurs, they are rapidly activated and secrete large quantities of cytokines leading to the activation and recruitment of leukocytes to the wound site [14], [95], [96]. Bacteria, damaged cells and dead neutrophils are recognized by macrophages that effectively eliminate them by phagocytosis [95], [96]. Such elimination is essential to the healing progression and defects in neutrophil clearance contributes to DFU pathology [96]. During the proliferation phase, macrophages are involved in cell proliferation and ECM deposition [14]. Macrophages produce GFs that promote cell proliferation and protein synthesis, which are essential for tissue formation, including VEGF which is essential for angiogenesis [14], [96]. Thus, the first main role of macrophages in wound healing is the elimination of debris, induction of proliferation of other cells and release reactive oxygen species (ROS) to eliminate pathogens [97].

The depletion of dermal macrophages during the inflammatory phase delayed wound healing. The lack of macrophages decreases the cell proliferation rate, which leads to less formation of new tissue and less vascularisation, and an abnormal epithelialization. When the depletion occurs in the proliferative phase, wound healing stagnates at this stage and was not able to proceed to the next phases with a consequence of an incapacity for wound closure [98]. Although the presence of macrophages in the maturation phase is not mandatory and essential [98], they are important at this stage since they are involved in ECM remodelling [97].

Macrophages are also of utter importance in inflammation resolution during the healing process. In the early stages of wound healing, the inflammation is essential to wound healing and elimination of pathogens and M1 macrophages promote this by releasing pro-inflammatory mediators. However, in the final stages the inflammation needs to be resolved in order for the healing process to be completed. For this, M1 macrophages have to be converted into M2 macrophages which releases anti-inflammatory mediators that will promote wound closure [99].
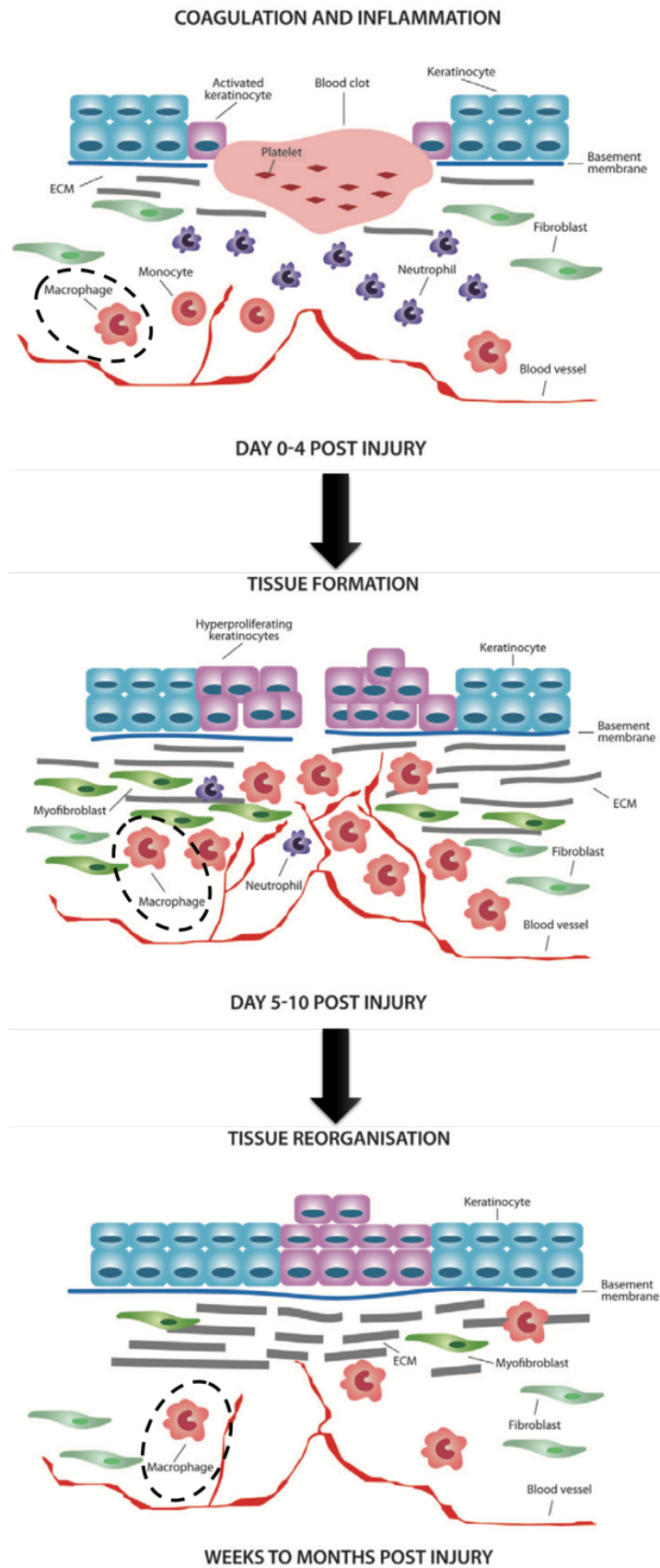
Figure 7 - Macrophages have a role and are present in all phases of wound healing (Adapted with permission from Minutti *et al*, 2016 [14], Copyright by the authors).

1.3.3. Impaired wound healing in diabetes

DFUs are a type of chronic wound with failed or poor healing. Chronic diabetic ulcers are present for more than 4 weeks with very slow healing, or no healing at all [100] and are characterised by excessive inflammation, poor pathogen control, high levels of pro-inflammatory cytokine, which maintain an inflammatory state, and of ROS, that cause damage in the cells, poor angiogenesis, decreased ECM production and increased ECM breakdown [87], [101]–[103]. Normally, chronic wounds are retained in inflammation phase of healing and do not progress to proliferative and maturation phases [70], [99].

In chronic wounds, a high number of cells (keratinocytes, endothelial cells, fibroblasts, and macrophages) are in senescence, not being able to proliferate normally or to respond to wound healing stimuli. This senescence is correlated with impaired wound healing [104], [105]. Other marker of chronic wounds is the presence of high amounts of activated neutrophils that lead to an overexpression of matrix metalloproteinases (MMPs) leading to the destruction of ECM and growth factors and their receptors. This destruction does not allow the wound to progress to the proliferative phase and leads to the attraction of more inflammatory cells increasing the inflammatory environment in the wound [104]–[106]. Thus, the inflammatory cytokines predominate and the factors that promote proliferation and the resolution of inflammation are in very low number [106]. The large number of immune cells that are accumulated in the wound site in chronic wounds produce large amounts of ROS, that in low concentrations is a defence mechanism against pathogens but in high concentrations is dangerous leading to damage in ECM and cell membranes promoting of cell senescence. ROS is also involved in the production of high levels of MMPs, that as referred before, are prejudicial to wound healing [70], [87].

The reepithelization process does not occur in chronic wounds. In this process, KC migration and proliferation are essential, and, for this, a large range of growth factors are required. The problem is that in chronic wounds these factors and their activity are aberrant or degraded by MMPs as described previously [104], [105].

Role of macrophages in chronic wound healing

When the macrophage function is impaired, wound healing is disrupted [99], [107]. Macrophages present in chronic wounds have less phagocytic capacities, not being able to phagocyte dead cells, like neutrophils, that will stay in the wound and increase the inflammatory environment [99], [108]. Furthermore, macrophages secrete a lower number of cytokines and growth factors like TGF- β, VEGF, and insulin-like growth factor 1 (IGF-1) that are essential in the wound healing process [104], [108].

The conversion of the pro-inflammatory M1 macrophages into anti-inflammatory M2 macrophages is essential for wound closure, and in chronic wound this conversion does not occur delaying the resolution of the inflammatory phase, which explains the higher number of M1 macrophages found in chronic wounds [99], [108].

1.4. Protein Tyrosine Phosphatase 1B (PTP1B)

Tyrosine phosphorylation and dephosphorylation are two essential and important processes in cell signalling cascades. Protein tyrosine kinases (PTKs) are responsible for phosphorylation and protein tyrosine phosphatases (PTPs) for dephosphorylation, coordinating and controlling cell signalling. The role of protein kinases is currently well known however the role of protein phosphatases still remains little known and has recently gained emphasis and interest being already known that these proteins play essential roles in cells [109], [110]. The classical or tyrosine-specific PTPs can be divided into two categories: receptor-like PTPs and non-transmembrane PTPs [109], [111].

PTP1B is a non-transmembrane PTP, it was the first PTP isolated in humans [112] and since then it has been widely studied. Until now it is known that PTP1B is ubiquitous, being present in several tissues, works as a negative regulator of several metabolic pathways, including insulin and leptin, and has an important role in diabetes [113]–[115]. The C-terminal of PTP1B contains a side extension containing a proline-rich region, which is involved in the recruitment of substrates, and a hydrophobic region, which is inserted into the membrane of the endoplasmic reticulum [113]. This protein is also involved in processes such as glucose uptake, proliferation, differentiation, motility, adhesion and invasion [116], [117], all with essential roles in wound healing. In the last years, evidence has emerged that inhibition of PTP1B may assist in wound healing enabling this protein to be a good therapeutic target for the treatment of chronic wounds.

1.4.1. Role of PTP1B in insulin signalling and T2DM

When IR is activated, it undergoes autophosphorylation and it interacts with the IRS that also undergo phosphorylation in order to trigger the activation of PI3K and, consequently, the translocation of glucose transporters to the plasma membrane. Thus, dephosphorylation of IR and IRS is necessary for the down regulation of the insulin pathway and this dephosphorylation is performed in part by PTP1B, which plays an essential role in the regulation of the insulin pathway and in glucose homeostasis [113], [118] (**Figure 8**).

Termination or decrease in insulin signalling requires the dephosphorylation of important residues in proteins of the insulin signalling cascade and, because of this, one of the hypotheses is that abnormalities and dysfunctions in PTP1B activity may be associated with insulin resistance. In

addition, there is evidence that PTP1B expression and activity is increased in insulin resistance conditions, which is associated with obesity and diabetes [115], [118]. PTP1B KO mice have high insulin sensitivity and do not develop resistance to insulin when treated with a high fat diet, which shows the potent role of this enzyme in T2DM therapy [119].
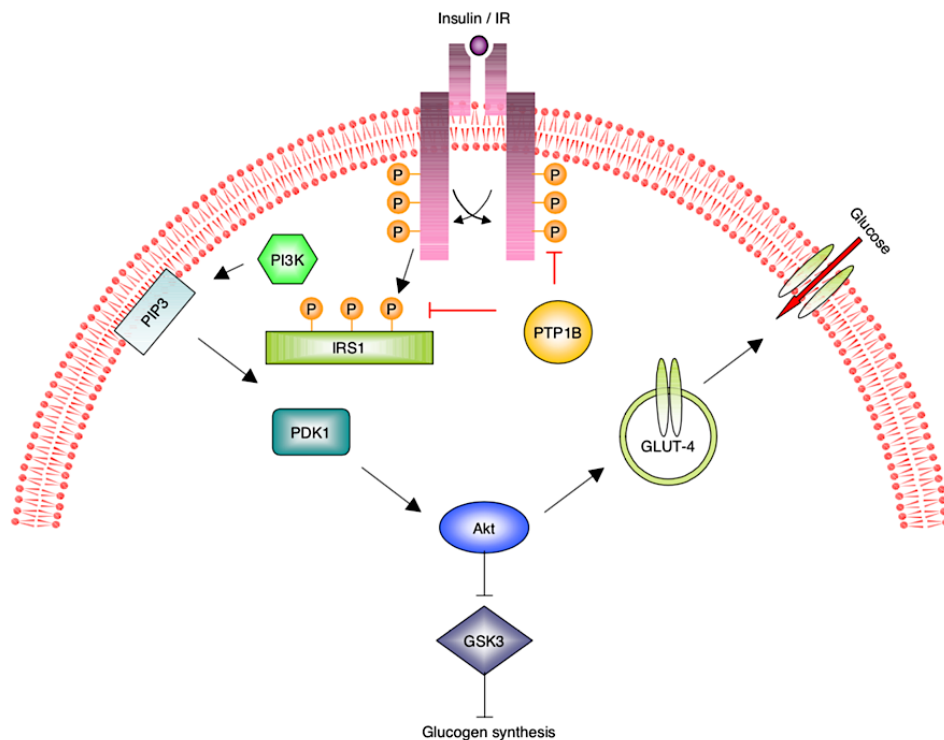
Figure 8 - Role of PTP1B in insulin signalling (Reproduced with permission from Zhang *et al*, 2003 [118], Copyright Ashley Publications).

1.4.2. Beneficial effects of PTP1B inhibition on wound healing

Due to the role of PTP1B in insulin signalling and to the fact that PTP1B is overexpressed in diabetic conditions [120] , various studies have addressed the role of PTP1B in wound healing. Kakazu *et al.* [121] showed that *in vitro* inhibition of PTPs, including PTP1B, led to the activation of a PI3K/PKB pathway involved in wound healing. PTP1B downregulates this pathway, impairing wound healing, and its inhibition reverts this phenotype. This article was one of the first publications to show the relation between PTP1B and impaired wound healing. After this article, many more came out raising the potential role of PTP1B in wound healing.

Inhibition of PTP1B reverses endothelial dysfunction

Angiogenesis is one of the most important events in wound healing in order to create new blood vessels and the restoration of the endothelial network (reendothelization) at the wound site

after an injury [122]. For this to occur, it is necessary that endothelial cells are functional and produce NO, which will trigger a cascade of events essential for wound healing to occur [123] and it is responsible for vasodilatation. However, when endothelial cells are dysfunctional NO production is affected, probably due to dysfunctions in the activation of the pathways responsible for NO synthesis. Phosphorylation is essential for the activation of these pathways and endothelial NO synthase (eNOS) activation, indicating that failures in phosphorylation may be the main reason for endothelial dysfunction and failure of NO production in response to flow [124]. One of the hypotheses to circumvent this dysfunction is the inhibition of PTPs present in the endothelium. PTP1B is expressed in many parts of the body, including the endothelium which forms the inner layer of blood vessels, as demonstrated by immunolocalization [124]. Vercauteren *et al.* demonstrated that by inhibiting this protein in arteries with endothelial dysfunction using selective inhibitors, a large increase in flow-mediated dilation (FMD; a measure of endothelial function [125]) is observed, due to stimulation of NO production via PI3K/Akt pathway, one of the essential pathways for NO synthesis, and increasing eNOS phosphorylation [124].

In addition to PTP1B inhibition, the deletion of this protein in blood vessels also seems to prevent endothelial dysfunction in mice with chronic heart failure, as demonstrated by Gomez *et al.* [126]. In their work, they demonstrated that the inhibition or deletion of PTP1B leads to an increase in FMD, a bigger activation of eNOS (due to an increase in its phosphorylation) and an increase in NO production.

In a more recent study, a whole body PTP1B deletion was performed to evaluate the effects on endothelial dysfunction [127]. The authors found that the deletion of this PTP prevented endothelial dysfunction in aortas of diabetic mice by increasing levels of prostacyclin (PGI_2), a potent vasodilator. Diabetes reduces the NO bioavailability, which affects vasodilation since NO cannot perform its vasodilator function. According to the authors, the depletion of PTP1B increases the expression of cyclooxygenase-2 (COX-2) in endothelial cells. COX-2 is one of the main sources of PGI_2. Thus, increased COX-2 expression will inevitably lead to an increase in the production of the PGI_2, which will compensate for the NO reduction observed during endothelial dysfunction.

Observing all these results, PTP1B appears to contribute to endothelial dysfunction and its inhibition may reverse this dysfunction.

Inhibition of PTP1B in proliferation and migration of endothelial cells and angiogenesis

As mentioned, reendothelialization and angiogenesis play an important role in wound healing. For these processes to occur, in addition to functional endothelial cells, their migration to the lesion site as well as their onsite proliferation are important [128]. Migration and proliferation of these cells is controlled by VEGFs [129]. VEGF acts by binding to its VEGF type 2 receptor

(VEGFR2) inducing its phosphorylation and leading to its activation that will promote migration, since it leads to the breakdown of vascular endothelial (VE)-cadherin-mediated cell-cell adhesions, and proliferation of endothelial cells [130], [131]. It has been demonstrated that PTP1B negatively regulates the activation of VEGFR2 and leads to dephosphorylation of the VE-cadherin, preventing cell-cell adhesions between endothelial cells from being broken, and the activation of endothelial cells proliferation [131]. Therefore, deletion of PTP1B leads to increased activation of VEGFR2 leading consequently to increased phosphorylation of VE-cadherin and reduction of VE-cadherin-mediated cell-cell adhesion, promoting migration of endothelial cells, and also endothelial cells proliferation that increase angiogenesis [131].

In other two studies, the same was observed. Lanahan *et al.* concluded that the endothelial-specific deletion of PTP1B increased VEGFR2 activation leading to a higher migration and proliferation of endothelial cells [132]. They also observed that the mice in which PTP1B was deleted showed increased angiogenesis and, consequently, accelerated wound healing. Besnier *et al.* also showed that both inhibition and silencing of PTP1B promotes the migration and proliferation via VEGF, enhancing angiogenesis [133].

However, PTP1B inhibition can enhance and promote migration of endothelial cells even in the absence of VEGFR2 signalling [122]. When VEGFR2 signalling is compromised or inhibited, PTP1B inhibition appears to promote p130Cas/DOCK180/Rac1 pathway, a pathway involved in integrin signalling, increasing mobility and migration of endothelial cells that lead to enhanced angiogenesis.

In conclusion, inhibition of PTP1B leads to an increase in VEGF2 signalling or to the activation of other pathways, which promotes an increased proliferation and migration of endothelial cells leading to increased angiogenesis which is essential for a faster wound healing.

PTP1B inhibition improves endoplasmic reticulum stress

Endoplasmic reticulum (ER) is the main responsible for the synthesis and folding of proteins in the cell [134], [135]. ER stress is caused by stressors that are responsible for disturbances in the normal functioning of the endoplasmic reticulum [134]. This incorrect functioning of ER is responsible for an inefficient folding of proteins leading to an accumulation of unfolded or misfolded proteins in the reticulum [134], [136]. The accumulation of unfolded proteins leads to the development of the unfolded protein response (UPR) which is strongly associated with inflammation [136], [137]. Excessive and persistent inflammation are present in chronic wound, contributing to the impairment of healing [87]. Furthermore, it is also known that ER stress participates in endothelial dysfunction, which, as mentioned previously, contributes to the failure of wound healing [138].

PTP1B is present in the ER membrane and has been identified as a regulator of ER stress in various tissues [138]–[141] and its inhibition may help to reduce ER stress. This role of PTP1B was first discovered in non-cardiovascular tissues. Studies with PTP1B$^{-/-}$ fibroblasts have demonstrated that the absence of this protein protects cells from the induction of ER stress and, consequently, these cells are more resistant to apoptosis induced by ER stress [141]. Also, liver-specific deletion of PTP1B appears to protect cells from ER stress [139]. The absence of this protein seems to impair ER stress signalling. In order to investigate the role of PTP1B in the regulation of ER stress in the neuronal system, Jeon *et al.* inhibited this protein in neuronal cells [140]. They found that PTP1B inhibition decreases the level of ER stress markers and thus attenuates ER stress in neuronal cells.

Recently, Thiebaut *et al.* carried out a study with the objective of studying for the first time the role of PTP1B in the regulation of ER stress in cardiovascular tissue [138]. They have demonstrated that PTP1B plays a very important role in the regulation of ER stress in the endothelium. Both inhibition and deletion of PTP1B in mouse arteries reduce ER stress. Therefore, PTP1B inhibition may protect the endothelium from ER stress. The authors think that the reduction of endothelial ER stress is due to the stimulation of the protein kinase RNA-like ER kinase (PERK) protective pathway. UPR is activated to try to compensate ER stress and regain normal ER function. For the activation of this response, it is necessary the signalling of three molecular stress sensors: PERK, Inositol-requiring protein 1α (IRE1α) and activating transcription factor 6 (ATF6) [136], [142]. Therefore, the inhibition of PTP1B activates the PERK pathway, attenuating ER stress.

These results show that inhibition of PTP1B can modulate ER stress. This stress is associated with endothelial dysfunction and the development of inflammation, two factors closely related to the failure to heal wounds. Thus, by preventing ER stress, PTP1B inhibition may potentiate wound healing.

Reduction of inflammation in the absence of PTP1B activity

PTP1B inhibition can reduce inflammation by reducing ER stress, but also through other mechanisms. Immediately after injury, inflammation occurs in order to repair damage to tissues and to eliminate pathogens that have infiltrated into the site of injury [96], [143], [144]. However, prolonged and exaggerated inflammation can lead to tissue destruction and impair healing [143]. Macrophages play an essential role in this process as they are responsible for the production of various signals such as cytokines and growth factors [143], [145]. These signals can be pro-inflammatory or anti-inflammatory and will promote and control the inflammatory response [145]. PTP1B is expressed in immune cells, such as macrophages, and its expression is known to be increased with a pro-inflammatory stimuli [146], [147]. Taking this into account, PTP1B may be a good target for the control of inflammation.

In microglia, resident macrophages which act as the first line of defence of the central nervous system [148], it is known that overexpression of PTP1B leads to an increase in the levels of certain pro-inflammatory cytokines, which seems to indicate that PTP1B leads to a pro-inflammatory response. Treatment of a mouse model of neuroinflammation with a PTP1B inhibitor leads to a decrease in the expression levels of these pro-inflammatory cytokines and has an anti-inflammatory action [147].

PTP1B also seems to play an important role in hypothalamic inflammation. It has recently been discovered that a deficiency of PTP1B in the hypothalamic microglia leads to increased expression of Interleukin-10 (IL-10) mRNA, decreased levels of the pro-inflammatory cytokine TNF-α, and to the activation of the Janus kinase 2 (JAK2)–signal transducer and activator of transcription 3 (STAT3) signalling pathway, which will improve and reduce the hypothalamic inflammation [149]. IL-10 is one of the first anti-inflammatory cytokines released when inflammation occurs and leads to the activation of JAK-STAT signalling pathways which promotes the expression of genes involved in the elimination of inflammation [150]. Therefore, PTP1B inhibition may result in the suppression of inflammatory responses. *In vitro* experiments with macrophages corroborate these results [151]. The deletion of PTP1B in macrophages leads to an increase in IL-10 expression as well as to a decrease in TNF-α levels. In addition to these anti-inflammatory effects, it has also been observed that PTP1B deletion promotes a greater activation of STAT3. Pike *et al.* also found that the IL-10-dependent activation of STAT3 is much higher in macrophages of mice without PTP1B compared to mice expressing this phosphatase [150]. The anti-inflammatory potential of inhibition of PTP1B is thus reinforced.

However, it is not only in the brain that PTP1B is involved in the control of inflammation. Experiments performed in PTP1B-null mice have shown that these mice are more resistant to the development of colitis (inflammation in the large intestine) than mice expressing PTP1B [152]. It was found that the lack of PTP1B led to a higher activation of JAK2 and STAT3 which promotes the production of myeloid-derived suppressor cells (MDSCs), a heterogeneous population of immature myeloid cells, which includes for example macrophage precursors. MDSCs have the ability to reduce and control inflammation by protecting PTP1B-null mice from the development of colitis. Thus, the elimination of PTP1B leads to an increased production of MDSCs which in turn prevents the installation of inflammation in the intestine.

By bringing together all of this knowledge with the above information, PTP1B appears to be an excellent target to combat inflammation at the wound site and thus provide better and faster healing.

Deficiency of PTP1B contributes to tissue regeneration

The lack of PTP1B function also appears to be involved in promoting tissue regeneration. In a study using PTP1B-deficient mice, it was observed that in the absence of PTP1B there is an increase in cell proliferation markers in the liver and an improvement in hepatic regeneration [153]. Another study observed the same increase in tissue regeneration with PTP1B inhibition. Zebrafish treated with a PTP1B inhibitor, showed increased regeneration of the amputated caudal fin which is constituted by bone, connective, skin, vascular and nervous tissues; and also an increase in cardiomyocyte proliferation which led to a faster heart regeneration [154]. Taking all together, the inhibition of PTP1B may lead to an increase in regeneration at the wound site contributing to a faster healing.

1.5. Trodusquemine – a specific PTP1B inhibitor

Trodusquemine (or MSI-1436) with the molecular formula $C_{37}H_{72}N_4O_5S$ (**Figure 9**) is a non-competitive and allosteric inhibitor of PTP1B that specifically inhibits this enzyme preventing it from being able to dephosphorylate IR, which leads to increased insulin signalling and consequently lower blood glucose levels [155]–[157].
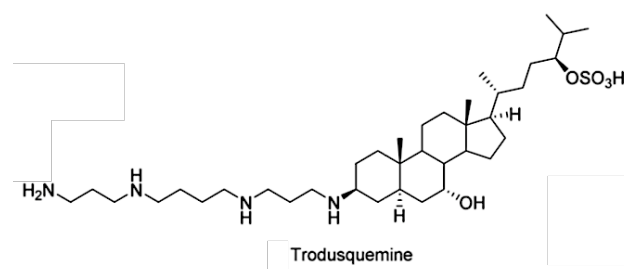
Figure 9 - Molecular structure of Trodusquemine (Adapted with permission from He *et al*, 2016[158], Copyright by the authors).

Trodusquemine appears to suppress appetite, which leads to weight loss, increases sensitivity to insulin and leads to glucose homeostasis, being at the moment in phase 2 clinical trials to assess its safety and efficacy in the treatment of obese or overweight type 2 diabetics [156], [157], [159], [160]. Considering that PTP1B inhibitors are in phase 2 clinical trials for diabetes treatment, these could easily be repurposed for diabetic foot ulcer treatment.

As already mentioned, one of the main reasons for wound healing failure is the establishment of infections due to the proliferation of microorganisms at the injured site [161]. Therefore, one of the main goals is to eliminate the infection in order to promote wound healing. As previously explained, it is known that the use of PTP1B inhibitors improves endothelial function and promotes angiogenesis, however there have been indications that analogues of Trodusquemine may have

direct antimicrobial activities against various strains of fungi and bacteria [162]. When these microorganisms are present in the wound and they are not removed efficiently, a prolonged inflammation can set in and slow or even prevent wound healing [163]. PTP1B inhibitors may thus help to clean the wound of microorganisms preventing the introduction of harmful inflammations.

This finding reinforces the potential of PTP1B inhibitors usage in wound healing, since a simple inhibition could lead to the promotion of mechanisms involved in wound healing and to the elimination of infections at the wound site.

1.6. Aims

DFUs are one of the most devastating and costly complications of diabetes. Classic treatments sometimes cannot cure DFUs and recurrence is very common. Thus, it is necessary to develop new treatments capable of addressing non-healing DFUs. PTP1B has been linked to failure to cure chronic ulcers and therefore may be a good therapeutic target. The main hypothesis of this work is that topical inhibition of PTP1B will improve wound repair in diabetic chronic ulcers. To determine whether inhibition of PTP1B improves wound healing the following aims will be evaluated:

1.   Monocytes, that will be isolated from the blood of diabetic patients with and without DFUs as well as healthy volunteers, and THP-1 cells cultured under normal and high glucose conditions will be treated with Trodusquemine and differentiated into macrophages to assess the effects of PTP1B inhibition on the release of inflammatory cytokines and wound healing mediators in these cells.

2.   In an *in vivo* setting, Trodusquemine will be applied topically (at the wound site) using the streptozotocin-induced diabetic mouse model.

It is expected that this work will lead to the development of new promising and effective treatment for DFUs.

Chapter 2: Materials and Methods

2.1. Reagents

The *secondary antibodies Goat Anti-Rat Alexa Fluor 568, Anti-Rabbit Alexa Fluor 488, Goat Anti-Mouse Alexa Fluor 488* and *Anti-Mouse Alexa Fluor 568* were obtained from Molecular Probes, MA, USA. The reagents *Hydrochloric acid* (*HCL), Triton X-100, Isopropanol, Ethanol for molecular biology* and *Entellan* were purchased from Merck, MA, USA. *Anti-human PTP1B antibody* was obtained from Calbiochem, Merck, CA, USA. The *primary antibodies anti-human CD163, anti-human TNF-α,* the *Pierce™ BCA Protein Assay Kit,* the *Horseradish peroxidase (HRP) secondary antibodies (anti-rabbit, anti-goat and anti-mouse)* and the *enhanced chemiluminescence (ECL) reagent* were purchased from Thermo Fisher Scientific, MA, USA, as well as the applied *Biosystems™ High-Capacity cDNA Reverse Transcription* and *Dihydroethidium (DHE)*.

In addition, the *protease inhibitor cocktail (complete Mini)* and the *phosphatase inhibitor cocktail (PhosSTOP)* were purchased from Roche, Switzerland. The *primary antibodies p-AMPKα (Thr 172), p-JAK2 (Tyr 1007/Tyr 1008), AMPKα2 (C-20), JAK2* and *anti-mouse CD206* were obtained from Santa Cruz Biotechnology, CA, USA. *p-AKT (Ser473)* and *AKT* were purchased from Cell Signalling Technology, MA, USA, and *anti- mouse Ki-67* was acquired from Invitrogen, CA, USA.

Furthermore, the primary *antibody* anti-mouse *CD31* and the *Polyvinylidene difluoride (PVDF) membranes* were obtained from Millipore, MA, USA. Moreover, the *primary antibody anti-mouse TNF-α* and the reagent *Acrylamid/BisSolution* were purchased from Bio-Rad AbD Serotec Ltd, CA, USA. The *LEGENDplex™ Multi-Analyte Flow Assay, Human Th Cytokine Panel (13-plex) kit* was obtained from Biolegend, CA, USA.

RNase free water, *PerfeCTa® SYBR® Green FastMix®* were from Quanta Biosciences, Canada, and the primary antibodies *anti-mouse and anti-human CD68 antibodies* were both purchased from Abcam Plc, Cambridge, UK.

Finally, all *primers* were obtained from Integrated DNA technologies, IA, USA. *QIAzol^{TM} Lysis Reagent* was from Qiagen, Germany, and the *anti-mouse and human HO-1 antibody* were from Enzo Life Sciences Inc., NY, USA. Additionally, the *normal goat serum* from Life Technologies, CA, EUA, and *MSI-1436* from MedChem Express Europe, Sweden.

Lastly, the *density gradient medium Lymphoprep^{TM}* was from Stemcell Technologies, Canada, and the *anti-human CD14 MicroBeads* from Miltenyi Biotec, Bergisch Gladbach, Germany.

All the remaining reagents were purchased from Sigma-Aldrich, MO, USA or VWR, Portugal.

2.2. THP-1 cell culture

The human monocytic cell line THP-1 was kindly supplied by Doctor Maria da Conceição Pedroso de Lima (Vectors and Gene Therapy Group, Center for Neuroscience and Cell Biology, University of Coimbra). THP-1 cells were cultured using a glucose-free RPMI 1640 medium supplemented with non-heat-treated 10% fetal bovine serum (FBS), 1% Penicillin-Streptomycin and 2 g/L of sodium bicarbonate at 37°C in a humidified 5% CO_2 atmosphere. The cells were grown in normal and high glucose, adding 1 g/L or 4.5 g/L of glucose to the medium to obtain the concentration of 5.5 or 25 mM of glucose, respectively.

Cells were subcultured when cell concentration reached $8-10 \times 10^5$ cells/mL in a 75 cm^2 flask and the RPMI medium was replaced every 3-4 days of culture. In order to decrease the area of adhesion of the cells to the plastic, the culture flasks were always used vertically, and the cells were grown in suspension.

Afterwards, cells were centrifuged at 200-300×g for 5min and resuspended in fresh serum-free medium in the desired concentration and seeded in 6-, 12-, or 24-well depending upon the experiment being conducted. To increase cell adhesion to the well bottom, cells were left in serum-free medium overnight and the serum was added to the medium on the next day, 30 min before the treatment of the cells. The number of viable cells was evaluated using Trypan Blue.

2.2.1. Differentiation of THP-1 monocytes into macrophages and treatment

THP-1 monocytes were differentiated into macrophages using phorbol 12-myristate-13-acetate (PMA). Cells were incubated 48h with 50 ng/mL PMA [164]. The differentiation of PMA treated cells was approximately 99%. The differentiation was confirmed by the presence of CD68, a pan-macrophage marker [165]. After 48h of PMA treatment, the PMA-containing medium was removed and fresh medium was added after the cells were washed with warm phosphate-buffered saline (PBS, pH 7.4). The cells were allowed to rest 30 min before any manipulation.

THP-1 differentiated macrophages were incubated with lipopolysaccharide (LPS) (1 μg/mL) for 24h, in the presence or absence of MSI-1436 added 30 min prior LPS stimulation. Two different concentrations (500 nM and 1 μM) of MSI-1436 were tested. The cells were stimulated with LPS and/or treated with 500 nM or 1 μM of MSI-1436 or left untreated (control).

2.3. Isolation of human monocytes from whole blood

Monocytes from peripheral blood of diabetic patients without DFUs (*n*=3), diabetic patients with acute DFUs (ulcer <3 months) (*n*=1), diabetic patients with chronic DFUs (ulcer > 3 months)

(*n*=3), and healthy volunteers (*n*=3), all age and sex-matched, were isolated to evaluate the effect of PTP1B inhibition in human macrophages activation and differentiation. The blood samples were collected by venepuncture into EDTA tubes at Centro Hospitalar do Porto - Hospital de Santo António. Both patient and control sample collection were approved by the local ethics committee and were performed after informed written consent. History of neoplastic malignancies or autoimmune disorders and clinically detectable infection at the time of sample collection (other than the foot infection in the case of DFU patients) were exclusion criteria for all patients and controls enrolled in this study.

2.3.1. Isolation of peripheral blood mononuclear cells (PBMCs)

PBMCs were isolated from the whole blood by a density gradient centrifugation method using the density gradient medium Lymphoprep™ (**Figure 10**). The blood (15-20 mL of each donor) was 1:1 diluted with PBS. Approximately 30 mL of diluted blood was layered over 15 mL of Lymphoprep™ in a 50 mL tube, very carefully to avoid mixing the Lymphoprep™ with blood. The tubes were centrifuged 30 min at 400×g, 20 °C, without brake to avoid mixing the Lymphoprep™ with blood. After the centrifugation, the mononuclear cell layer was carefully transferred to a new 50 mL tube, avoiding Lymphoprep™ contamination since it is cytotoxic. The separated layer was washed with 50 mL PBS at 300×g for 10 minutes at 20 °C. Following centrifugation, the supernatant was completely removed, and the cell pellet was resuspended in 50 mL of PBS and centrifuged at 200×g for 15 minutes at 20 °C, for platelet removal and to increase the purity of isolated cells in the subsequent cell separation. The supernatant was completely removed, and the cell pellet resuspended in 10 mL of PBS.
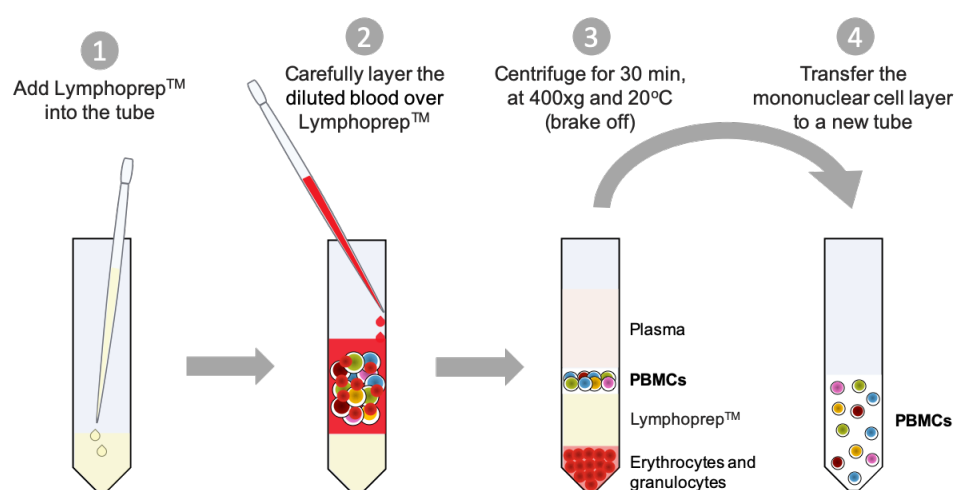
Figure 10 - PBMCs isolation using density gradient centrifugation method. After the centrifugation of diluted blood layered on top of the separation medium it is clear the four separated layers; PBMCs are between the plasma and the Lymphoprep™ layers.

2.3.2. Isolation of CD14+ monocytes by magnetic labelling

CD14 is highly expressed in monocytes therefore this protein was used to isolate monocytes from PBMCs [166]. The isolation of CD14+ monocytes from the PBMCs was performed by using an anti-CD14 MicroBeads and a MACS separation column system following the manufacturer´s instructions (Miltenyi Biotec) (**Figure 11**).

After the PBMCs isolation, the cell number was determined using Trypan Blue and the cell suspension was centrifugated for 10 minutes at 300×g and 20°C. The supernatant was completely removed, and the cell pellet was resuspended in 80 μL of MACS buffer (PBS, pH 7.2; 0.5% bovine serum albumin (BSA); 2mM EDTA) per 10^7 total cells. MACS buffer was freshly prepared and kept to a maximum of one month at 4°C. Then, cells were incubated with CD14 MicroBeads (20 μL of MicroBeads per 10^7 total cells) for 15 minutes at 4°C. Following incubation, the cells were washed by adding 1−2 mL of MACS buffer per 10^7 cells and centrifuged at 300×g for 10 minutes at 20°C. The supernatant was removed completely, and the cells resuspended in 500 μL of MACS buffer. For the magnetic separation, LS Columns were used. The column was placed in the magnetic field of a MACS Separator and prepared with 3 mL of MACS buffer. Then, the sample was applied onto the column and washed 3 times with 3 mL of MACS buffer. The magnetically labelled CD14+ cells were retained in the column while unlabelled cells passed through the column and were discarded. Afterwards, the column was removed from the Separator and placed onto a tube. To access the isolated monocytes, 5 mL MACS buffer was added onto the column and flushed out by firmly pushing the plunger into the column. The number of cells was determined, and PBS was added to the cell suspension and centrifuged at 400×g for 5min at 4°C. Following centrifugation, the supernatant was removed, and cells were resuspended in the necessary volume to obtain 4×10^5 cells per mL of complete culture medium. The cells were seeded for differentiation to macrophages in 24-well plates (4×10^5 cells/well). Monocytes were cultured using RPMI 1640 medium supplemented with non-heat-treated 10% FBS, 1% Penicillin-Streptomycin and 2 g/L of sodium bicarbonate at 37°C in a humidified 5% CO_2 atmosphere.

Cells were maintained for 3 days without any stimulation or treatment in order to rest and recover from isolation and ensure the results obtained were not influenced by the manipulation performed during the isolation technique. After 3 days of resting the medium was replaced and the cells were differentiated into macrophages.

2.3.3. Differentiation of isolated monocytes into macrophages and treatment

Human monocytes were differentiated into macrophages in the same manner as THP-1 cells. Cells were incubated 48h with 50 ng/mL PMA, then, the medium was removed and, after the

cells were washed with warm PBS and fresh medium was added. Cells were allowed to rest 30 min before any manipulation and the differentiated macrophages were incubated with LPS (1 µg/mL) for 24h, in the presence or absence of MSI-1436 added 30 min prior to LPS stimulation. One concentration (1 µM) of MSI-1436 was tested.
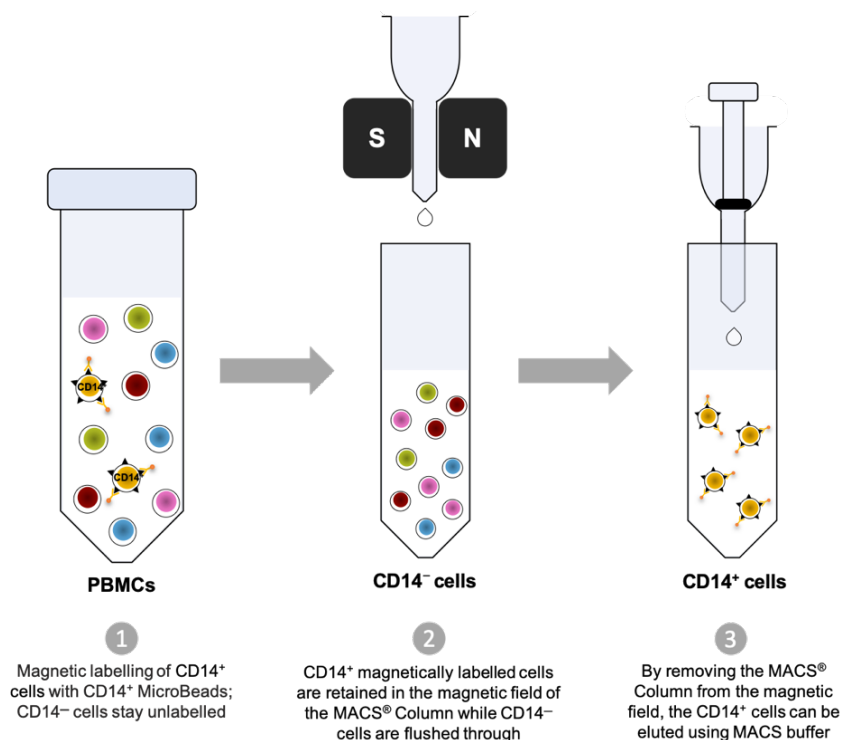
Figure 11 - Isolation of CD14$^+$ monocytes using MACS$^®$ Technology.

2.4. MTT assay to assess cell viability

In order to determine cell viability, 2×10^5 THP-1 cells per well were seeded in 24-well plates, differentiated into macrophages and stimulated with MSI-1436 (500 nM or 1 µM) and LPS (1 µg/mL). This assay was performed in both cells, cell line and primary cells, grown in high and normal glucose.

The MTT assay is a colorimetric assay where the soluble yellow compost MTT (3-(4,5-dimethylthiazol-2-yl)-2,5-diphenyltetrazolium bromide) that is positively charged, passes through the cell membrane into the cells. Inside the cells, this compost is converted by mitochondrial succinate dehydrogenases to formazan insoluble crystals with purple colour. The formazan crystals were dissolved using acidic isopropanol and the absorbance of the obtained purple colour solution was measured using a spectrophotometer. Only viable cells with intact and functional mitochondria, and active metabolism are able to convert MTT into formazan crystals; dead cells do not have an active metabolism therefore are unable to produce formazan crystals. Thus, the measured absorbance will be proportional to the number of viable cells [167], [168].

Briefly, the cells were left with 450 µL of medium and 50 µL MTT (5 mg/mL; prepared in PBS) was added to each well. The cells were incubated at 37ºC for 1-2 hours in a humidified 5% CO_2 atmosphere with MTT and following the incubation the supernatants were carefully removed. The formazan crystals formed were dissolved by adding 250 µl acidic isopropanol (0,04 N) to each well and mixed in order to dissolve completely the crystals. The acidic isopropanol solution was collected to a 96-well plate and the absorbance of the solution measured using a microplate spectrophotometer (SpectraMax® Plus 384 Microplate Reader), at 570 nm with a reference wavelength of 620 nm.

2.5. Immunocytochemistry

Immunocytochemistry assay was performed to confirm THP-1 macrophage differentiation by CD68 staining. To evaluate the number of M2 macrophages a double staining with CD68 and CD163 was used [169], and the inflammatory state of macrophages were evaluated with TNF-α staining. Furthermore, the levels of the enzyme heme oxygenase 1 (HO-1) were also measured using this assay. HO-1 is an enzyme, related to oxidative stress, actuating as a protective mechanism against oxidative tissue damages and having anti-inflammatory and antioxidant properties [170]–[173].

For this assay, THP-1 cells (1×10^5 cells/well) were seeded in 24-well plates with 12 mm glass coverslips, differentiated into macrophages and treated as previously explained. After all treatments, the medium was removed, the cells were washed with PBS (37 ºC; 1 mL/well) and fixed with 4% paraformaldehyde in PBS (PFA) for 10 minutes at room temperature (RT). Following fixation, the cells were washed with PBS 0.03% BSA 2 times for 5 minutes, permeabilized with 0.1% Triton X-100 in PBS for 10 at RT and washed with PBS + 0.03% BSA 3 times for 5 minutes. Then, the coverslips were incubated on the top of a parafilm, well adhered to the bench with water and surrounded with wet paper to maintain a humid atmosphere around the coverslips in order to avoid dehydration of the cells. For the blocking step, the cells were incubated with normal goat serum (1:10 in PBS; 50 µL/coverslip) for 30 min. After the blocking step, all the serum was removed, and the cells were incubated with the respective primary antibody (1:100 in PBS; 30 µL/coverslip). The cells were washed 3 times for 5 min each with PBS + 0.03% BSA and incubated with DAPI (1:1000 in PBS) together with the secondary antibody (1:500 in PBS+DAPI; 30 µL/coverslip) for 1h at RT, in the dark. The cells were again washed 3 times for 5 min each with PBS + 0.03% BSA and mounted in slides with mounting medium. The images were acquired with an LSM 710 confocal microscope (Carl Zeiss) and the optimal acquisition parameters and settings were maintained throughout the experiment. The number of M2 macrophages and the fluorescence intensities (TNF-α and HO-1) were measured using the open-source software Fiji.

2.6. Dichloro-dihydro-fluorescein diacetate (DCFH-DA) assay

DCFH-DA assay is a long-established assay which allows the detection of oxidative stress using a fluorogenic dye that measures ROS activity inside the cell [173]. Low and controlled levels of ROS are essential in wound healing since it provides protection against pathogens which try to invade the wound and are involved in the promotion of angiogenesis. However, the presence of high levels of ROS in wounds are related to the pathogenesis of chronic wounds since they lead to oxidative stress that have destructive and negative effects in wound repair and healing [175], [176]. Consequently, determining the level of oxidative stress present in the wound can be important to understand whether the treatment with MSI-1436 can modulate the ROS production and improve wound healing.

In this assay, live cells are incubated with 2′,7′-dichlorodihydrofluorescein diacetate (DCFH$_2$-DA) which can pass through the cell membrane and is converted in 2′,7′-dichlorodihydrofluorescein (DCFH$_2$) by intracellular esterases that cleave the acetate groups of DCFH$_2$-DA. The oxidation of DCFH$_2$ in the presence of general ROS leads to the generation of 2′,7′- dichlorofluorescein (DCF) which emits fluorescence that can be measured [174] (**Figure 12**). Therefore, the presence of a greater amount of ROS will lead to a higher emission of fluorescence.

THP-1 cells were cultured as previously described in the immunocytochemistry assay; 1×10^5 cells/well were seeded in 24-well plates with 12 mm glass coverslips, differentiated into macrophages and treated. The medium was removed, the cells washed with warm PBS and incubated with 1mL of free-serum medium to rest and stabilize for 30 min. Then, cells were incubated with 10 nM of DCFH- DA probe for 30 min. Both incubations were performed at 37 ºC in a humidified 5% CO_2 atmosphere. At the end of this time, the medium was removed, the cells were washed two times with warm PBS and immediately observed in the fluorescence microscope (Axio Imager Z2, Carl Zeiss). The fluorescence intensity was measured using the open-source software Fiji.
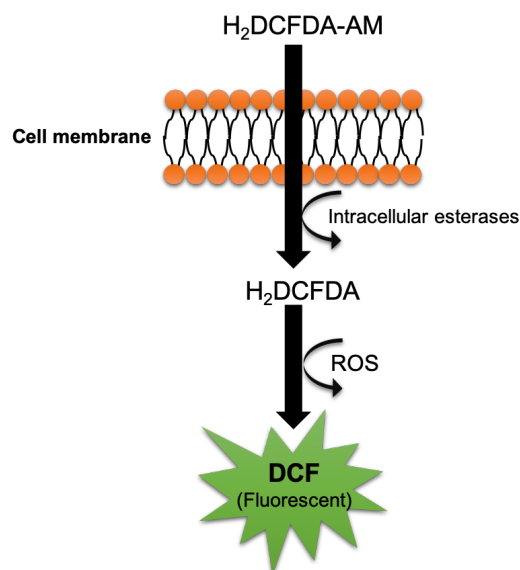
Figure 12 - Principle of the DCFH-DA assay. After the acetate groups cleavage of $DCFH_2$-DA by intracellular esterases, the interaction of ROS with $DCFH_2$ leads to the generation of the fluorescent compound DCF.

2.7. Western blotting

2.7.1. Cell lysates preparation

THP-1 cells (8×10^5 cells/well) were plated in 12-well plates and differentiated into macrophages as described before. To study the activation of relevant pathways to the study, the phosphorylated state of key pathway proteins was evaluated when the cells were incubated for 30 min with two different concentrations of MSI-1436 (500 nM and 1 µM) prior to incubation with 1 µg/mL of LPS for 15 min and 30 min. To evaluate the total expression of other proteins, the cells were treated was described before.

After all incubations, the cells were washed with warm PBS and 150 µL of ice-cold RIPA buffer (150 mM NaCl, 50 mM Tris-base, 5 mM EGTA, 10% Triton X-100, 0.5% sodium deoxycholate (DOC), 0.1% sodium dodecyl sulphate (SDS), protease inhibitors, phosphatase inhibitors, dithiothreitol (DTT) 1 mM, milli-Q H_2O; pH 7.5) were added to each well and the plate placed on ice. Cell lysates were collected and kept on ice for 30 min, being homogenized every 10 min, and then frozen at -80 ºC until use.

Before protein denaturation, cell lysates were sonicated three times, 10 seconds each, with intervals of 4 seconds between them and always on ice, using a Vibra Cell sonicator. The cell lysates were then centrifuged at 3000×g for 5 min, and the supernatant collected to perform protein denaturation.

2.7.2. Protein quantification using the bicinchoninic acid (BCA) method

BCA method is a widely used method for protein quantification based on the protein conversion of Cu^{2+} to Cu^+ in alkaline conditions; Cu^+ reacts with BCA, producing a purple colour solution. The colour produced can be measured using a spectrophotometer, at 540-570 nm, and the colour intensity is proportional to protein concentration. In this method, the protein concentration from samples can be calculated by correlation with known protein concentration standards [177], [178].

Cell lysates were defrosted and very well mixed. The protein standards were prepared using a range of dilution of BSA (2 mg/mL) in an increasing concentration between 12.5 µg/mL and 800 µg/mL and the absorbance values obtained were used to originate a standard linear curve to determine protein concentration. To perform this assay, 25 µL of diluted cell lysates (1:10), water or BSA protein standard, and 25 µL diluted RIPA buffer (1:20) were added to each well in a 96-well plate. In the end, 200 µL of BCA reagent were added to each well and the plate was stirred for 30 seconds and incubated at 37 ºC for 30 min, protected from light. Following the incubation, the absorbance of the colour produced in each well was measured using a microplate spectrophotometer (SpectraMax® Plus 384 Microplate Reader) at 570 nm.

2.7.3. Immunoblotting

Immunoblotting was performed to analyse the phosphorylation and/or total expression of some proteins involved in signal pathways, where PTP1B plays an important role, in order to confirm the inhibition of this phosphatase. In addition, the immunoblotting was used to analyse the cellular protein levels and expression of PTP1B in high and normal glucose condition, in the presence or absence of MSI-1436.

In this assay, 30 µg of protein from each sample were mixed with sample buffer (6x: 0.125 M Tris; 2% SDS; 100 mM DTT; 10% glycerol and bromophenol blue; pH 6.8) and denatured at 99 ºC for 5 min. The denatured proteins along with the molecular weight marker were loaded onto a 7.5 or 10% (V/V) sodium dodecyl sulphate polyacrylamide gel electrophoresis (SDS-PAGE) and ran for 1–2 h at 80-100 V. Afterwards, the proteins were transferred from the gel to an activated PVDF membrane for 1h at 100 V. To confirm the transference of proteins, Ponceau S staining was performed in the membrane. Shortly, the membrane was submersed in Ponceau solution and, following confirmation of a successful transfer, the solution of Ponceau S was removed from the membrane by washing it several times with TBS-T (Tris-buffered saline + 0.02% of Tween 20, pH 7.4). Then, the membrane was blocked using a blocking buffer (TBS-T + 5% BSA) for 1h at RT. After blocking, the membrane was incubated with the desired primary antibody, using the dilution recommended by the

manufacturer (**Table 2**), at 4ºC and overnight. In the following day, the membrane was washed 3 times for 15 min each, with TBS-T and incubated for 1h at RT with the specific secondary antibody (1:5000). After incubation, the membrane was washed again 3 times for 15 min each, the bands were obtained using an ECL Western Blotting Substrate and the images acquired by the ChemiDoc™ Imaging System (Bio-Rad). The results were analysed using the FIJI software.

Table 2 - Primary antibodies used in the immunoblotting and respective dilutions.

Antibody	Dilutions
p-AMPKα (Thr 172)	1:1000
p-AKT (Ser473)	1:1000
p-JAK2 (Tyr 1007/Tyr 1008)	1:1000
AMPKα	1:1000
AKT	1:1000
JAK2	1:1000
HO-1	1:1000
PTP1B	1:1000
β-Actin	1:5000

Legend: p-AMPKα → Phospho-AMP-activated protein kinase α subunit; p-PKB/AKT → Phospho-Protein kinase B; p-JAK2 → Phospho-Janus kinase 2; AMPKα → AMP-activated protein kinase α subunit; PKB/AKT → Protein kinase B; JAK2 → Janus kinase 2; HO-1→ Heme oxygenase 1; PTP1B → Protein tyrosine phosphatase 1B.

2.8. Real-Time quantitative polymerase chain reaction (qRT-PCR)

2.8.1. RNA extraction

THP-1 cells (1×10^6 cells/well) or human isolated macrophages (4×10^5 cells/well) were cultured in 6-well plates or 24-well plates, respectively, and treated as described before. The cells were washed once with PBS to removed dead cells and incubated with QIAzol™ Lysis Reagent (1 mL/10 cm^2) for 5 min at RT, scraped and collected, passing the cell lysate several times through a pipette. For each mL of QIAzol™ used, 200 µL of chloroform were added to the samples then, after vigorously mixed for 15 seconds, samples were left at RT for 3 min. The samples were centrifuged for 15 min at 12000×g, 4ºC, and a separation between the three phases is clear, the RNA is in the aqueous phase in the top of the tube (**Figure 13**). In order to precipitate the RNA, the aqueous phase containing the RNA was transferred to a new tube and 500 µL of isopropanol was added to the tube, which was left at RT for 10 min and centrifuged for 10 min at 12000×g, 4ºC. The supernatant was

removed and carefully 1 mL of 75% ethanol per mL of QIAzol™ used was added. The tubes were very well mixed and centrifuged for 5 min at 7500×g,4ºC. After the centrifugation, all the ethanol was removed, and the tubes were kept at RT to dry completely with the lid open for 5 to 10 minutes. Finally, the RNA pellet was dissolved in 40 µL of 70ºC heated RNase free water and the RNA concentration was determined by OD260 measurement using a Nanodrop spectrophotometer (Wilmington, DE, USA). The isolated RNA was used to perform the cDNA synthesis or stored at -80ºC.
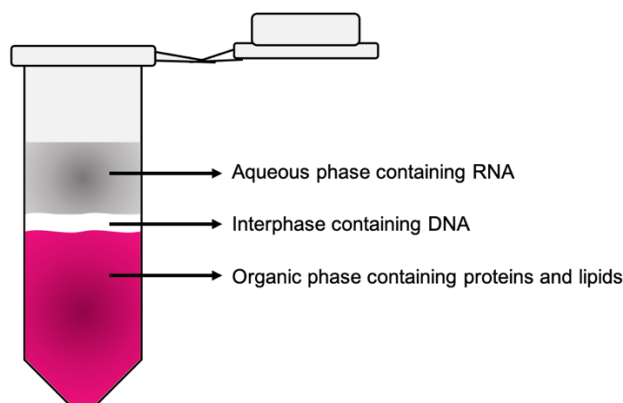
Figure 13 - Phase separation after addition of chloroform and centrifugation. The upper aqueous phase is rich in RNA, while the interphase is rich in DNA; the lower layer is rich in organic content like proteins and lipids

2.8.2. Quantification of mRNA with qRT-PCR assay

Genes of interest can be amplified using specific primers, and the inclusion of the SYBR green dye in the double-stranded DNA molecules allows to measure the gene amplification, which is important to compare the amount of gene expression in the cell, in a control or treatment situation.

The conversion of RNA to cDNA by reverse transcription was done with the Applied BiosystemsTM High-Capacity cDNA Reverse Transcription kit using 1 µg of RNA. Shortly, 2 µl of 10X RT Buffer, 0.8 µl of 25X dNTP Mix (100 mM), 2µl of 10X RT Random Primers, 1 µl of MultiScribe® Reverse Transcriptase (50 U/µL) and RNase free water up to 14.2 µL were added to the required amount of RNA sample (1 µg). The 20 µl reaction was added to a Thermal cycler (VWR) with the protocol for cDNA synthesis: 10 min at 25 ºC, 2h at 37ºC, 5 min at 85 ºC and then kept at 4 ºC. After the cDNA transcription, the samples were diluted 10 times with RNase-free water.

The qRT-PCR reaction was done in 10 µl and include 2.5 µl cDNA, 5 µl PerfeCTa$^®$ SYBR$^®$ Green FastMix$^®$, 0.03 µl of each primer (100 nM of final primer concentration) and 2.44 µl of RNase-free water. The following protocols were performed using the Bio-Rad My Cycler iQ5:

- 95 ºC for 3 min, 40 cycles of 10 sec at 95 ºC and 30 sec at 60 ºC

- 95 ºC for 30 sec, 40 cycles of 3 sec at 95 ºC, 15 sec at 55 ºC and 10 sec at 68 ºC

The list of primers used, and respective sequences are in **Table 3**. After amplification, a threshold was set for each gene and the Ct-values were calculated for all samples. The results were normalised using the reference gene TATA binding protein (TBP).

Table 3 - List of primers and respective sequences.

Primers	Forward sequence	Reverse sequence
TBP	TTCCACTCACAGACTCTC	ACAATCCCAGAACTCTCC
IL-8	TTGGCAGCCTTCCTGATTTC	AACTTCTCCACAACCCTCTG
IL-6	GTAGTGAGGAACAAGCCAGAG	CATGCTACATTTGCCGAAGAG
IL-1β	GCTTGGTGATGTCTGGTC	GCTGTAGAGTGGGCTTATC
MCP-1	AAACTGAAGCTCGCACTCTC	AATCCTGAACCCACTTCTGC
TGF-β	CAACAATTCCTGGCGATACT	GCTAAGGCGAAAGCCCTCAT
VEGF	CAGAATCATCACGAAGTG	TCTGCATGGTGATGTTGGA
PDGF	GAGATGCTGAGTGACCACTCGA	GTCATGTTCAGGTCCAACTCGG
PTP1B	ATAAAGACTGCCCCATCAAGG	GTAACTCAGTGCATGGTCCTC
TNF-α	CCTGTGAGGAGGAGGAAC	CGAAGTGGTGGTCTTGTTG
EGF	AATCATGGCTGTACTCTTGGG	CAGGACAGAAACATAAGGGAC

Legend: TBP → TATA binding protein; IL-8 → Interleukin 8; IL-6 → Interleukin 6; IL-1β → Interleukin 1 beta; MCP-1 → Monocyte chemoattractant protein-1; TGF-β → Transforming growth factor beta; VEGF → Vascular endothelial growth factor; PDGF → Platelet-derived growth factor; PTP1B → Protein-tyrosine phosphatase 1B; TNF-α → Tumour necrosis factor alpha; EGF → Epidermal growth factor.

2.9. LEGENDplex^{TM} Multi-Analyte Flow Assay

The quantification of the inflammatory cytokines of interest was performed using a LEGENDplex^{TM} Multi-Analyte Flow Assay, Human Th Cytokine Panel (13-plex). For that, the supernatant of the cells used for qRT-PCR was collected, centrifuged at 220×g for 5 min and stored at -80 ºC until use. This assay is a bead-based immunoassay that follows the same basis of sandwich immunoassays. The capture beads are conjugated with specific antibodies that, when incubated with a sample containing target analytes, will bound to the analytes. Then, specific biotinylated detection

antibodies are added, and each antibody binds to its specific bead conjugated antibody. In the end, streptavidin-phycoerythrin (SA-PE) is added and it binds to the biotinylated detection antibodies, providing fluorescent signal with intensities that are proportional to the amount of the analyte. The concentration of the analytes is determined using a known standard curve and the LEGENDplex™ data analysis software [179].

For this assay the manufacturer´s instructions were followed. First, the lyophilized Human Th Panel Standard Cocktail with 250 µL Assay Buffer was reconstituted with 250 µL assay buffer, mixed and left for 10 min at RT. This was used as the top standard C7 (**Table 4**). Then, a serial 1:4 dilutions were performed to obtain C6, C5, C4, C3, C2 and C1 standards. The assay buffer was used as the 0 pg/mL standard (C0).

To prepare the samples and standards, 25 µL Assay Buffer, 25 µL of each standard or each sample, 25 µL of the pre-mixed beads and 25 µL Detection Antibodies were added to all tubes. The tubes were incubated for 2h at RT, protected from light and in continuous shaking. Without washing, 25 µL SA-PE to were added to each tube and the tubes were incubated for 30 min at RT with shaking and protected from light. After incubation, the tubes were centrifuged at 1000×g for 5 min, the supernatant was removed, the tubes were washed with 200 µL of 1X Wash Buffer and centrifuged at 1000×g for 5 min. The supernatant was then removed, and the beads resuspended in 200 µL of 1X Wash Buffer. The samples were immediately read on BD FACSCalibur™ flow cytometer following the manufacturer´s instructions.

Table 4 - Standard concentrations and preparation (Adapted from BioLegend instructions).

Standard ID	Serial Dilution	Assay Buffer to add (µL)	Standard to add	Final Concentration (pg/mL)
C7	-	-	-	10,000
C6	1:4	75	25 µL of C7	2,500
C5	1:16	75	25 µL of C6	625
C4	1:64	75	25 µL of C5	156.3
C3	1:256	75	25 µL of C4	39.1
C2	1:1024	75	25 µL of C3	9.8
C1	1:4096	75	25 µL of C2	2.4
C0	-	75	-	0

2.10. Mouse model of wound healing

For this experiment, 8-9-week-old male C57BL/6J WT mice (Charles River Corporation Inc, Barcelona, Spain) were used. The animals were kept at normal room temperature on a 12 h light/dark cycle, with free access to food and water. All experiments were conducted according to the National and European Community Council directives on animal care.

2.10.1. Diabetes induction

Mice weighing 22-28 g received an intraperitoneal injection of 50 mg/kg Streptozotocin (STZ) in citrate buffer (pH 4.5) for consecutive 5 days [175]. One week after the last injection the blood glucose levels were measured and the animals with blood glucose levels above 250 mg/dL were considered diabetic. STZ induces diabetes by the destruction of the beta cells in pancreatic islets [181]. The animals were kept diabetic for 6 weeks of diabetes prior the wound healing procedure.

2.10.2. Wound healing model and treatments

The mice were anaesthetised with inhalation of 3-5% isoflurane combined with oxygen with a flow rate of 1 L/min and the anaesthesia maintenance dose was 2.5% isoflurane. The hair was removed from the back, the skin was disinfected, and two 6 mm diameter full-thickness excisional wounds were created with a biopsy punch. After the wound healing procedure, the animals were maintained in individual cages. The wound area was measured using acetate tracing every day to follow the rate of wound closure up to 10 days post-wounding. The wound size was analysed using the FIJI software.

The mice were divided in four different groups: the groups with wounds treated with 1 µg, 10 µg or 25 µg MSI-1436, and the control group with wounds treated with saline, every day until sacrifice. The animals were sacrificed at day 3 or day 10 after wounding and the tissue harvested. The skin was embedded in optimal cutting temperature (OCT) compound and frozen to perform immunohistochemistry and ROS staining assays.

2.11. Immunohistochemistry assay

The immunostaining was performed for detection of M1 and M2 macrophages (CD68 + TNF-α and CD68 + CD206, respectively), proliferation (Ki-67), for the evaluation of the neovascularisation in the wounded skin (CD31) and to detect the presence of HO-1.

Skin cryosections (10 µm) were fixed in ice-cold acetone for 10 min and rinsed three times in PBS-T (PBS 1X + 0.1% Tween 20) for 5 min each. To permeabilize the samples these were incubated at RT with PBS-T + 0.1 % Triton X-100 for 10 min. After this, samples were washed with PBS-T and blocked with 40 µL of 5% goat serum in PBS-T for 30 min in a humidified chamber at RT. The blocking solution was removed, and the cells incubated overnight at 4°C in a humidified chamber with 40 µL of primary antibody in PBS-T + 1% goat serum (dilutions on **Table 5**). In the following day, the samples were washed three times with PBS-T, 5 min each, and incubated with 40 µL of secondary antibody (1:500) in PBS-T+1% goat serum plus DAPI (1:1000) for 1h at RT in the dark. The samples were rinsed three times with PBS-T, 5 min each, and mounted with mounting media (Entellan) and left to dry at RT for 1-2 h. The images of M1 and M2 macrophages, ki-67 and HO-1 staining, were obtained using the LSM 710 confocal microscope (Carl Zeiss) and for CD31 was used the fluorescence microscope Axio Imager Z2 (Carl Zeiss). The optimal acquisition parameters and settings were maintained throughout the experiment.

The number of M1 and M2 macrophages, proliferative cells and the number of vessels as well as fluorescence intensities (HO-1) were measured using the open-source software Fiji.

Table 5 - Primary antibodies used in the immunostaining and respective dilutions.

Antibody	Dilutions
CD68	1:100
TNF-α	1:200
CD206	1:200
Ki-67	1:500
CD31	1:100
HO-1	1:200

Legend: CD68 → Cluster of differentiation 68; TNF-α → Tumour necrosis factor alpha; CD206 → Cluster of differentiation 206 or mannose receptor; CD31 → Cluster of differentiation 31 or platelet endothelial cell adhesion molecule; HO-1 → Heme oxygenase 1.

2.12. ROS staining

As mentioned before, the presence of high ROS levels in the wound are prejudicial to wound healing. Thus, the quantification of ROS levels allows to know whether the treatment affects the oxidative stress at the wound site.

Cross-sections of unfixed skin (30 µm) were washed with PBS for 5 min at RT. Then, samples were incubated with 1 µM DHE for 30 min at 37 ºC in a humidified chamber and protected from light. DHE, like DCFH-DA, is a probe that, when in the presence of superoxide, an important ROS, undergoes oxidation leading to a red fluorescence emission. After incubation, the samples

were washed twice with PBS and fixed with 4% PFA for 5 min at RT. The slides were washed once with PBS, stained with DAPI (1:2000) for 5 min and washed once again. Slides were mounted with mounting media (Entellan) and observed immediately with the LSM 710 confocal microscope (Carl Zeiss). The fluorescence intensity was measured using the open-source software Fiji.

2.13. Statistical analysis

The results are expressed as mean ± standard error of the mean (SEM) of the indicated number of experiments. Statistical analysis was performed using t-test and for multiple group comparisons was used the One-Way ANOVA test, with a Newman–Keuls post-test. The tests were performed using GraphPad Prism, version 6 (GraphPad Software, San Diego, CA, USA). p values lower than 0.05 were considered statistically significant.

Chapter 3: Results

3.1. Results in THP-1 cells

Macrophages are essential in the wound healing process. When injury occurs, macrophages are rapidly activated. M1 macrophages are the first players in healing, responsible for the phagocytose of exogenous pathogens and death cells, and also for the secretion of large quantities of pro-inflammatory cytokines that are essential for the initiation of wound healing [14], [182]. In the later stages of tissue repair, macrophages change to the M2 phenotype, were they play an important role. These macrophages release essential anti-inflammatory cytokines and growth factors to the resolution of inflammation, and promotion of cell proliferation and tissue formation [181], [182]. When macrophage function is impaired, wound healing is compromised [99], [107]. In chronic wounds, macrophages are associated with the impairment in tissue repair. M1 macrophages are not able to change to the M2 phenotype, contributing to the maintenance of the inflammatory phase and delaying its resolution [99]. Thus, macrophages can be a potential therapeutic target for chronic wounds.

To evaluate the effect of PTP1B inhibition on the functional properties of macrophages related to wound healing, the THP-1 cell line was used. The THP-1 cell line is a human leukaemia monocytic cell line which has been widely used as a model for human monocyte and macrophage cells. When the goal is the study of human monocytes or macrophages, using this cell line has numerous advantages since access to human macrophages from patients is very limited, including the number of monocytes obtainable per patient [184].

THP-1 cells were grown in normal (5.5 mM) and high (25 mM) glucose medium, differentiated into macrophages and incubated with two different concentrations of MSI-1436 (500 nM and 1 µM of PTP1Bi) and/ or LPS (1 µg/mL), during different time periods. These concentrations were chosen based on previous work [183].

3.1.1. THP-1 differentiated macrophages

THP-1 cells were differentiated into macrophages by incubation with 50 ng/mL PMA for 48h. During the process of differentiation, cell morphology changes by increasing cytoplasmic volume, increasing in size and adhering to the bottom [180], [181] (**Figure 14A**). These changes were observed using a light microscopy during the 48h of differentiation. After 48h of incubation with PMA, both cell conditions, grown in normal or in high glucose concentrations, appeared completely differentiated, showing macrophage morphology. Cells were then incubated with or without MSI-1436 and LPS for 24h. Macrophage differentiation has been confirmed by the presence of the macrophage differentiation marker CD68 [183], in normal (NG) (**Figure 15B**) or high (**Figure 14C**) glucose (HG). The differentiation of PMA treated cells was approximately 99%.
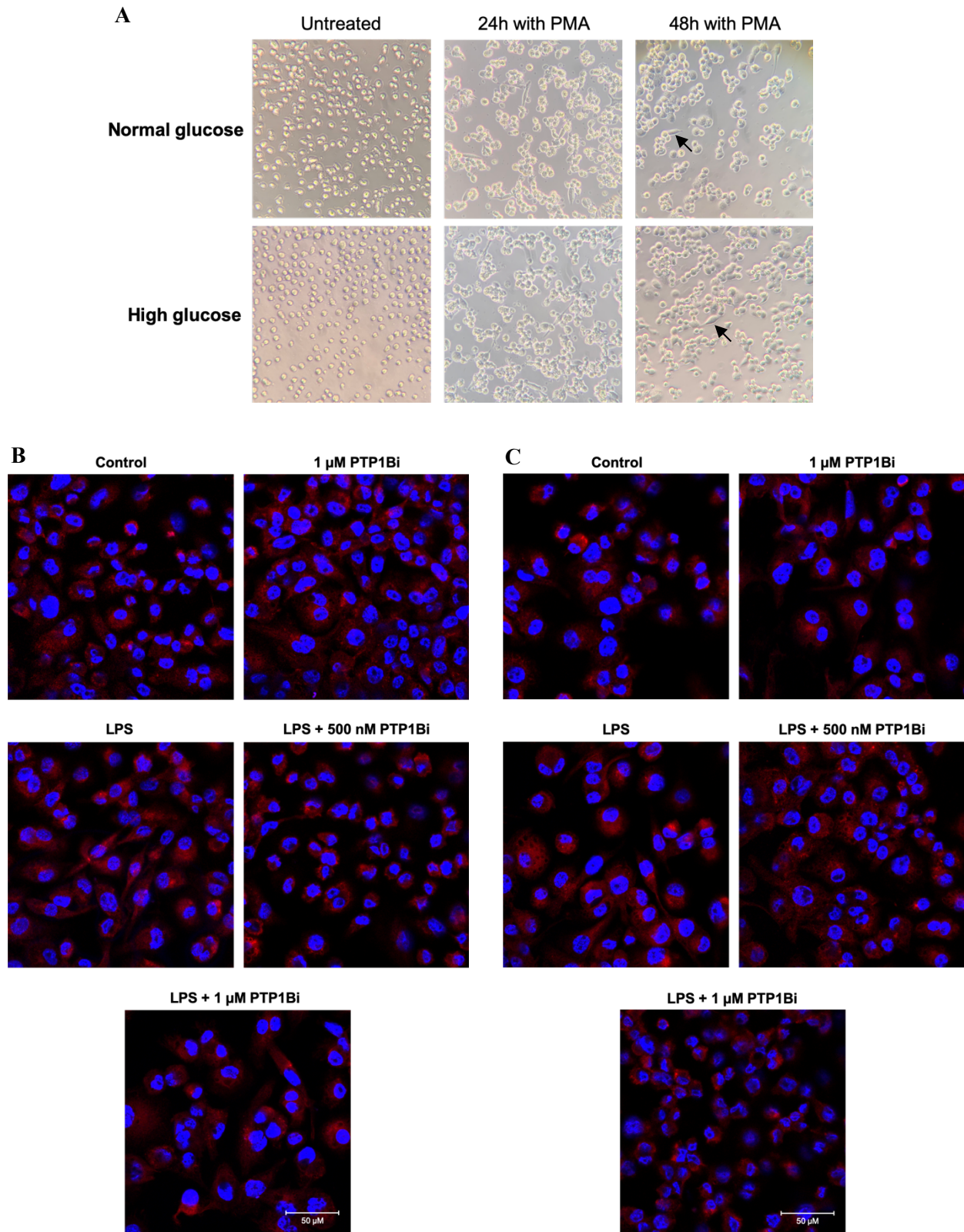
Figure 14 - Macrophage differentiation of THP-1 cell line. (A) Bright field images of THP-1 cells before and after 24h and 48h of PMA stimulation; it is possible to see changes and enlargement of the cytoplasm during the two days of differentiation, with 200x magnification. The black arrow indicates a differentiated cell with adherent and flattened morphology. (B) Representative 400x magnification images of THP-1 cells grown in normal or (C) high glucose stained with CD68 after all treatments, showing that the

differentiation was successful in both conditions. DAPI (nuclei, blue), CD68 (macrophage differentiation marker, red); scale bar is 50 μm.

3.1.2. MSI-1436 did not affect THP-1 cell viability under LPS-induced inflammatory conditions

Bacterial lipopolysaccharides, also known as LPS, is an endotoxin present, in large number, in the outer-membrane of Gram-negative bacteria [189]. LPS can promote cytotoxicity through the induction of high levels of oxidative stress in cultured cells [190].

MSI-1436, or Trodusquemine, is a naturally occurring aminosterol currently in clinical trials for the treatment of cancer, obesity, diabetes and other diseases [154], [191]. This PTP1B inhibitor is well tolerated by patients and seems to have a cytostatic instead of cytotoxic effect [153], [191].

Thus, in order to determine whether LPS has a strong cytotoxic effect and to confirm the low cytotoxicity of MSI-1436, THP-1 cells were differentiated into macrophages and maintained untreated (control) or incubated with 500 nM or 1 μM of PTP1Bi and/or 1 μg/mL of LPS during 24h. The cell viability was determined by the MTT assay. The influence of HG on cells has also been evaluated since there are reports that HG can promote oxidative stress that is toxic to cells [193].
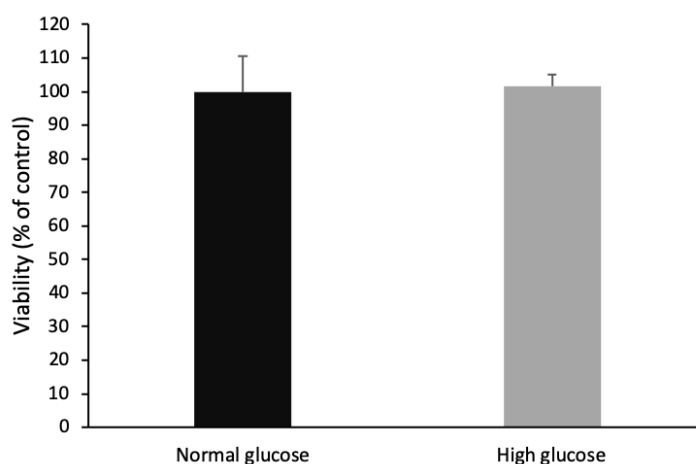
Figure 15 - Effect of high glucose concentration (25 mM) on THP-1 cell viability. THP-1 cells were grown in normal or high glucose concentration and its viability was determined by the MTT assay. High glucose concentration seems to not affect the viability of THP-1 cells when compared to normal glucose concentration. For statistical evaluations a student t-test was performed, and no statistical differences were observed. The results are presented as percentage of viable cells relatively to the normal glucose and data are presented as mean ± SEM (*n*=2).
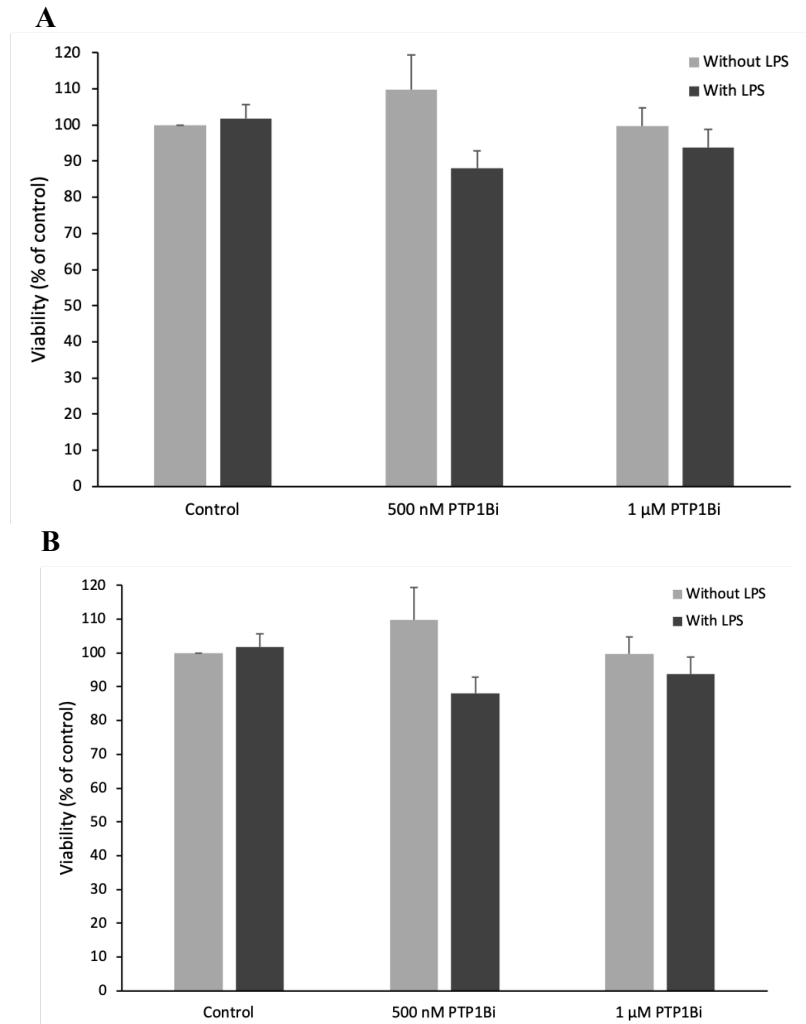
Figure 16 - Effect of LPS and PTP1Bi on THP-1 cell viability. Cells were grown in (A) normal or (B) high glucose concentration and maintained untreated (control) or incubated with 500 nM or 1 μM of PTP1Bi and/or 1 μg/mL of LPS during 24h and the viability of cells was determined by the MTT assay. Neither LPS nor PTP1Bi significantly affected the viability of cells grown in normal or high glucose. For statistical evaluations a one-way ANOVA, followed by a Newman-Keuls post-test, was performed, and no statistical differences were observed. The results are presented as percentage of viable cells relatively to the control and data are represented as mean ± SEM (*n*=6).

HG did not affect cell's viability when compared to NG (101.65 ± 3.36%) (**Figure 15**). Therefore, contrary to observations in other cell types, high glucose concentrations are neither harmful nor toxic to THP-1 cells, under these conditions.

Both PTP1Bi concentrations did not alter THP-1 viability of cells grown in NG or HG (**Figure 16**). In normoglycemic conditions (**Figure 16A**), PTP1Bi did not affect viability when cells were treated with 500 nM (109.70 ± 9.65%) or 1 μM of PTP1Bi (99.75 ± 4.87%). In addition, in HG conditions (**Figure 16B**), 500 nM or 1 μM of PTP1Bi did not significantly alter viability of cells when compared to control, to 94.84 ± 7.24 % and 94.50 ± 6.31%, respectively.

In control cells, NG with LPS during 24h did not change the viability of the cells (101.70 ± 3.94%), however, HG with LPS seems to slightly decrease the cell's viability (87.16 ± 4.19%). THP-1 cells were also incubated with LPS and 500 nM or 1 µM of PTP1Bi for 24h. Both NG and HG grown cells treated with LPS and 500 nM or 1 µM showed a decrease in cell's viability. In normoglycemic conditions, the viability of cells treated with LPS and 500 nM of PTP1Bi decreased to 87.99 ± 4.89% and the viability of cells treated with LPS and 1 µM of PTP1Bi decreased to 93.68 ± 5.18% when compared to control (**Figure 16A**). In turn, HG decreased viability to 82.18 ± 9.32% in cells treated with LPS and 500 nM and to 84.22 ± 6.09% in cells treated with LPS and 1 µM of PTP1Bi (**Figure 16B**).

Taking into account all the data, it is possible to conclude neither LPS nor PTP1Bi significantly affect the viability of THP-1 cells under normal or high glucose conditions.

3.1.3. High glucose increased PTP1B expression in THP-1 cells

PTP1B expression has been shown to increase under diabetic condition [120]. It is also known that some cell types in high glucose conditions show increased expression of this protein [194], [195]. Furthermore, it was also demonstrated that microglial cells have increased PTP1B expression after LPS stimulation [147]. Thus, to test whether elevated glucose levels and LPS stimulation lead to an increase in PTP1B expression in THP-1 macrophages and if this expression is affected by PTP1B inhibition, PTP1B expression was evaluated by qRT-PCR (**Figure 17A**) and by western blot (**Figure 17B and 17C**). THP-1 cells were cultured in NG and HG medium and differentiated into macrophages, and then incubated with LPS and/or PTP1Bi for 24h.

HG slightly reduced PTP1B mRNA expression levels (0.86 ± 0.12-fold change from control) when compared to normoglycemic conditions, while, PTP1B protein levels were significantly increased under HG conditions (1.44 ± 0.14) when compared with NG conditions ($p<0.05$, $n=3$).

Under NG, the expression of PTP1B seems to be increased by LPS stimulation. The PTP1B mRNA levels were increased (1.29 ± 0.16-fold) when compared with control. This increase was also observed in PTP1B protein levels to 1.31 ± 0.12 when compared with control. In HG, the PTP1B mRNA levels were also increased after LPS treatment to 1.49 ± 0.45-fold comparing to HG without LPS (0.86 ± 0.12-fold), however the PTP1B protein levels slightly decrease to 1.22 ± 0.20 when compared to control (1.44 ± 0.14). Although none of these results are statistically significant, it indicates that LPS, as occurs in other cell types, tends to increase PTP1B expression.

The PTP1Bi treatment lead to a small decrease in PTP1Bi mRNA levels to 0.84 ± 0.20-fold in NG and 0.76 ± 0.10-fold in HG when compared to control, but PTP1Bi treated cells appear to have a small increase in the protein levels to 0.94 ± 0.21 in NG and a small decrease to 1.36 ± 0.17 in HG. When cells were treated with both LPS and 500 nM of PTP1Bi, in NG the mRNA

levels were increased to 2.58 ± 1.53-fold and in HG to 1.07 ± 0.23. In NG, LPS and 500 nM of PTP1Bi increased PTP1B protein levels to 1.29 ± 0.12 when compared to control but in HG, the protein level decreased to 0.90 ± 0.59 comparing to control. The treatment with both LPS and 1 μM of PTP1Bi, when compared to control, does not appear to influence PTP1B mRNA levels in NG (1.06 ± 0.14-fold) and in HG, LPS and 1 μM of PTP1Bi increased the PTP1B mRNA levels to 1.23 ± 0.20-fold. The PTP1B protein level had an increase of 1.83 ± 0.40 when compared to control but in HG the results showed a decrease to 0.61 ± 0.21. However, none of the changes were statistically significant, which indicates that PTP1B inhibition does not appear to alter significantly PTP1B expression under NG and HG conditions.

A

B
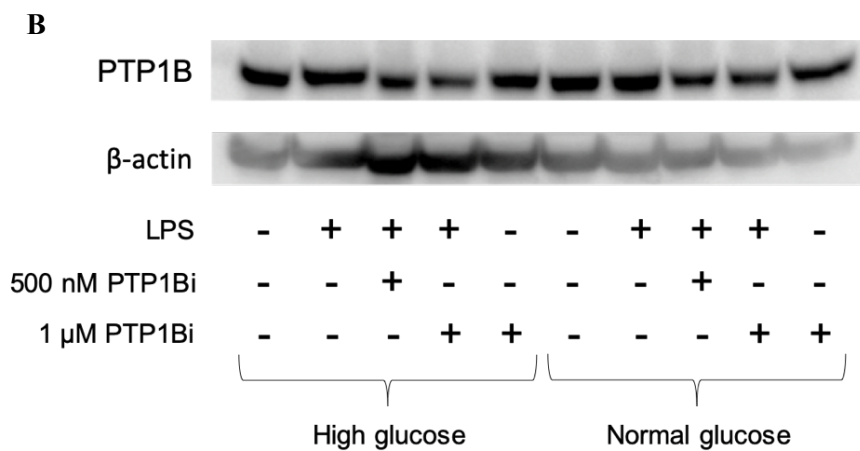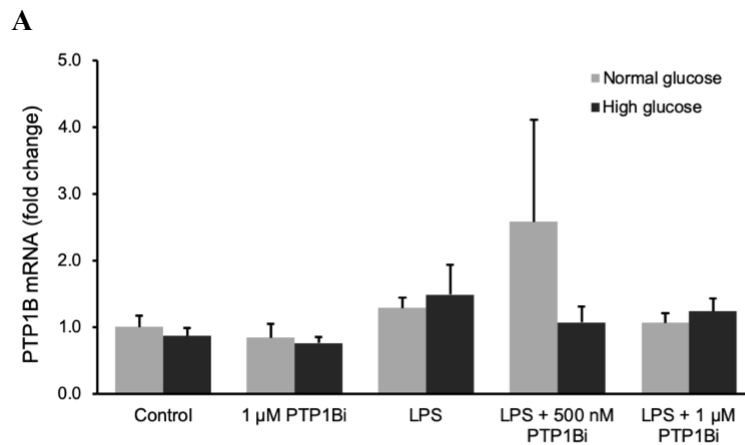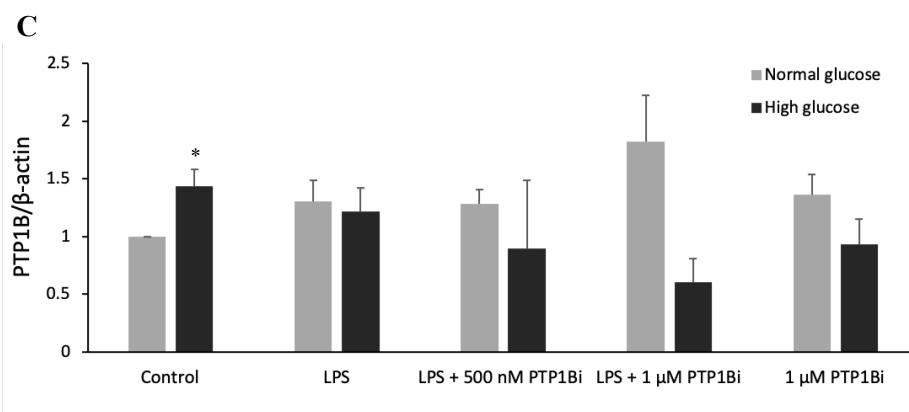
Figure 17 - Effect of PTP1B inhibition on PTP1B expression in THP-1 cells cultured under NG and HG with or without LPS stimuli for 24h. (A) PTP1B mRNA levels in THP-1 cells cultured under NG and HG and untreated or treated with PTP1Bi and/or LPS. (B) Representative Western blot of PTP1B protein expression. β-actin was used as a loadin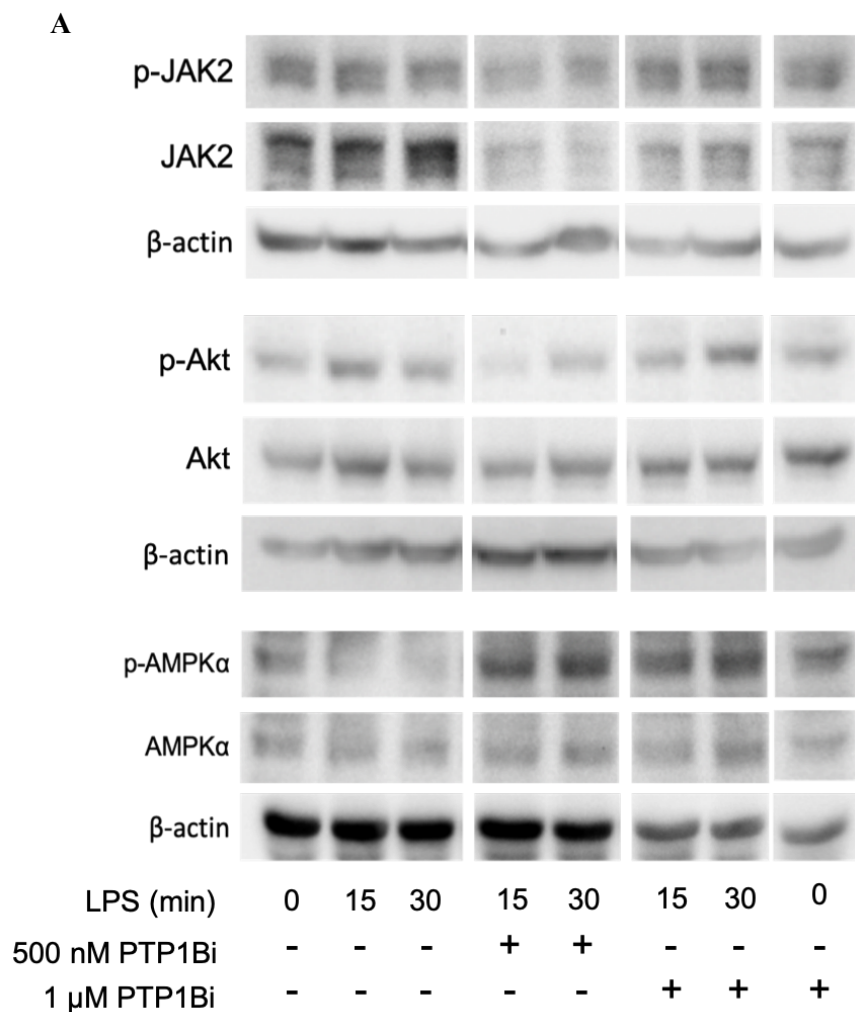g control. (C) Quantification of PTP1B western blot, presented as a ratio of β-actin value. For statistical analysis a one-way ANOVA, followed by a Newman-Keuls post-test, was performed to compare the different conditions in NG and in HG independently, and no statistical differences were observed. A student t-test was performed to compare the NG control condition with the HG control condition. The results are presented as fold change of NG control and data are represented as mean ± SEM (*n*=3). * *p*<0.05, t-test NG control *vs* HG control.

3.1.4. PTP1B inhibition increased phosphorylation of JAK2, PKB/Akt and AMPKα proteins

PTP1B negatively regulates leptin and insulin pathways, dephosphorylating IR and the leptin receptor and its downstream signalling components such as JAK2, PKB/Akt and AMPKα [113]. Thus, the inhibition of PTP1B is expected to increase phosphorylation of these components. To evaluate the PTP1B inhibition and the increase in the phosphorylation of proteins involved in insulin and leptin pathways, THP-1 macrophages were cultured under NG or HG conditions or left untreated (control) or treated with LPS and/or PTP1Bi for 15 or 30 min. Then, the phosphorylation levels of JAK2, PKB/Akt and AMPKα proteins were measured by western blot (**Figure 18A and 19A**).

Under NG conditions, cells treated for 15 or 30 min with LPS showed an increase on p-JAK2 levels when compared to untreated cells (1.46 ± 0.35 and 2.24 ± 1.12, respectively). THP-1 cells treated with LPS together with PTP1Bi, showed increased levels of p-JAK2 by both PTP1Bi concentrations after 15 min of incubation when compared to LPS-induced phosphorylation (**Figure 18B**). The 500 nM of PTP1Bi treatment increased p-JAK2 levels to 1.65 ± 0.38 while the concentration of 1 µM caused an increase to 1.77 ± 0.44. After 30 min of treatment with LPS, 500 nM (1.87 ± 0.48) or 1 µM (1.71 ± 0.45) of PTP1Bi were not able to increase p-JAK2 levels when compared to LPS. In addition, cells treated only with 1 µM of PTP1Bi also demonstrated a small increase on p-JAK2 levels (1.15 ± 0.19). Cells treated with LPS for 15 and 30 min seem not to alter

p-PKB/AKT (0.97 ± 0.16 and 1.00 ± 0.23, respectively) when compared to control. However, these levels demonstrate an increase when cells were treated with 500 nM combined with LPS after 15 min (1.13 ± 0.51) or 30 min (1.40 ± 0.59) of incubation, when compared to LPS treatment (**Figure 18C**). After 30 min of incubation with 1 µM of PTP1Bi and LPS increased p-PKB/AKT levels (1.57 ± 0.46), whereas after 15 min of incubation the level of p-PKB/AKT levels seems not to change with this treatment (0.99 ± 0.25). The treatment with 1 µM of PTP1Bi did not change p-PKB/AKT levels (0.73 ± 0.26). The phosphorylation of AMPKα was not increased by LPS treatment for 15 and 30 min (0.79 ± 0.05 and 0.59 ± 0.03, respectively) relatively to control (**Figure 18D**). After 15 min of incubation, the levels of p-AMPKα were not altered (0.89 ± 0.35) with LPS and 500 nM treatment, however, an increase to 1.14 ± 0.33 with LPS and 1 µM of PTP1Bi was observed. After 30 min of incubation, LPS and 500 nM or 1 µM of PTP1Bi did not alter p-AMPKα (1.04 ± 0.30 and 1.14 ± 0.33, respectively). The treatment with 1 µM of PTP1Bi increased AMPKα phosphorylation levels to 1.15 ± 0.32 when compared to control.
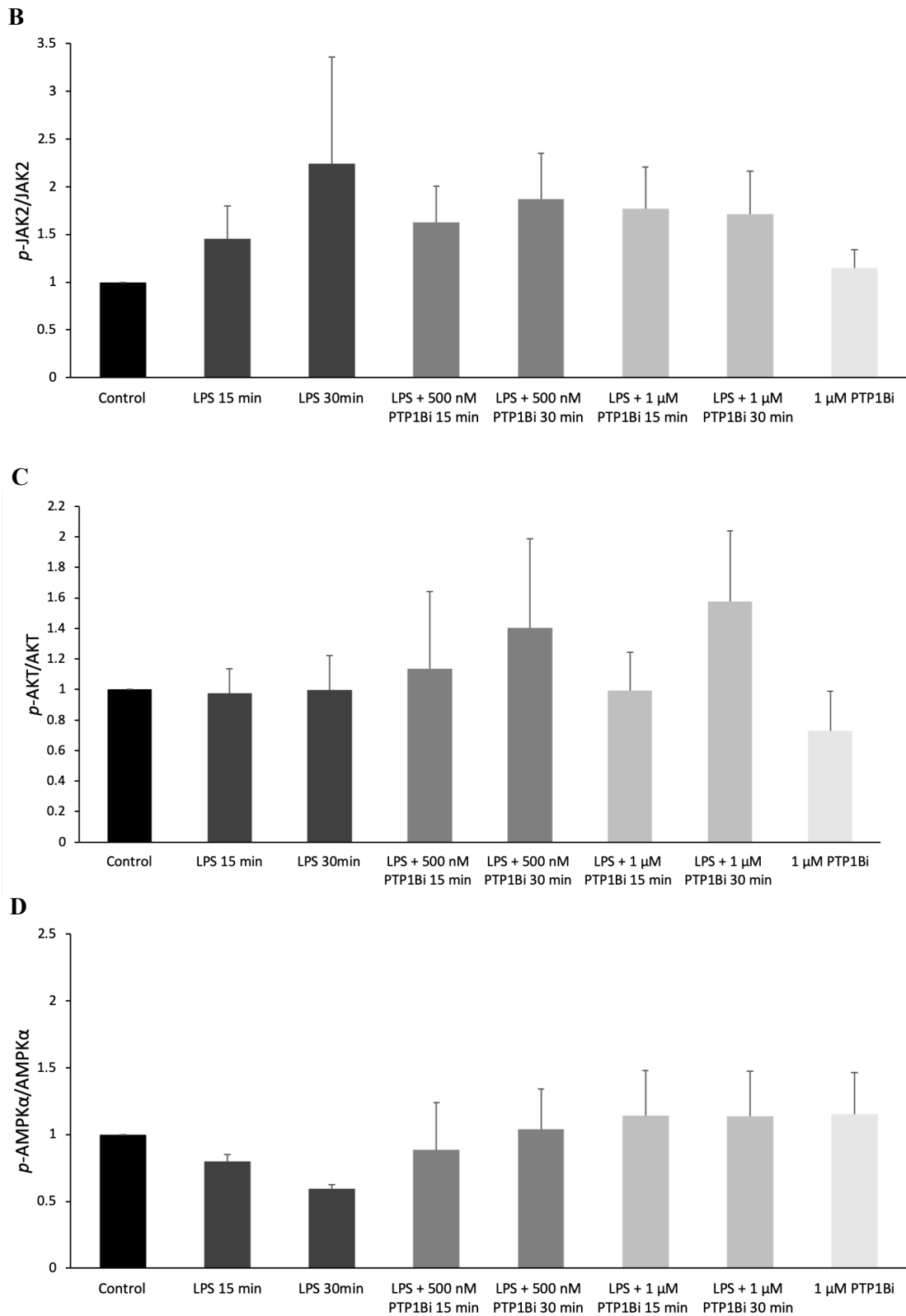
Figure 18 - Effect of PTP1B inhibition on JAK2, PKB/Akt and AMPKα phosphorylation in THP-1 cells cultured under NG and maintained untreated (control) with or without LPS stimuli for 15 or 30 minutes. (A) Representative Western blot of p-JAK2, p-PKB/Akt and p-AMPKα and total JAK2, PKB/Akt and AMPKα expression. β-actin was used as a loading control. (B) Quantification of p-JAK2, (C) p-PKB/Akt and (D) p-AMPKα, presented as a ratio of total protein and β-actin values. For statistical analysis a one-way ANOVA,

Under HG conditions, cells treated for 15 or 30 min with LPS also present an increase on p-JAK2 levels when compared to untreated cells (1.42 ± 0.76 and 1.70 ± 0.63, respectively). However, cells treated with LPS together with PTP1Bi did not increase the p-JAK2 levels when compared to LPS-induced phosphorylation (**Figure 19B**). Cells treated for 15 min with LPS and 500 nM of PTP1Bi showed a p-JAK2 level of 0.87 ± 0.41 and cells treated for 30 min showed a level of 0.79 ± 0.42, while cells treated with LPS and 1 μM of PTP1Bi for 15 min showed a p-JAK2 level of 0.79 ± 0.15 and cells treated for 30 min showed a level of 0.72 ± 0.15, relatively to only LPS. Furthermore, the levels of p-JAK2 did not increase in cells treated with only 1 μM of PTP1Bi (0.65 ± 0.00). The level of PKB/Akt phosphorylation in cells treated with LPS for 15 (0.89 ± 0.23) and 30 min (0.79 ± 0.09) did not increase when compared to control (**Figure 19C**). However, these levels demonstrated an increase when treated with LPS and PTP1Bi for either 15 or 30 min. After 15 min of incubation with LPS and 500 nM of PTP1Bi the phosphorylation levels of PKB/Akt were increased to 1.44 ± 0.10 and the incubation with LPS and 1 μM of PTP1Bi increased the levels to 1.34 ± 0.25 comparing to LPS-induced phosphorylation. After 30 min of treatment, the levels increased to 0.99 ± 0.34 and to 1.35 ± 0.10, respectively. The treatment with 1 μM of PTP1Bi alone did not increase PKB/Akt phosphorylation levels (0.91 ± 0.27). Cells treated with LPS, for 15 or 30 min, did not change AMPKα phosphorylation level (1.08 ± 0.23 and 0.70 ± 0.12, respectively) when compared to control (**Figure 19D**). The LPS and 500 nM of PTP1Bi treatment for 15 (0.58 ± 0.21) and 30 min (0.54 ± 0.08) did not increase p-AMPKα levels when compared to LPS. Regarding the LPS and 1 μM of PTP1Bi treatment for 15 min, these levels also did not suffer an increase (0.83 ± 0.09) but cells treated for 30 min with these compounds showed an increase in p-AMPKα levels to 1.21 ± 0.05. As observed in NG, the treatment with only 1 μM of PTP1Bi increased the p-AMPKα levels to 1.77 ± 0.70 when compared to control.

Although not statistically significant, these results indicate that PTP1B inhibition tends to increase the phosphorylation of key proteins in the signalling pathways where PTP1B is involved.

A

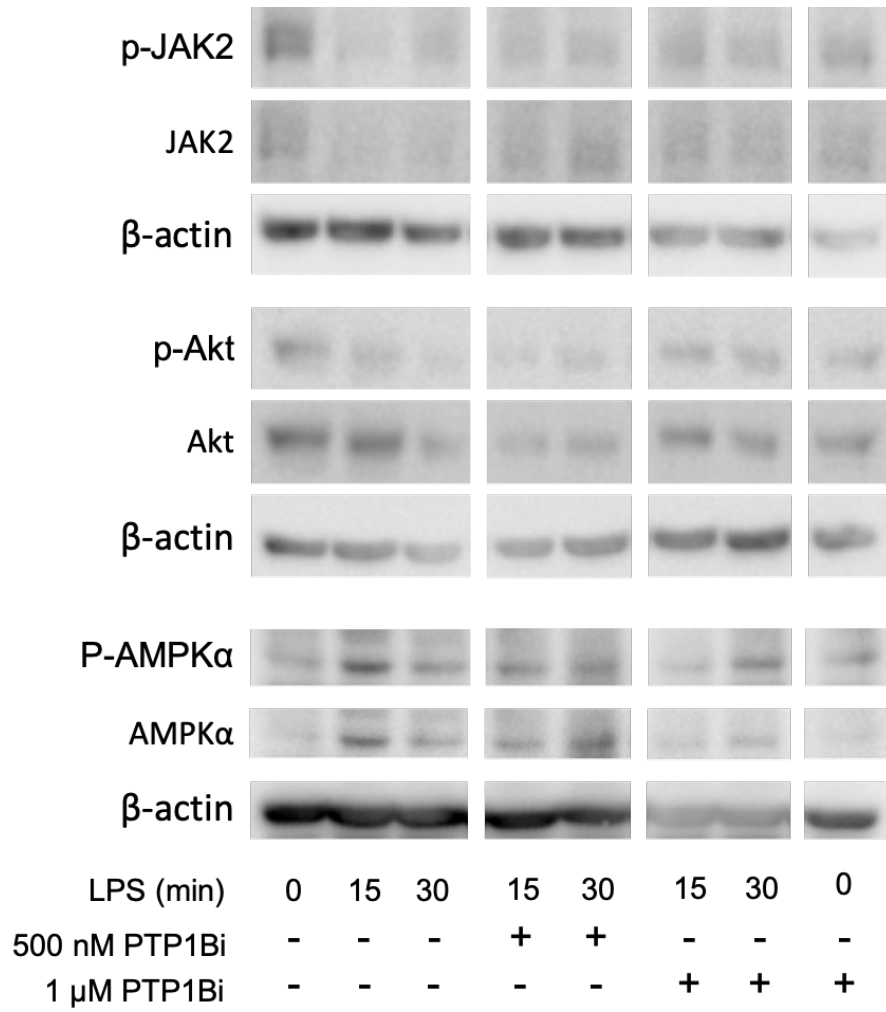|								
LPS (min)	0	15	30	15	30	15	30	0
500 nM PTP1Bi	-	-	-	+	+	-	-	-
1 µM PTP1Bi	-	-	-	-	-	+	+	+

B
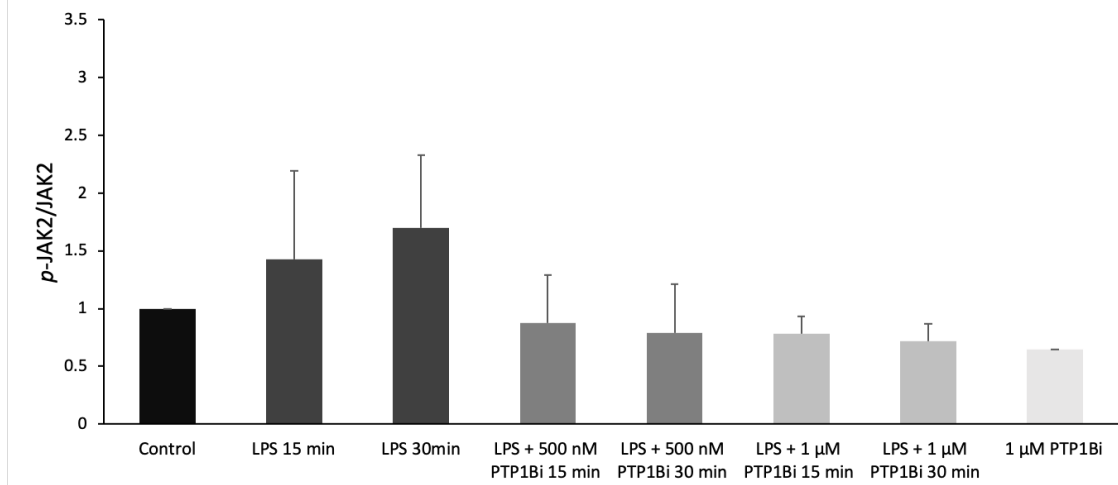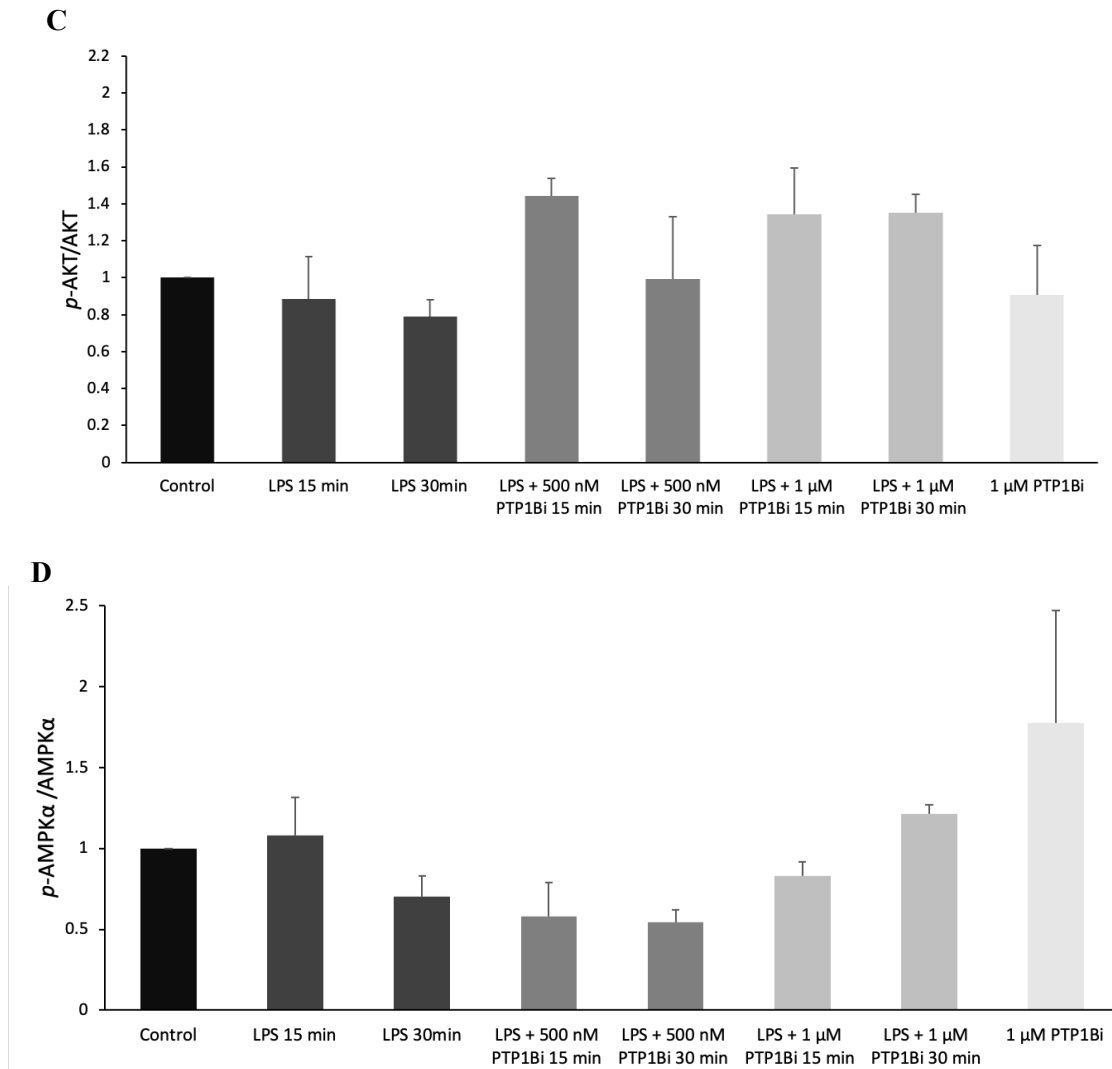
Figure 19 - Effect of PTP1B inhibition on JAK2, PKB/Akt and AMPKα in THP-1 cells cultured under HG and maintained untreated (control) with or without LPS stimuli for 15 or 30 minutes. (A) Representative Western blot of p-JAK2, p-PKB/Akt and p-AMPKα and total JAK2, PKB/Akt and AMPKα expression. β-actin was used as a loading control. (B) Quantification of p-JAK2, (C) p-PKB/Akt and (D) p-AMPKα, presented as a ratio of total protein and β-actin values. For statistical analysis a one-way ANOVA, followed by a Newman-Keuls post-test, was performed and no statistical differences were observed. The results are presented as fold change of control and data are represented as mean ± SEM (*n*=3).

3.1.5. PTP1B inhibition decreased the pro-inflammatory environment via modulation of macrophage phenotype under normoglycemic and high glucose conditions

Macrophages are present in all wound healing phases playing a key role in essential functions [14]. A depletion of macrophages during the inflammatory or the proliferative phase do not allow the wounds to heal [97]. Thus, when the macrophage function is impaired, wound healing is disrupted [99], [107]. One of the most important functions of macrophages during wound healing is the resolution of inflammation, and at the final stages of wound healing process M1 macrophages are converted into M2 macrophages releasing anti-inflammatory mediators that will promote wound closure [98]. In chronic wounds, such as diabetic ulcers, macrophages are known to secrete a lower number of factors essential to the healing process, and the conversion of the pro-inflammatory M1 macrophages into anti-inflammatory M2 macrophages does not occur delaying the resolution of the inflammatory phase, and the accumulation of M1 macrophages in the wound site leads to a pro-inflammatory environment [98], [103], [107].

One of the hypotheses of this work is that PTP1Bi treatment can reduce the pro-inflammatory cell environment promoting the conversion of M1 into M2 macrophages, as well as the release of cytokines and growth factors essential for wound healing. To test this hypothesis, THP-1 macrophages were cultured under either NG or HG conditions and left untreated (control) or treated with LPS and/or PTP1Bi for 24h, then the number of M1 and M2 macrophages was evaluated. For the detection of M1 macrophages, immunolocalization of CD68 (pan-macrophage marker, red) and TNF-α (M1 specific marker, green) was used, and CD68 (green) and CD163 (M2 specific marker, red) immunolocalization was used for M2 detection.

Initially, the effect HG conditions on macrophage polarisation was analysed. It is known that macrophages cultured in HG conditions are known to undergo M1-like inflammatory polarisation and the same is observed in patients with hyperglycaemia [196]. This effect of HG on macrophages polarisation was observed in THP-1 cells (**Figure 20A**), where HG increased M1 macrophages to 107. 62 ± 2.68% when compared to NG (100%) (**Figure 20B**). As expected, the LPS treatment increased the M1 number of cells both under NG and HG conditions. In NG, LPS increased M1 macrophages to 121.98 ± 8.11% while in HG M1 macrophages significantly increased to 131.63 ± 8.38% ($p<0.05$, n=4). Regarding M2 macrophages, it seems to occur a slight increase in their number in HG (131.37 ± 27.87%) when compared to NG (100%) (**Figure 20C and D**). After LPS treatment, it was also observed an increase in M2 number to 157.45 ± 19.18% in NG and to 166.76 ± 28.33% in HG.

A

TNF-α CD68 TNF-α + CD68 + DAPI

NG Control

HG Control

NG LPS

HG LPS

B

64
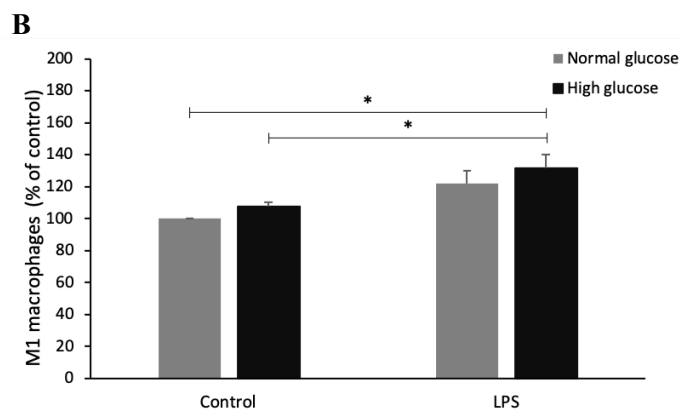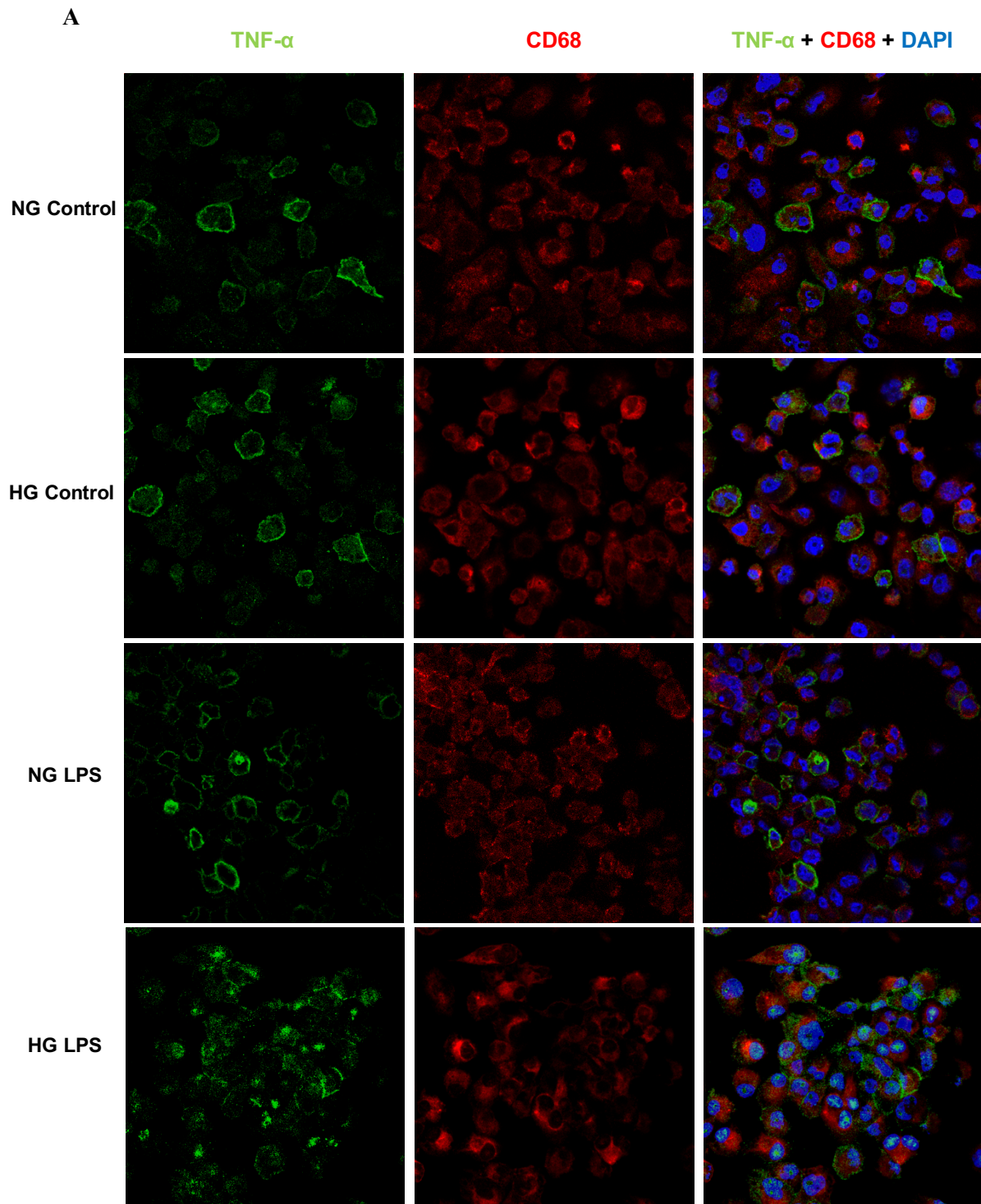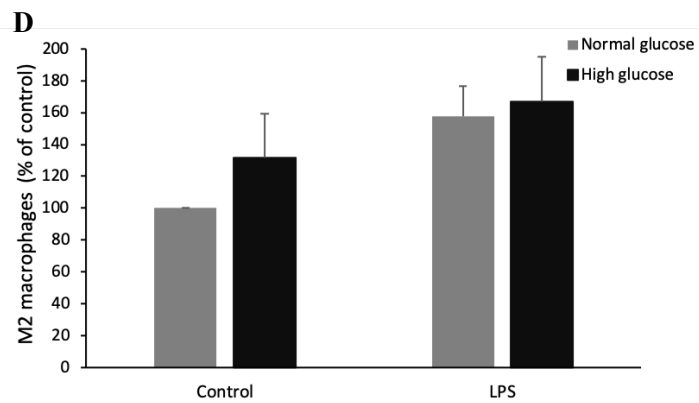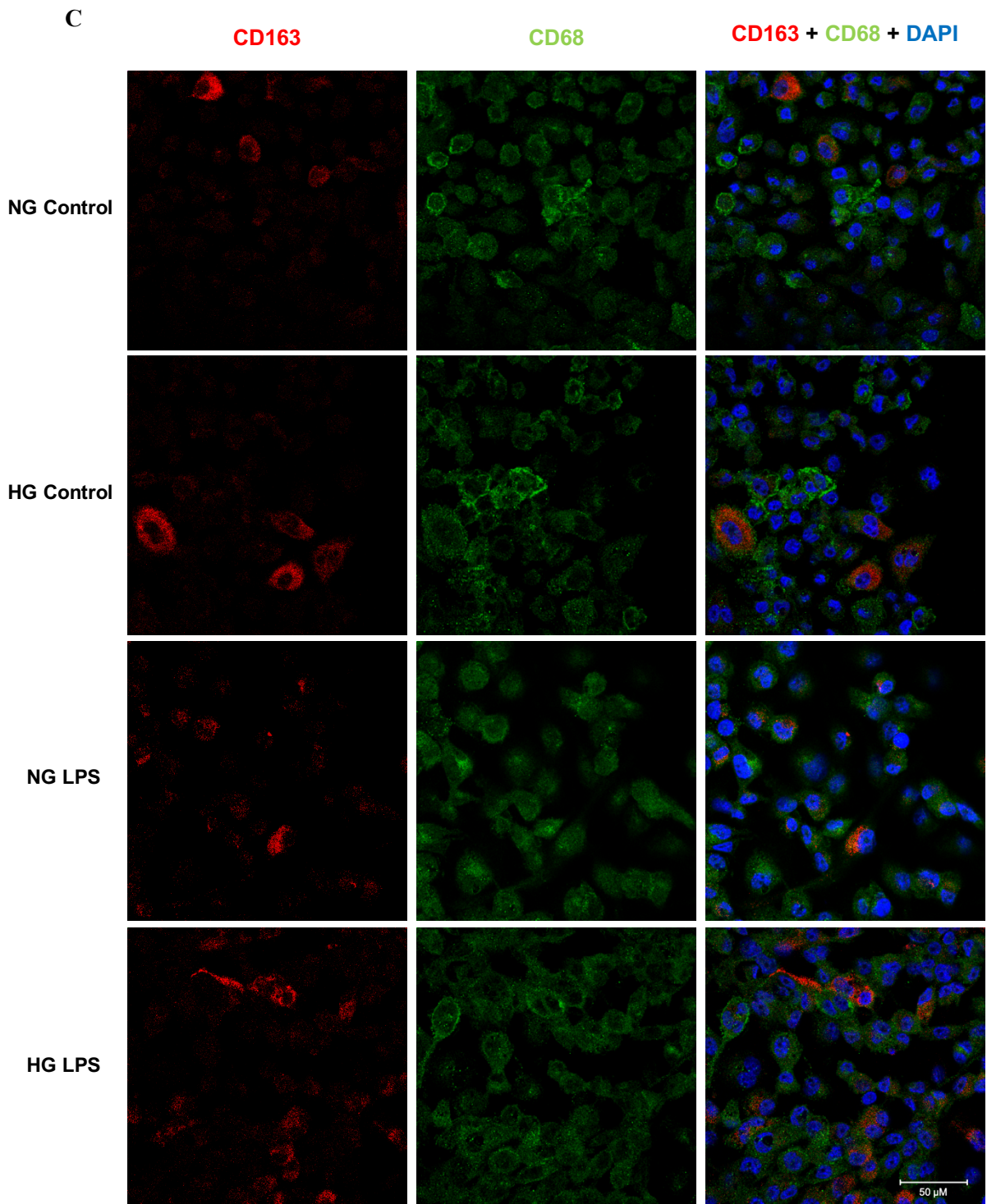
Figure 20 - Effect of HG and LPS on macrophage polarisation of differentiated THP-1 cells. (A) Representative 400x magnification images of the macrophage marker proteins CD68 (pan-macrophage

marker, red) and TNF-α (M1 specific marker, green). (B) Representative 400x magnification images of the macrophage marker proteins CD68 (green) and CD163 (M2 specific marker, red). (C) Quantification of M1 macrophages (CD68 + TNF-α double-positive cells). (D) Quantification of M2 macrophages (CD68 + CD163 double-positive cells). For statistical analysis a one-way ANOVA, followed by a Newman-Keuls post-test, was performed. Nuclei were stained with DAPI (blue). Scale bar is 50 μm. The results are presented as percentage of NG control cells and represented as mean ± SEM (n=4). * p<0.05.

Under NG conditions, the PTP1B inhibitory effect on the number of M1 macrophages was evaluated through immunofluorescence (**Figure 21A**). PTP1B inhibition decreased the M1 macrophage number under NG conditions. As previously described, the higher number of M1 cells was obtained with LPS treatment, under inflammatory conditions. The treatment LPS + 500 nM of PTP1Bi decreased M1 macrophages to 111.74 ± 9.94% whereas the LPS + 1 μM of PTP1Bi treatment further decreased the number to 100.74 ± 9.22%, when compared to LPS treated cells (121.98 ± 8.11%) (**Figure 21C**). Therefore, PTP1B inhibition seems to cause a reduction in M1 cell number in a PTP1Bi concentration-dependent manner. In basal condition, without inflammatory stimulus (LPS), the treatment with 1 μM of PTP1Bi also caused a decrease in the M1 macrophages to 96.30 ± 7.30% when compared to control.

The number of M2 macrophages was also evaluated under similar conditions (**Figure 21B**). The effect of PTP1B was also evaluated under inflammatory conditions. Under inflammatory conditions, it was observed that 500 nM of PTP1Bi increased significantly M2 macrophages to 231.05 ± 13.57% (p<0.01, n=4), as well as the 1 μM of PTP1Bi significantly increased M2 macrophages (231.87 ± 18.07%) (p<0.01, n=4), when compared to LPS treatment (157.45 ± 19.20%) (**Figure 21D**). PTP1B inhibition under basal conditions, showed an increase in M2 macrophages to 141.52 ± 52%, when compared to control.

The effect of PTP1B inhibition on the number of M1 and M2 macrophages was also tested in THP-1 cells cultured under HG. Similarly to NG conditions, in the presence of inflammatory conditions, the treatment with 500 nM decreased M1 macrophages to 112.19 ± 5.34% and the 1 μM of PTP1Bi significantly decreased M1 macrophages to 101.70 ± 9.49% (p<0.05, n=4), when compared to cells treated with only LPS (131.63 ± 8.38%) (**Figure 22A and C**).

In basal conditions, without LPS incubation, the treatment with 1 μM of PTP1Bi promoted a decrease in M1 macrophages (82.75 ± 7.29%) when compared to control (107.62 ± 2.68%). This can be extremely important, since HG conditions lead to an increase of the M1 cell phenotype, thus PTP1B inhibition can contribute to a reduction of hyperglycaemia-induced inflammation.

A

TNF-α	CD68	TNF-α + CD68 + DAPI

Control

1 µM PTP1Bi

LPS

LPS + 500 nM
PTP1Bi

LPS + 1 µM
PTP1Bi

50 µM

B

	CD163	CD68	CD163 + CD68 + DAPI
Control			
1 µM PTP1Bi			
LPS			
LPS + 500 nM PTP1Bi			
LPS + 1 µM PTP1Bi			

50 µM
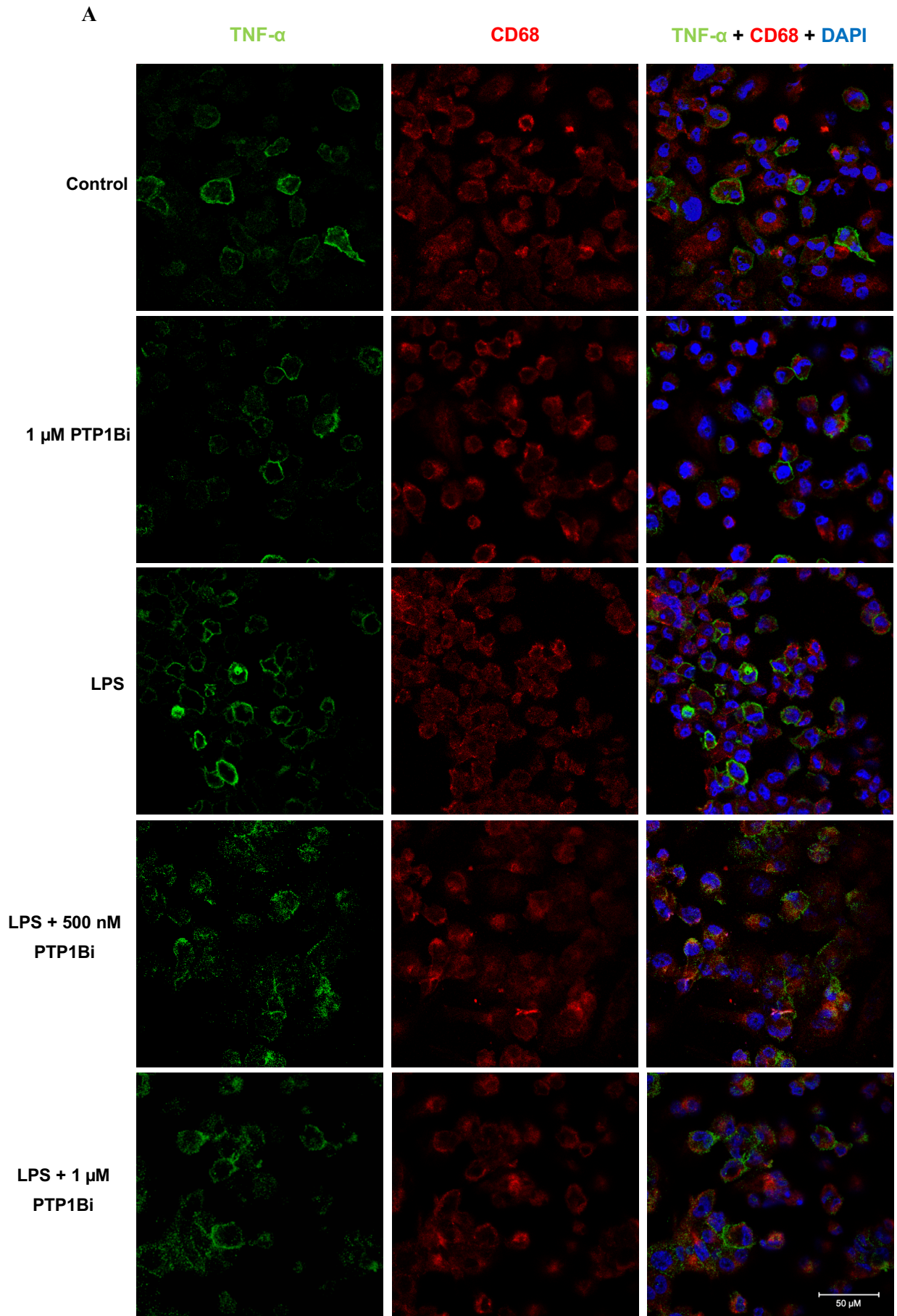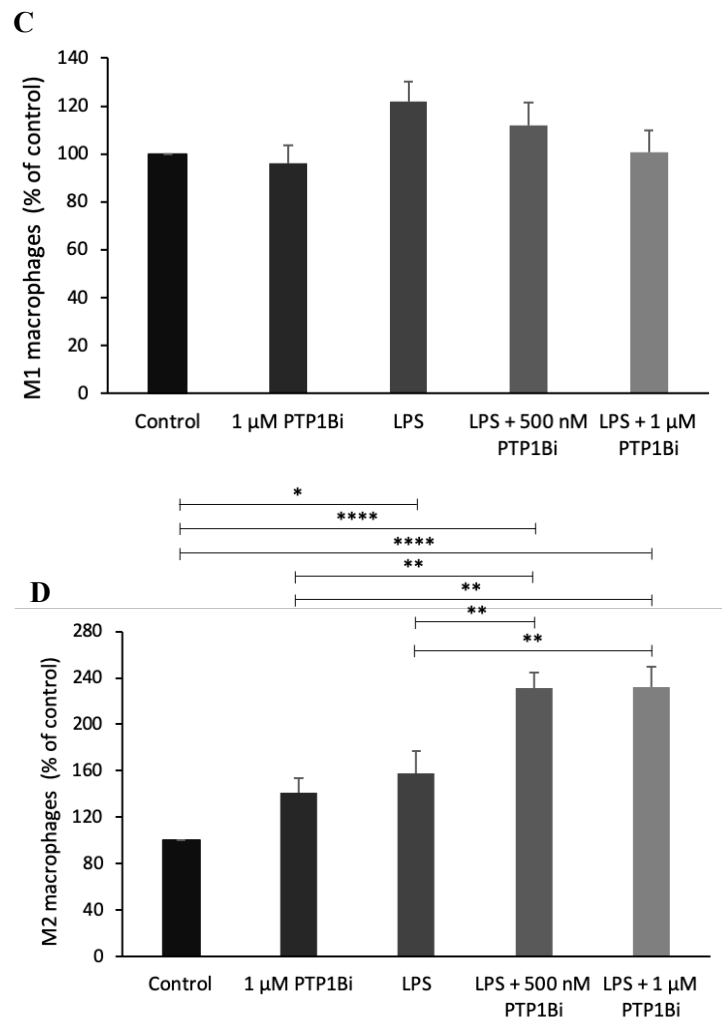
Figure 21 - Effect of PTP1B inhibition on macrophage phenotypes of differentiated THP-1 cells cultured under NG conditions with or without LPS stimuli for 24h. Treatment with PTP1Bi shows a decreased number of M1 macrophages and an increased number of M2 macrophages. (A) Representative 400x magnification images of the macrophage marker proteins CD68 (red) and TNF-α (green). (B) Representative 400x magnification images of the macrophage marker proteins CD68 (green) and CD163 (red). (C) Quantification of M1 macrophages (CD68 + TNF-α double-positive cells). (D) Quantification of M2 macrophages (CD68 + CD163 double-positive cells). For statistical analysis a one-way ANOVA, followed by a Newman-Keuls post-test, was performed. Nuclei were stained with DAPI (blue). Scale bar is 50 μm. The results are presented as percentage of NG control cells and represented as mean ± SEM (*n*=4). * *p*<0.05, ** *p*<0.01, **** *p*<0.0001.
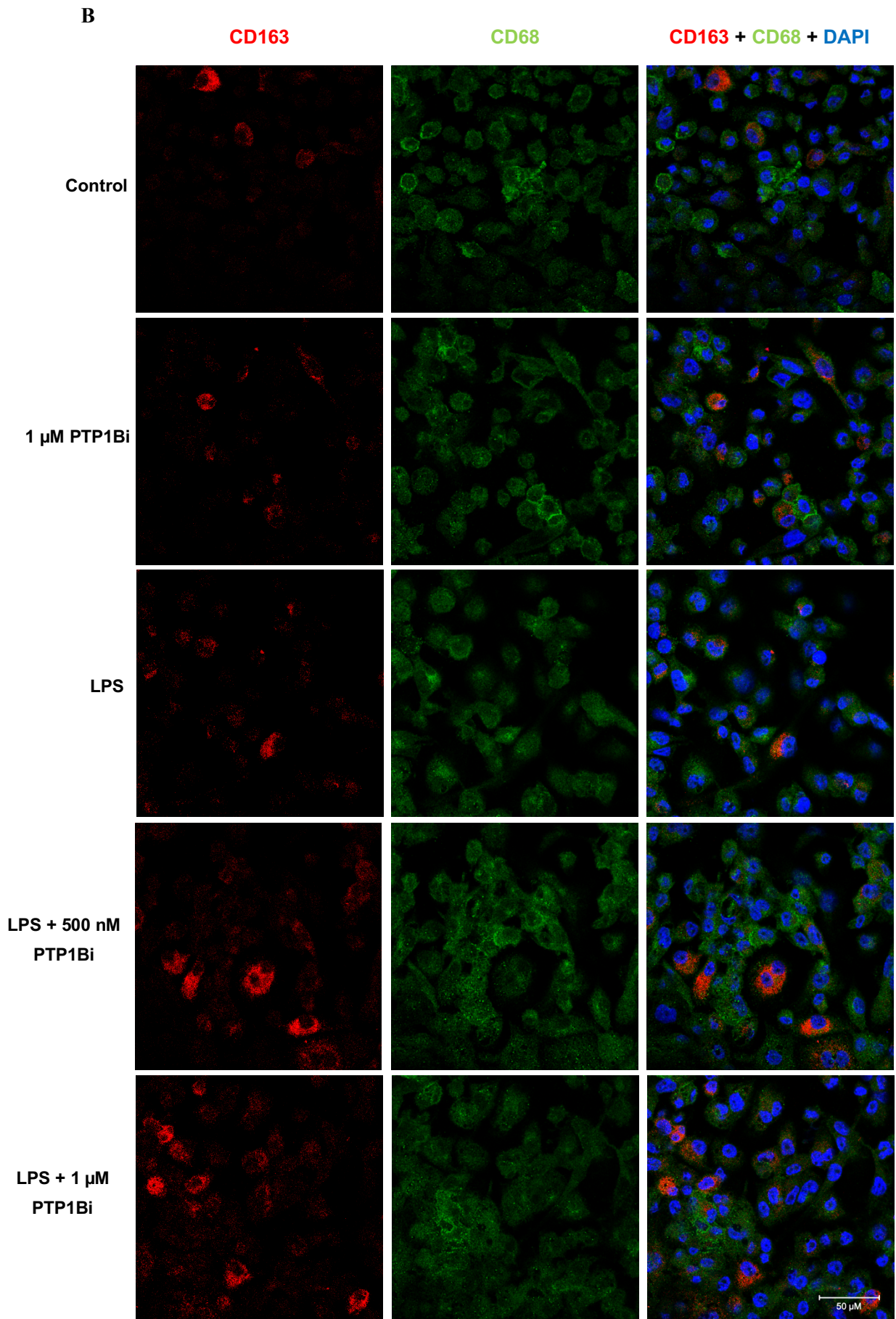
In addition, as observed in NG, PTP1B inhibition also had a similar effect on M2 macrophages under HG conditions (**Figure 22B**). The effect of PTP1B was evaluated under inflammatory conditions and 500 nM of PTP1Bi showed an increase in M2 macrophages to 213.08 ± 33.41%. Moreover, the treatment with 1 µM of PTP1Bi also resulted in an increase in M2 macrophages (246.39 ± 26.49%), when compared to LPS treatment only (166.76 ± 28.33%) (**Figure 22D**). Also, PTP1B inhibition under basal (no LPS) HG conditions increased M2 macrophages to 146.50 ± 28.23% when compared to control (131.37 ± 27.87%).

Taking all this into account, inhibition of PTP1B can promote changes of the pro-inflammatory M1 macrophages into anti-inflammatory M2 macrophages, decreasing the number of accumulated M1 macrophages in chronic diabetic wounds and reducing the pro-inflammatory environment.

Macrophages from diabetic patients, as well as macrophages cultured under HG conditions, show an increase in TNF-α production [197]. Although TNF-α is very important during the proliferative phase of wound healing, exaggerated levels of this pro-inflammatory cytokine promote chronic inflammation and it is related to impaired healing [198]. This increase in TNF-α levels is associated with the presence of a larger number of M1 macrophages, since they are responsible for most of this cytokine production [197], [198]. Macrophages release large amounts of TNF-α when are exposed to inflammatory stimulus, like LPS**.** To investigate the role of PTP1B inhibition in TNF-α production, THP-1 cells cultured under NG or HG were differentiated in macrophages and treated with LPS and/or PTP1Bi for 24h and TNF-α was determined by immunocytochemistry.

As expected, cells cultured in HG had a small increase of TNF-α levels (**Figure 23A and B**). HG conditions increased TNF-α levels to 105.65 ± 16.17% comparing to NG (100%) (**Figure 23B**). In addition, when cells were treated with an inflammatory stimuli (LPS) TNF-α levels were increased. In NG, LPS increased TNF-α levels to 147.43 ± 15.55%, and in HG the incubation with LPS increased the levels of TNF-α to 169.27 ± 30.59%.

Under NG and inflammatory conditions, the treatment with LPS and 500 nM or 1 µM of PTP1Bi decreased TNF-α levels (**Figure 24A**). TNF-α levels observed in cells treated with 500 nM were reduced to 116.08 ± 26.45% and in cells treated with 1 µM to 115.28 ± 15.82%, lower values than those were observed in cells treated with LPS (147.43 ± 15.55%) (**Figure 24B**). Under basal conditions, without LPS treatment, cells treated with 1 µM PTP1Bi also showed a slight decrease in TNF-α levels to 89.49 ± 7.08% when compared to control (100%).

PTP1B inhibition decreased TNF-α levels in HG conditions. TNF-α levels, under inflammatory conditions (**Figure 24C**), were decreased with 500 nM of PTP1Bi to 105.12 ± 28.08%. Also, 1 µM of PTP1Bi decreased TNF-α levels to 114.78 ± 28.69% (**Figure 24D**) when compared to LPS (169.27 ± 30.59%). As observed in NG, HG cultured cells treated only with 1 µM of PT1Bi also decreased TNF-α values to 68.40 ± 31.07% comparing to control (105.65 ± 16.17%).

A

	TNF-α	CD68	TNF-α + CD68 + DAPI
Control			
1 μM PTP1Bi			
LPS			
LPS + 500 nM PTP1Bi			
LPS + 1 μM PTP1Bi			

B

| CD163 | CD68 | CD163 + CD68 + DAPI |

Control

1 μM PTP1Bi

LPS

LPS + 500 nM PTP1Bi

LPS + 1 μM PTP1Bi

50 μM
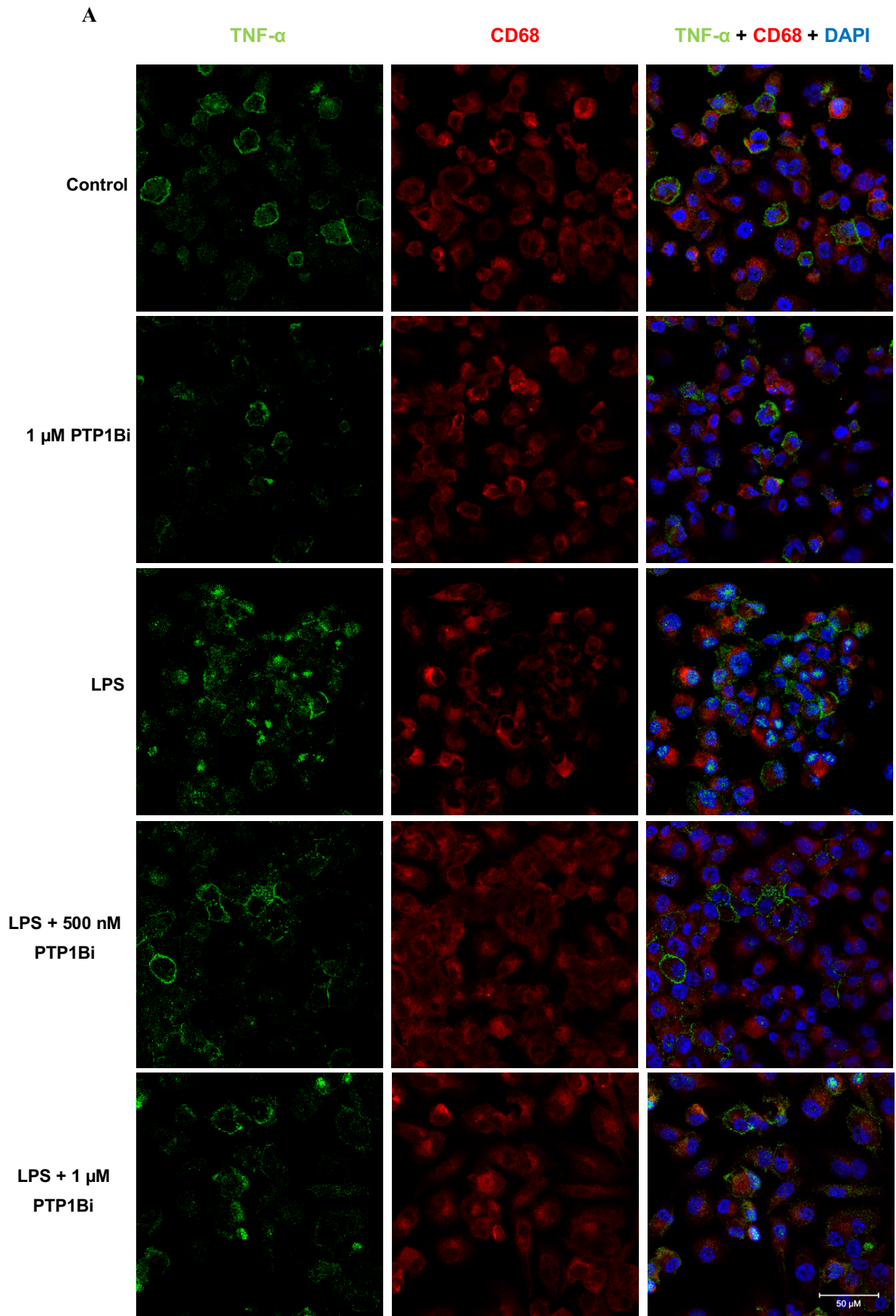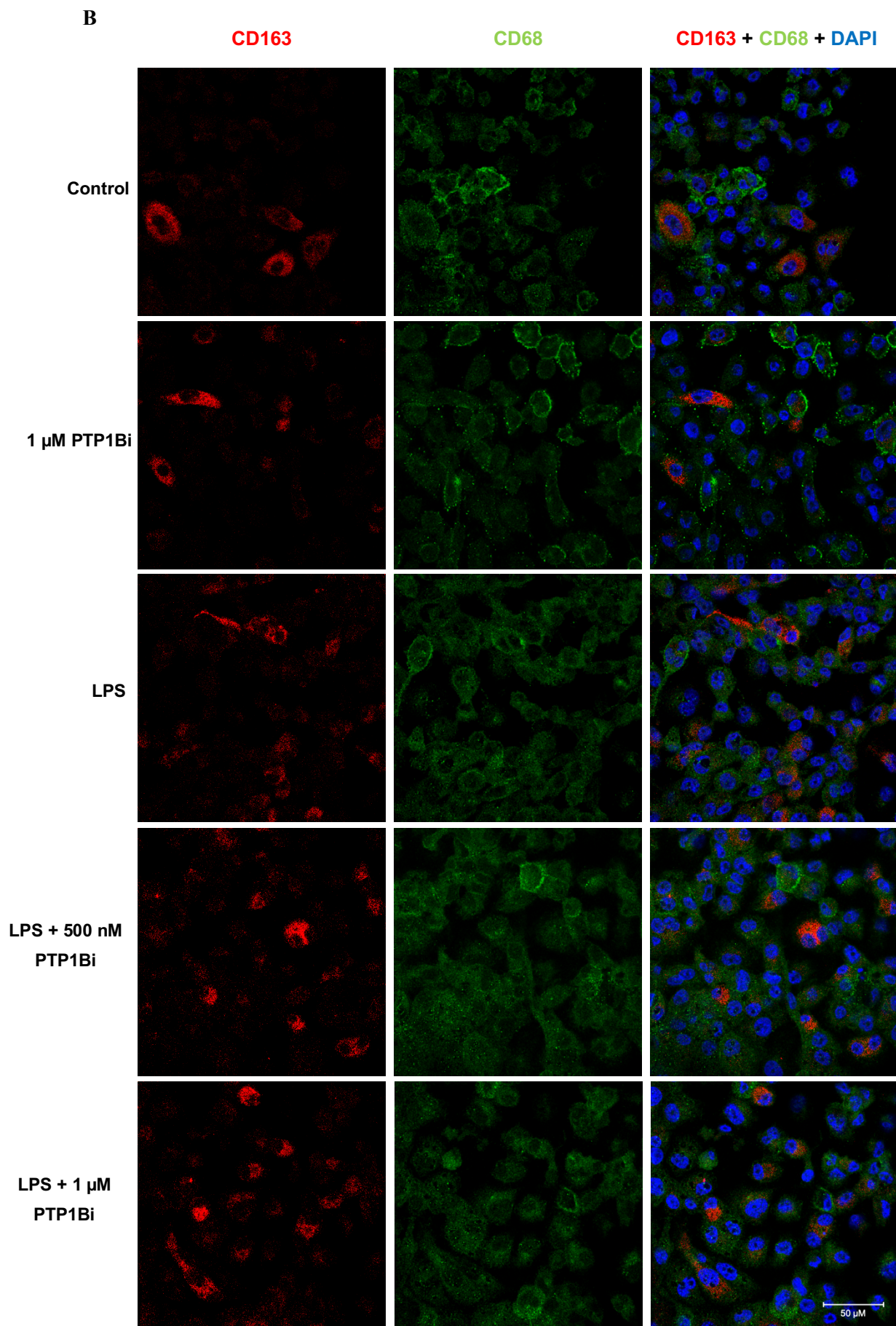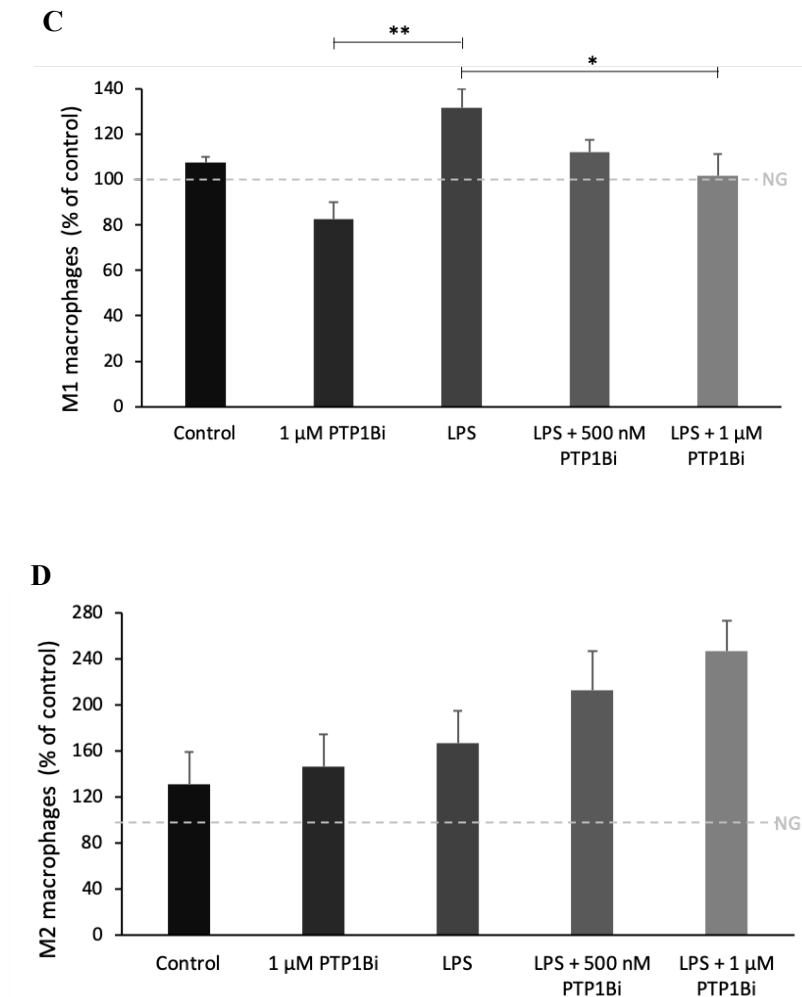
Figure 22 - Effect of PTP1B inhibition on macrophage phenotypes of differentiated THP-1 cells cultured under HG conditions with or without LPS stimuli for 24h. PTP1Bi showed a decrease in M1 macrophages and an increase in M2 macrophages. (A) Representative 400x magnification images of the macrophage marker proteins CD68 (red) and TNF-α (green). (B) Representative 400x magnification images of the macrophage marker proteins CD68 (green) and CD163 (red). (C) Quantification of M1 macrophages (CD68 + TNF-α double-positive cells). (D) Quantification of M2 macrophages (CD68 + CD163 double-positive cells). For statistical analysis a one-way ANOVA, followed by a Newman-Keuls post-test, was performed. Nuclei were stained with DAPI (blue). Scale bar is 50 μm. The results are presented as percentage of NG control cells and represented as mean ± SEM ($n=4$). * $p<0.05$, ** $p<0.01$.

Figure 23 - TNF-α expression in THP-1 cells cultured in NG and HG before and after LPS treatment. (A) Representative 400x magnification images of TNF-α (green) and (B) corresponding quantification. For statistical analysis a one-way ANOVA, followed by a Newman-Keuls post-test, was performed and no

statistical differences were observed. Nuclei were stained with DAPI (blue). Scale bar is 50 μm. The results are presented as percentage of NG control cells and represented as mean ± SEM (*n*=4).

In addition to TNF-α, macrophages produce other cytokines, chemokines and growth factors that are directly involved in inflammation and wound healing. Therefore, it is important to analyse the effect of PTP1B inhibition in the production of these molecules. THP-1 macrophages were cultured under NG and HG conditions and left untreated (control) or treated with LPS and/or 500 nM or 1 μM of PTP1Bi for 24h and the expression of IL-8, IL-6, IL-1β, TNF-α and MCP-1 was analysed by qRT-PCR (**Figure 25**). Furthermore, the levels of IL-6, IL-10 and TNF-α were also analysed (**Table 6**).

The results showed that, in NG conditions without the inflammatory stimuli, 1 μM of PTP1Bi increased IL-8 mRNA levels to 2.50 ± 2.02-fold (**Figure 25A**). Also, in the presence of LPS, 1 μM or 500 nM of PTP1Bi increased IL-8 mRNA to 703.26 ± 191.24-fold and 921.64 ± fold, respectively, and this increase was higher than in cells treated with LPS alone (690.16 ± 234.93-fold). However, 1 μM of PTP1Bi in HG conditions, IL-8 mRNA levels decreased (1.62 ± 0.49-fold) comparing to control (4.48 ± 2.45-fold). More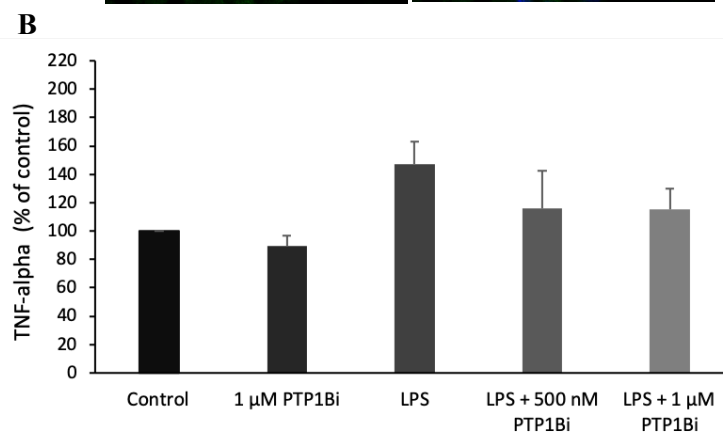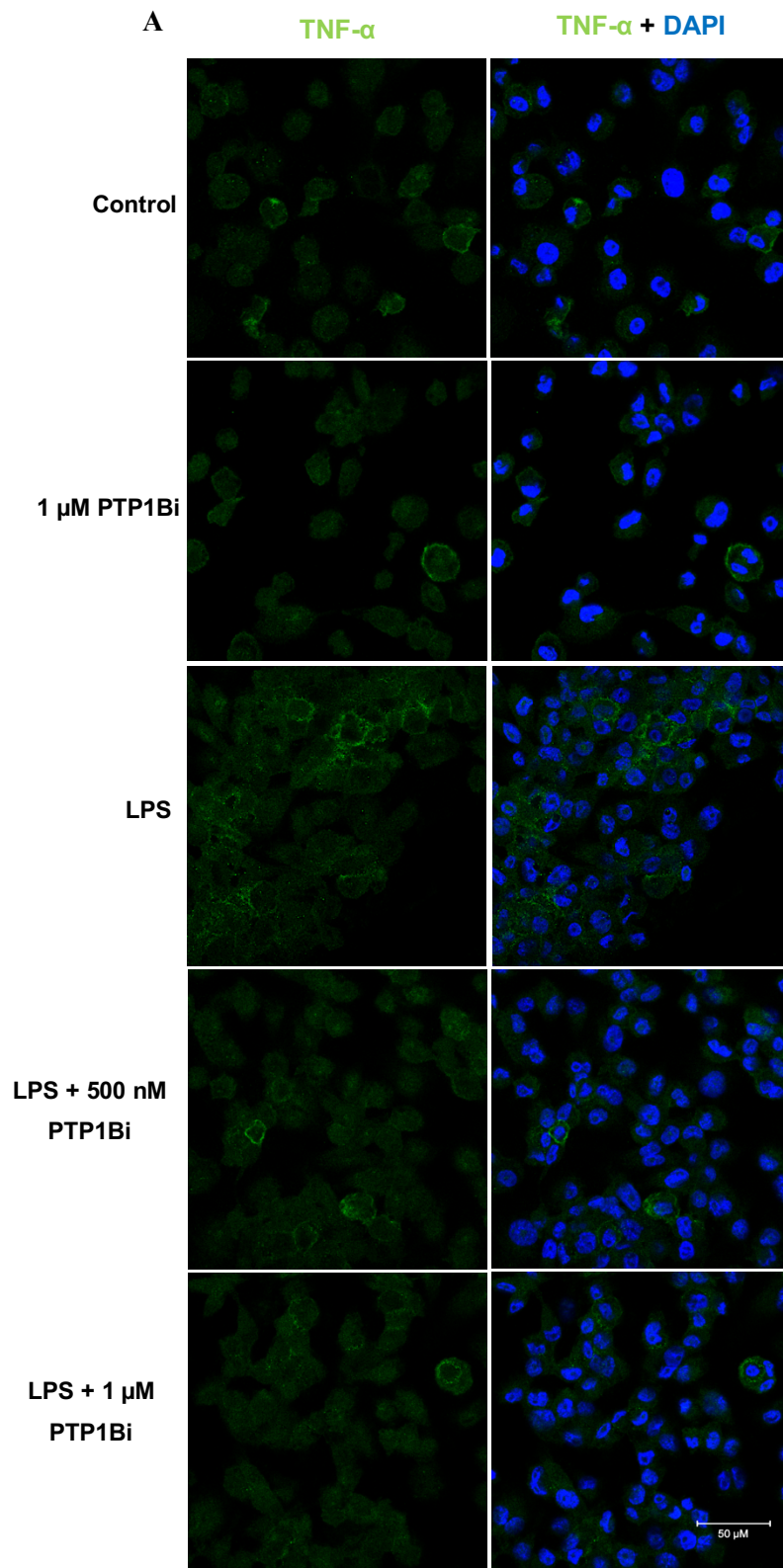over, in LPS conditions 500 nM and 1 μM of PTP1Bi decreased IL-8 mRNA (452.89 ± 127.73 and 541.24 ± 91.26-fold, respectively), when compared to LPS (575.40 ± 184.87-fold).

IL-6 mRNA levels were also quantified (**Figure 25B**). Cells in NG conditions treated with 1 μM of PTP1Bi without LPS decreased IL-6 mRNA (0.80 ± 0.90-fold), however, when the inhibitor was applied together with LPS, IL-6 mRNA levels increased. LPS increased IL-6 mRNA to 303.57 ± 184.54-fold when compared to control. The treatment with 500 nM of PTP1Bi and LPS increased IL-6 mRNA to 334.61 ± 251.25-fold whereas 1 μM of PTP1Bi with LPS increased IL-6 mRNA to 487.81 ± 373.11-fold. Under HG conditions, 1 μM of PTP1Bi without LPS decreased IL-6 expression to 0.41 ± 0.27-fold when compared with HG conditions (1.64 ± 0.98-fold). In the presence of LPS, 500 nM and 1 μM of PTP1Bi decreased IL-6 mRNA levels to 134.34 ± 32.73-fold and 144.55 ± 22.56-fold, respectively, when compared to LPS (157.82 ± 42.28-fold). In addition, IL-6 levels were also measured, in both NG and HG conditions (**Figure 26A**). Under NG conditions, IL-6 levels of 0.57 ± 0.08 pg/mL were measured for basal conditions. The treatment with 1 μM of PTP1Bi without LPS slightly increased IL-6 levels to 0.69 ± 0.09 pg/mL. When LPS was added, IL-6 levels increased to 6074.86 ± 4843.44 pg/mL. Both 500 nM and 1 μM of PTP1Bi, in the presence of LPS, decreased Il-6 levels to 1561. 90 ± 844.89 pg/mL and to 329.97 ± 163.75 pg/mL, respectively. In HG conditions, 1 μM of PTP1Bi did not have an effect in IL-6 levels (0.61 ± 0.05 pg/mL) when compared to control (0.62 ± 0.08 pg/mL). As expected, LPS increased IL-6 levels to 1564.31 ± 919.96 pg/mL and 500 nM of PTP1Bi decreased IL-6 levels to 854.81 ± 712.97 pg/mL. However, 1 μM of PTP1Bi increased IL-6 levels to 1907.75 ± 660.35 pg/mL when compared to LPS.
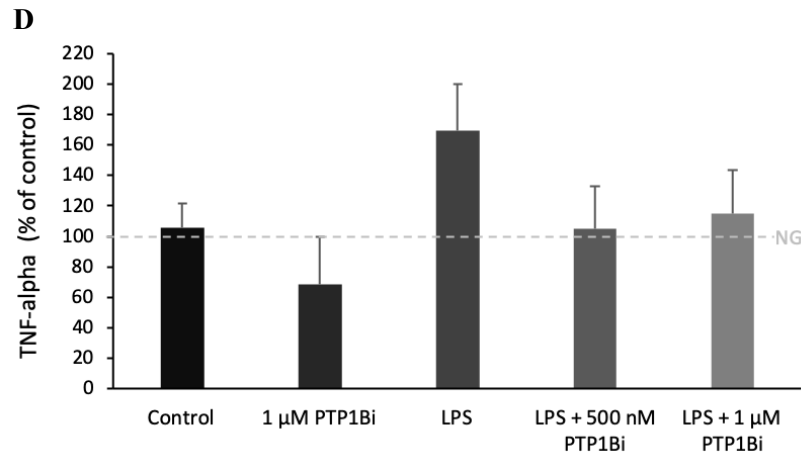
A

TNF-α   TNF-α + DAPI

Control

1 µM PTP1Bi

LPS

LPS + 500 nM
PTP1Bi

LPS + 1 µM
PTP1Bi

50 µM

B

	TNF-α	TNF-α + DAPI
Control		
1 µM PTP1Bi		
LPS		
LPS + 500 nM PTP1Bi		
LPS + 1 µM PTP1Bi		

C

Figure 24 - TNF-α expression in THP-1 cells cultured in NG and HG and treated with LPS and/or PTP1Bi. (A) Representative 400x magnification images of TNF-α (green) and (B) quantification of TNF-α. (C) Representative 400x magnification images of TNF-α (green) and (D) corresponding quantification. For statistical analysis a one-way ANOVA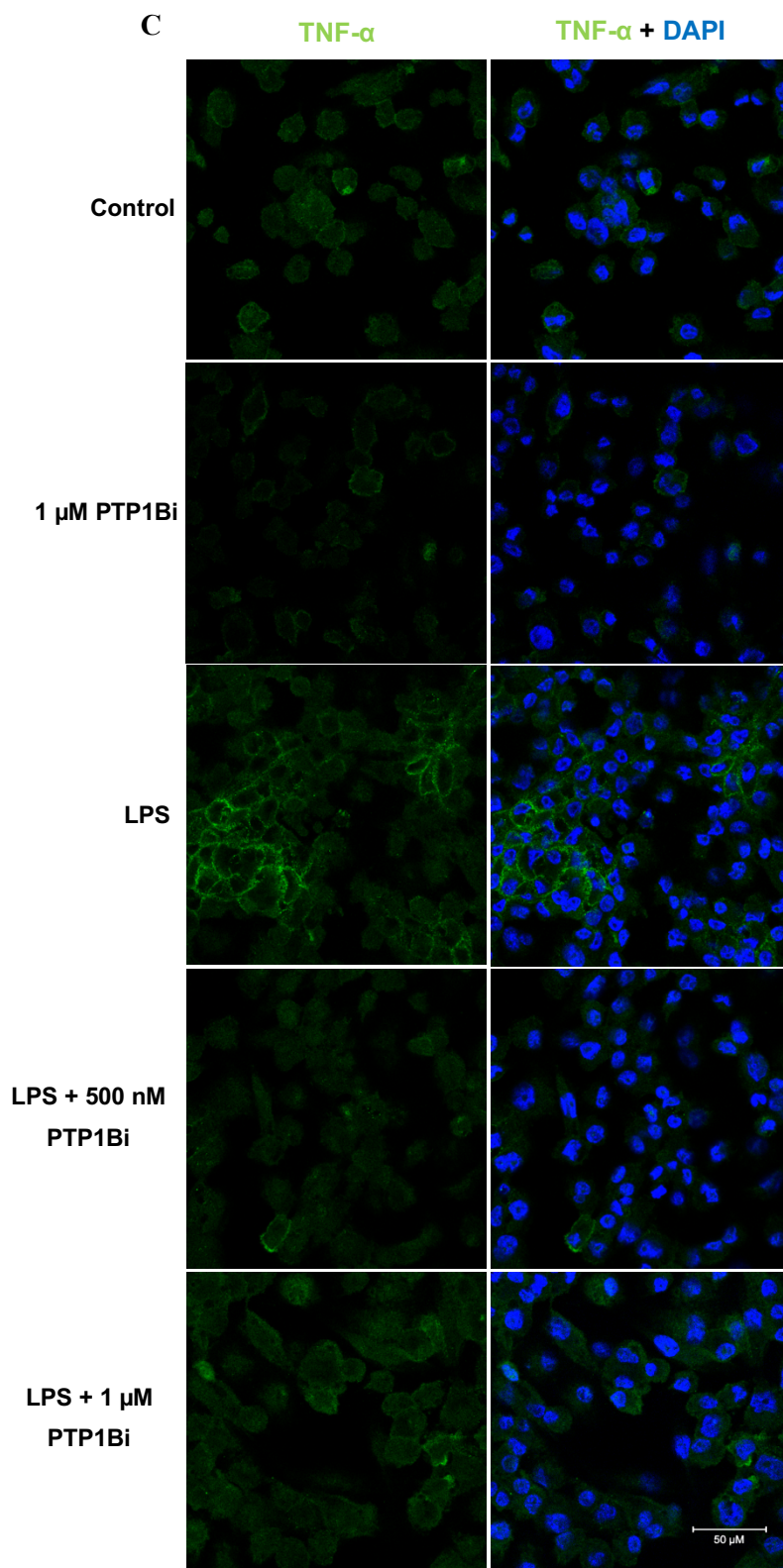, followed by a Newman-Keuls post-test, was performed and no statistical differences were observed. Nuclei were stained with DAPI (blue). Scale bar is 50 μm. The results are presented as percentage of NG control cells and represented as mean ± SEM (*n*=4).

Additionally, the IL-1β mRNA levels were measured in NG and HG conditions (**Figure 25C**). In NG basal conditions, IL-1β mRNA levels did not change with 1 μM of PTP1Bi (1.00 ± 0.90 pg/mL) when compared to control (1.00 ± 0.92 pg/mL). When the treatment of either 1 μM or 500 nM of PTP1Bi was applied together with LPS, IL-1β mRNA levels slightly increased to 23.50 ± 7.40-fold and 27.93 ± 9.01-fold, respectively, when compared to LPS treatment (22.22 ± 13.06-fold). Under HG conditions, 1 μM of PTP1Bi decreased IL-1β mRNA levels (0.55 ± 0.03-fold) when compared to control (0.66 ± 0.16-fold). In addition, LPS treatment increased IL-1β mRNA levels (21.16 ± 7.31-fold) and both 500 nM and 1 μM PTP1Bi concentrations decreased IL-1β mRNA levels (18.95 ± 3.95-fold and 18.62 ± 1.32-fold, respectively).

Moreover, TNF-α mRNA levels, in NG conditions, increased to 1.25 ± 0.32-fold with 1 μM of PTP1Bi without LPS when compared to control (**Figure 25D**). LPS increased TNF-α mRNA levels to 36.14 ± 11.55-fold, but in the presence of 500 nM of PTP1Bi TNF-α were slightly decreased (35.56 ± 9.06-fold). However, 1 μM of PTP1Bi in the presence of LPS, increased TNF-α mRNA levels (48.26 ± 17.97-fold) when compared with LPS alone. In HG conditions, 1 μM of PTP1Bi decreased TNF-α mRNA levels (0.70 ± 0.15-fold) when compared to control (0.91 ± 0.27-fold). LPS treatment increased TNF-α mRNA levels (24.27 ± 6.11-fold), however, regardless of the concentration of PTP1Bi, the values of mRNA remained nearly unaltered (24.89 ± 4.02-fold for 500 nM of PTP1Bi; 24.50 ± 3.55-fold for 1 μM of PTP1Bi). The evaluation of TNF-α levels (**Figure 26B**) showed that, in NG conditions, the application of 1 μM without LPS caused an increase on the levels of TNF-α (1.78 ± 0.18 pg/mL) when compared to control (1.61 ± 0.11 pg/mL). LPS

promoted a high increase in TNF-α production (12954.82 ± 7449.02 pg/mL) and both PTP1Bi treatments decreased TNF-α levels (9979.77 ± 5720.01 pg/mL for 500 nM of PTP1Bi; 3668.00 ± 2505.69 pg/mL for 1 μM of PTP1Bi). In HG basal conditions, TNF-α levels increased slightly with 1 μM of PTP1Bi treatment (1.83 ± 0.17 pg/mL) when compared to control (1.44 ± 0.04 pg/mL). LPS highly increased TNF-α levels (6375.22 ± 3477.86 pg/mL), however, in the presence of 500 nM of PTP1Bi TNF-α levels decreased to 4028.13 ± 5720.10 pg/mL, whereas 1 μM of PTP1Bi treatment increased TNF-α levels to 12169.24 ± 2505.69 pg/mL.

The MCP-1 mRNA levels were also analysed (**Figure 25E**). In NG conditions, MCP-1 mRNA levels increased to 2.11 ± 1.41-fold with 1 μM of PTP1Bi when compared to control. LPS increased the MCP-1 mRNA levels (381.37 ± 178.82-fold) but this increase was reduced with 500 nM and 1 μM of PTP1Bi (283.99 ± 130.59-fold and 289.04 ± 102.06-fold, respectively). Similar results were observed in HG conditions. The levels of MCP-1 mRNA remained unchanged when cells were treated with 1 μM of PTP1Bi (2.33 ± 0.57-fold) when compared to control (2.38 ± 0.94-fold). LPS increased MCP-1 mRNA levels (579.65 ± 230.74-fold), but the mRNA levels increase, promoted by LPS, was lower in the presence of 500 nM and 1 μM of PTP1Bi (458.13 ± 122.77-fold and 430.02 ± 83.71-fold, respectively).

Finally, the evaluation of IL-10 levels in NG and HG conditions showed a wide range of variations (**Figure 26C**). Firstly, NG cells treated with 1 μM PTP1Bi showed an increase to 1.19 ± 0.19 pg/mL of IL-10 when compared to control (0.96 ± 0.03 pg/mL). LPS treatment stimulated IL-10 production (13.64 ± 6.70 pg/mL), which did not change with 500 nM of PTP1Bi treatment (12.14 ± 6.81 pg/mL), however, 1 μM of PTP1Bi resulted in a decrease of IL-10 levels (4.17 ± 1.60 pg/mL). In HG conditions, 1 μM of PTP1Bi had no impact on IL-10 level (1.14 ± 0.02 pg/mL) when compared to control (1.23 ± 0.04 pg/mL). IL-10 levels were increased with LPS (8.80 ± 3.00 pg/mL). In LPS conditions, 500 nM treatment promoted a decrease on IL-10 levels (6.88 ± 3.58 pg/mL) whereas 1 μM of PTP1Bi treatment resulted in an increase on IL-10 levels (11.79 ± 3.60 pg/mL).

Interestingly, the expression of the pro-inflammatory cytokines IL-8, IL-6 and MCP-1 were increased in cells in HG conditions.

The expression of the growth factors TGF-β, VEGF, PDGF and EGF was also analysed before and after the treatment with PTP1Bi, however, there were no relevant modifications (data not shown)

80
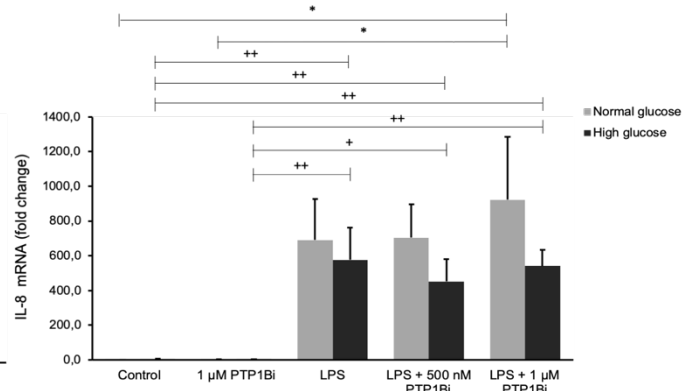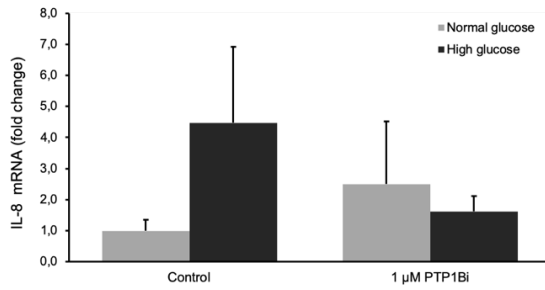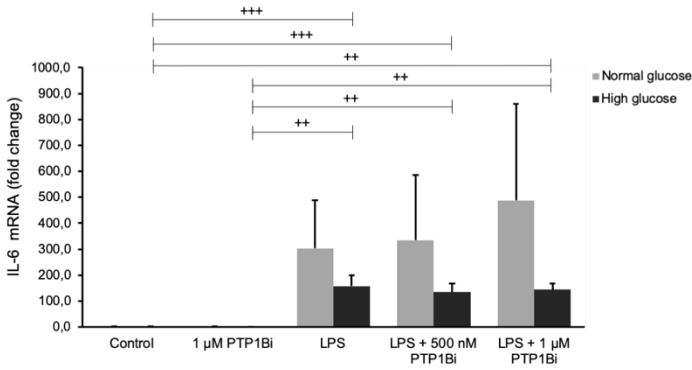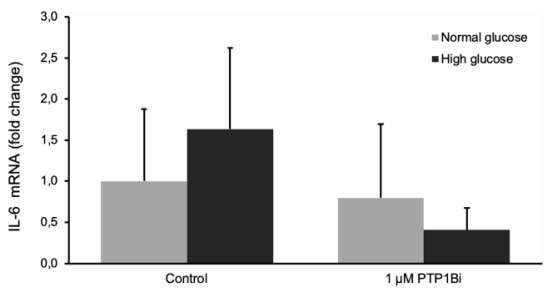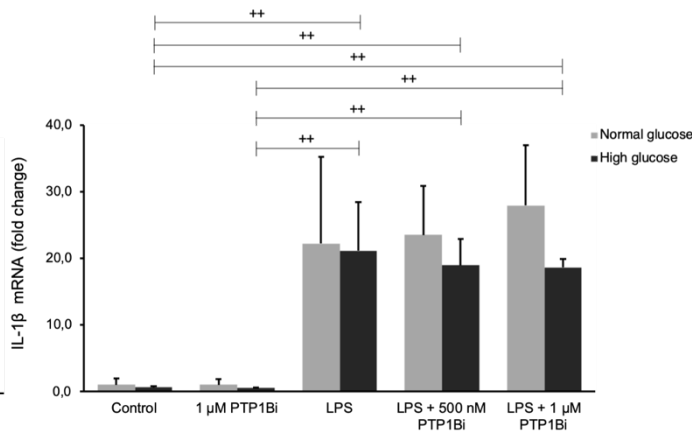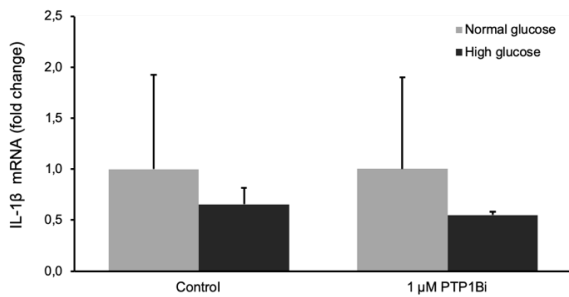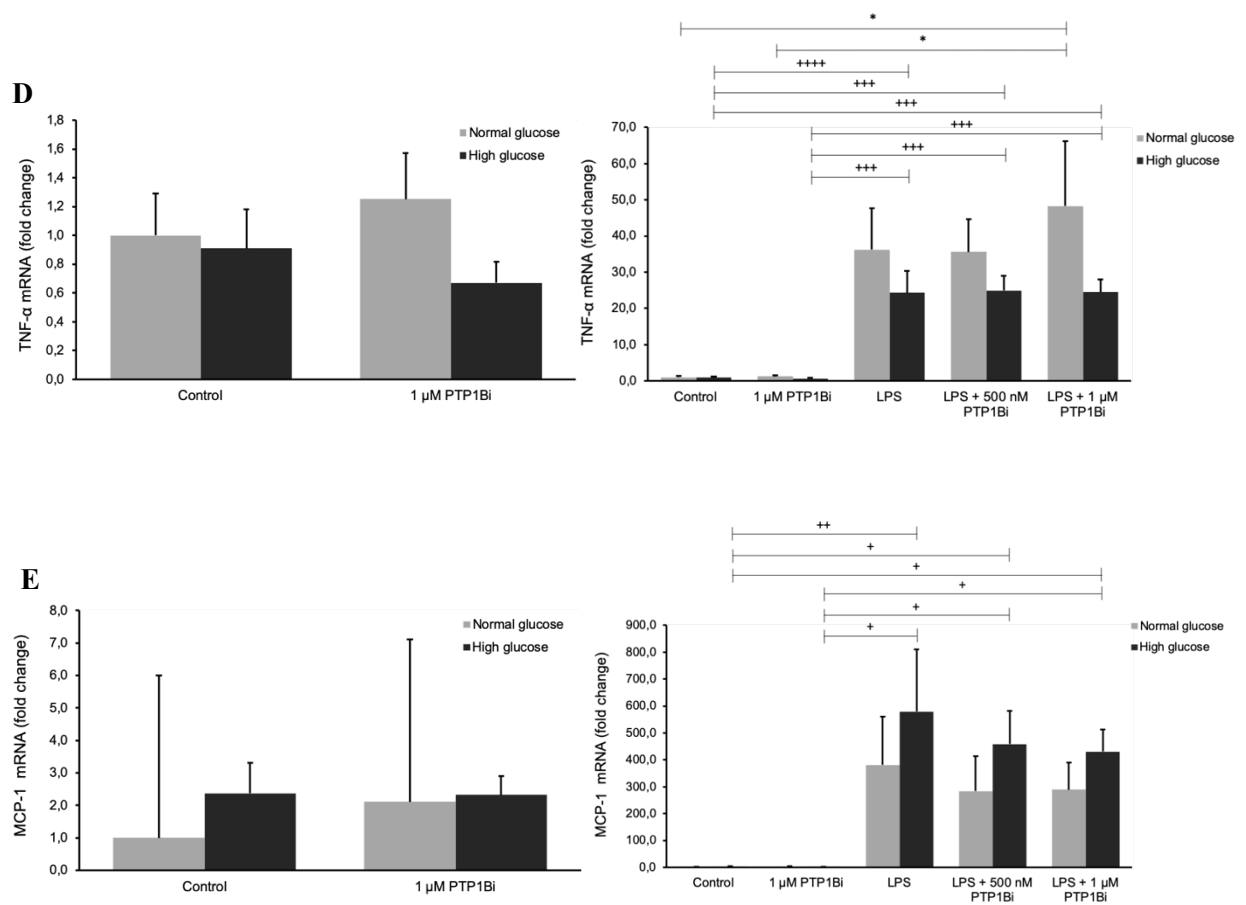
Figure 25 - The effect of PTP1B inhibition on IL-8, IL-6, IL-1β, TNF-α and MCP-1 expression in THP-1 cells cultured under NG or HG conditions. THP-1 cells were maintained untreated (control) or incubated with 500 nM or 1 µM of PTP1Bi and/or 1 µg/mL of LPS during 24h and the expression of (A) IL-8, (B) IL-6, (C) IL-1β, (D) TNF-α, and (E) MCP-1 was measured using qRT-PCR. The mRNA expression for each gene was normalized to TBP and calculated as the fold change of the NG control group. For statistical analysis a one-way ANOVA, followed by a Newman-Keuls post-test, was performed to compare the different conditions in NG and in HG independently. A student t-test was performed to compare the NG control condition with the HG control condition and no statistical differences were observed. The results are represented as mean ± SEM (n=4). * $p<0.05$ *vs* NG control, + $p<0.05$ *vs* HG group, ++ $p<0.01$ *vs* HG group, +++ $p<0.001$ *vs* NG group. **Legend:** IL-8 → Interleukin 8; IL-6 → Interleukin 6; IL-1β → Interleukin 1 beta; TNF-α → Tumour necrosis factor alpha; MCP-1 → Monocyte chemoattractant protein-1; TBP → TATA binding protein.

Table 6 - Summary of the levels of IL-6, TNF-α and IL-10 in THP-1 cells cultured under NG or HG conditions and left untreated (control) or incubated with 500 nM or 1 μM of PTP1Bi and/or 1 μg/mL of LPS for 24h. For statistical analysis a one-way ANOVA, followed by a Newman-Keuls post-test, was performed to compare the different conditions in NG and in HG independently and no statistical differences were observed. The results are represented as mean ± SEM (n=4).

Cytokine	Glucose level	Conditions				
		Control	1 μM PTP1Bi	LPS	LPS + 500 nM PTP1Bi	LPS + 1 μM PTP1Bi
IL-6	NG	0.58 ± 0.08	0.69 ± 0.09	6074.86 ± 4843.44	1561.90 ± 844.89	329.97 ± 163.75
(pg/mL)	HG	0.62 ± 0.05	0.61 ± 0.04	1564.31 ± 919.96	854.81 ± 712.97	1907.75 ± 660.35
TNF-α	NG	1.61 ± 0.11	1.78 ± 0.18	12954.83 ± 7449.02	9979.77 ± 5720.10	3668.00 ± 2505.69
(pg/mL)	HG	1.44 ± 0.04	1.83 ± 0.17	6375.22 ± 3477.86	4028.13 ± 2879.94	12169.24 ± 3957.26
IL-10	NG	0.96 ± 0.03	1.19 ± 0.19	13.64 ± 6.70	12.14 ± 6.81	4.17 ± 1.57
(pg/mL)	HG	1.23 ± 0.04	1.14 ± 0.02	8.80 ± 3.00	6.86 ± 3.58	11.79 ± 3.60

Legend: IL-6 → Interleukin 6; TNF-α → Tumour necrosis factor alpha; IL-10 → Interleukin 10.
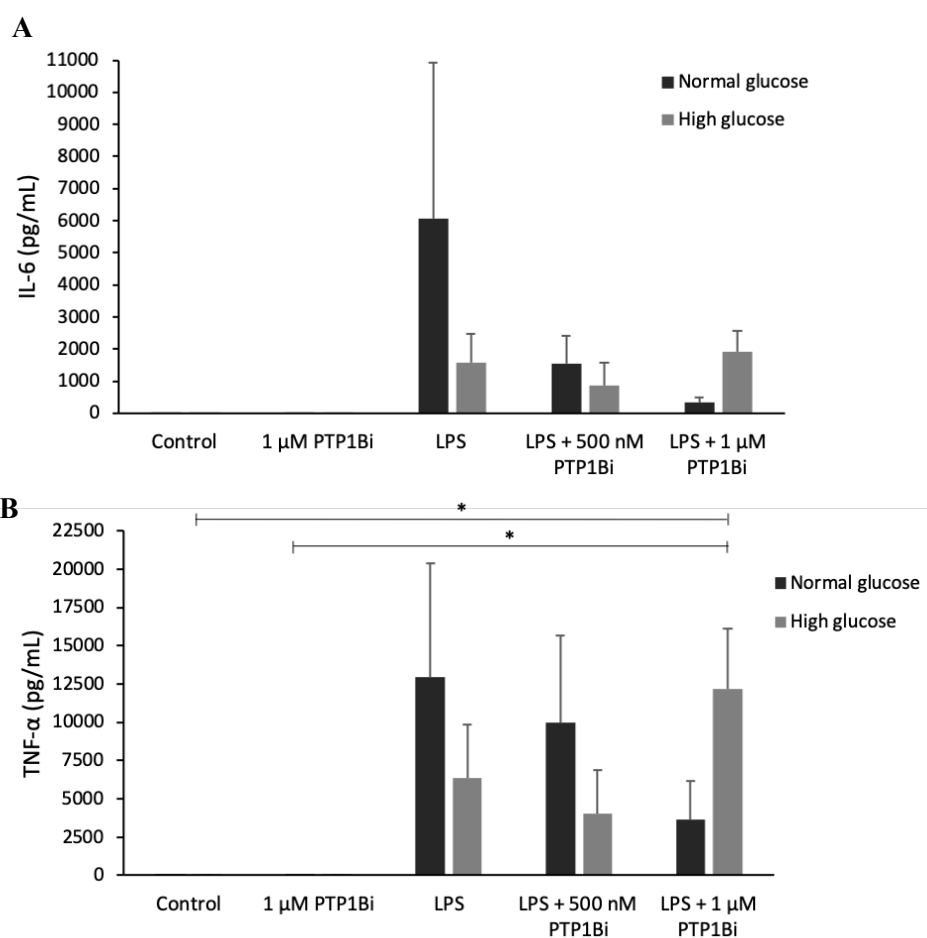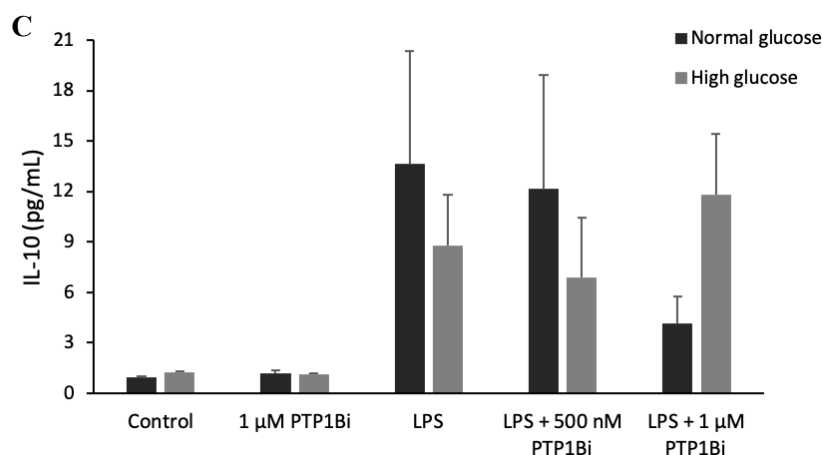
Figure 26 - The effect of PTP1B inhibition on IL-6, TNF-α and IL-10 levels in THP-1 cells cultured under NG or HG conditions. THP-1 cells were maintained untreated (control) or incubated with 500 nM or 1 μM of PTP1Bi and/or 1 μg/mL of LPS for 24h and the levels of (A) IL-6, (B) TNF-α, and (C) IL-10 was measured using a LEGENDplex™ Multi-Analyte Flow Assay. For statistical analysis a one-way ANOVA, followed by a Newman-Keuls post-test, was performed to compare the different conditions in NG and in HG independently and no statistical differences were observed. The results are represented as mean ± SEM (n=4). **Legend:** IL-6 → Interleukin 6; TNF-α → Tumour necrosis factor alpha; IL-10 → Interleukin 10.

3.1.6. Inhibition of PTP1B decreased oxidative stress in normal and high glucose conditions

As mentioned before, macrophages play a really important role in wound healing and are present in all wound healing phases [14]. These immune cells produce ROS when stimulated with an inflammatory stimulus like LPS [199]. ROS can cause damage in the cells and impair angiogenesis being prejudicial to wound healing [87], [200]. In fact, murine and human macrophages cultured in HG conditions have increased ROS formation which is associated with the promotion of the pro-inflammatory M1 phenotype and it can result in damage to macrophage cell structures disturbing its normal function [201].

One of the hypotheses of this dissertation is that PTP1B inhibition may help to reduce oxidative stress levels in human macrophages. To test this hypothesis, THP-1 cells cultured in NG and HG were differentiated in macrophages and treated with LPS and/or PTP1Bi for 24h. Then, ROS levels were measured by DCFH-DA assay.

Hyperglycaemia is known to lead to an increase in ROS levels and some cell types, as endothelial cells or fibroblasts, when exposed to HG conditions have an increase in ROS levels [202]–[204]. When comparing the basal levels of ROS present in untreated THP-1 cells cultured in NG and HG it is clear that ROS levels were increased in HG (**Figure 27A**). In HG, the ROS levels were increased to $130.22 \pm 62.32\%$ compared to the levels observed in NG ($100 \pm 16.17\%$) (**Figure 27B**). To evaluate the effect of PTP1B inhibition on ROS production in inflammatory condition, the

cells were incubated for 24h with LPS. Following incubation with LPS, ROS levels in both NG and HG cells increased significantly to $178.61 \pm 25.42\%$ and to $202.91 \pm 26.29\%$ respectively, compared to baseline levels. These levels served as baseline levels for further evaluation of the effect of PTP1Bi treatment on the modulation of ROS levels.

A
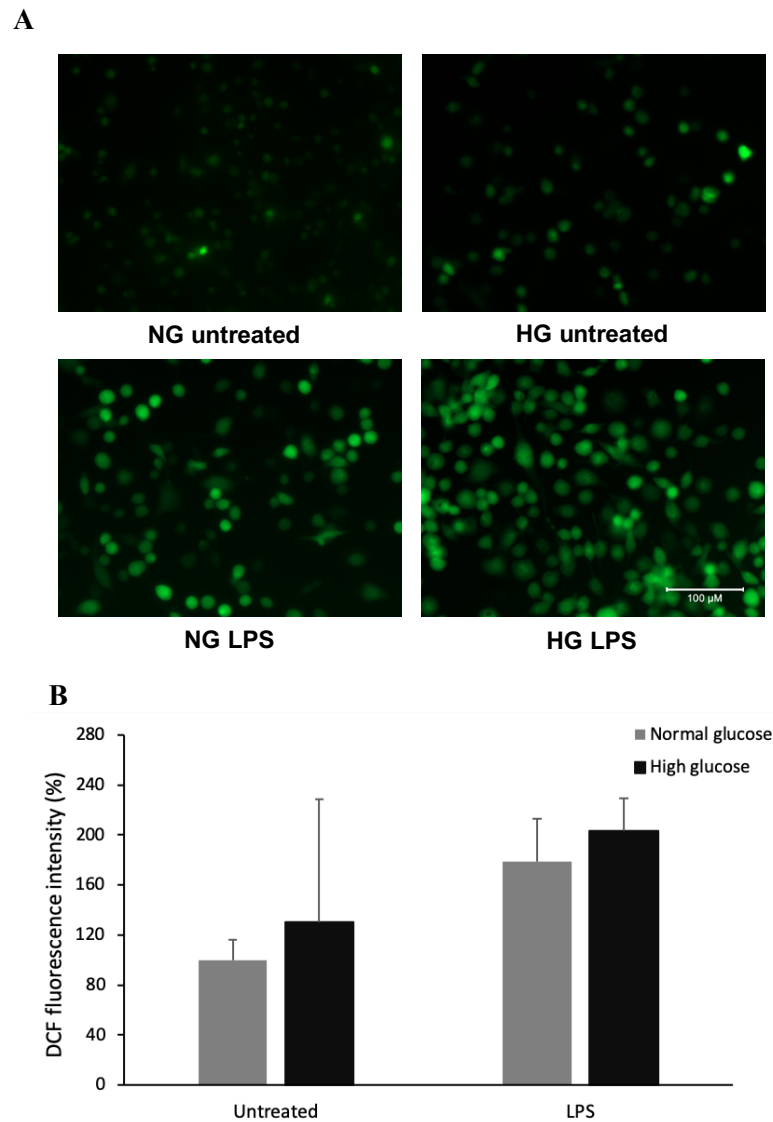
Figure 27 - ROS levels in THP-1 cells cultured in NG and HG before and after LPS treatment. (A) Representative 200x magnification images of DCFH-DA staining (green) and (B) respective ROS quantification. Scale bar is 100 μm. For statistical analysis a one-way ANOVA, followed by a Newman-Keuls post-test, was performed and no statistical differences were observed. The results are presented as percentage of NG untreated cells and data are represented as mean ± SEM (*n*=6).

To evaluate the effect of PTP1Bi treatment in ROS levels, cells cultured in NG and HG were treated with LPS and 500 nM or 1 μM of PTP1Bi or left untreated. In cells cultured in NG conditions, treatment with PTP1Bi decreased ROS levels in the cellular environment in a concentration-dependent manner (**Figure 28A**). Thus, the lower concentration of 500 nM of PTP1Bi

led to a decrease in ROS levels to $78.70 \pm 9.77\%$ while the 1 µM concentration significantly reduced the levels to $63.13 \pm 1.76\%$, when compared to the maximum ROS levels obtained with LPS (100%) ($p<0.05$, $n=4$) (**Figure 28B**). Surprisingly, the levels obtained with 1 µM of PTP1Bi were lower than those observed in untreated cells ($66.30 \pm 10.60\%$). Similar results were observed in cells cultured in HG conditions (**Figure 28C**). In this case, 500 nM of PTP1Bi treatment decreased the ROS levels to $85.43 \pm 4.35\%$ and 1 µM of PTP1Bi treatment decreased the levels to $77.75 \pm 9.71\%$ when compared to the maximum ROS levels obtained with LPS treatment (100%) (**Figure 28D**). Although these decreases in ROS levels with PTP1Bi in HG cultured cells are not statistically significant, they can be biologically relevant, since as occurs in NG, PTP1B inhibition is able to modulate ROS levels in the cellular environment and reduce them to levels closer to normal.
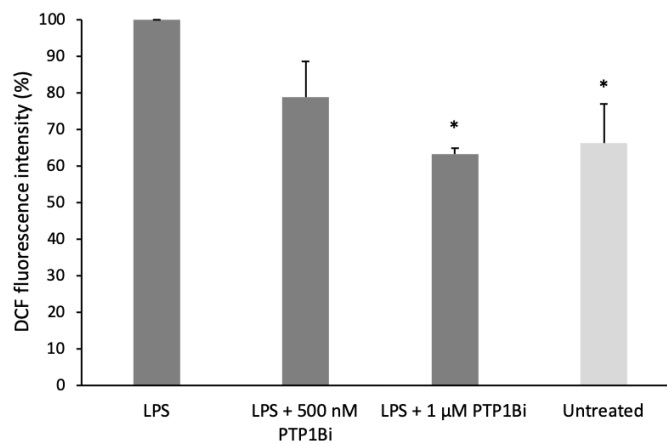
C

D

Figure 28 - ROS levels in THP-1 cells cultured in NG and HG and treated with LPS and/or PTP1Bi. (A) Representative 200x magnification images of DCFH-DA staining (green) and (B) respective ROS quantification. (C) Representative 200x magnification images of DCFH-DA staining and (D) respective ROS quantification. LPS treatment was considered as the maximum ROS levels. Scale bar is 100 μm. For statistical analysis a one-way ANOVA, followed by a Newman-Keuls post-test, was performed. The results are presented as percentage of respective LPS treated cells and data are represented as mean ± SEM (*n*=4). * *p*<0.05.

3.1.7. HO-1 levels increase in cells treated with MSI-1436

In macrophage, HO-1 expression is increased when cells are exposed to an inflammatory stimuli, like LPS, as a response against inflammation and stress oxidative damages [205]. Furthermore, this antioxidant and anti-inflammatory enzyme has been linked to enhanced polarisation towards an anti-inflammatory M2 macrophage and has antioxidant capacities [206], [207]. Thus, it is important to study the effect PTP1B inhibition in the expression of this enzyme. For this, HO-1 expression in THP-1 cells cultured in NG and HG, differentiated in macrophages and treated with LPS and/or PTP1Bi for 24h was determined using immunoblotting and immunofluorescent staining.

Cells cultured in HG cells have an increased HO-1 protein level (**Figure 29A and B**). The protein levels are significantly increased to 1.77 ± 0.19 when compared with NG ($p<0.05$, $n=3$). This increase was also observed in the immunofluorescence assay (**Figure 30A**). The results of this assay showed a lower increase of HO-1 levels to $104.03 \pm 15.11\%$ comparing to NG (100%) (**Figure 30B**). As a consequence of ROS levels increase, due to high glucose, cells may attempt to compensate the augmented oxidative stress through an increase on HO-1 production.

As expected, LPS treatment increased HO-1 expression. In NG, LPS significantly increased HO-1 protein level to 3.76 ± 0.49 ($p<0.05$, $n=3$) when compared to control. This increase was confirmed by immunofluorescence, where LPS increased HO-1 levels to $148.79 \pm 9.33\%$ ($p<0.05$, $n=4$). The same was observed in HG, LPS increased HO-1 protein levels to 4.42 ± 0.57, and this increase was confirmed by immunofluorescence where the increase of HO-1 level was to $180.46 \pm 9.04\%$ ($p<0.001$, $n=4$). This increase in HG after LPS treatment was significantly greater than that observed in NG ($p<0.05$, $n=4$).
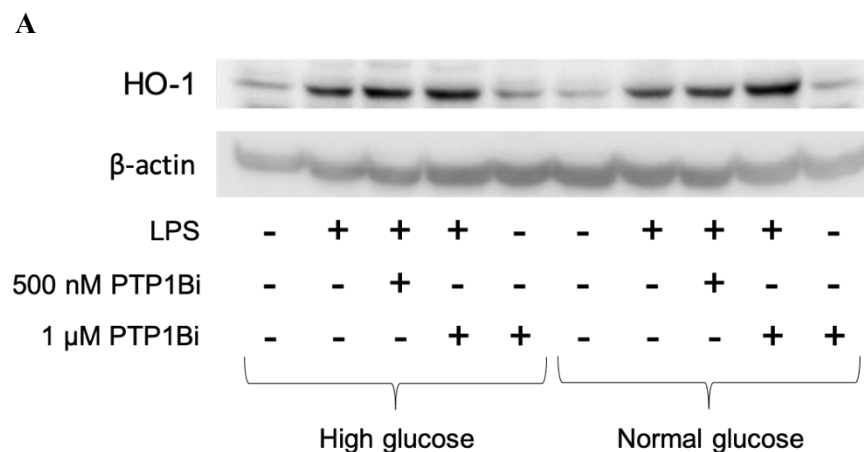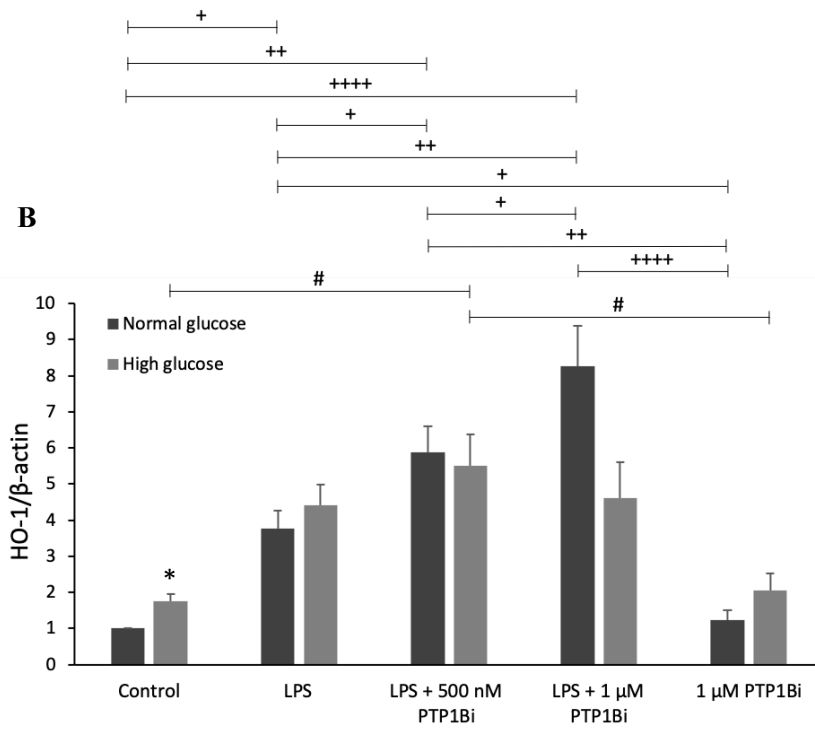
Figure 29 - The effect of PTP1B inhibition in HO-1 expression in THP-1 cells cultured under NG and HG with or without LPS stimuli for 24h. (A) Representative Western blot of HO-1 protein expression. β-actin was used as a loading control. (B) Quantification of HO-1, presented as a ratio of β-actin value. For statistical analysis a one-way ANOVA, followed by a Newman-Keuls post-test, was performed to compare the different conditions in NG and in HG independently. A student t-test was performed to compare the NG control condition with the HG control condition. The results are relative to NG control and data are represented as mean ± SEM (*n*=3). * *p*<0.05, NG control *vs* HG control, + *p*<0.05 *vs* NG group, ++ *p*<0.01 *vs* NG group, ++++ *p*<0.0001 *vs* NG group, # *p*<0.05 *vs* HG group.

Under NG and inflammatory conditions, the treatment with PTP1Bi increased the HO-1 levels in a concentration dependent manner. When cells were treated with 500 nM of PTP1Bi, HO-1 protein levels were significantly increased to 5.89 ± 0.71 when compared to an inflammatory environment containing only LPS (3.76 ± 0.49) (*p*<0.05, *n*=3). A greater effect was observed with 1 μM of PTP1Bi, where the HO-1 protein levels raised to 8.27 ± 1.12 (*p*<0.01, *n*=3). (**Figure 29A and B**). The immunofluorescence images confirm PTP1B inhibition effect. The quantification of HO-1 intensity present in these images demonstrated that under inflammatory conditions (**Figure 31A**), 500 nM of PTP1Bi increased HO-1 expression to 199.28 ± 23.40% whereas 1 μM treatment caused an increase to 214.36 ± 23.57 % (**Figure 31C**), relatively to LPS (148.79 ± 9.33%).

A

HO-1 HO-1 + DAPI

NG Control

HG Control

NG LPS

HG LPS

50 µM
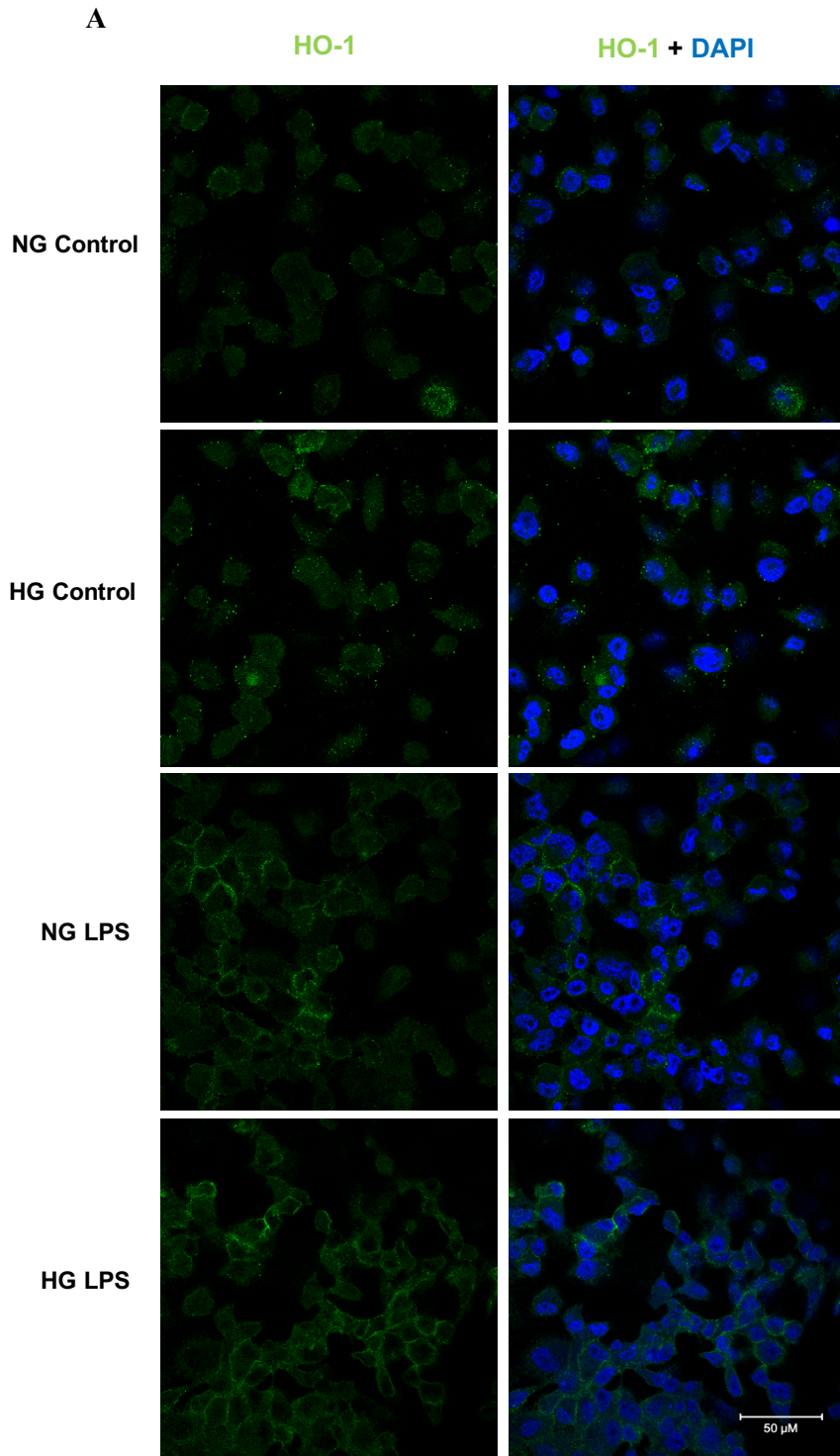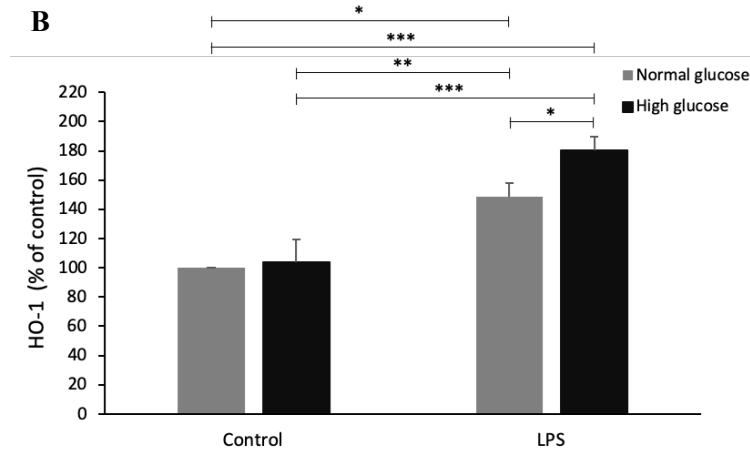
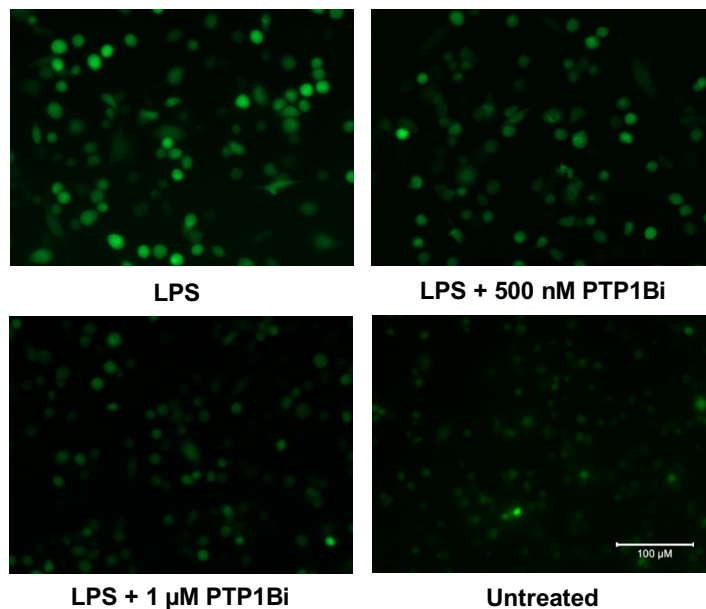**Figure 30 -** HO-1 levels in THP-1 cells cultured in NG and HG before and after LPS treatment. (A) Representative 400x magnification images of HO-1 (green) and (B) respective quantification in THP-1 cells. For statistical analysis a one-way ANOVA, followed by a Newman-Keuls post-test, was performed. Nuclei were stained with DAPI (blue). Scale bar is 50 μm. The results are presented as percentage of NG control cells and represented as mean ± SEM (n=4). * p<0.05, ** p<0.01, *** p<0.001.

Interestingly, under basal conditions, without LPS treatment, cells treated with 1 μM PTP1Bi also presented a slight increase on HO-1 expression, showed by immunoblotting and fluorescence assays. Following PTP1Bi treatment, cells showed a slight increase in HO-1 protein level to 1.24 ± 0.27 when compared to control, confirmed with fluorescence assay since HO-1 expression increased to 148.58 ± 14.97% comparing to control (100%). This increase was similar to the induced by LPS.

A similar effect of PTP1B inhibition was observed in cells cultured in HG, however the most efficient concentration in this case was the 500 nM of PTP1Bi. The immunoblotting results showed that cells treated with 500 nM of PTP1Bi significantly increased HO-1 protein levels to 5.50 ± 0.88 when compared to an inflammatory environment containing only LPS (4.42 ± 0.57). The 1 μM of PTP1Bi potentiated a smaller increase to 4.62 ± 1.00 (**Figure 29A and B**). Similar results were observed with the immunofluorescence images (**Figure 31B**), where the quantification of HO-1 intensity demonstrated that, under inflammatory conditions, 500 nM and 1 μM of PTP1Bi increased HO-1 expression to 290.45 ± 41.15% (p<0.05, n=4) and 289.98 ± 22.92 % (p<0.05, n=4), respectively, comparing to LPS treatment (180.46 ± 9.04%) (**Figure 31D**). Under basal conditions, cells treated with 1 μM PTP1Bi increased HO-1 expression observed in both immunoblotting (2.06 ± 0.47) and fluorescence assays (186.04 ± 19.54%) when compared to control (1.77 ± 0.19 for immunoblotting and 104.03 ± 15.11% for immunofluorescence). The increase promote by PTP1Bi treatment was higher than the one promoted by LPS (180.46 ± 9.04%).

A

B

HO-1   HO-1 + DAPI

Control
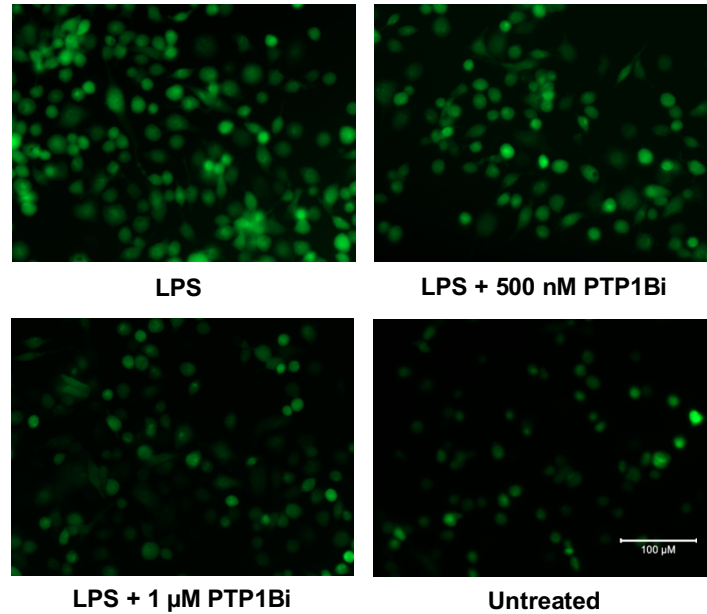
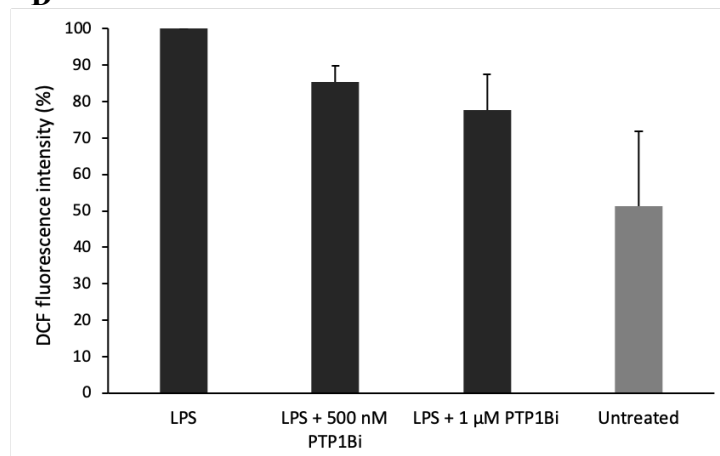1 µM PTP1Bi

LPS

LPS + 500 nM
PTP1Bi

LPS + 1 µM
PTP1Bi

50 µM
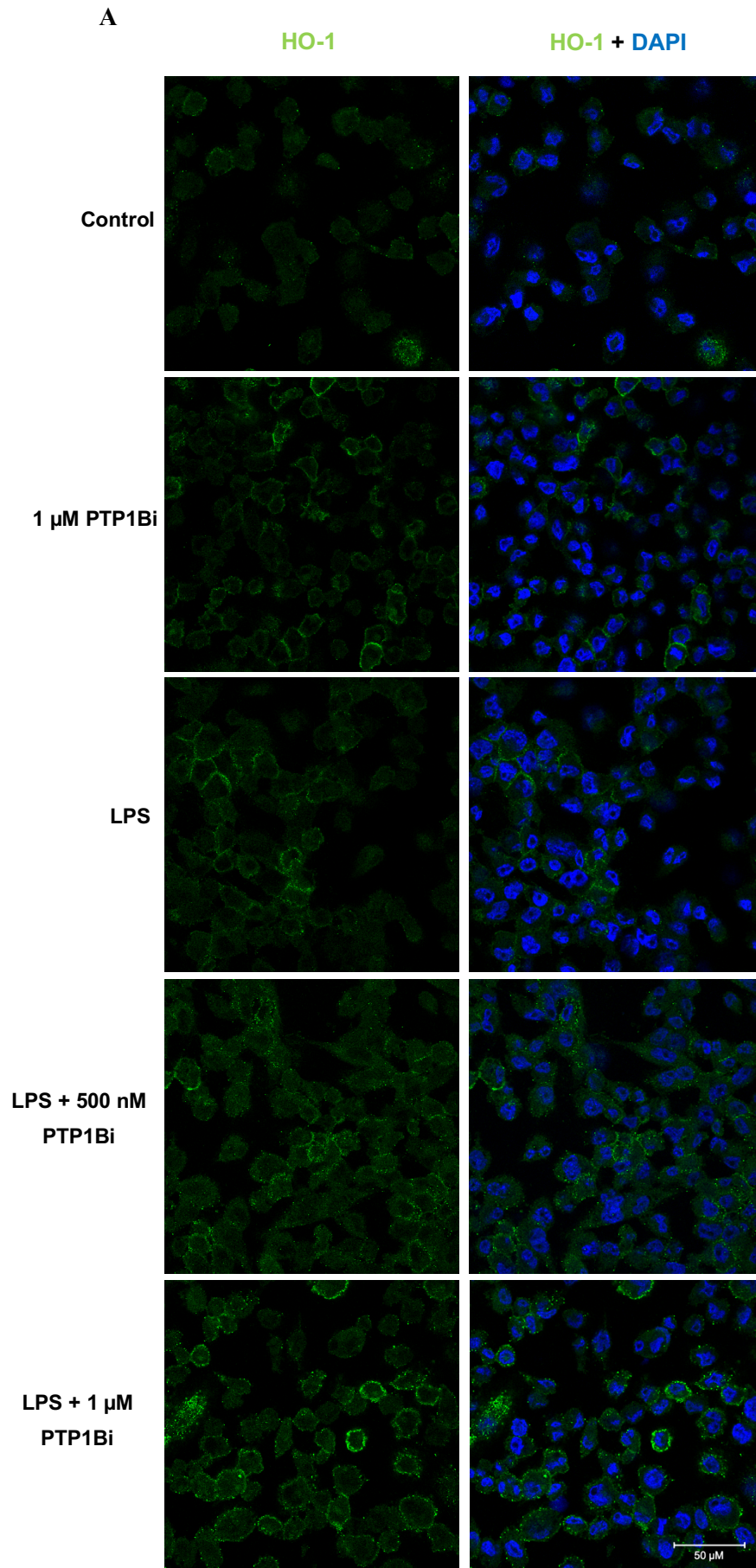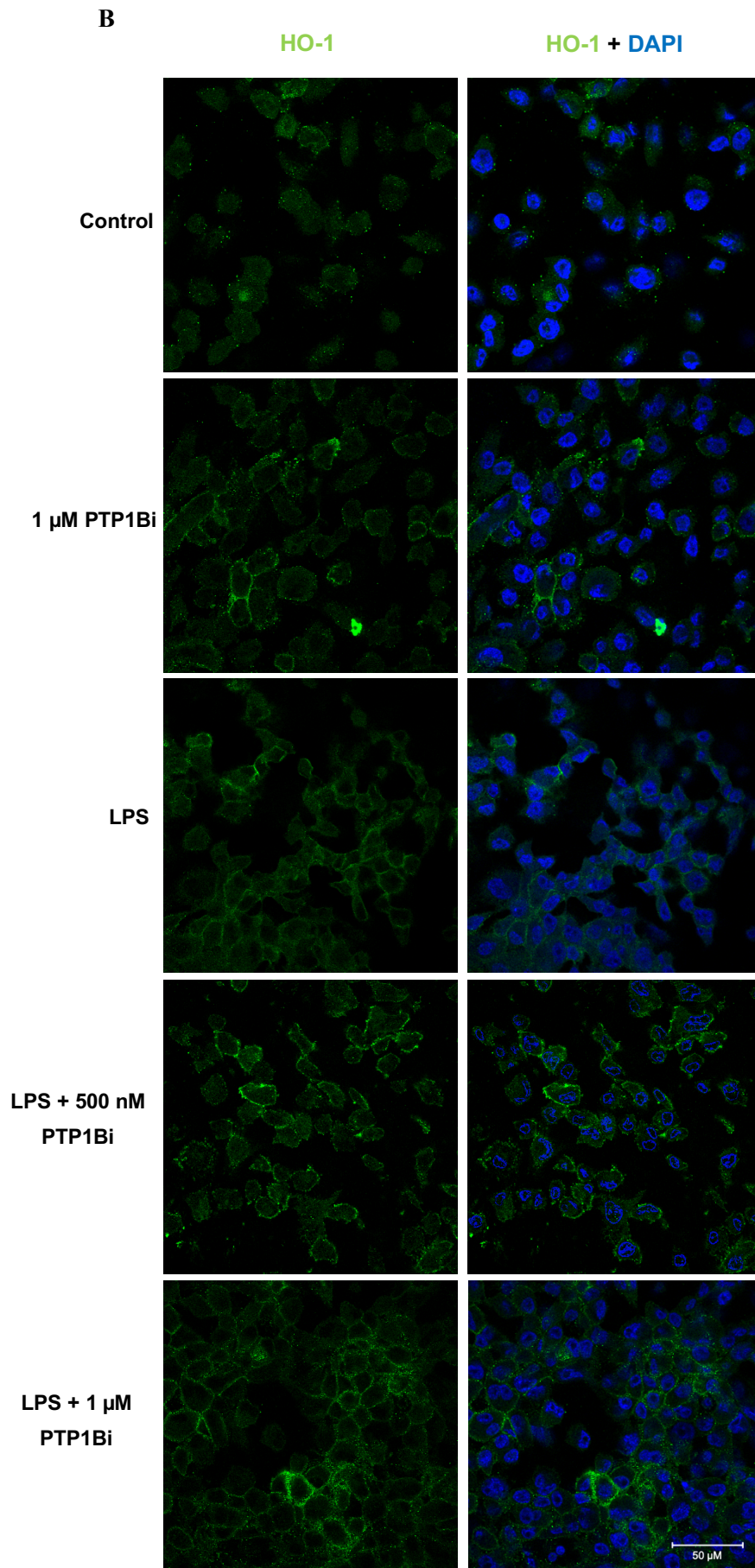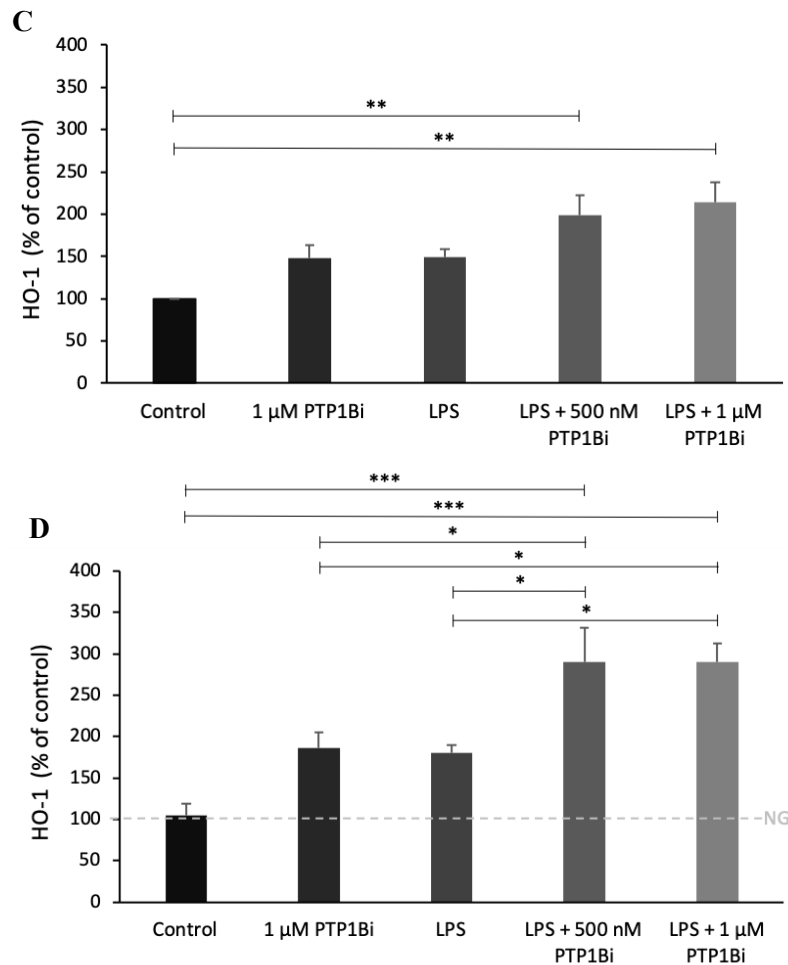
Figure 31 - HO-1 levels in THP-1 cells cultured in NG and HG and treated with LPS and/or PTP1Bi. (A) Representative 400x magnification images of HO-1 (green) in THP-1 cells. (B) Representative 400x magnification images of HO-1 (green) in THP-1 cells. (C) Quantification of HO-1 in THP-1 cells cultured under NG conditions and (D) under HG conditions. For statistical analysis a one-way ANOVA, followed by a Newman-Keuls post-test, was performed. Nuclei were stained with DAPI (blue). Scale bar is 50 µm. The results are presented as percentage of NG control cells and represented as mean ± SEM (n=4). * p<0.05, ** p<0.01, *** p<0.001.

When cells are exposed to an inflammatory stimulus, which causes an increase on ROS level, they attempt to decrease oxidative stress level by increasing HO-1 production, although sometimes this increase is insufficient to regulate ROS levels. HO-1 production is potentiated by PTP1B inhibition, which in turn highly decreases ROS levels, thus indicating that PTP1Bi treatment have an important effect in the modulation of excessive ROS production, improving macrophage functions and reducing the inflammatory environment.

3.2. Results in peripheral blood isolated monocytes

As mentioned before, the THP-1 cell line is widely used as a model for human monocytes and macrophages and is extremely useful for studying these cells since the access to human cells from patients is very limited. However, this cell line has limitations as a model for primary cells. They are immortalized cells which causes their physiological behaviour to be different from human peripheral blood monocytes [184], [208]. Thus, these cells may have different responses to stimuli compared to human peripheral blood monocytes. Several studies have shown that THP-1 cells respond to various stimuli similarly to human peripheral blood monocytes, however, other studies have also reported some differences in gene expression and cytokine release between these cells when presented with the same stimulus [208]. Thus, it is important to validate the responses observed using THP-1 cells in studies using cell cultures of human peripheral blood monocytes.

To evaluate the effects of PTP1B inhibition on monocytes-derived macrophages from peripheral blood, it was used blood from diabetic patients without DFUs, diabetic patients with acute DFUs (ulcer < 3 months), diabetic patients with chronic DFUs (ulcer >3 months), and healthy volunteers, all age and sex-matched. The blood samples were collected at Centro Hospitalar do Porto - Hospital de Santo António, and both patient and control sample collections were approved by the local ethics committee and were performed after informed written consent. History of neoplastic malignancies or autoimmune disorders and clinically detectable infection at the time of sample collection were exclusion criteria for all patients and controls enrolled in this study. After isolation, cells were left to rest for 3 days before any manipulation and then differentiated into macrophages and treated with MSI-1436 (1 µM PTP1Bi) and/or LPS (1 µg/mL) during 24h. The 1 µM concentration of PTP1Bi was chosen because, analysing all the results obtained in THP-1 cells, it seems to be the most effective concentration. The characterisation of the groups used in this study are exhibited on **Table 7**, unfortunately the complete details of the groups were not available because the Hospital could not provide the full relevant data timely. The results presented are only preliminary, since the number of patients and macrophages used was very small. More studies need to be done in order to consolidate the results obtained.

Table 7 - Patient groups and control group known parameters. Results are represented as mean ± SEM.

	Age (years)	Sex Male	Sex Female	n
Control group	48.33 ± 0.88	2	1	3
Diabetic group	-	3	0	3
Diabetic with acute ulcer group	-	1	0	1
Diabetic with chronic ulcer group	-	2	1	3

3.2.1. Human monocyte-derived macrophages morphology

Human peripheral blood monocytes were differentiated into macrophages by incubation with 50 ng/mL PMA for 48h. As described for THP-1 cells, during the process of differentiation, there is an increase in cytoplasmic volume, the cells adhere to the bottom and become noticeably larger (**Figure 32**). These changes were observed using a light microscopy during the 48h of differentiation. After 48h of incubation with PMA, cells appeared to be completely differentiated, showing macrophage morphology.
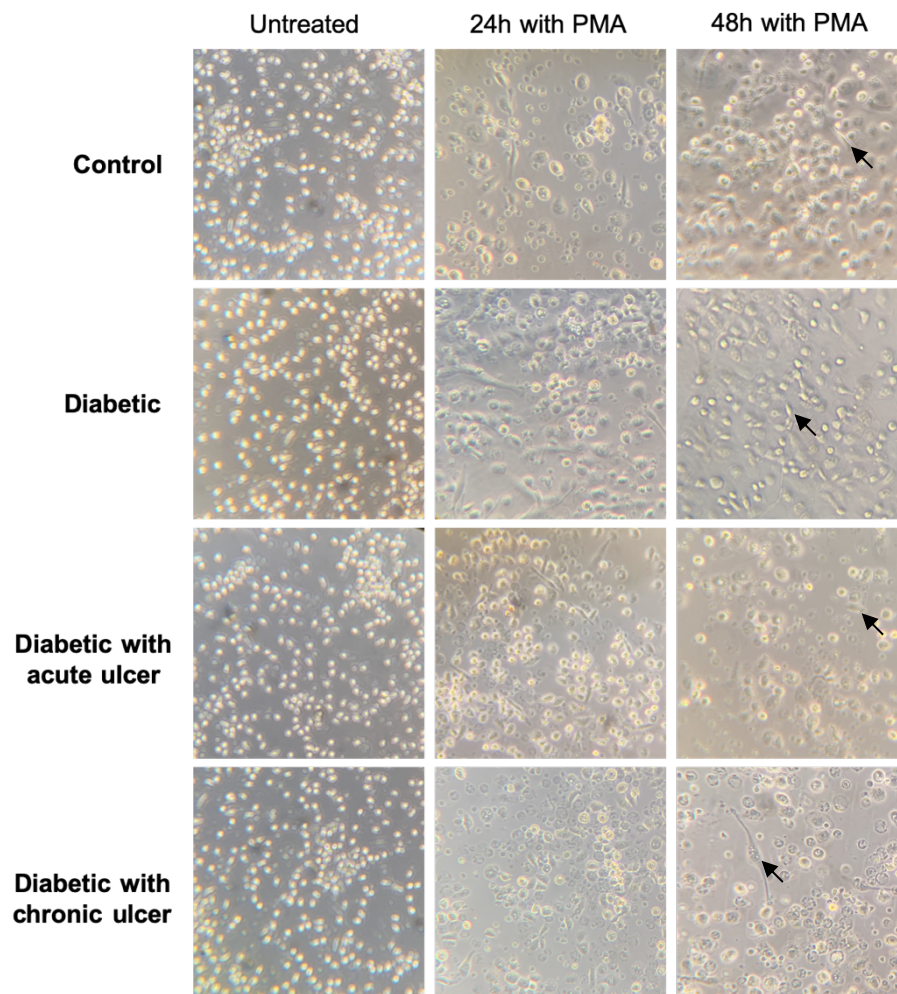
Figure 32 - Morphology of human peripheral blood monocytes-derived macrophages after 48h. (A) Bright field images of human monocytes before and after 24h and 48h of PMA stimulation; it is possible to observe changes and enlargement of the cytoplasm during the two days of differentiation with 200x magnification images. The black arrow indicates a differentiated cell with adherent and flattened morphology.

3.2.2. MSI-1436 did not affect human monocyte-derived macrophages cell viability

MSI-1436 seems to be well tolerated by THP-1 cells not affecting their cell viability. However, it is not known what effect it has on human peripheral blood monocytes viability. Thus, in order to determine MSI-1436 cytotoxicity in human peripheral blood, human cells from control group were differentiated into macrophages and maintained untreated (control) or incubated with 1 µM of PTP1Bi during 24h and the viability was determined by MTT assay. This viability assay was performed on control cells only, since the number of samples and cells obtained from patients is very limited.

PTP1Bi did not affect cell viability in cells treated with 1 µM of PTP1Bi ($96.16 \pm 16.40\%$) (**Figure 33**).
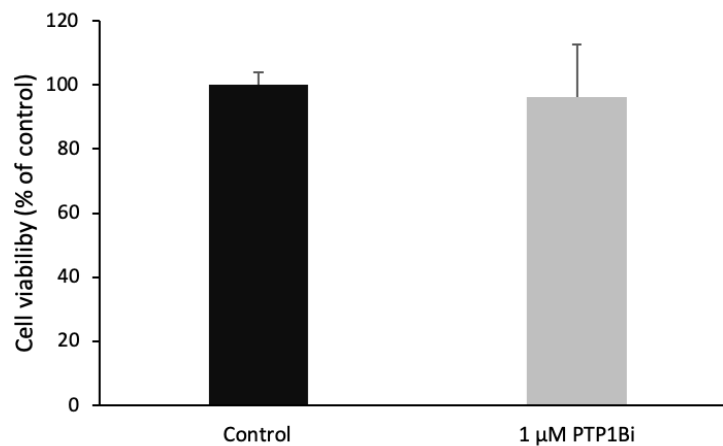
Figure 33 - Effect of PTP1B inhibition on human peripheral blood monocytes viability from control group. Cells were maintained untreated (control) or incubated with 1 µM of PTP1Bi during 24h and cell viability was determined by MTT assay. PTP1Bi did not affect the cell viability. For statistical analysis a student t-test was performed, and no statistical differences were observed. The results are presented as percentage of viable cells relatively to control cells and data are represented as mean ± SEM (*n*=3).

3.2.3. PTP1B inhibition decreased the pro-inflammatory environment in diabetic conditions

As mentioned before, macrophages produce a large number of cytokines, chemokines and growth factors that are directly involved in inflammation and wound healing, and it is important to analyse the effect of PTP1B inhibition in the production of these molecules. Human peripheral blood monocytes were left untreated (control) or treated with LPS and LPS together with 1 µM of PTP1Bi for 24h and the expression of IL-8, IL-6, IL-1β, TNF-α, MCP-1, EGF and PDGF was

analysed by qRT-PCR (**Figure 34**). Furthermore, the IL-6, TNF-α and IL-10 levels were also analysed (**Table 8**).

IL-8 mRNA baseline levels are decreased in the diabetic (0.50 ± 0.11-fold), diabetic with acute ulcer (0.37-fold) and diabetic with chronic ulcer (0.40 ± 0.25-fold) groups when compared to control group (**Figure 34A**). As expected, LPS increased IL-8 mRNA expression in every group (26.39 ± 21.29-fold for control group; 53.73 ± 31.24-fol for diabetic group; 7.04-fold for diabetic with acute ulcer group; 2.06 ± 0.38-fold for diabetic with acute ulcer group), especially in diabetic group. However, the cells of diabetic with acute ulcer and diabetic with chronic ulcer groups showed a lower response to the LPS stimulus. The treatment with 1 μM of PTP1Bi showed different responses for every group. Regarding the control group, 1 μM of PTP1Bi increased IL-8 mRNA levels (73.17 ± 76.52-fold) when compared to LPS treatment while in the diabetic group IL-8 mRNA levels were decreased (38.89 ± 15.52-fold). For the diabetic with both acute and chronic ulcers groups, there was a slight increase in IL-8 mRNA levels (20.76-fold and 2.98 ± 0.50-fold respectively).

IL-6 mRNA expression was only possible to determine in control and diabetic groups. As observed before for IL-8, the baseline levels of IL-6 mRNA were lower in the diabetic group (0.21 ± 0.12-fold) when compared to control group (**Figure 34B**). The LPS stimulus induced an increase in IL-6 mRNA levels (60.55 ± 69.05-fold for control group; 69.88 ± 39.07-fold for diabetic group), particularly in diabetic group. While cells from the control group treated with 1 μM of PTP1Bi increased IL-6 mRNA levels (262.98 ± 319.29-fold), the opposite effect was found in the diabetic group (52.53 ± 6.60-fold). In addition to mRNA expression, the IL-6 levels were measured. As IL-6 mRNA results, the basal levels of IL-6 in diabetic (0.51 ± 0.07 pg/mL), diabetic with acute ulcer (0.53 pg/mL) and diabetic with chronic ulcer (0.56 ± 0.12 pg/mL) groups were lower when compared to control group (0.75 ± 0.15 pg/mL) (**Table 8 and Figure 35A**). The LPS treatment increased IL-6 levels in all groups (21.07 ± 20.21 pg/mL for control group; 10.76 ± 8.69 pg/mL for diabetic group; 4.50 pg/mL for diabetic with acute ulcer group; 0.99 ± 0.29 pg/mL for diabetic with chronic ulcer group), however, the cells of the diabetic with chronic ulcer group seem to be less responsive to LPS stimulation. The pattern observed in mRNA levels was also observed in the control and diabetic groups, demonstrating, respectively, an increase (27.71 ± 25.55 pg/mL) and a decrease (2.53 ± 0.59 pg/mL) of IL-6 levels with 1 μM of PTP1Bi treatment. For diabetic with acute ulcer, a decrease in IL-6 levels was observed with PTP1Bi treatment (3.22 pg/mL) when compared to LPS treatment. In diabetic with chronic ulcer group, PTP1Bi treatment did not have effect on IL-6 levels (1.00 ± 0.44 pg/mL).

The analysis of IL-1β mRNA baseline levels showed a lower expression of IL-1β in the diabetic (0.61 ± 0.12-fold), diabetic with acute ulcer (0.10-fold) and diabetic with chronic ulcer (0.41 ± 0.24-fold) groups when compared to control group (**Figure 35C**). LPS increased IL-1β production in every group (32.16 ± 30.10 pg/mL for control group; 48.52 ± 24.36-fold for diabetic

group; 2.74-fold for diabetic with acute ulcer group; 1.25 ± 0.44-fold for diabetic with chronic ulcer group), particularly in diabetic group. Conversely, the cells of diabetic with acute ulcer and diabetic with chronic ulcer groups showed a lower response to LPS stimulus. In the control group, PTP1Bi treatment increased IL-1β mRNA levels (65.31 ± 72.72-fold) when compared to LPS treatment, while in the diabetic group the same treatment decreased IL-1β mRNA levels (30.39 ± 9.78-fold). In diabetic with acute ulcer groups, PTP1Bi treatment increased IL-1β mRNA levels (13.18-fold), however, in the diabetic with chronic ulcer group, PTP1Bi treatment did not change IL-1β expression (1.30 ± 0.41-fold).

The basal expression of TNF-α mRNA was decreased in the diabetic (0.36 ± 0.08-fold), diabetic with acute ulcer (0.13-fold) and diabetic with chronic ulcer (0.61 ± 0.85-fold) groups when compared to control group (**Figure 34D**). LPS increased TNF-α mRNA in all groups, especially in the diabetic group (5.09 ± 0.73-fold for control group; 7.21 ± 1.80-fold for diabetic group; 1.90-fold for diabetic with acute ulcer group; 0.91 ± 0.29-fold for diabetic with chronic ulcer group). However, the cells of diabetic with acute ulcer and diabetic with chronic ulcer groups showed a lower response to LPS stimulus. For control group, PTP1Bi treatment increased TNF-α mRNA levels (7.52 ± 4.98-fold) when compared to LPS treatment whereas for diabetic group, the same treatment, decreased TNF-α mRNA levels (5.41 ± 1.60-fold). For the diabetic with acute ulcers and diabetic with chronic ulcers, TNF-α mRNA levels increased with PTP1Bi treatment (6.38-fold and 1.86 ± 0.35-fold, respectively). Similar results were found with TNF-α levels, higher levels of TNF-α were found in the control when compared with the other groups (2.21 ± 0.41 pg/mL for control group; 1.53 ± 0.09 pg/mL for diabetic group; 1.61 pg/mL for diabetic with acute ulcer group; 1.70 ± 0.22 pg/mL for diabetic with chronic ulcer group) (**Table 8 and Figure 35B**). LPS increased TNF-α levels in every groups (31.43 ± 27.57 pg/mL for control group; 9.15 ± 3.93 pg/mL for diabetic group; 19.53 pg/mL for diabetic with acute ulcer group; 4.88 ± 1.86 pg/mL for diabetic with chronic ulcer group) and the treatment with 1 μM of PTP1Bi induced an increase in control (40.15 ± 33.50 pg/mL) and diabetic with acute ulcer (24.21 pg/mL) whereas for diabetic (4.37 ± 1.08 pg/mL) and diabetic with chronic ulcers (4.42 ± 1.16 pg/mL), TNF-α levels were decreased with a higher effect in the diabetic group.

The MCP-1 mRNA levels were not detected in the diabetic with acute ulcers group. The baseline values of MCP-1 mRNA were higher for control group (1.00 ± 0.59-fold) than for diabetic (0.55 ± 0.28-fold) and diabetic with chronic ulcers groups (0.63-fold) (**Figure 34E**). The LPS treatment increased MCP-1 mRNA levels in control (11.49 ± 10.85-fold) and diabetic (18.52 ± 16.11-fold) groups but, surprisingly, induced a decrease in diabetic with chronic ulcer (0.28 ± 0.24-fold). Additionally, the PTP1Bi treatment increased MCP-1 mRNA levels in control group (66.61 ± 79.94-fold) and decreased MCP-1 mRNA levels in diabetic (12.07 ± 8.70-fold) and diabetic with chronic ulcer (0.20 ± 0.13-fold) groups.

The levels of IL-10 were also determined (**Table 8 and Figure 35C**). The basal IL-10 levels are very similar across the different groups (0.95 ± 0.04 pg/mL for control group; 0.91 ± 0.04 pg/mL for diabetic group; 0.87 pg/mL for diabetic with acute ulcer group; 0.90 ± 0.01 pg/mL for diabetic with chronic ulcer group). The treatment with LPS resulted in an increase of IL-10 levels in all groups (2.53 ± 1.48 pg/mL for control group; 2.64 ± 1.55 pg/mL for diabetic group; 1.26 pg/mL for diabetic with acute ulcer group; 0.94 ± 0.00 pg/mL for diabetic with chronic ulcer group), nonetheless this increase was very low for the diabetic with chronic ulcer group. Moreover, the PTP1B inhibitor induced an increase in IL-10 levels in the control (2.98 ± 1.85 pg/mL) and diabetic (1.39 ± 0.21 pg/mL) groups while did not have an impact on diabetic with acute (1.27 pg/mL) and chronic (0.92 ± 0.04 pg/mL) ulcer group.

Finally, the EGF and PDGF mRNA expression were also measured. EGF expression was only possible to detect in control and diabetic groups. In basal conditions, EGF mRNA levels were decreased in the diabetic group (0.16 ± 0.13-fold) when compared to control group. LPS increased EGF mRNA expression in both groups (1.12 ± 1.09-fold for control group; 0.69 ± 0.49-fold for diabetic group) and the treatment with 1 µM of PTP1Bi induced a decrease in EGF mRNA levels in control group (0.75 ± 0.42-fold) and an increase in diabetic group (1.17 ± 0.63-fold) when compared to LPS. For PDGF, in baseline levels the control group (1.00 ± 0.44-fold) showed a higher expression than the other groups (0.20 ± 0.08-fold for diabetic group; 0.12-fold for diabetic with acute ulcer group; 0.56 ± 0.27-fold for diabetic with chronic ulcer group). LPS decreased PDGF mRNA levels in all groups (0.35 ± 0.10-fold for control group; 0.07-fold for diabetic with acute ulcer group; 0.40 ± 0.12-fold for diabetic with chronic ulcer group) except for diabetic group where occurred a slight increase (0.29 ± 0.01-fold). In this case, the application of 1 µM of PTP1Bi increased PDGF expression in every group (0.51 ± 0.24-fold for control group; 0.50 ± 0.17 for diabetic group; 0.34-fold for diabetic with acute ulcer group; 0.55 ± 0.12-fold for diabetic with chronic ulcer group).

The expression of the growth factors TGF-β and VEGF was also analysed before and after the treatment with PTP1Bi, however, there were no relevant changes (data not shown).

Through the analysis of all data, it was possible to observe that PTP1B inhibition seems to lead to a decrease of pro-inflammatory environment in diabetic conditions. Macrophages derived from monocytes of the diabetic with acute and chronic ulcers showed to be less responsive to stimulus than the cells from the other two groups, which may compromise the effect of PTP1Bi treatment.

A

B

C

D

E

F

G
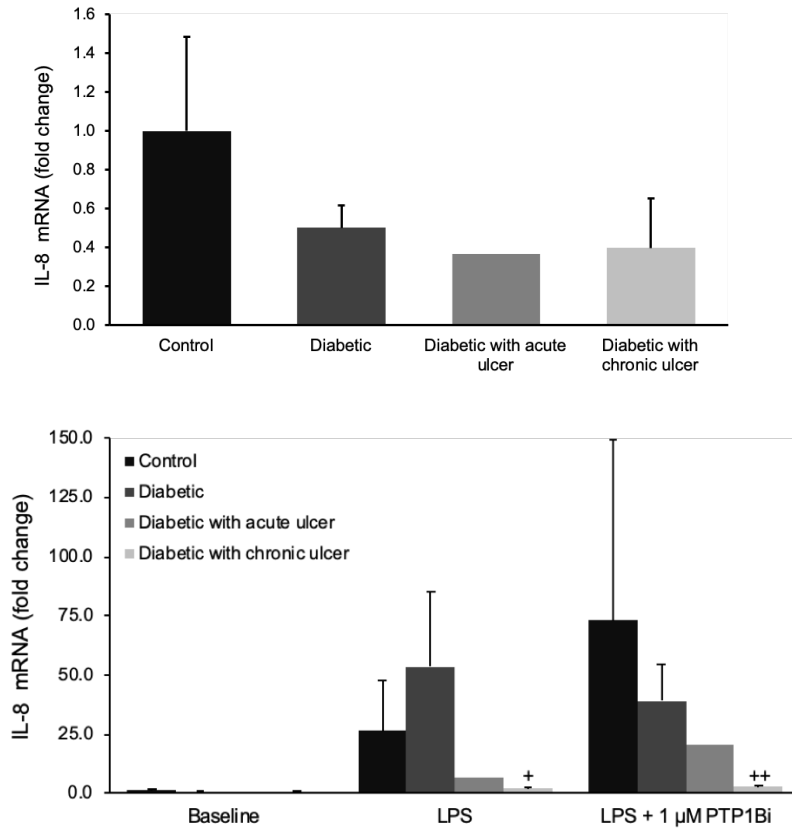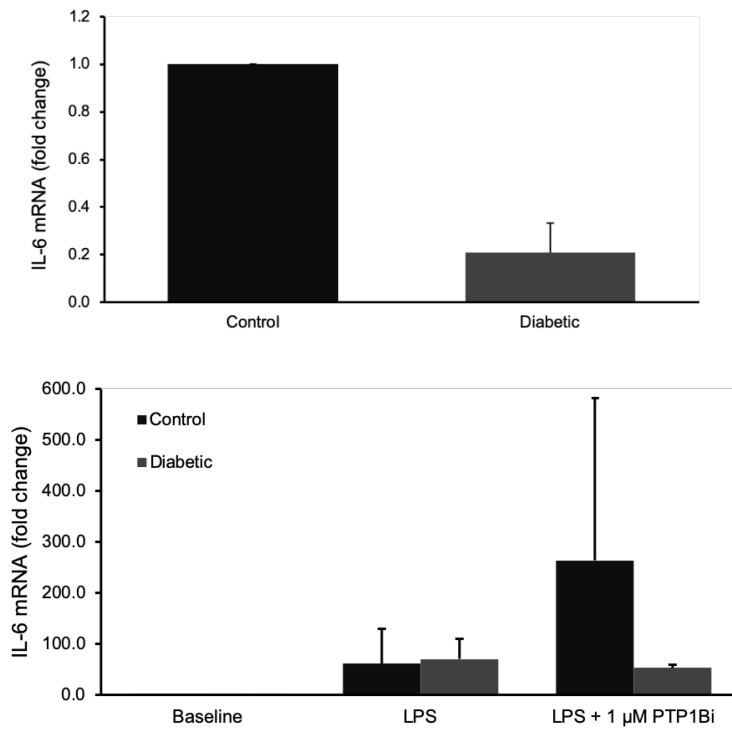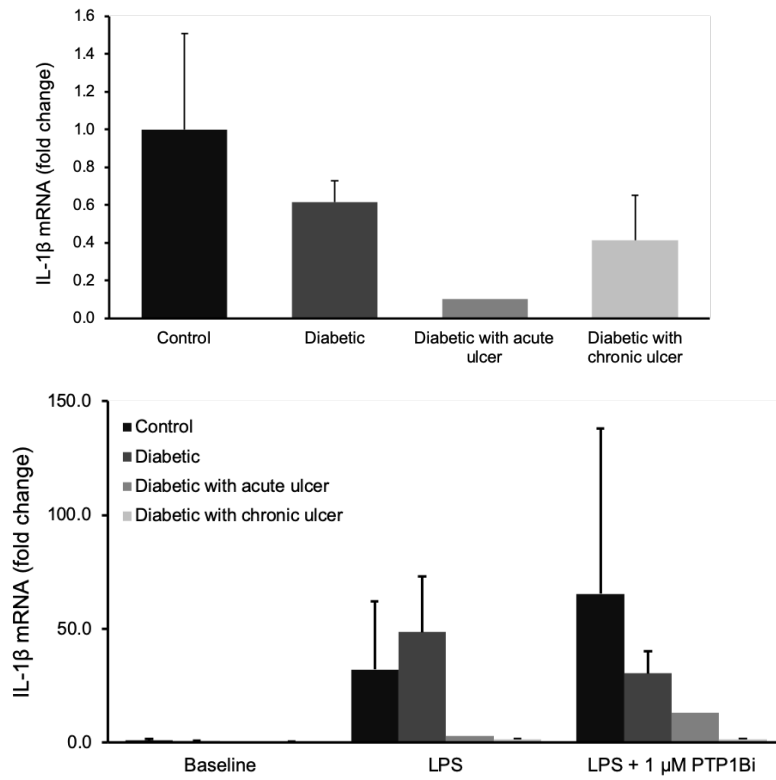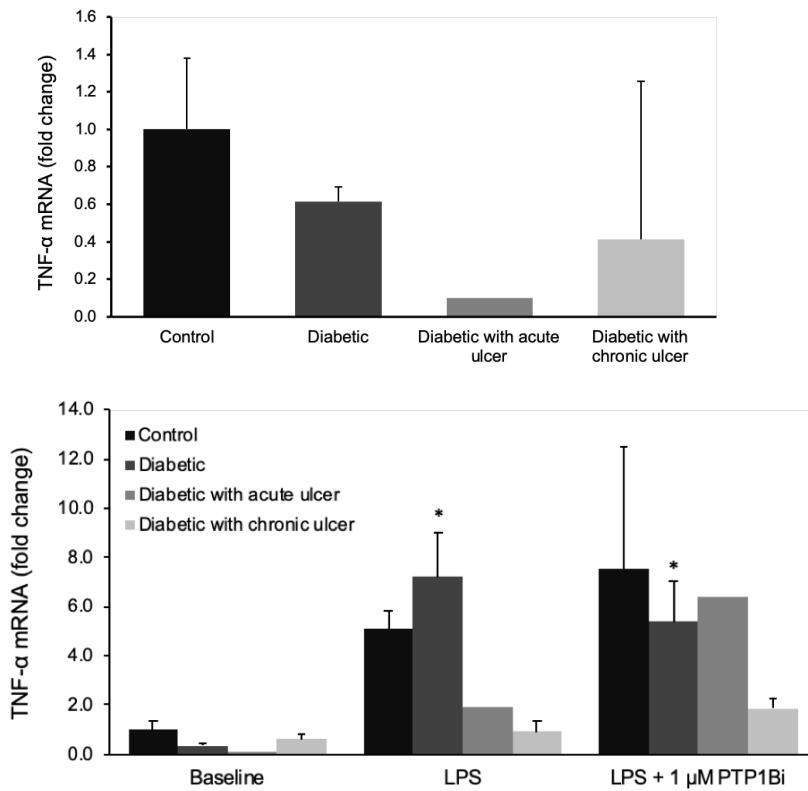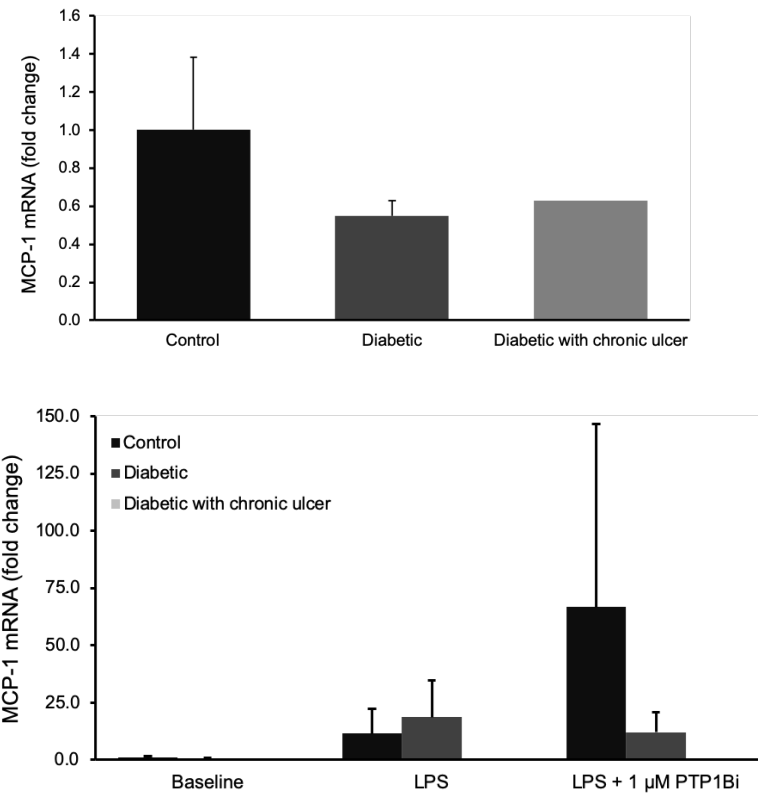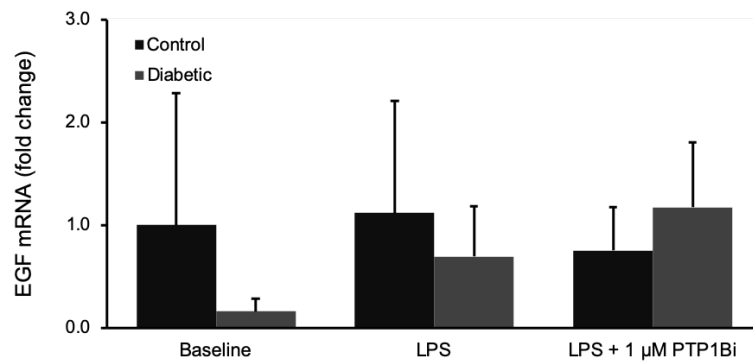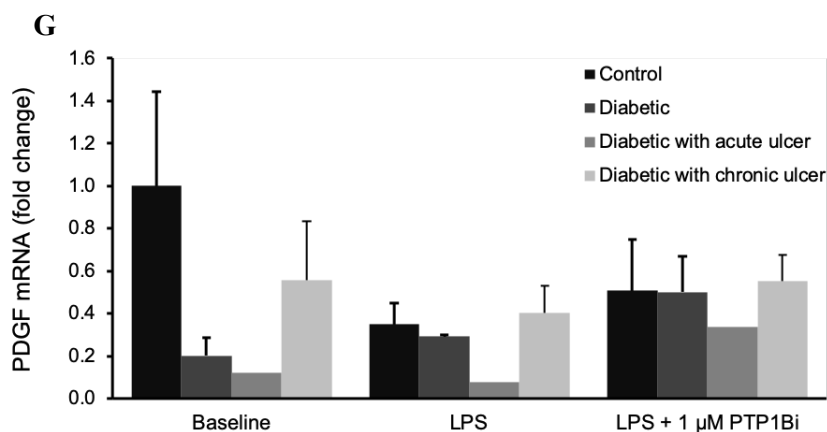
Figure 34 - Effect of PTP1B inhibition on IL-8, IL-6, IL-1β, TNF-α, MCP-1, EGF and PDGF expression in human peripheral blood monocytes from control and patient groups. Cells were left untreated (control) or incubated with 1 µg/mL of LPS or LPS together with 1 µM of PTP1Bi during 24h. The expression of (A) IL-8, (B) IL-6, (C) IL-1β, (D) TNF-α, (E) MCP-1, (F) EGF and (F) PDGF was measured using qRT-PCR. The mRNA expression for each gene was normalized to the housekeeping gene TBP and calculated as the fold change of the baseline of control group. For statistical analysis a one-way ANOVA, followed by a Newman-Keuls post-test, was performed to compare the different groups independently. The results are represented as mean ± SEM ($n=3$ for control, diabetic and diabetic with chronic ulcer groups; $n=1$ for diabetic with acute ulcer group). * $p<0.05$ *vs* diabetic group; + $p<0.05$ *vs* diabetic with chronic ulcer group; ++ $p<0.01$ *vs* diabetic with chronic ulcer group. **Legend:** IL-8 → Interleukin 8; IL-6 → Interleukin 6; IL-1β → Interleukin 1 beta; TNF-α → Tumour necrosis factor alpha; MCP-1 → Monocyte chemoattractant protein-1; EGF → Epidermal growth factor; PDGF → Platelet-derived growth factor; TBP → TATA binding protein.

Table 8 - IL-6, TNF-α and IL-10 levels in human peripheral blood monocytes from control and patient groups. Cells were left untreated (control) or incubated with 1 µg/mL of LPS or LPS together with 1 µM of PTP1Bi during 24h. For statistical analysis a one-way ANOVA, followed by a Newman-Keuls post-test, was performed to compare the different groups independently and no statistical differences were observed. The results are represented as mean ± SEM ($n=3$ for control, diabetic and diabetic with chronic ulcer groups; $n=1$ for diabetic with acute ulcer group).

Cytokine	Patients	Conditions		
		Baseline	LPS	LPS + 1 µM PTP1Bi
IL-6 (pg/mL)	Control	0.75 ± 0.15	21.07 ± 20.21	27.71 ± 25.55
	Diabetic	0.51 ± 0.07	10.76 ± 8.69	2.53 ± 0.59
	Diabetic with acute ulcer	0.53	4.50	3.22
	Diabetic with chronic ulcer	0.56 ± 0.12	0.99 ± 0.29	1.00 ± 0.44
TNF-α (pg/mL)	Control	2.21 ± 0.41	31.43 ± 27.57	40.15 ± 33.50
	Diabetic	1.53 ± 0.09	9.15 ± 3.93	4.37 ± 1.08
	Diabetic with acute ulcer	1.61	19.53	24.21
	Diabetic with chronic ulcer	1.70 ± 0.22	4.88 ± 1.86	4.42 ± 1.16
IL-10 (pg/mL)	Control	0.95 ± 0.04	2.53 ± 1.48	2.98 ± 1.85
	Diabetic	0.91 ± 0.04	2.64 ± 1.55	1.39 ± 0.21
	Diabetic with acute ulcer	0.87	1.26	1.27
	Diabetic with chronic ulcer	0.90 ± 0.01	0.94 ± 0.03	0.92 ± 0.04
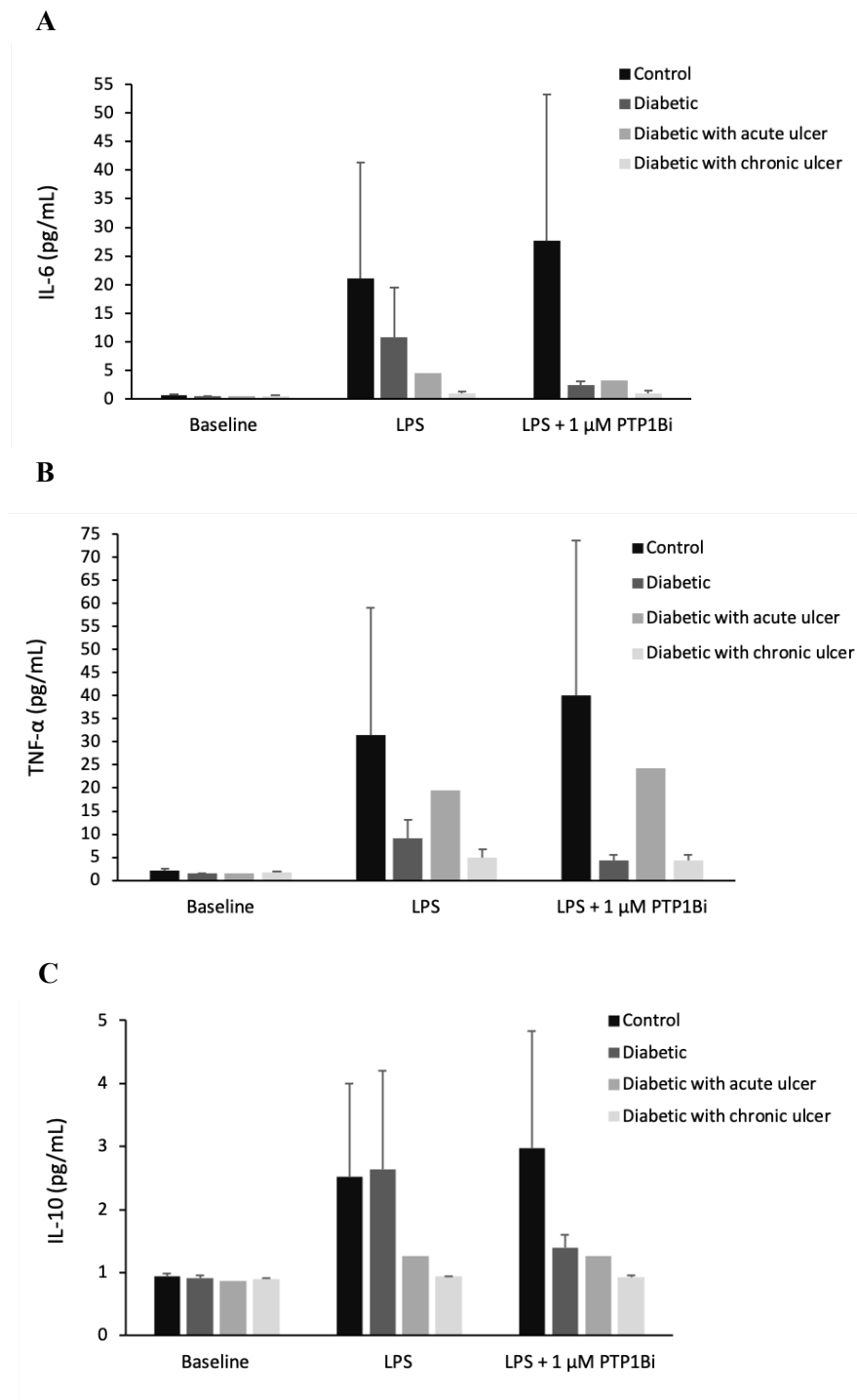
Figure 35 - The effect of PTP1B inhibition on IL-6, TNF-α and IL-10 levels in human peripheral blood monocytes from control and patient groups, left untreated (control) or incubated with 1 μg/mL of LPS or LPS together with 1 μM of PTP1Bi during 24h and the levels of (A) IL-6, (B) TNF-α, and (C) IL-10 was measured using a LEGENDplex^TM Multi-Analyte Flow Assay. For statistical analysis a one-way ANOVA, followed by a Newman-Keuls post-test, was performed to compare the different groups independently and no statistical differences were observed. The results are represented as mean ± SEM (*n*=4). **Legend:** IL-6 → Interleukin 6; TNF-α → Tumour necrosis factor alpha; IL-10 → Interleukin 10.

3.3. Animal experiments

In order to determine whether PTP1B inhibition (Trodusquemine, MSI-1436) improves diabetic wound healing, an STZ-induced diabetic mouse model was used. Streptozotocin, originally identified as an antibiotic, is extracted from the gram-negative bacteria *Streptomyces achromogenes* whose diabetogenic properties were described, for the first time, in 1963 [209]–[211]. When administered to mice, STZ is highly cytotoxic to pancreatic β-cell leading to the death and destruction of these cells resulting in hyperglycaemia and insulin deficiency, which are characteristics of human TD1M. STZ-induced diabetic mouse is being widely used as an animal model for diabetes, mainly due to its low cost and great similarity to TD1M observed in humans [210], [211].

To determine which dose of MSI-1436 (PTP1Bi) would be the most effective for wound healing, STZ-induced diabetic mice were divided into four different groups: the groups with wounds topically treated with 1 µg, 10 µg or 25 µg of PTP1Bi, and the control group whose wounds were treated with saline. Two wounds were created in each mouse with 6 weeks of diabetes and the animals were treated with the respective PTP1Bi dose every day until sacrifice, which occurred at day 10 after wounding. As a result of this experiment, the 1 µg dose was chosen as the most effective and a second experiment was performed wherein animals were treated only with this dose every day until sacrifice. The animals were sacrificed at day 3 to assess acute inflammatory phase and at day 10 to assess the proliferation and remodelling phase of wound healing.

On the day of surgery (day 0) and after 6 weeks of diabetes, mice from different groups weighed between 22-28 g and had blood glucose levels between 320-520 mg/dL (**Table 9**). All animals were diabetic at the time of surgery since they had a blood glucose level above 250 mg/dL. No significant differences were found between the weights and glycemia of the animals from the different groups.

Table 9 - Body weight and blood glucose levels of mice from different groups at day 0. For statistical evaluations a student t-test and a one-way ANOVA, followed by a Newman-Keuls post-test, were performed, and no statistical differences were observed; data are represented as mean ± SEM.

	Body Weight, g	**Glycaemia, mg/dL**	***n***
Control Group	24.05 ± 0.61	433 ± 18	10
Group 1 µg PTP1Bi	24.7 ± 0.53	422 ± 14	10
Group 10 µg PTP1Bi	24.27 ± 1.47	464 ± 13	3
Group 25 µg PTP1Bi	26.3 ± 1.72	446 ± 12	3

3.3.1. PTP1B inhibition improved wound healing in diabetes

As mentioned before, a preliminary experiment was performed in order to assess the ideal dose for PTP1Bi. For that, mouse wounds were treated topically at the wound site with 1 µg, 10 µg or 25 µg of PTP1Bi, and with saline. The wound area was measured using acetate tracing every day to follow the rate of wound closure up to 10 days post-wounding.
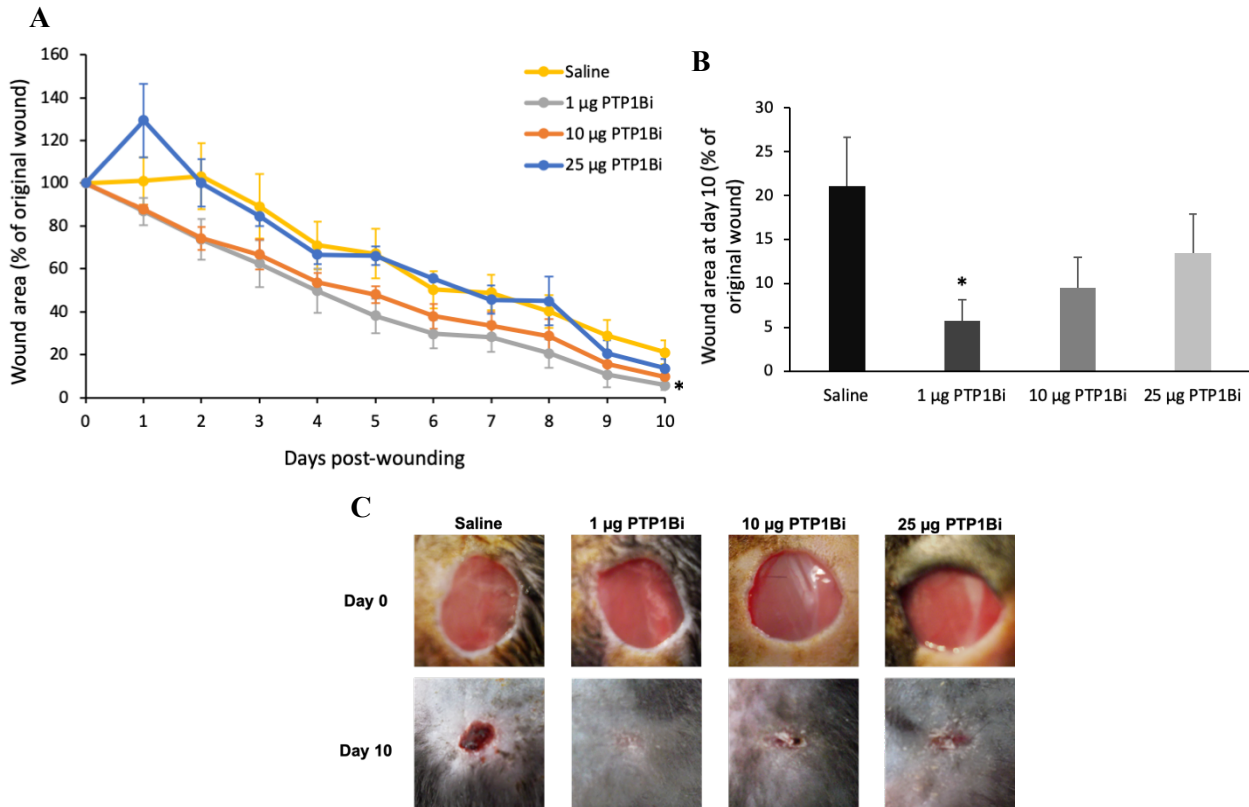
Figure 36 - Effect of PTP1Bi in diabetic wound healing. (A) Percentage of original wound area during the 10 days of experiment in all groups, (B) percentage of original wound area at day 10 in mice treated with 1 µg, 10 µg or 25 µg of PTP1Bi, and saline-treated mice. Results are presented as percentage of original wound. (C) Representative images of the wounds at day 0 and day 10. Day 0 pictures were taken immediately after wounding. For statistical evaluations a student t-test was performed, and data are represented as mean ± SEM (*n*=6 wounds per group). * *p*<0.05 compared to saline.

The wounds treated with 1 and 10 µg of PTP1Bi exhibited a faster wound closure when compared to saline treated wounds (**Figure 36A**). Wounds treated with 25 µg of PTP1Bi exhibited a wound closure progression very similar to saline. The wounds at day 10 were more closed with 1 ug of PTP1Bi treatment, with only 5.75 ± 2.38% of the initial wound size, being significantly different from control wounds (*p*<0.05, *n*=6 wounds) (**Figure 36B**). PTP1Bi treatment with 10 µg and 25 µg also accelerated wound closure to 9.55 ± 3.40% and 13.47 ± 4.43% respectively, however, this decrease in wound size was not significantly different from saline-treat wounds with 21.08 ± 5.58% of original wound size. At day 10, the beneficial effect of PTP1B inhibition in wound healing was clear between the wounds size of the different groups, especially in 1 µg of PTP1Bi

with the wound is almost completely closed, as represented by the wound pictures (**Figure 36C**). This pilot study, in addition to other observations described later, 1 µg of PTP1Bi was defined as the most effective. Thus, another animal experiment was performed where the animal wounds were treated with 1 µg of PTP1Bi to evaluate how the inhibition of PTP1B is improving diabetic wound healing. The animals were then sacrificed at day 3 to evaluate the acute inflammatory phase and at day 10 to evaluate the proliferative and remodelling phase of wound healing.
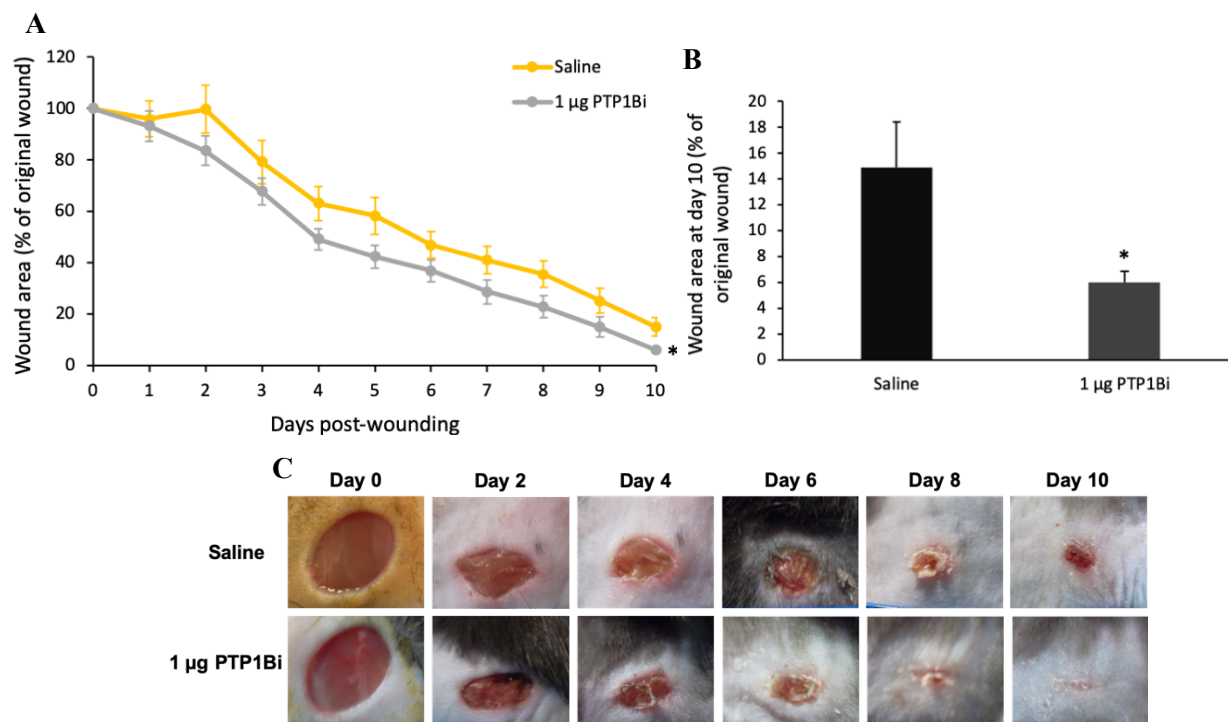
Figure 37 - The effect of 1 µg of PTP1Bi in diabetic wound healing. (A) Percentage of original wound area during the 10 days and (B) percentage of original wound area at day 10 in mice treated with1 µg of PTP1Bi or saline. Results are presented as percentage of original wound. (C) Representative images of the wounds at days 0, 2, 4, 6, 8 and 10. Day 0 pictures were taken immediately after wounding. For statistical evaluations a student t-test was performed, and data are represented as mean ± SEM (*n*=12 wounds per group). * *p*<0.05 compared to saline.

In the second experiment, the PTP1Bi effectiveness and contribution to wound healing was confirmed. During all wound healing process, it was possible to observe that PTP1Bi led to an accelerated wound closure when compared with saline-treated wounds (**Figure 37A and C**). This difference became more significant at day 10 since the PTP1Bi treated wounds were almost totally closed (5.96 ± 0.88% of the original wound) when compared with saline-treated wounds (14.90 ± 3,55%, *p*<0.05, *n*=12 wounds) (**Figure 37B**). The observation of the representative images on **Figure 37C** suggest that the applied treatment decreased the wound size specially at days 8 and 10 comparing to saline, nearly achieving the complete closure of the wound. In order to evaluate how PTP1Bi improves wound healing it was investigated, at the wound site, the pro-inflammatory environment, oxidative stress, angiogenesis as well as the proliferation and remodelling phases of wound healing.

3.3.2. PTP1B inhibition decreased the pro-inflammatory environment at the wound site

One of the main problems associated with delayed wound healing in diabetes is the substantial pro-inflammatory environment present in the wounds. This environment is mainly caused by an elevated number of M1 macrophages present in the diabetic wound. Since the inflammatory environment does not allow the M1 macrophages to convert into anti-inflammatory M2 macrophages, the resolution of the inflammatory phase is delayed and the M1 macrophages present in the wound release high levels of pro-inflammatory cytokines, which leads to a substantial pro-inflammatory environment at the wound site. One of the hypotheses of this work is that the application of PTP1Bi at the wound site will reduce the pro-inflammatory environment promoting the conversion of M1 to M2 macrophages and improving wound healing. To test this hypothesis, the wounded skin from mice treated with 1 µg, 10 µg and 25 µg of PTP1Bi, or saline was harvested after 10 days of treatment, embedded in OCT compound and frozen to perform immunohistochemistry assays. For detection of M1 macrophages, it was used a double staining with CD68 (pan-macrophage marker, green) and TNF-α (M1 specific marker, red) (**Figure 38A**), and for M2 macrophages, it was used the CD68 and CD206 (M2 specific marker, red) (**Figure 38C**). The yellow fluorescence present in the merged image represents the places where double staining occurs. The M1/M2 ratio was also evaluated since increased M1/M2 values are correlated with a high inflammatory environment while decreased values are more related with an anti-inflammatory environment. One second animal experiment was performed using the 1 µg of PTP1Bi and the animals were sacrificed either at day 3 or at day 10.

PTP1Bi treatment decreased the number double-positive for CD68 and TNF-α stained cells at the wound site (**Figure 38B**). The treatment that cause a higher decrease on the inflammatory M1 macrophages number was the 10 µg of PTP1Bi to $71.35 \pm 9.74\%$ when compared to saline ($100 \pm 10.54\%$); 25 µg of PTP1Bi decreased the M1 number to $85.12 \pm 20.76\%$ and 1 µg of PTP1Bi to $93.57 \pm 13.77\%$. Although this result was not statistically significant it may have biologically significance since this reduction in the number of M1 macrophages possibly leads to a reduction in the pro-inflammatory environment present in the wound. On the other hand, PTP1Bi treatment increased the number of anti-inflammatory M2 macrophages at the wound site (**Figure 38D**). In this case, the treatment that was the most effective was the 1 µg of PTP1Bi, since it increased the M2 number to $141.86 \pm 13.73\%$ when compared to saline ($100 \pm 14.04\%$). A small increase was also observed in 10 µg of PTP1Bi treatment, where the M2 number increased to $104.49 \pm 10.25\%$. However, 25 µg of PTP1Bi appears to have no effect on the number of M2 macrophages present at the wound site ($85.71 \pm 6.07\%$ comparing to saline). These *in vivo* data can indicate that PTP1B treatment modulates the macrophage phenotype present in the wound towards an anti-inflammatory M2 macrophage. This result supports the idea that PTP1B inhibition may lead to a reduction in the

pro-inflammatory environment present in the wound which can contribute to an accelerated wound healing. To confirm this hypothesis, the M1/M2 ratio was also calculated and it is clear that the treatment with 1 µg and 10 µg of PTP1Bi decreased the M1/M2 ratio when compared to saline (**Figure 38E**). The M1/M2 ratio for 1 µg of PTP1Bi was 0.56 ± 0.09 and for 10 µg of PTP1Bi it was 0.58 ± 0.05. The 25ug of PTP1Bi had a similar M1/M2 ratio to saline (0.85 ± 0.14 and 0.85 ± 0.09 respectively). Taking all this into account, it was possible to conclude that the treatment with 1 µg, as well as 10 µg of PTP1Bi led to a decrease in the pro-inflammatory environment present in the wound contributing to faster wound closure.

B

C

| | CD206 | CD68 | CD206 + CD68 + DAPI |

Saline

1 µg PTP1Bi

10 µg PTP1Bi

25 µg PTP1Bi

50 µM

D

E
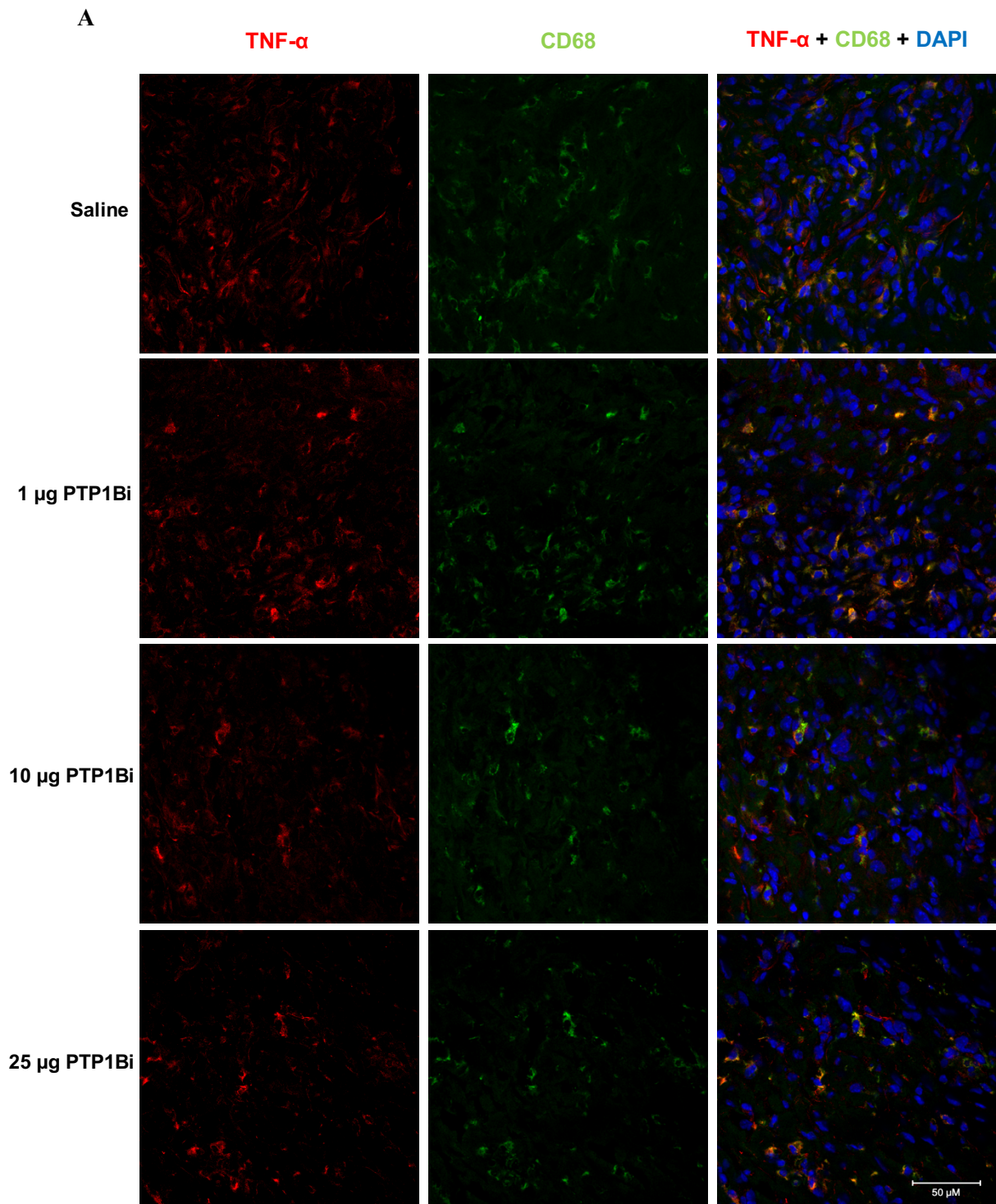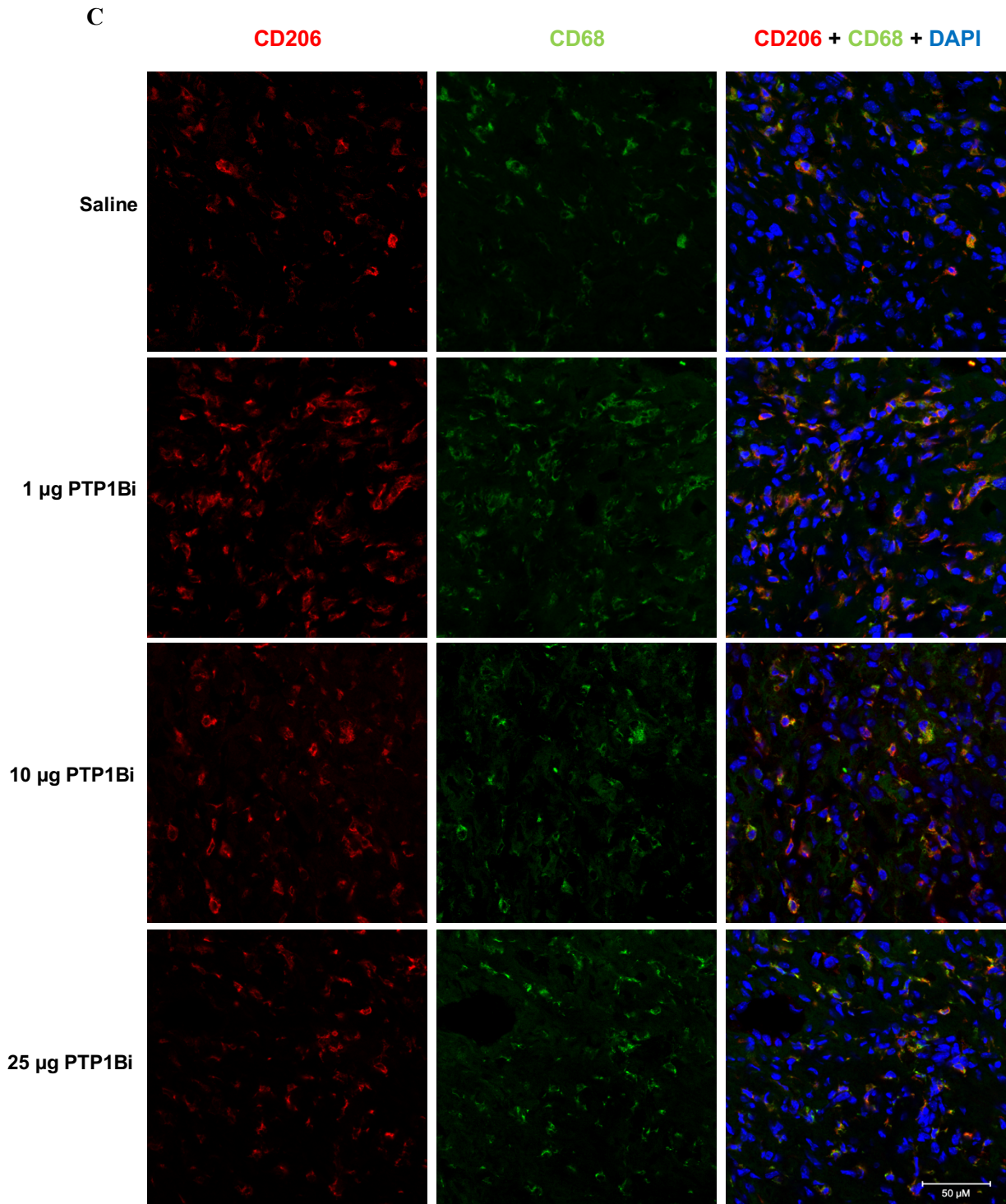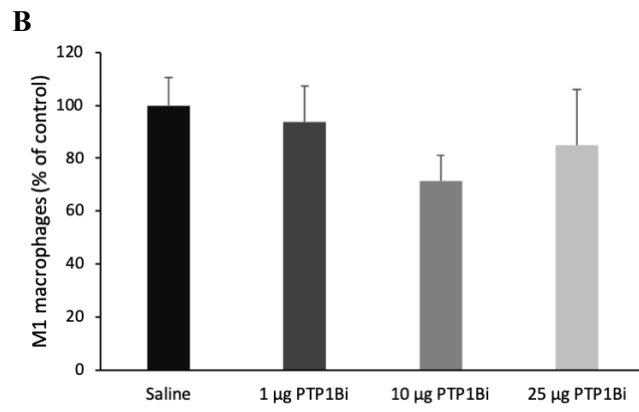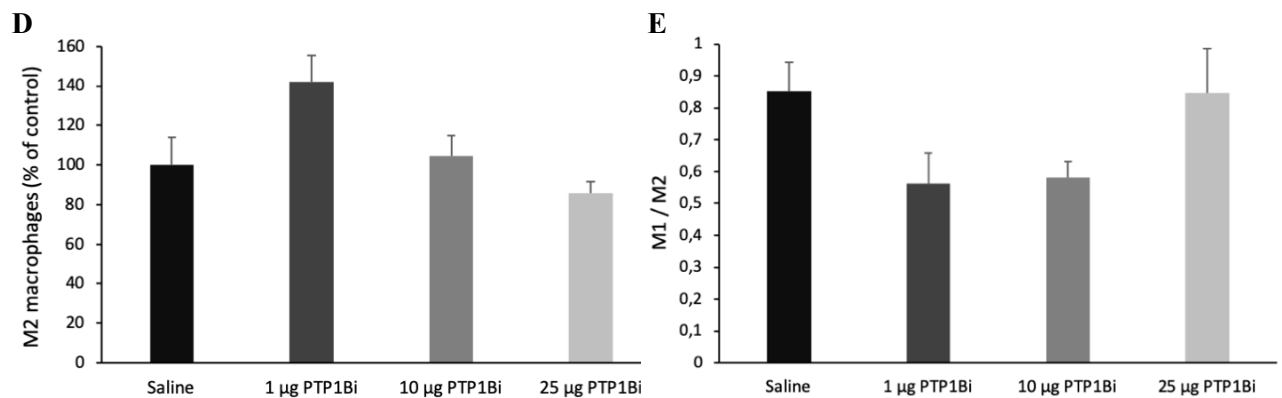
Figure 38 - The treatment with PTP1Bi altered the macrophage phenotype towards an anti-inflammatory environment in diabetic wounds at day 10. (A) Representative 400x magnification images of the macrophage marker proteins CD68 (pan-macrophage marker, green) and TNF-α (M1 marker, red), showing that PTP1Bi treatment decreased the co-localization of CD68 and TNF-α, indicating a total decrease of M1 macrophages (yellow). (B) Quantification of M1 macrophages (CD68 + TNF-α double-positive cells) present in the wound at day 10. (C) Representative 400x magnification images of the macrophage marker proteins CD68 and CD206 (M2 marker, red), showing that PTP1Bi treatment increased the co-localization of CD68 and CD206, indicating a total increase of M2 macrophages (yellow). (D) Quantification of M2 macrophages (CD68 + CD206 double-positive cells) present in the wound at day 10. (E) M1/M2 ratio for the treatment groups and saline group, the doses 1 μg and 10 μg of PTP1Bi decreased M1/M2 ratio. For statistical analysis a student t-test was performed to compare the treatment groups with the saline-treated group, and no statistical differences were observed. Nuclei were stained with DAPI (blue). Scale bar is 50 μm. The results are presented as percentage of macrophage (M1 or M2) number in saline-treated wounds and represented as mean ± SEM (n=3 mice per group).

As mentioned before, the dose 1 μg of PTP1Bi was selected to further evaluate the role of PTP1B inhibition in diabetic wound healing. For this experiment, the wounded skin from mice treated with 1 μg of PTP1Bi, and saline mice was harvested after 3 or 10 days of treatment and analysed by immunohistochemistry assays. The day 3 post-wounded skin was used to assess the acute inflammatory phase, and M1 (**Figure 39A**) and M2 macrophages (**Figure 39C**) were quantified by immunohistochemistry, as described before.

The wounds at day 3 showed that the treatment with 1 μg of PTP1Bi decreased the number of inflammatory M1 macrophages to $85.80 \pm 6.73\%$ when compared to saline ($100 \pm 3.11\%$) (**Figure 39B**) and increased significantly the number of M2 macrophages (**Figure 39D**) to $129.51 \pm 3.71\%$ comparing to saline ($100 \pm 4.83\%$) ($p<0.01$, n=4 mice), these results suggest that PTP1B inhibition prevents the exaggerated inflammation in a very early state of the wound healing process. The value of M1/M2 ratio of 1 μg of PTP1Bi treatment (0.53 ± 0.03) was significantly lower than the control value (0.81 ± 0.04) ($p<0.01$, n=4 mice) (**Figure 39E**), which corroborates the idea that inhibition of PTP1B may be essential for the initial fight against exacerbated inflammation.

A

TNF-α | CD68 | TNF-α + CD68 + DAPI

Saline

1 μg PTP1Bi

50 μM

B

C

CD206 | CD68 | CD206 + CD68 + DAPI

Saline

1 μg PTP1Bi

50 μM
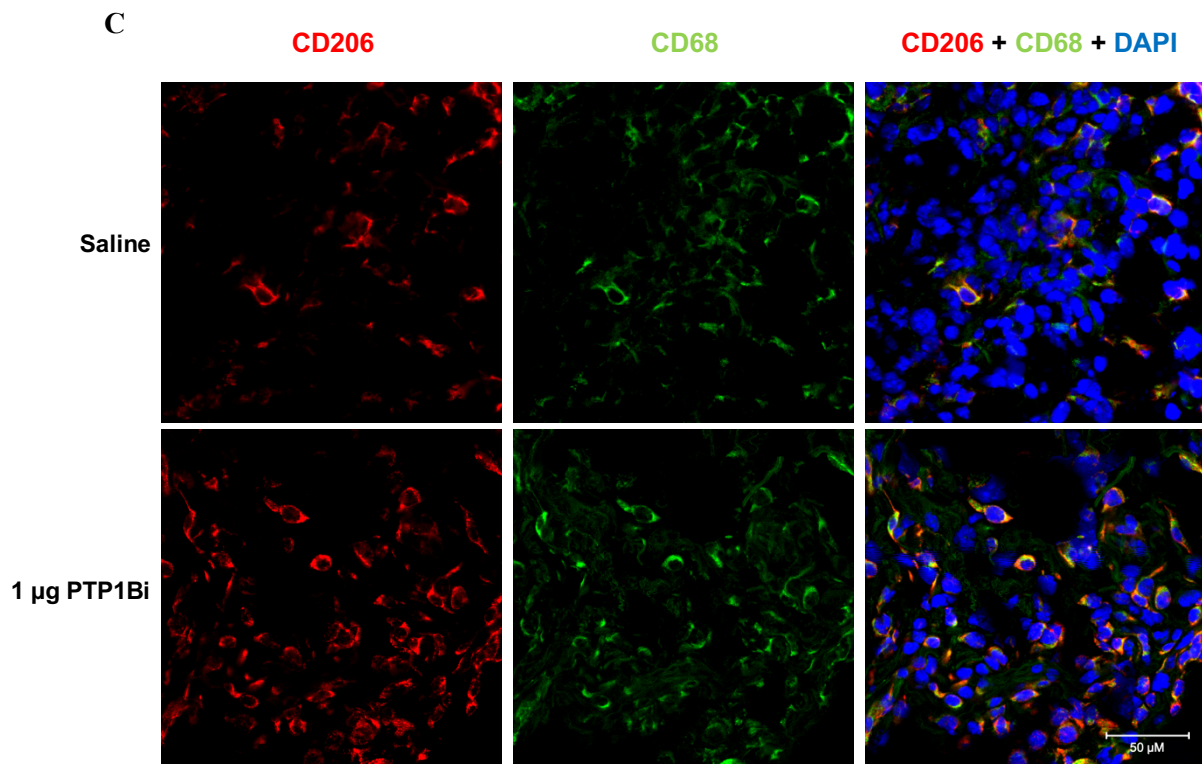
Figure 39 - The treatment with 1 μg of PTP1Bi altered the macrophage phenotype towards a decreased inflammatory environment in diabetic wounds at day 3. (A) Representative 400x magnification images of the macrophage marker proteins CD68 (green) and TNF-α (red), showed that 1 μg of PTP1Bi decreased the co-localization of CD68 and TNF-α, indicating a total decrease of M1 macrophages (yellow). (B) Quantification of M1 macrophages (CD68 + TNF-α double-positive cells) in the wound at day 3. (C) Representative 400x magnification images of the macrophage marker proteins CD68 (green) and CD206 (red), showed that 1 μg of PTP1Bi increased the co-localization of CD68 and CD206, indicating a total increase of M2 macrophages (yellow). (D) Quantification of M2 macrophages (CD68 + CD206 double-positive cells) in the wound at day 3. (E) M1/M2 ratio for 1 μg PTP1Bi treatment and saline, 1 μg of PTP1Bi significantly decreased M1/M2 ratio. For statistical analysis a student t-test was performed to compare the treatment group with the saline-treated group. Nuclei were stained with DAPI (blue). Scale bar is 50 μm. The results are presented as percentage of macrophage (M1 or M2) number in saline-treated wounds and represented as mean ± SEM (n=4 mice per group). ** p<0.01 compared to saline.

The wounds at day 10 confirmed the results observed in the pilot experiment (**Figure 40A and C**). The treatment with 1 μg of PTP1Bi decreased the number of inflammatory M1 macrophages to 88.78 ± 6.51% comparing to saline (100 ± 6.21%) (**Figure 40B**) and increased significantly the number of M2 macrophages to 132.34 ± 7.46% comparing to saline (100 ± 8.88%) (p<0.05, n=6 mice) (**Figure 40D**). The value of M1/M2 ratio of 1 μg of PTP1Bi treatment was 0.6 ± 0.05 and the value of saline treatment was 0.91 ± 0.09 (p<0.05, n=6 mice) (**Figure 40E**).

One of the major problems in diabetic wounds is the accumulation of M1 macrophages that maintain an exaggerated inflammation and delay or stall the normal wound closure. The treatment with 1 μg of PTP1Bi appears to counteract this accumulation of M1 and promote its conversion to M2 facilitating the environment for wound closure. The increase in the number of M2 macrophages at day 10, during the proliferation and remodelling phases of wound healing, in the wounds treated with PTP1B inhibitor have a relevant role since M2 macrophages release several growth factors essential for cell proliferation and have an important role in tissue remodelling and repair. Thus, in addition to the decrease in the pro-inflammatory environment, the inhibition of PTP1B also promotes an increase in the number of M2 macrophages, facilitating wound closure.

A

TNF-α CD68 TNF-α + CD68 + DAPI

Saline

1 μg PTP1Bi

50 μM

B

C

CD206 CD68 CD206 + CD68 + DAPI

Saline

1 μg PTP1Bi

50 μM

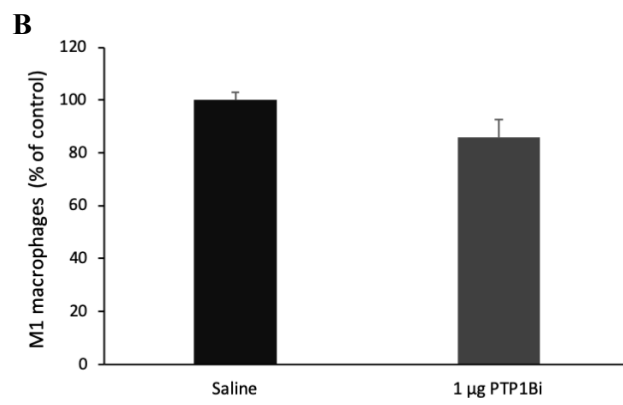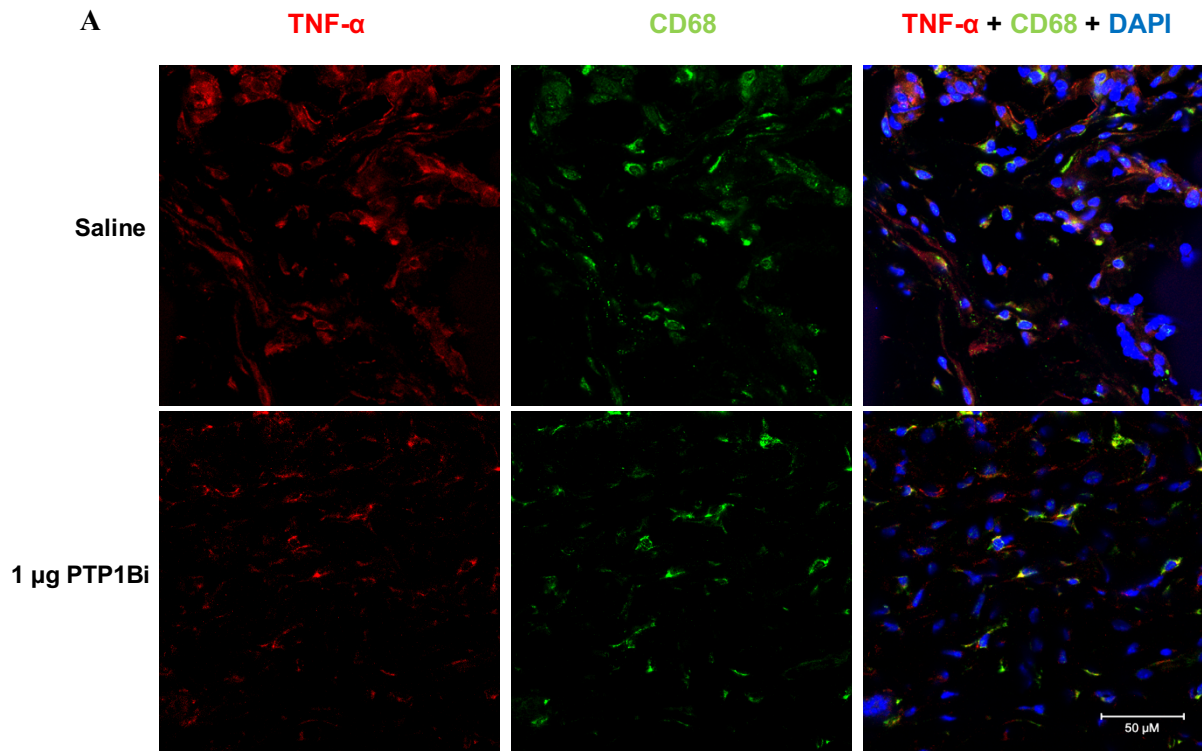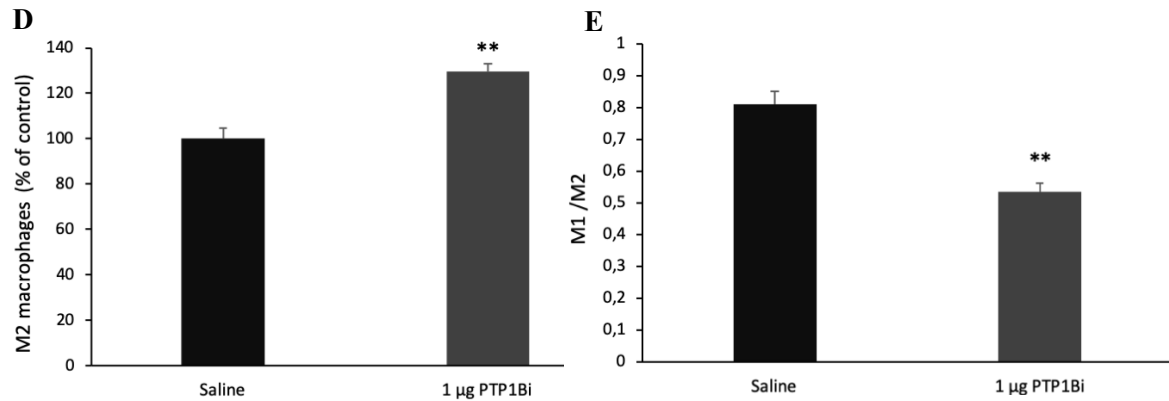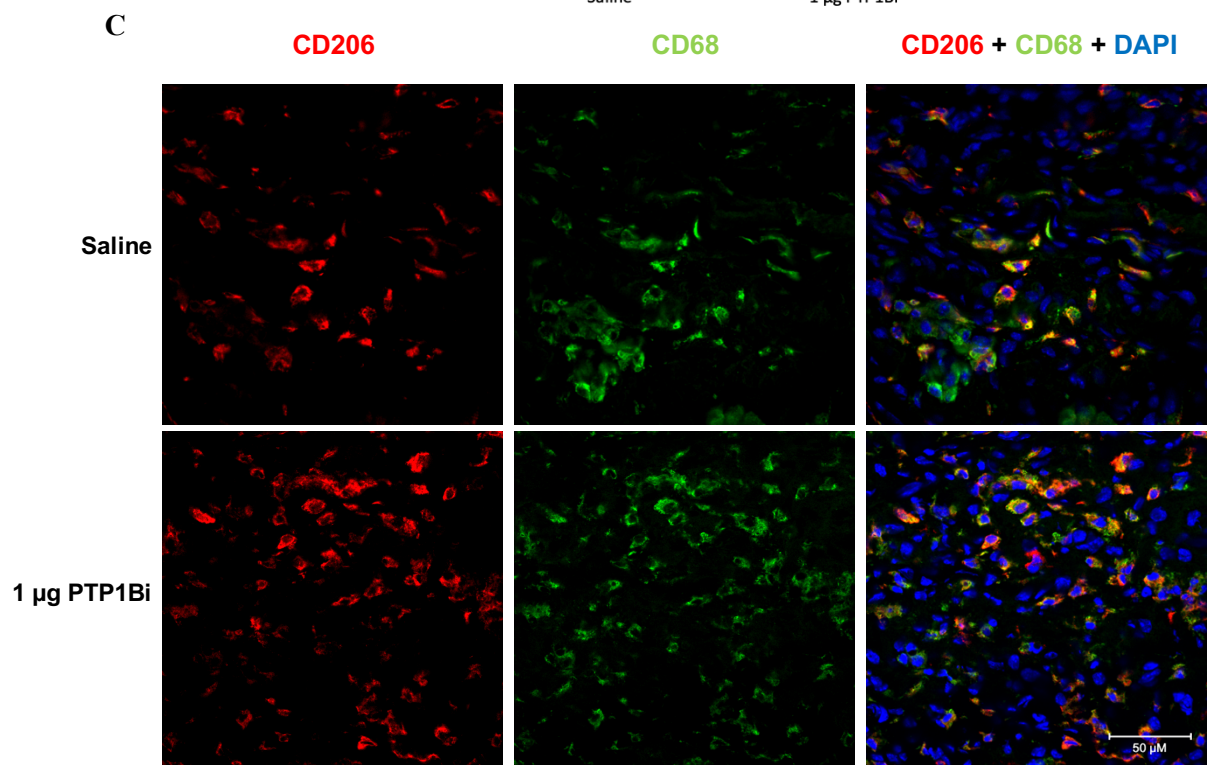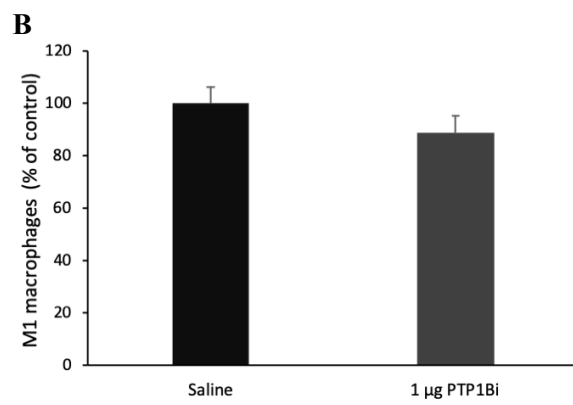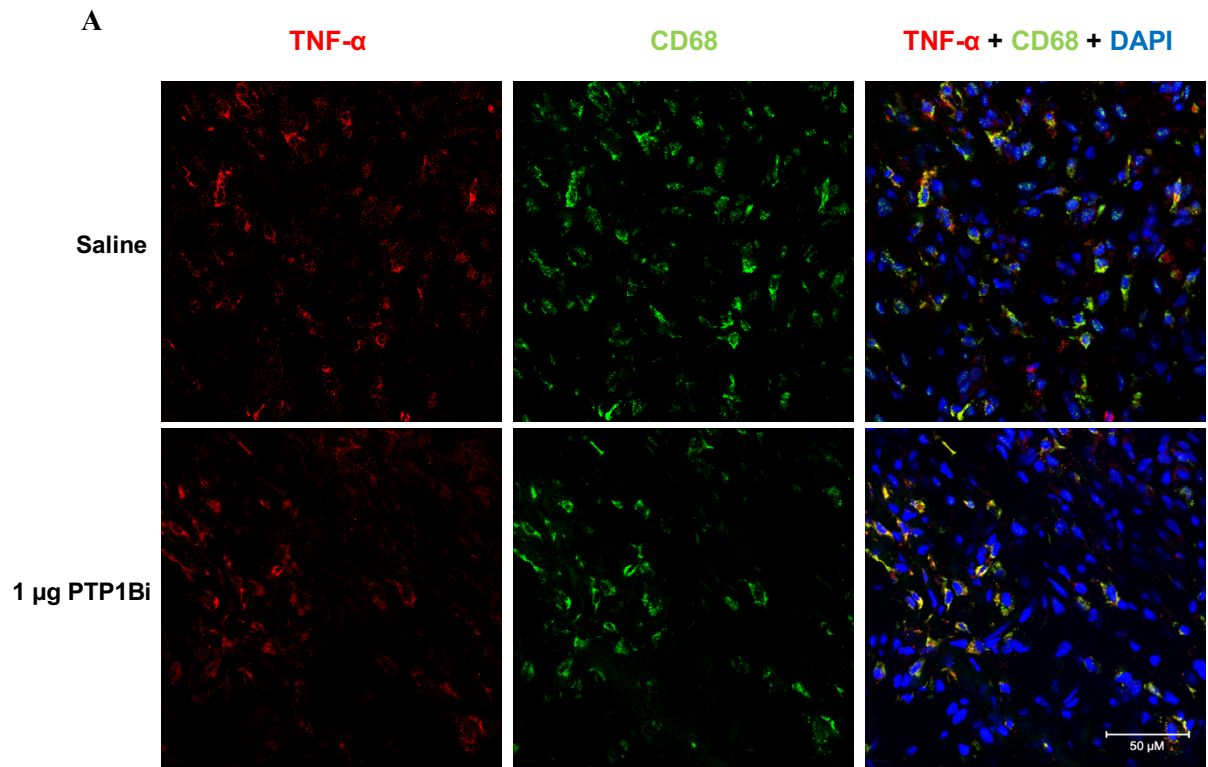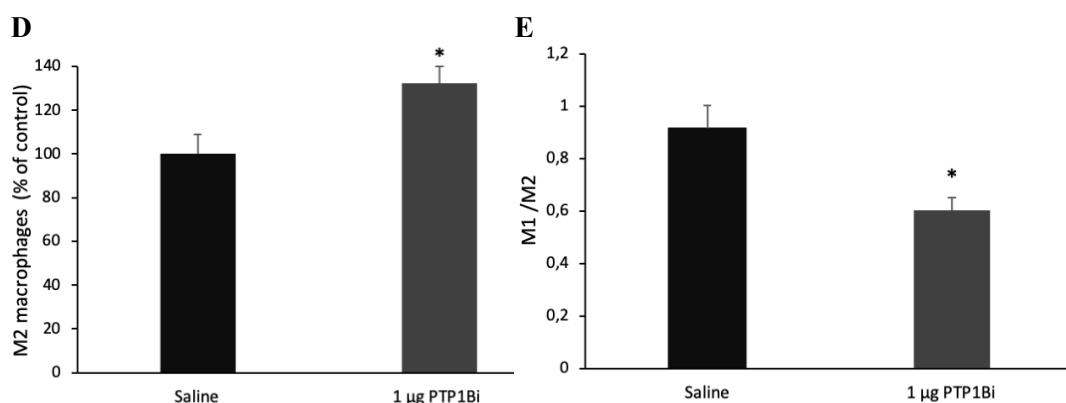**Figure 40 -** The treatment with 1 μg of PTP1Bi altered the macrophage phenotype towards a decreased inflammatory environment in diabetic wounds at day 10. (A) Representative 400x magnification images of the macrophage marker proteins CD68 (green) and TNF-α (red), showed that 1 μg of PTP1Bi decreased the co-localization of CD68 and TNF-α, indicating a total decrease of M1 macrophages (yellow). (B) Quantification of M1 macrophages (CD68 + TNF-α double-positive cells) present in the wound at day 10. (C) Representative 400x magnification images of the macrophage marker proteins CD68 and CD206 (red), showed that 1 μg of PTP1Bi increased the co-localization of CD68 and CD206, indicating a total increase of M2 macrophages (yellow). (D) Quantification of M2 macrophages (CD68 + CD206 double-positive cells) in the wound at day 10. (E) M1/M2 ratio for 1 μg of PTP1Bi treatment and saline,1 μg of PTP1Bi significantly decreased M1/M2 ratio. For statistical analysis a student t-test was performed to compare the treatment group with the saline-treated group. Nuclei were stained with DAPI (blue). Scale bar is 50 μm. The results are presented as percentage of macrophage (M1 or M2) number in saline-treated wounds and represented as mean ± SEM (*n*=6 mice per group). * *p*<0.05 compared to saline.

3.3.3. The inhibition of PTP1B decreased ROS levels at the wound site

Chronic wounds have high levels of ROS which are produced in large amounts by the numerous immune cells accumulated at the wound site. ROS can cause damage in the cells, poor angiogenesis, decreased ECM production and increased ECM breakdown which is prejudicial to wound healing [87], [200]. Furthermore, in chronic diabetic wounds there is an increase in ROS production, as well as a reduction in antioxidant defences which will lead to a redox imbalance [191, [192] . Thus, in order to promote wound closure, it will be very important to reduce the high levels of ROS.

To test the hypothesis that PTP1B inhibition could possibly contribute to reduce the oxidative stress levels at the wound site, the wounds were treated with 1 μg, 10 μg and 25 μg of PTP1Bi, or saline and then harvested after 10 days of treatment. ROS levels were evaluated by DHE assay (**Figure 41A**). The effect of PTP1B inhibitor, particularly the 1 μg of PTP1Bi dose was also evaluated, as described before, at the inflammatory (day 3) and proliferation phase (day 10), in ROS levels.

ROS levels were significantly decreased with 1 μg of PTP1Bi treatment, to 59.46 ± 11.09% when compared to the saline (100 ± 10.82%) (*p*<0.05, *n*=3 mice) (**Figure 41B**). A significant

reduction was also observed with the 10 µg of PTP1Bi dose (66.08 ± 8.04%) ($p<0.05$, $n=3$ mice), however, this reduction was not as high as the observed with the lower PTP1Bi dose. Although not as efficient, the treatment with 25 µg of PTP1Bi also led to a reduction to 79.44 ± 24.55% of the levels of ROS at the wound site when compared to saline. These results suggest that the inhibition of PTP1B has an effect in the reduction of oxidative stress which can lead to normal levels of ROS in diabetic wounds usually characterised with a high oxidative stress environment.

B
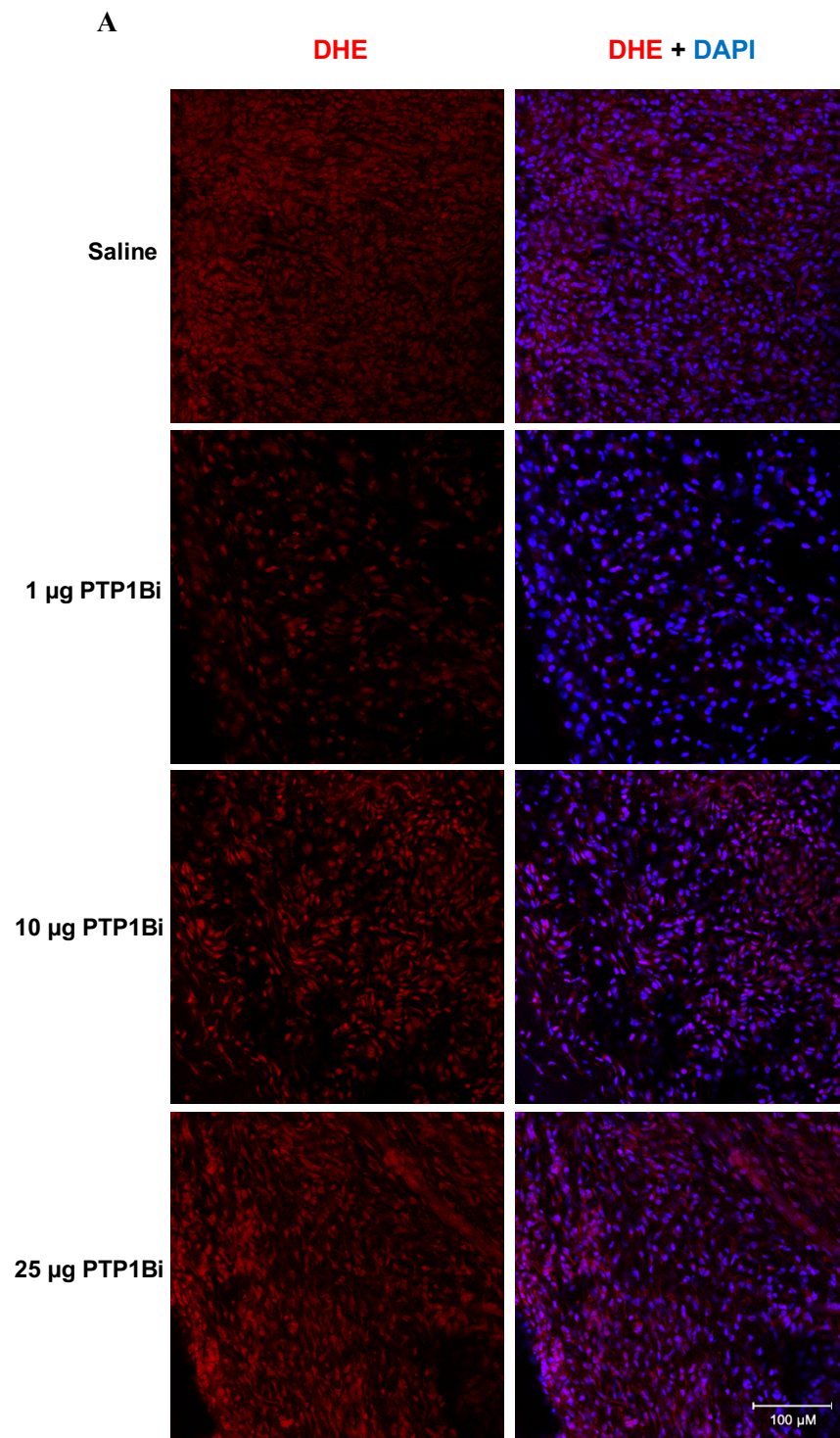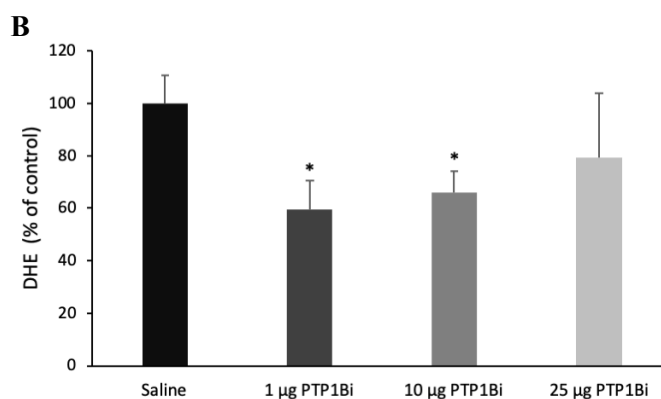
Figure 41 - The inhibition of PTP1B decreased reactive oxygen species levels in the wound site at day 10. (A) Representative 200x magnification images of DHE (red) and (B) respective quantification in mice wounds treated with 1 μg, 10 μg and 25 μg of PTP1Bi, or saline. For statistical analysis a student t-test was performed to compare the treatment groups with the saline-treated group. Nuclei were stained with DAPI (blue). Scale bar is 100 μm. The results are presented as percentage of ROS in saline-treated wounds and represented as mean ± SEM (*n*=3 mice per group). * *p*<0.05 compared to saline.

At day 3 (**Figure 42A and B**), the treatment with 1 μg of PTP1Bi slightly decreased ROS levels to 79.12 ± 17.68% comparing to saline (100 ± 8.36%). Although this decrease was not statistically significant, it can indicate that early on at the wound site, ROS levels can be modulated by PTP1Bi in order to reach only moderate levels. Moreover, during the inflammatory phase, although ROS levels can be exaggerated and caused damage to the tissue, ROS play a very important role in fighting external pathogens that invade the wound, so a very high reduction of ROS levels could jeopardise this function of fighting dangerous pathogens.

A

B
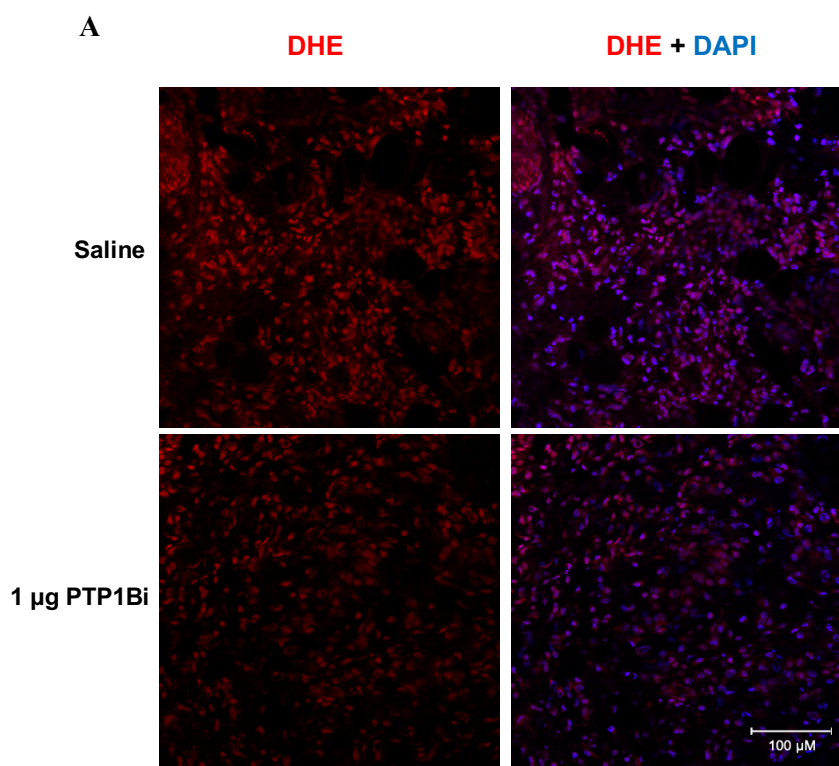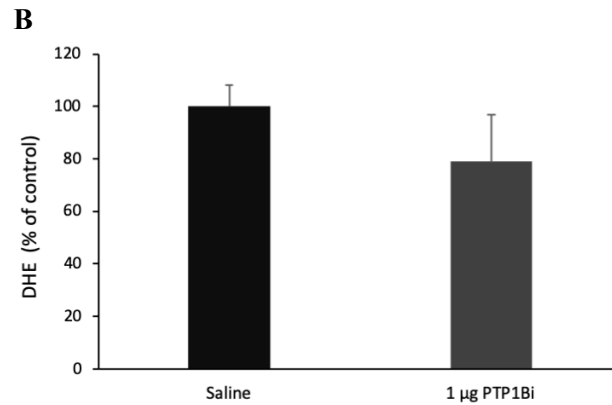
Figure 42 - The effect of 1 µg of PTP1Bi in reactive oxygen species levels in the wound site at day 3. (A) Representative 200x magnification images of DHE (red) and (B) respective quantification in mice wounds treated with 1 µg of PTP1Bi, or saline. Scale bar is 100 µm. For statistical analysis a student t-test was performed to compare the treatment group with the saline-treated group and no statistical differences were observed. Nuclei were stained with DAPI (blue). Scale bar is 100 µm. The results are presented as percentage of ROS in saline-treated wounds and represented as mean ± SEM (n=4 mice per group).

The treatment with 1 µg of PTP1Bi significantly decreased the ROS levels to 58.62 ± 8.21% when compared to saline (100 ± 6.17%) (p<0.001, n=6 mice) at day 10 (**Figure 43A and B**), similar to what was observed in previous experiments. These results suggest that PTP1B inhibition can be a very effective antioxidant strategy, being able to reduce the ROS levels present in the wound. This effect will allow to overcome the excessive ROS production in diabetic wounds and promote a better wound healing.

A

B

3.3.4. The PTP1B inhibition increased HO-1 expression in the wound

HO-1 is an enzyme that is able to protect against oxidative tissue damages. Several properties of this enzyme have been studied, including its anti-inflammatory effect, linked to enhanced polarisation toward an anti-inflammatory M2 macrophage phenotype, and antioxidant capacities [170]–[173]. The overexpression of HO-1 is associated with a high ROS elimination contributing to the redox balance [195], [196]. Studies with HO-1-deficient cells demonstrated that in the absence of HO-1 activity, cells produce high levels of ROS and have reduced stress defences [213]. The overexpression of HO-1 is also related to a high vascularisation and angiogenesis [214]. Thus, this enzyme seems to potentiate several very important factors for the wound healing process. In fact, studies have shown that the overexpression of this enzyme promotes wound healing in diabetic mouse and rat models [215], [216]. Thus, since the inhibition of PTP1B accelerates wound closure, the presence of HO-1 at the wound site of mouse wounds treated for 10 days with 1 μg, 10 μg and 25 μg of PTP1Bi or saline, was analysed by immunohistochemistry in order to understand whether PTP1B inhibition could promote HO-1 expression.

All doses of PTP1Bi promoted an increase in HO-1 expression (**Figure 44A and B**). The 25 μg of PTP1Bi promoted the lowest HO-1 expression increase (253.9 ± 10.06%), however, still significant when compared to saline (100 ± 16.97%) (p<0.01, n=3 mice). The treatment with 10 μg of PTP1Bi promoted a significant increase in HO-1 levels to 338.08 ± 19.38%, comparing to saline (p<0.05, n=3 mice). The lower dose of PTP1Bi showed the highest significant increase in HO-1 levels to 521.46 ± 17.42% (p<0.05, n=3 mice) when compared to saline, clearly indicating that the dose 1 μg of PTP1Bi is the most effective for the treatment of diabetic mouse ulcers.

A

HO-1   HO-1 + DAPI

Saline

1 µg PTP1Bi

10 µg PTP1Bi

25 µg PTP1Bi

B

Figure 44 - The effect of PTP1B inhibition in HO-1 levels in the wound site at day 10. (A) Representative 400x magnification images of HO-1 (red) and (B) respective quantification in mice wounds treated with 1 µg, 10 µg, 25 µg of PTP1Bi, or saline. For statistical analysis a student t-test was performed to compare the treatment group with the saline group. Nuclei were stained with DAPI (blue). Scale bar is 50 µm. The results are presented as percentage of saline-treated wounds and represented as mean ± SEM (*n*=3 mice per group). * *p*<0.05, ** *p*<0.01 compared to saline.

As before, mouse wounds were treated for 3 or 10 days with 1 µg of PTP1Bi and HO-1 levels were assessed at the wound site (**Figure 45A**). Similarly to what was observed at day 10, 1 µg of PTP1Bi treatment increased very significantly HO-1 levels to 321.58 ± 2.49% when compared to saline (100 ± 5.62%) (*p*<0.0001, *n*=4 mice) (**Figure 45B**). This increase can be related to the reduction on ROS levels and to the increase of M2 macrophages observed at day 3. After a few days of PTP1B inhibition, HO-1 levels seem to be increased in order to promote wound healing as early as at the inflammatory phase.

A

B
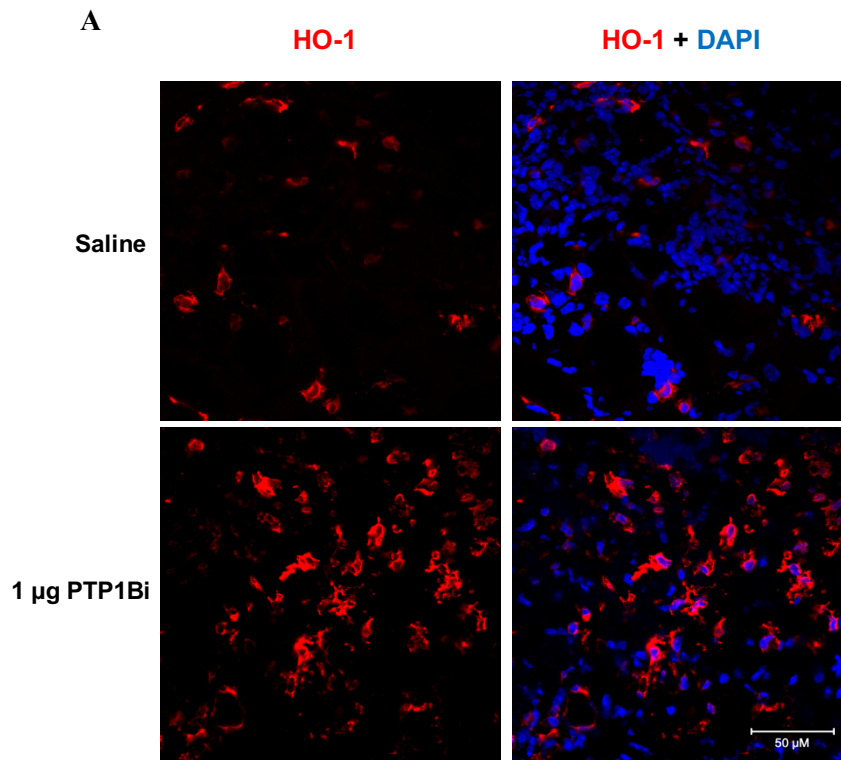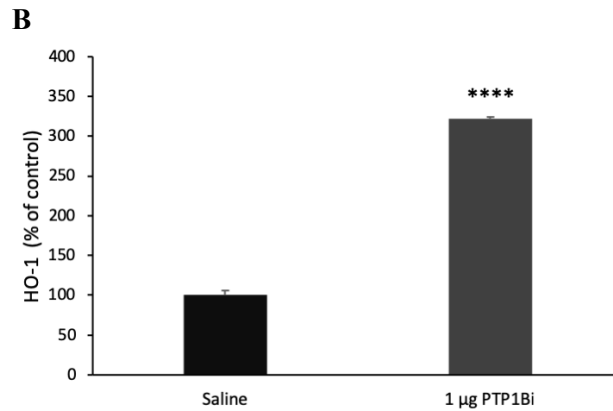
Figure 45 - The effect of 1 µg of PTP1Bi treatment in HO-1 levels in the wound site at day 3. (A) Representative 400x magnification images of HO-1 (red) and (B) quantification of HO-1 in mice wounds treated with 1 µg of PTP1Bi, or saline. For statistical analysis a student t-test was performed to compare the treatment group with the saline-treated group. Nuclei were stained with DAPI (blue). Scale bar is 50 µm. The results are presented as percentage of saline-treated wounds and represented as mean ± SEM (*n*=4 mice per group). **** *p*<0.0001 compared to saline.

Mice wounds were again treated with 1 µg of PTP1Bi for 10 days in order to confirm what was observed in the first pilot experiment, and the HO-1 expression was assessed by immunohistochemistry (**Figure 46A**). As before, HO-1 expression was significantly increased with 1 µg of PTP1Bi treatment to 363.15 ± 11.22% when compared to saline (*p*<0.001, *n*=6 mice) (**Figure 46B**). The increase of HO-1 levels is consistent with the increase in the number of M2 macrophages, the decrease in the pro-inflammatory environment and the reduction in the ROS levels at the wound site, promoting wound healing. These results indicate that inhibition of PTP1B improves diabetic wound healing via the increase in HO-1 levels which in turn will promote a decrease in oxidative stress and an anti-inflammatory environment.
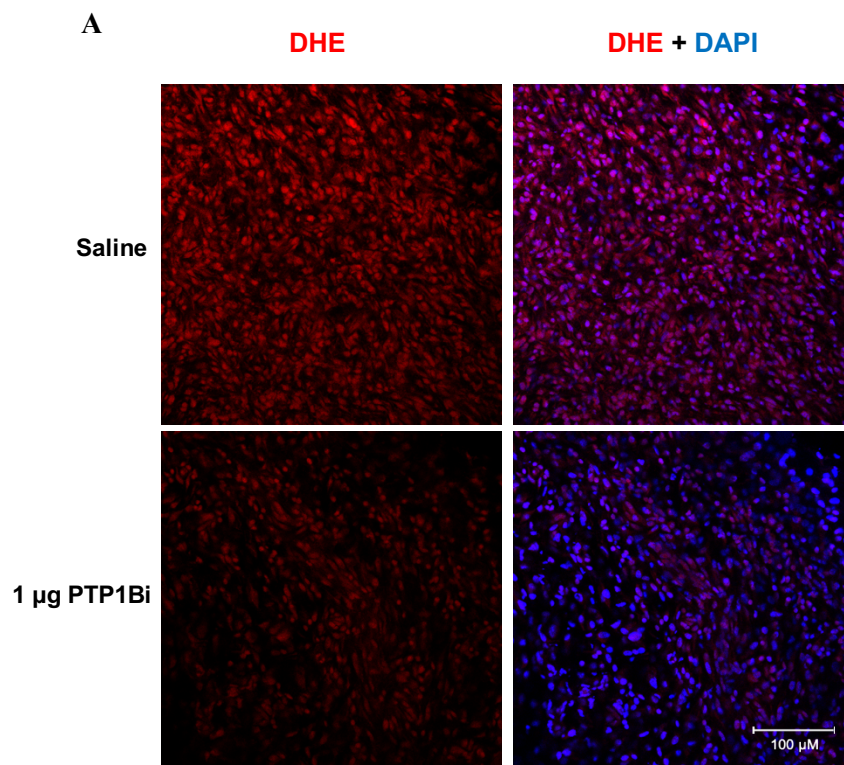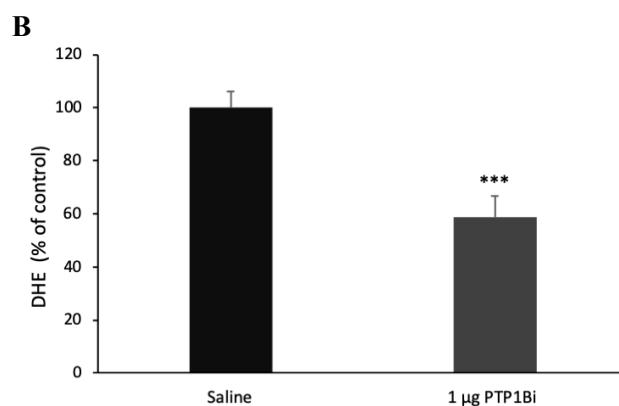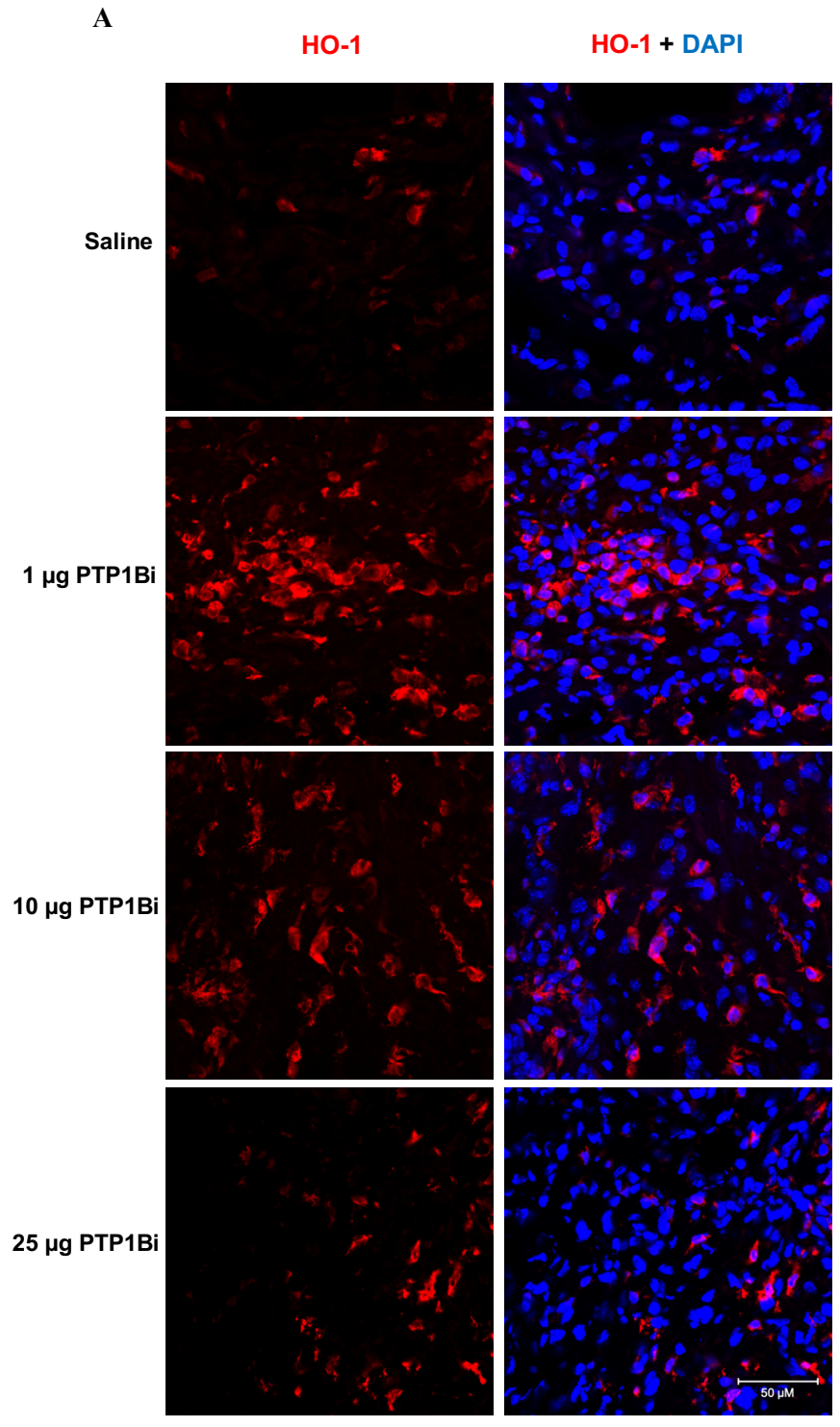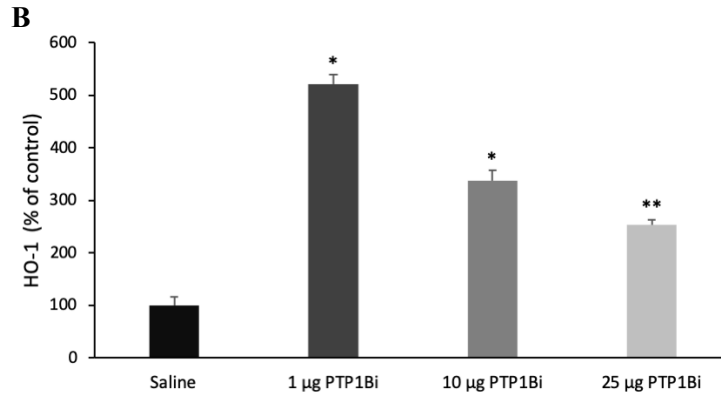
A

B
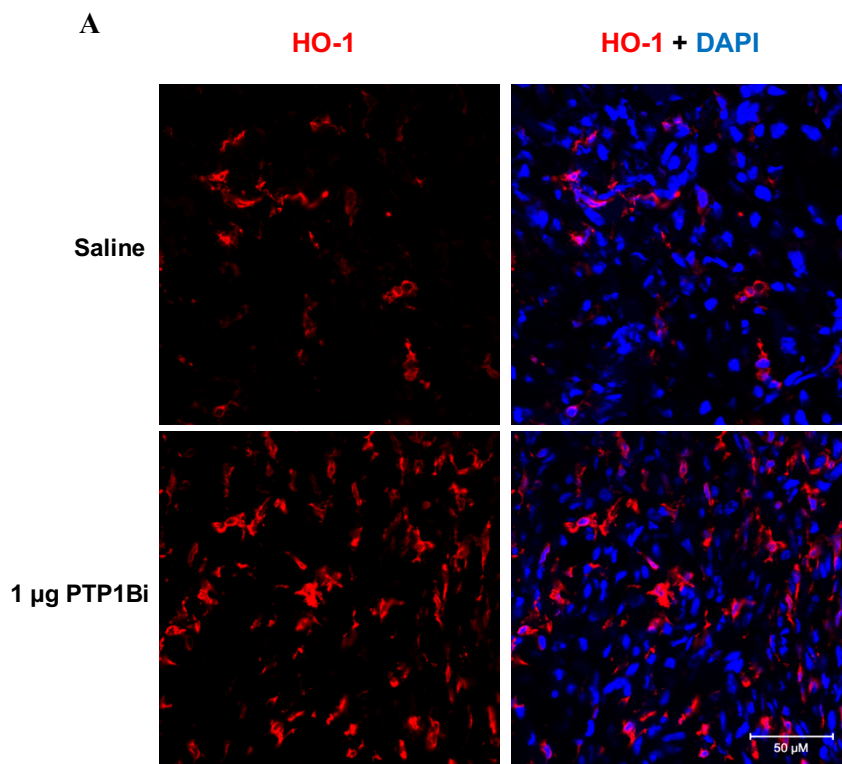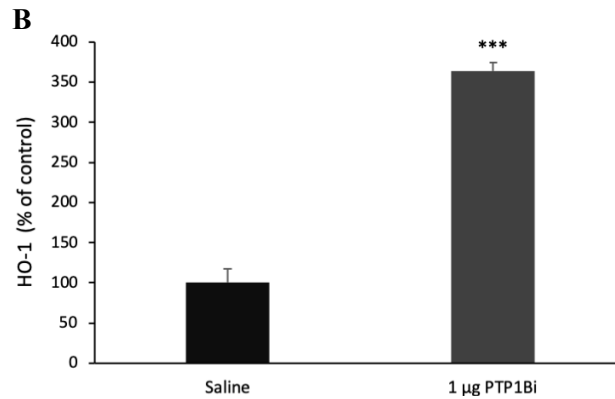
Figure 46 - The effect of 1 μg of PTP1Bi treatment in HO-1 levels in the wound site at day 10. (A) Representative 400x magnification images of HO-1 (red) and (B) respective quantification in mice wounds treated with 1 μg of PTP1Bi, or saline. For statistical analysis a student t-test was performed to compare the treatment group with the saline-treated group. Nuclei were stained with DAPI (blue). Scale bar is 50 μm. The results are presented as percentage of control mice and represented as mean ± SEM (*n*=6 mice per group). *** *p*<0.001 compared to saline.

3.3.5. The treatment with MSI-1436 increased wound vascularisation

Chronic diabetic wounds are characterised by impaired angiogenesis. Diabetic ulcers have insufficient angiogenesis that results in poor blood flow which prevents the necessary nutrients from reaching the wound, as well as promotes hypoxia contributing to delayed wound healing [202]. One of the strategies which can improve wound healing is to increase angiogenesis at the wound site and therefore high blood flow. Thus, it is important to investigate the effect of PTP1B inhibition on angiogenesis. For that, the mouse wounds treated for 10 days with 1 μg, 10 μg and 25 μg of PTP1Bi or saline were stained with the endothelial cell marker, CD31 (red), and the number of vessels present at the wound site were quantified. Again, a second experiment was done with mice treated for 3 or 10 days with only 1 μg of PTP1Bi. CD31 is a protein found on the surface of endothelial cells, being widely used as a marker for endothelial cells and to detect angiogenesis [218], [219].

In the pilot study, it was found that PTP1Bi treatment increased angiogenesis at the wound site (**Figure 47A**). Surprisingly, the higher dose, 25 μg of PTP1Bi, was the most effective to promote angiogenesis, in opposition to previous results where 1 μg of PTP1Bi was the most effective dose. Mouse wounds treated with this dose increased to 142.32 ± 12.41% the number of blood vessels comparing to saline wounds (100 ± 4.23%) (**Figure 47B**). The dose 1 μg of PTP1Bi increased the number of vessels to 104.21 ± 3.5% comparing to saline. In turn, the 10 μg dose appears to have no effect on angiogenesis, with even a slight decrease in angiogenesis compared to saline (98.73 ± 12.72% against 100% ± 4.23% of saline). These results are not statistically significant probably due to a low *n* value, however they may be biologically significant, indicating that PTP1B inhibition may promote angiogenesis.

A

	CD31	CD31 + DAPI
Saline		
1 µg PTP1Bi		
10 µg PTP1Bi		
25 µg PTP1Bi		

100 µM
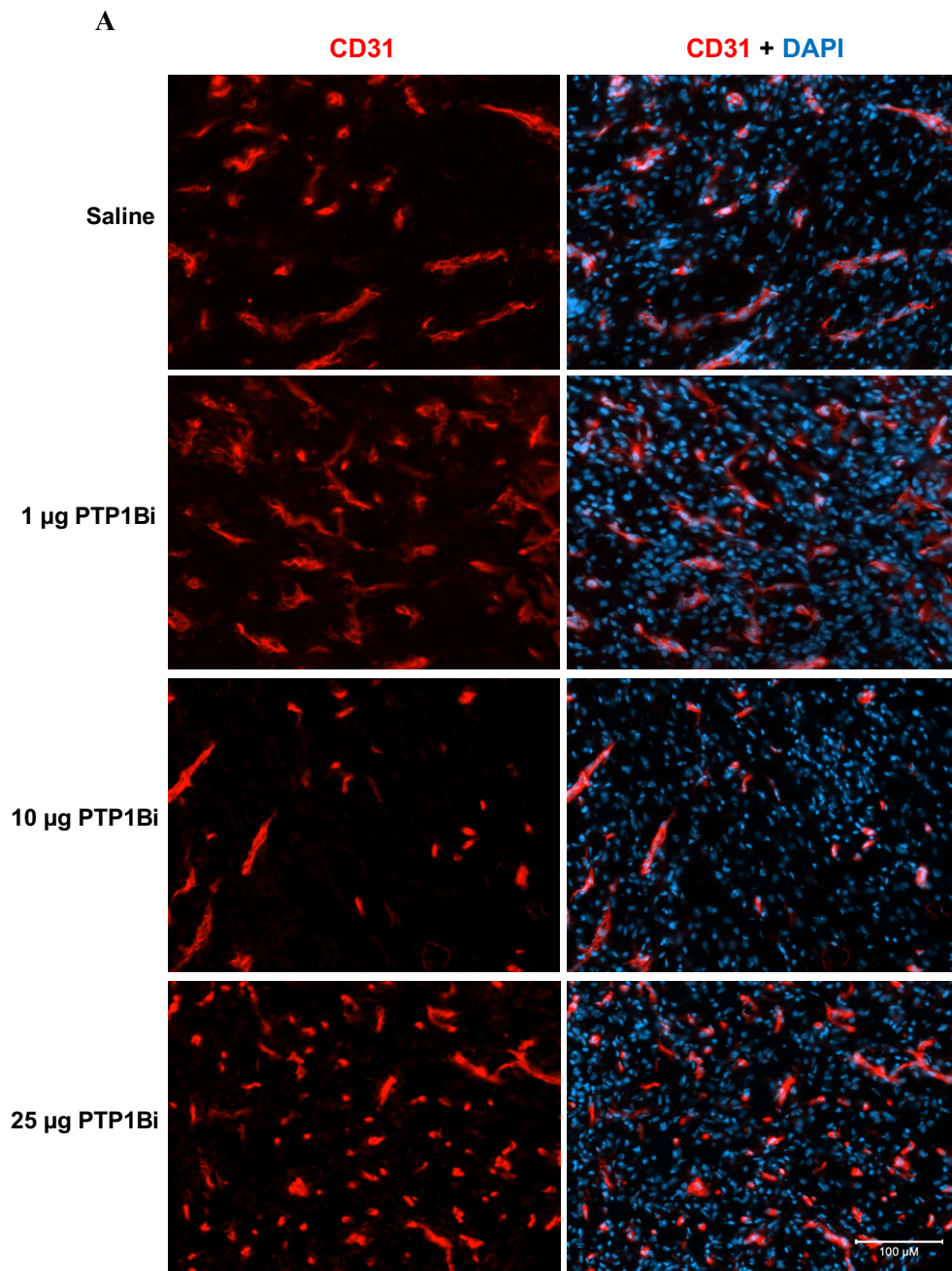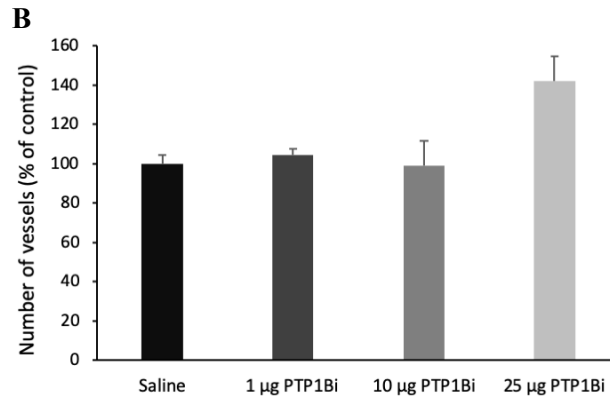
Figure 47 - The effect of the PTP1B inhibition in the number of vessels present in the wound site at day 10. (A) Representative 200x magnification images of the number of vessels stained using CD31 (endothelial cells specific marker, red) (B) respective quantification in mice wounds treated with 1 µg, 10 µg, 25 µg of PTP1Bi, or saline. For statistical analysis a student t-test was performed to compare the treatment group with the saline-treated group and no statistical differences were observed. Nuclei were stained with DAPI (blue). Scale bar is 100 µm. The results are presented as percentage of the number of vessels in saline-treated wounds and represented as mean ± SEM (n=3 mice per group).

Although 1 µg is not the dose that promote more angiogenesis, taken all the other results into account, this dose seems to be the most efficient and was the one that led to the best result in wound healing. So, to evaluate the effect of this treatment on wound angiogenesis, the mouse wounds treated for 3 or 10 days only with 1 µg of PTP1Bi were analysed to quantify the number of vessels.

At day 3, the treatment with 1 µg of PTP1Bi increased the number of vessels at the wound site to 131.4 ± 13.79% (**Figure 48A**) compared to saline (100 ± 2.66%) (**Figure 48B**). This supports the idea that the beneficial effect of PTP1B inhibition begins to be noticed very early in the wound healing process.

B
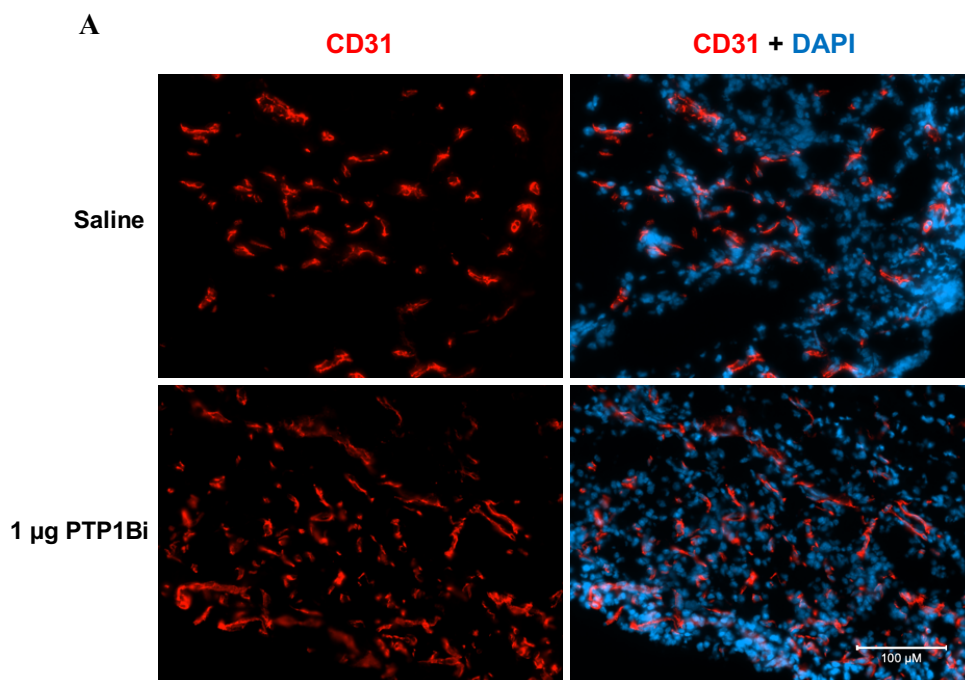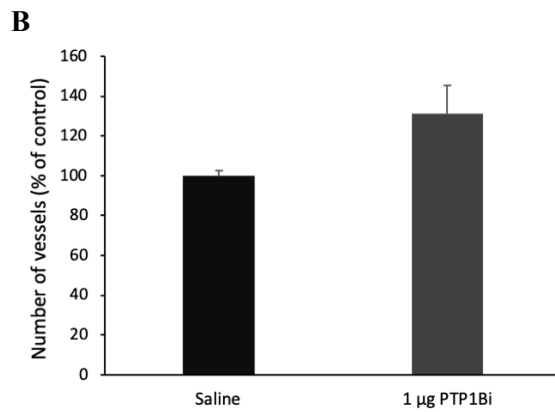
Figure 48 - The effect of 1 µg of PTP1Bi in the number of vessels present in the wound site at day 3. (A) Representative 200x magnification images of the number of vessels stained using CD31(red) and (B) respective quantification in mice wounds treated with 1 µg of PTP1Bi, or saline. For statistical analysis a student t-test was performed to compare the treatment group with the saline-treated group and no statistical differences were observed. Nuclei were stained with DAPI (blue). Scale bar is 100 µm. The results are presented as percentage of the number of vessels in saline-treated wounds and represented as mean ± SEM (*n*=4 mice per group).

The effect of the treatment with 1 µg of PTP1Bi at day 10 was also investigated. In this second experiment, the wounds treated with 1 µg of PTP1Bi showed a higher number of blood vessels than the wounds treated with saline (**Figure 49A**). The treatment increased significantly the number of vessels to $111.54 \pm 2.78\%$ when compared to saline ($100 \pm 2.56\%$) ($p<0.05$, *n*=6 mice) (**Figure 49B**). PTP1B inhibition appears to promote angiogenesis which contributes to the closure of diabetic ulcers since poor angiogenesis is one of the causes of the delayed healing observed in diabetic wounds. The increase in angiogenesis together with all the previously observed beneficial effects of PTP1B inhibition will lead to a more effective and faster wound closure. This effect of PTP1B inhibition on angiogenesis is consistent with what has been observed in previous studies [122], [132], [220].

A

B
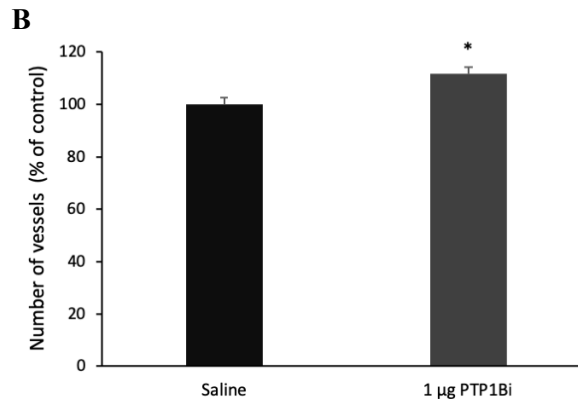
Figure 49 - The effect of 1 µg of PTP1Bi in the number of vessels present in the wound site at day 10. (A) Representative 200x magnification images of the number of vessels stained using CD31(red) and (B) respective quantification in mice wounds treated with 1 µg of PTP1Bi, or saline. For statistical analysis a student t-test was performed to compare the treatment group with the saline-treated group. Nuclei were stained with DAPI (blue). Scale bar is 100 µm. The results are presented as percentage of the number of vessels in saline-treated wounds and represented as mean ± SEM (*n*=6 mice per group). * *p*<0.05 compared to saline.

3.3.6. PTP1B inhibition promoted cell proliferation at the wound site

In the proliferation phase of wound healing, the granulation tissue is formed, in order to rebuild the wound and create new tissue, and angiogenesis occurs to create new blood vessels that provide nutrients to the newly formed tissue. For this to occur, the cells present at the wound site need to proliferate and duplicate their number. This proliferation is promoted by growth factors released by various cells present at the wound site. One of the major problems in diabetic ulcers is the decrease in the expression of growth factors involved in healing which leads to a decrease in cell proliferation, for instance in fibroblasts or keratinocytes, which is essential for wound healing [76], [104], [105].

To investigate whether PTP1B inhibition can modulate cell proliferation at the wound site, wounds treated for 10 days with 1 µg, 10 µg and 25 µg of PTP1Bi or saline were stained for the presence of ki-67 (red) and the number of proliferating cells in the dermis of the wound was quantified (**Figure 50A**). Ki-67 is a protein involved in cell cycle and has been extensively used as a proliferation marker [221]. This protein is present in the nuclei of the cells that are proliferating, so the nucleus of a proliferating cell (ki-67 positive cells) will be stained.

All three different treatments seemed to increase cellular proliferation at the wound site. Again, the 1 µg of PTP1Bi proved to be the most efficient dose, increasing significantly the number of ki-67 positive cells to 269.18 ± 16.38% comparing to saline (100 ± 15.69%) (*p*<0.05, *n*=3 mice) (**Figure 50B**). The second best treatment was the 10 µg of PTP1Bi which increased the number of proliferating cells to 194.52 ± 19.39% when compared to saline. The highest dose of PTP1Bi was not as efficient, increasing the number of ki-67 positive cells to only 152.74 ± 12.83%. These last

two results were not statistically significant, although they demonstrated the tendency of PTP1Bi treatment to induce the increase of cellular proliferation at the wound site.

A

B

The dose 1 µg of PTP1Bi was used, as previously described, to evaluate the days 3 or 10. The number of ki-67 positive cells at day 3 was analysed (**Figure 51A**) and the treatment with PTP1Bi increased ki-67 positive cells number to 123.86 ± 8.48% comparing to saline (100 ± 10.56%) (**Figure 51B**). The obtained result is not statistically significant but indicate that PTP1B inhibition may be able to promote the transition from inflammatory to proliferative phase in wound healing. This transition is often stalled in diabetic ulcers and it is one of the causes for these wounds do not heal.

A

B
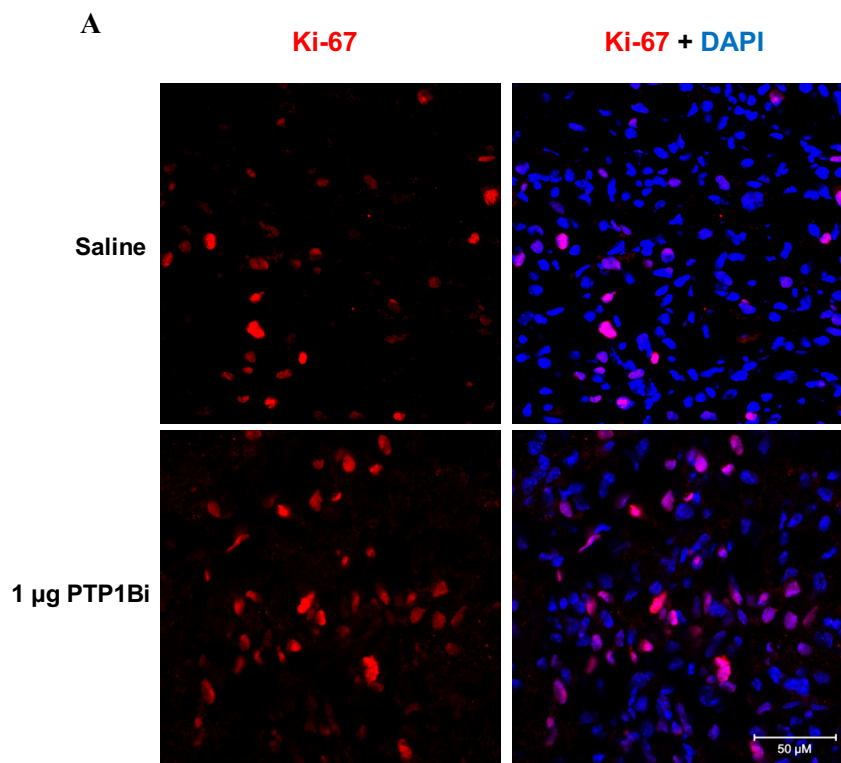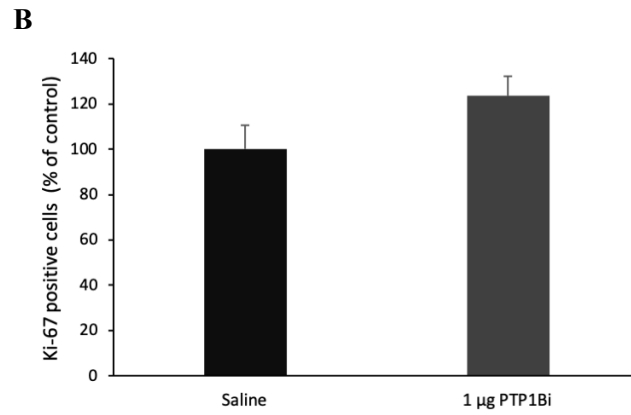
Figure 51 - The effect of 1 µg of PTP1Bi in the number of ki-67 positive cells present in the wound site at day 3. (A) Representative 400x magnification images of the number of ki-67 positive stained using ki-67 (red) and (B) respective quantification in mice wounds treated with 1 µg of PTP1Bi, or saline. Nuclei were stained with DAPI (blue). For statistical analysis a student t-test was performed to compare the treatment group to the saline group and no statistical differences were observed. Scale bar is 50 µm. The results are presented as percentage of the number of ki-67 positive cells in saline-treated wounds and represented as mean ± SEM (*n*=4 mice per group).

The number of ki-67 positive cells at day 10 was also analysed (**Figure 52A**). As observed in the first experiment, 1 µg of PTP1Bi increased the ki-67 positive cells number. In the second experiment, the increase was to $199.53 \pm 10.85\%$ comparing to saline $(100 \pm 11.04\%)$ *(p<0.01, n=6 mice)* (**Figure 52B**). Taking all these results into account, it could be concluded that PTP1B inhibition appears to promote cell proliferation at the wound site.
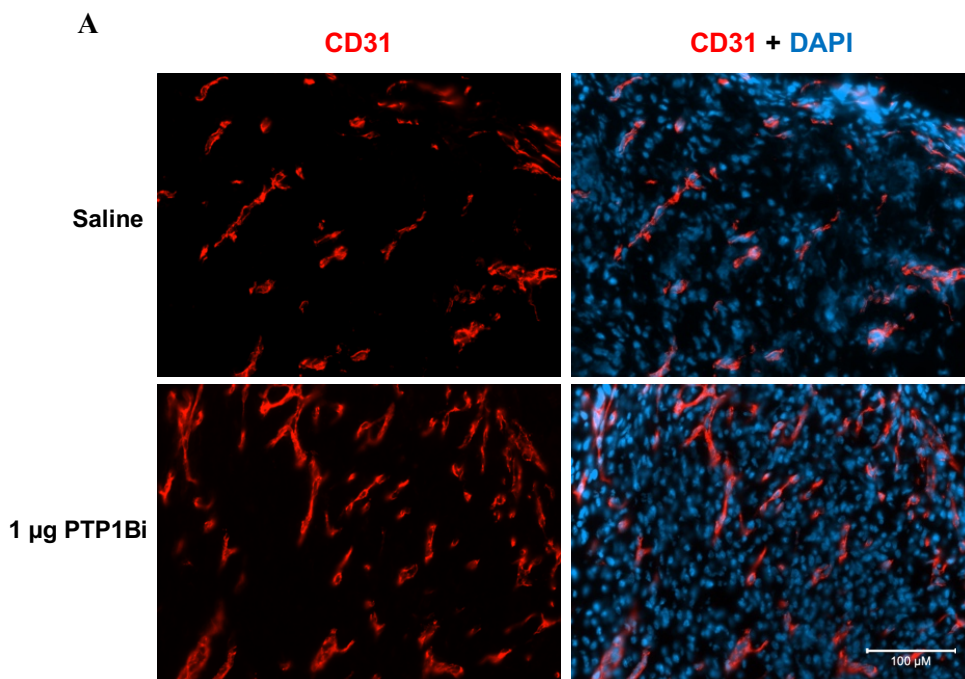
A

B
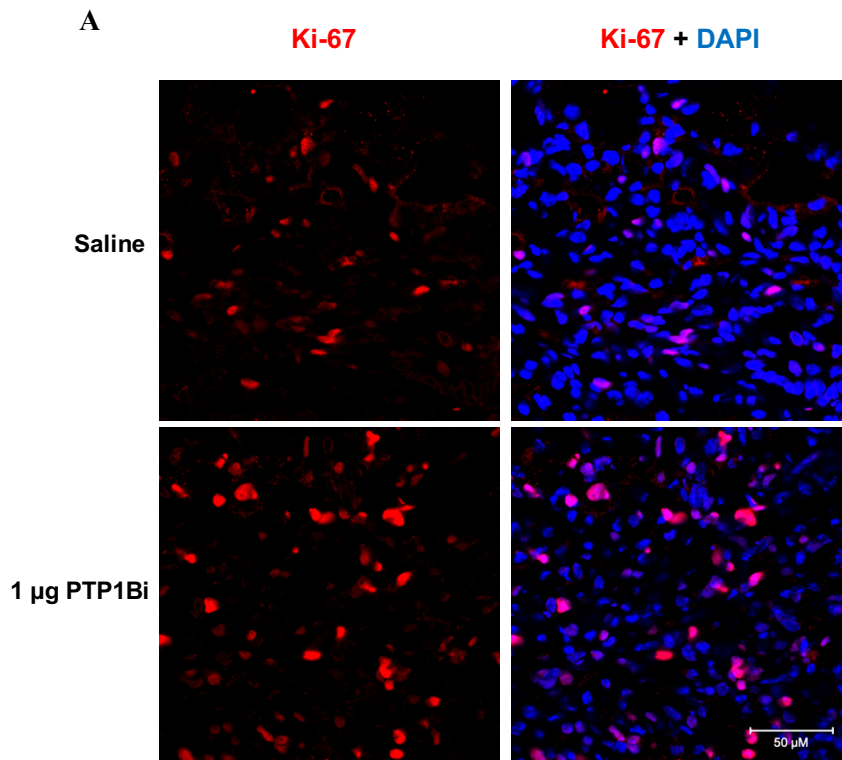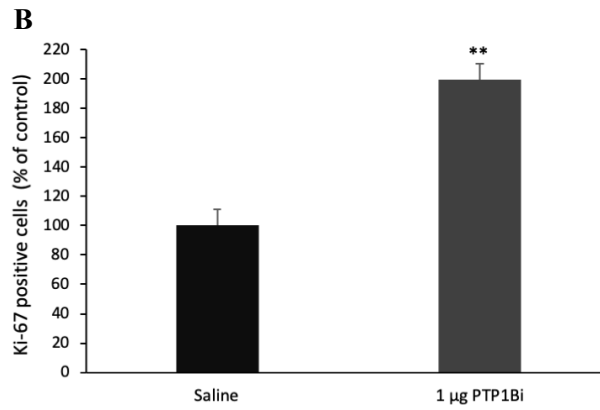
Figure 52 - The effect of 1 μg of PTP1Bi in the number of ki-67 positive cells present at wound site at day 10. (A) Representative 400x magnification images of the number of ki-67 positive stained using ki-67 (red) and (B) respective quantification in mice wounds treated with 1 μg of PTP1Bi, or saline. Nuclei were stained with DAPI (blue). For statistical analysis a student t-test was performed to compare the treatment group with the saline group and no statistical differences were observed. Scale bar is 50 μm. Results are presented as percentage of the number of ki-67 positive cells in saline-treated wounds and represented as mean ± SEM (*n*=6 mice per group). ** *p*<0.01 compared to saline.

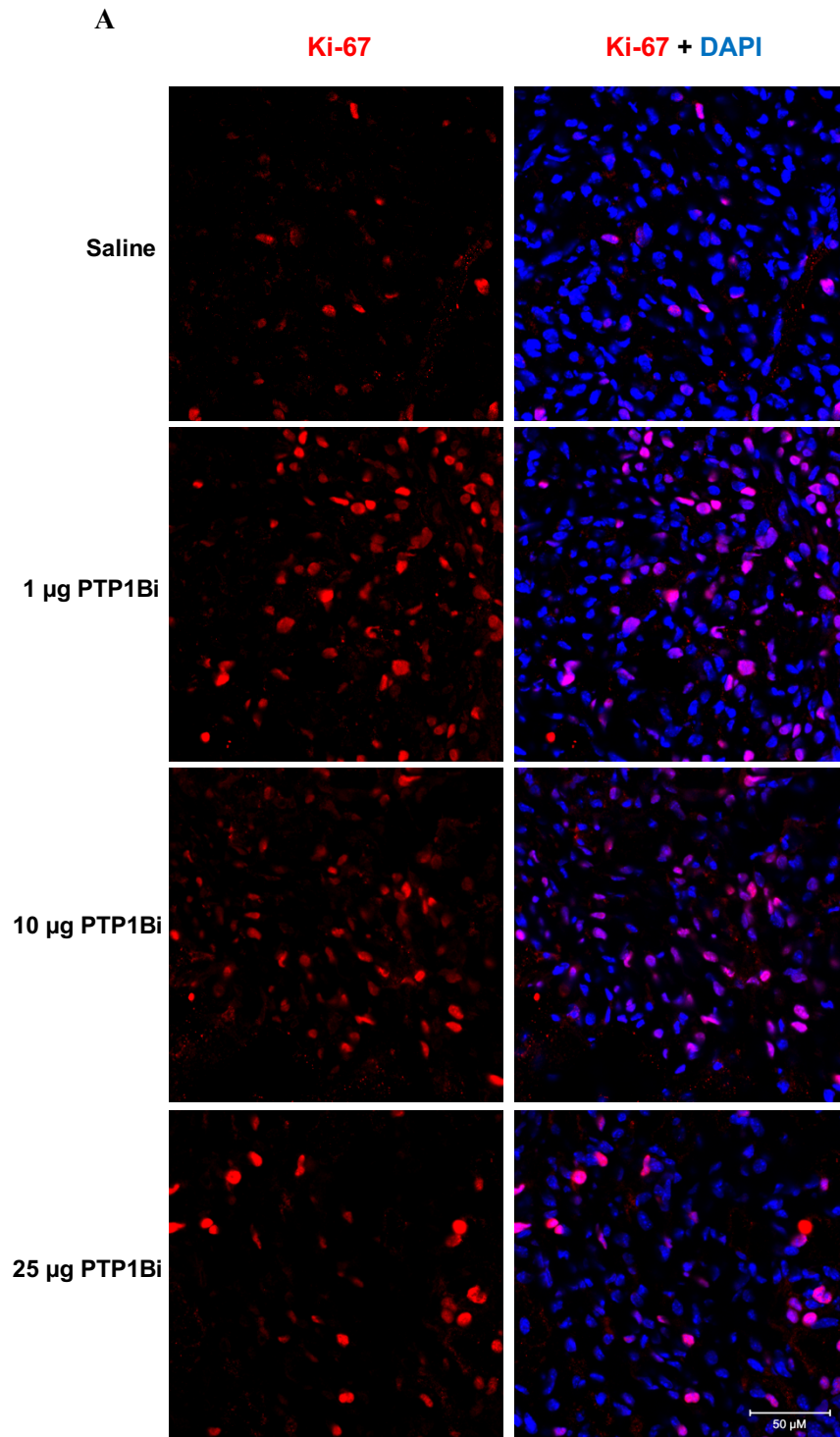# Chapter 4: Discussion and Conclusions

Diabetes is considered to be the new epidemic of the 21st century, especially T2DM which is responsible for about 90-95% of diabetes cases [222]–[224]. Over the last few years, the number of people suffering from this disease has been increasing wildly, as well as the complications associated with it. According to the World Health Organization, it was estimated that in 2014 around 422 million adults suffered from diabetes worldwide, and this number is estimated to reach 642 million by 2040 [31], [225]. This increase is mainly due to an increase in the numbers of adults with T2DM as a consequence of a dramatic rise in the incidence of obesity in the world [39]. The prevalence of diabetes in Portugal is approximately 9.9% in adults, one of the highest in Europe [32]. Persistent hyperglycemia observed in T1DM and T2DM is the principal responsible for the development of several complications, such as blindness, kidney failure, heart diseases and DFUs [31], [33], [37]. As the incidence of diabetes increases, more people suffer from these complications, increasing the need for highly specialised medical care, thus highly increasing the associated healthcare costs.

Approximately 15-25% of diabetic patients develop DFUs, also known as the diabetic foot, which are responsible for about 85% of amputations in diabetic patients [55]–[57]. The incidence of DFUs is higher in older patients with T2DM. As the number of patients with TD2M has been increasing over the years, so has the number of patients with DFUs [55], [58]. DFUs are responsible for a high mortality rate as well as for a high impact on the healthcare system and health economics, as they require high medical care and amputations have very elevated costs [59], [60], [82]. Peripheral neuropathy, peripheral arterial disease and infections are the main responsible for the development of DFUs [58], [63]. The most commonly used treatments to cure DFUs are based on strategies to combat and reduce the damage caused by those conditions, like revascularisation and infection control. However, these treatments often fail and are not able to completely cure DFUs, which causes about 10-15% of non-healing DFUs [58], [75]. Thus, it becomes evident the necessity to develop new effective treatments for non-healing DFUs.

Macrophages are present in all wound healing phases with important functions in each one of them [14]. They are responsible for the elimination of bacteria, damaged cells and other cellular debris present at the wound site, by phagocytosis [95], [96]. Furthermore, they produce a variety of factors that will promote cell proliferation and protein synthesis, which are essential for new tissue formation [14], [96]. Macrophages also play an important role in the final stages of wound healing, where the M1 macrophages are converted into M2 macrophages which will promote inflammation resolution and wound closure [99]. Their function in wounds and tissue repair is extremely important and when their function is impaired the wound healing process is disrupted, which has been proven in studies where the depletion of dermal macrophages during the inflammatory or proliferative phase delayed wound healing [98], [99].

The DFU pathology has been associated with dysfunctional phagocytosis of pathogens and cellular debris, abnormal macrophage secretion of cytokines and factors essential for wound

healing, and difficulties on the conversion of M1 into M2 macrophages, causing a delay in the resolution of the inflammatory phase [96], [99], [104], [108]. Thus, macrophages may be a good therapeutic target for chronic DFUs. Treatments capable of modulating and improving macrophage functions are good candidates to promote wound healing and tissue repair.

PTP1B was the first PTP isolated in humans [112] and since then its role in various pathologies has been widely studied. Since this protein works as a negative regulator of the insulin signalling pathway, its role in diabetes has been well studied and it has been proposed as a novel target for insulin resistance [113]–[115], [226]. Several studies have revealed that PTP1B expression and activity is increased in insulin resistance conditions [115], [118]. In addition, PTP1B KO mice show increased insulin sensitivity even under high fat diet [119]. These studies led to the finding and development of several PTP1B inhibitors, such as the naturally occurring MSI-1436, which is currently in clinical trials for approval to be used in diabetes treatment [227]. Furthermore, PTP1B is also involved in processes such as glucose uptake and cellular proliferation, differentiation, motility, adhesion and invasion [116], [117], which are essential in wound healing. In addition, PTP1B is overexpressed under diabetic conditions and in DFUs [120], which increases the interest in studying the role of PTP1B in diabetic wound healing, suggesting that PTP1B inhibition may be a good strategy to promote DFU healing. However, the role of PTP1B in this pathology remains unknown.

PTP1B is ubiquitously expressed and is located in the endoplasmic reticulum [150]. PTP1B is expressed in immune cells like macrophages, which can indicate that macrophage-PTP1B may have a role in chronic DFUs and its inhibition may be an important therapeutic approach.

The main hypothesis of this dissertation is that the inhibition of PTP1B, especially in macrophages, will improve wound repair in DFUs by modulating the macrophage phenotype, improving macrophage function during the healing process, and promoting other cell functions, including proliferation and differentiation. Considering that PTP1B inhibitors are in phase 2 clinical trials for diabetes treatment [228], these could easily be repurposed for diabetic foot ulcer treatment.

To evaluate the effect of PTP1B inhibition and its functional properties on macrophages during wound healing, THP-1 cells, a human leukaemia monocytic cell line widely used as a model for human monocytes and macrophages, were cultured in either NG or HG medium, differentiated into macrophages and treated with MSI-1436 under inflammatory conditions. In addition, primary cultures of human monocytes isolated from peripheral blood of diabetic patients without DFUs and with acute or chronic DFUs, as well as from healthy volunteers were used. Furthermore, MSI-146 was applied topically at the wound site, in streptozotocin-induced diabetic animals to study the role of PTP1B inhibition in wound healing and tissue repair.

The PTP1B inhibitor, MSI-1436, was well tolerated by human cells, since it did not alter the viability of THP-1 cells or isolated human monocytes. This supports other studies showing that MSI-1436 is well tolerated and has no relevant side or cytotoxic effects [154], [192], [229].

As mentioned before, studies revealed that PTP1B is overexpressed under diabetic conditions [115], [120]. Moreover, it is known that high glucose increases PTP1B expression in several cell types [194], [195]. The same was observed in this study, THP-1 cells cultured under HG conditions, showed higher PTP1B protein levels than cells cultured under NG conditions. These results suggest that PTP1B overexpression may be involved in macrophage dysfunction observed in diabetes and DFUs.

Chronic wounds are characterised by the presence of a higher number of M1 macrophages, suggesting that a strategy to improve wound healing can be the modulation of the macrophage phenotype by promoting the conversion of M1 macrophages into M2 macrophages [99], [108]. The literature shows that activated PTP1B reduces the phosphorylation of essential proteins in the pathway which leads to M2 polarisation, leading to a decrease in M2 levels [230]. Indeed, PTP1B inhibition has already been shown to increase M2 polarisation in murine macrophages [231], [232]. The results obtained in this dissertation are consistent with these studies, showing that THP-1 cells treated with MSI-1436, in the presence of an inflammatory stimulus, and cultured under NG or HG, showed an increase in M2 macrophages and a reduction in the number of M1 macrophages. Similar results were observed at the wound site in mice treated with MSI-1436. Diabetic mouse wounds treated with MSI-1436 showed a higher number of M2 macrophages and a reduction of M1 macrophages when compared to control (untreated) wounds. One of the major problems in diabetic wound is the exaggerated inflammation partly due to the accumulation of M1 macrophages. PTP1B inhibition promotes M2 polarisation, which is important for tissue repair and for the acceleration of wound healing, by reducing M1 macrophage accumulation and reducing the pro-inflammatory environment.

The expression of pro-inflammatory cytokines, IL-8, IL-6 and MCP-1 was increased in cells cultured under HG conditions when compared to NG conditions, indicating that there is a higher pro-inflammatory environment induced by HG. In this study, the expression of pro-inflammatory cytokines and chemokines IL8, IL-6, IL1β and MCP-1 was reduced with MSI-1436 treatment in THP-1 cells cultured under HG conditions. However, PTP1B inhibition did not have a relevant effect in the expression of these factors in NG cultured cells.

The levels of IL-6 and TNF-α in the medium were decreased with PTP1B inhibition in NG. In HG, only the lower concentration of MSI-1436 (500 nM) promoted a reduction in IL-6 and TNF-α. PTP1B inhibition increased IL-10 levels under HG, however this effect was not observed in NG condition. These results need to be repeated in order to corroborate what has been observed. However, the inhibition of PTP1B seems to lead to a reduction in the pro-inflammatory environment present in HG condition, but not under NG conditions. These results may be explained by the fact that, in a normal environment, macrophages are not dysfunctional, and they are able to modulate the inflammatory environment. In human monocyte-derived macrophages, PTP1B inhibition decreased the expression of IL-8, IL-6, IL1β, TNF-α and MCP-1 in the diabetic group. IL-6 levels

in the cell medium were reduced in cells from both diabetic and diabetic with acute ulcer groups with MSI-1436 treatment. The levels of TNF-α were also decreased in the human cells from the diabetic group. However, this effect was not observed in the control, diabetic with acute ulcer and diabetic with chronic ulcer groups. Curiously, PTP1B inhibition increased IL-10 levels in the control group but not in the other groups. Human monocyte-derived macrophages from diabetic patients with acute or chronic ulcers were hardly responsive to the given stimuli (LPS or MSI-1436). In addition, it was not possible to detect the expression of most cytokines reported in these groups. When the expression of cytokines was detected, in macrophages from diabetic patients with either acute or chronic ulcer, the response, after stimulation with LPS, was very low, indicating that these cells are compromised and do not respond correctly to either the inflammatory stimulus and/or the treatment. However, these are only preliminary data as the number of donors in each group is very small and further studies need to be performed. Another factor that may also have influenced the responses of these cells was the fact that the human monocyte-derived macrophages of the different groups were treated with PMA and LPS, which may have been excessive manipulation of these cells. Therefore, it is necessary to repeat these experiments in order to obtain better and more solid results.

The expression of the growth factors TGF-β; VEGF; PDGF and EGF was also analysed. In THP-1 cells, PTP1B inhibition did not change the expression of these growth factors. However, in human monocyte-derived macrophages, PTP1B inhibition increased EGF levels in cells from the diabetic group, and increased PDGF levels in all groups. Since PTP1B modulates growth factor signalling pathways by dephosphorylation of a variety of growth factor receptors, including the EGF receptor (EGFR) and PDGF receptor (PDGFR) [233], its inhibition may be beneficial to enhance growth factors signalling pathways, and not by modulating growth factor expression.

Chronic wounds have high level of ROS produced in large amounts by the numerous immune cells accumulated at the wound site. ROS is responsible for cell damage and impaired angiogenesis leading to poor wound healing [87], [200]. Furthermore, in chronic diabetic wounds, the increase in ROS production is also due to a reduction in the antioxidant defences creating a redox imbalance [191, [192]. It is also known that murine and human macrophages cultured under HG conditions have increased ROS formation, which is associated with the increase in the pro-inflammatory M1 phenotype [201]. The role of PTP1B in oxidative stress has been barely studied. A study done by Mobasher *et al.* revealed that PTP1B deficiency in mouse hepatocytes prevents ROS generation and enhances antioxidant defence [234]. In this study, PTP1B inhibition showed the ability to reduce ROS levels. The ROS levels in THP-1 cells treated with MSI-1436 and cultured under NG or HG, were decreased when compared to control cells. The same effect was observed in diabetic mouse wounds. PTP1B inhibition reduced the production of ROS at the wound site. These results suggest that PTP1B inhibition is capable of reducing ROS levels in the wound, accelerating wound healing under diabetic conditions.

Another biologic function impaired in chronic wounds is angiogenesis. It has been shown that DFUs have insufficient angiogenesis resulting in poor nutrient delivery and hypoxia, causing a delay in wound healing [202]. Diabetic wounds exhibit a reduction in vascularisation and capillary density at the wound site [217], [237]. This failure in angiogenesis may be associated with abnormalities observed in macrophages, as they are responsible for the production of various factors that promote angiogenesis, like VEGF [217]. Several studies have shown PTP1B playing a key role in angiogenesis. PTP1B negatively regulates the activation of VEGFR2 preventing the proliferation of endothelial cells, and PTP1B deletion leads to an increase in VEGFR2 activity causing an increase in endothelial cells proliferation and in angiogenesis, accelerating wound healing [131]–[133]. The results obtained in this work are consistent with previous studies, since diabetic mouse wounds treated with MSI-1436 showed a higher number of blood vessels comparing to control wounds. This effect of PTP1B inhibition will allow to obtain a better blood supply to the wound and, consequently, oxygen and nutrients essential for wound healing.

The proliferation of cell populations at the wound site, such as fibroblast, endothelial cells, macrophages and keratinocytes, is essential for reepithelization of the epidermis and, thus, for wound closure. However, in chronic wounds some cells populations have impaired proliferation and are unresponsive to signs that promote wound healing. This decrease in the proliferative capacity of cells is thought to be caused by high levels of oxidative stress that can cause cell cycle defects due to DNA damage [105]. Several authors have demonstrated that the absence of PTP1B activity leads to an increase in the proliferation of hepatocytes and cardiomyocytes improving hepatic and heart tissue regeneration [153], [154]. In addition, Zebrafish treated with a PTP1B inhibitor, showed increased tissue regeneration of the amputated caudal fin which is composed of bone, connective, skin, vascular and nervous tissues [154]. These data indicate that PTP1B inhibition may increase cell proliferation and tissue regeneration at the wound site contributing to a faster healing, which is supported by this study findings. PTP1B inhibition highly increased the number of proliferating cells at the wound site when compared to control wounds.

HO-1 is an enzyme with a protective role against oxidative tissue damage and its expression is induced by pro-oxidant and inflammatory stimulus [236]. This enzyme is known to have anti-inflammatory (enhances the polarisation toward anti-inflammatory M2 macrophage), antioxidant and anti-apoptotic properties [170]–[173], [236]. HO-1 overexpression in response to high ROS production contributes to the redox balance [171], [172]. The correlation between low HO-1 levels and tissue damage caused by high ROS levels was first observed by Yachie *et al.* in 1998. A patient with deficiencies in HO-1 production had lower antioxidant defences and protection against damage caused by ROS [236], [237]. Furthermore, HO-1-deficient cells produce high levels of ROS and have reduced stress defences [213]. The overexpression of HO-1 is also related to high vascularisation and angiogenesis, since this enzyme seems to protect the vessels from endothelial dysfunction [214], [234]. The increase in HO-1 expression also stimulates the proliferation of some

cell types as epidermal keratinocytes, endothelial cells and epithelial cells [238], [239]. Thus, HO-1 plays an important role in the wound healing process. In fact, some studies have demonstrated that the overexpression of HO-1 promotes mice and rat diabetic wound healing [215], [216]. In this work, it was found HO-1 gene expression and protein levels were significantly increased by PTP1B inhibition in THP-1 cells cultured in both NG and HG. Moreover, HO-1 protein levels were increased in diabetic wounds when compared to control. This effect of PTP1B inhibition on HO-1 levels had already been demonstrated in other studies. Xu *et al.* and Lee *et al.* have demonstrated that PTP1B inhibition leads to an overexpression of HO-1 in murine macrophages [231], [240]. However, to the best of my knowledge, this is the first report to show that PTP1B inhibition increases HO-1 levels in diabetic wounds. The increase in HO-1 levels is consistent with the increase in the number of M2 macrophages, the decrease in the pro-inflammatory environment and the reduction in the ROS levels at the wound site. Although pro-oxidant and inflammatory stimulus increase HO-1 production, sometimes this increase is not sufficient to regulate ROS levels. Thus, the inhibition of PTP1B seems to further increase the HO-1 production, suggesting a better protection for an increase in oxidative stress. The increase in HO-1 levels induced by PTP1B inhibition is also correlated with the reduction in the inflammatory environment and the increased angiogenesis and cell proliferation observed.

Previous studies have also shown that PTP1B inhibition improves wound healing [115], [220], however, the mechanisms involved are not well known particularly under diabetic conditions. The animal experiment showed that the dose 1 µg of MSI-1436 is the most effective in promoting wound healing.

Taken all together, although some of the results are preliminary, it is clear that PTP1B inhibition at the wound site promotes its healing by inducing an increase in HO-1 expression, which in turn leads to an increase in M2 macrophage polarisation, a decrease in inflammation, a decrease in oxidative stress and an increase in angiogenesis and proliferation. These effects will promote a faster and more efficient wound healing (**Figure 53**). These results suggest that the local modulation of PTP1B may be beneficial in the treatment of impaired wound healing in diabetes. PTP1B inhibition may be potentially effective in the treatment of DFUs and considering that PTP1B inhibitors are in phase 2 clinical trials for diabetes treatment [228], these could easily be repurposed for DFU treatment.

Although this study has shown very promising effects of PTP1B inhibition on the cure of DFUs, mores studies are need in order to consolidate the findings of this dissertation, as well as to better understand the mechanisms of PTP1B inhibition in diabetic wound healing and tissue repair.
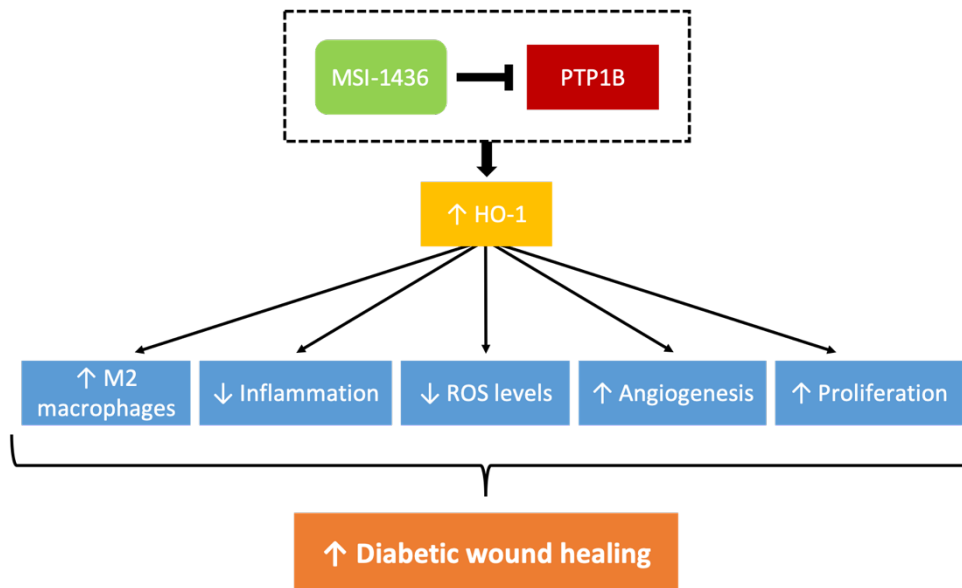
Figure 53 - Proposed mechanism for the effect of PTP1B inhibition in the promotion of diabetic wound healing. PTP1B inhibition leads to increased HO-1 expression which in turn induces an increase in M2 macrophages and a decrease in inflammation, a decrease in ROS levels and increases angiogenesis and proliferation at wound site, promoting diabetic wound healing.

Chapter 5: References

[1] R. F. Pereira, C. C. Barrias, P. L. Granja, and P. J. Bartolo, 'Advanced biofabrication strategies for skin regeneration and repair', *Nanomedicine*, vol. 8, no. 4, pp. 603–621, Apr. 2013.

[2] L. Yildirimer, N. T. K. Thanh, and A. M. Seifalian, 'Skin regeneration scaffolds: a multimodal bottom-up approach', *Trends in Biotechnology*, vol. 30, no. 12, pp. 638–648, Dec. 2012.

[3] E. McLafferty, C. Hendry, and A. Farley, 'The integumentary system: anatomy, physiology and function of skin', *Nursing Standard*, vol. 27, no. 3, pp. 35–42, Sep. 2012.

[4] 'Anatomy & Physiology. Chapter 5. The Integumentary System - 5.1 Layers of the Skin', 2018. [Online]. Available: http://library.open.oregonstate.edu/aandp/chapter/5-1-layers-of-the-skin/.

[5] G. J. Tortora and B. Derrickson, *Principles of Anatomy and Physiology*, 14th ed. John Wiley and Sons, Hoboken NJ, 2014.

[6] M. Yu, A. Finner, J. Shapiro, B. Lo, A. Barekatain, and K. J. McElwee, 'Hair follicles and their role in skin health', *Expert Review of Dermatology*, vol. 1, no. 6, pp. 855–871, Dec. 2006.

[7] B. D. Hodge and R. T. Brodell, 'Anatomy, Skin Sweat Glands. [Updated 2019 Apr 5]. In: StatPearls [Internet].', *Treasure Island (FL): StatPearls Publishing*, 2019. [Online]. Available: Available from: https://www.ncbi.nlm.nih.gov/books/NBK482278/.

[8] Z. Zaidi and S. W. Lanigan, 'Chapter 1 - Skin: Structure and Function', in *Dermatology in Clinical Practice*, London: Springer London, 2010, pp. 1–15.

[9] C. C. Zouboulis, 'Acne and sebaceous gland function', *Clinics in Dermatology*, vol. 22, no. 5, pp. 360–366, Sep. 2004.

[10] P. A. J. Kolarsick, M. A. Kolarsick, and C. Goodwin, 'Anatomy and Physiology of the Skin', *Journal of the Dermatology Nurses' Association*, vol. 3, no. 4, pp. 203–213, 2011.

[11] J. J. Wille and A. Kydonieus, 'Palmitoleic Acid Isomer (C16:1Δ6) in Human Skin Sebum Is Effective against Gram-Positive Bacteria', *Skin Pharmacol Physiol*, vol. 16, no. 3, pp. 176–187, 2003.

[12] M. Venus, J. Waterman, and I. McNab, 'Basic physiology of the skin', *Surgery (Oxford)*, vol. 28, no. 10, pp. 469–472, Oct. 2010.

[13] Z. Halata, M. Grim, and K. I. Baumann, 'Current understanding of Merkel cells, touch reception and the skin', *Expert Review of Dermatology*, vol. 5, no. 1, pp. 109–116, Feb. 2010.

[14] C. M. Minutti, J. A. Knipper, J. E. Allen, and D. M. W. Zaiss, 'Tissue-specific contribution of macrophages to wound healing', *Seminars in Cell & Developmental Biology*, vol. 61, pp. 3–11, 2016.

[15] O. Stojadinovic, N. Yin, J. Lehmann, I. Pastar, R. S. Kirsner, and M. Tomic-Canic, 'Increased

number of Langerhans cells in the epidermis of diabetic foot ulcers correlates with healing outcome', *Immunologic Research*, vol. 57, no. 1–3, pp. 222–228, Dec. 2013.

[16] F. O. Nestle, P. Di Meglio, J.-Z. Qin, and B. J. Nickoloff, 'Skin immune sentinels in health and disease', *Nature Reviews Immunology*, vol. 9, no. 10, pp. 679–691, Oct. 2009.

[17] E. Proksch, R. Fölster-Holst, and J.-M. Jensen, 'Skin barrier function, epidermal proliferation and differentiation in eczema', *Journal of Dermatological Science*, vol. 43, no. 3, pp. 159–169, Sep. 2006.

[18] K. C. Madison, 'Barrier Function of the Skin: "La Raison d'Être" of the Epidermis', *Journal of Investigative Dermatology*, vol. 121, no. 2, pp. 231–241, Aug. 2003.

[19] A. Matejuk, 'Skin Immunity', *Arch. Immunol. Ther. Exp.*, vol. 66, no. 1, pp. 45–54, Feb. 2018.

[20] P. Di Meglio, G. K. Perera, and F. O. Nestle, 'The Multitasking Organ: Recent Insights into Skin Immune Function', *Immunity*, vol. 35, no. 6, pp. 857–869, Dec. 2011.

[21] M. Zanetti, 'Cathelicidins, multifunctional peptides of the innate immunity', *Journal of Leukocyte Biology*, vol. 75, no. 1, pp. 39–48, Jan. 2004.

[22] D. Chomiczewska, E. Trznadel-Budźko, A. Kaczorowska, and H. Rotsztejn, 'The role of Langerhans cells in the skin immune system', *Polski merkuriusz lekarski : organ Polskiego Towarzystwa Lekarskiego*, vol. 26, no. 153, p. 173—177, Mar. 2009.

[23] B. Spellberg and J. E. Edwards, 'Type 1/Type 2 Immunity in Infectious Diseases', *Clinical Infectious Diseases*, vol. 32, no. 1, pp. 76–102, Jan. 2001.

[24] F. J. Dumont, 'Modulation of Th1 and Th2 responses for immunotherapy', *Expert Opinion on Therapeutic Patents*, vol. 12, no. 3, pp. 341–367, Mar. 2002.

[25] B. Wang, P. Amerio, and D. N. Sauder, 'Role of cytokines in epidermal Langerhans cell migration', *J Leukoc Biol*, vol. 66, no. 1, pp. 33–39, Jul. 1999.

[26] I. Harvima and G. Nilsson, 'Mast Cells as Regulators of Skin Inflammation and Immunity', *Acta Derm Venerol*, vol. 91, no. 6, pp. 644–650, 2011.

[27] N. Mascarenhas, Z. Wang, and A. Di Nardo, 'Mast Cells: Sentinels of Innate Skin Immunity', in *Clinical and Basic Immunodermatology*, A. A. Gaspari, S. K. Tyring, and D. H. Kaplan, Eds. Cham: Springer International Publishing, 2017, pp. 67–80.

[28] M. Pasparakis, I. Haase, and F. O. Nestle, 'Mechanisms regulating skin immunity and inflammation', *Nat Rev Immunol*, vol. 14, no. 5, pp. 289–301, May 2014.

[29] R. A. Clark, 'Skin-Resident T Cells: The Ups and Downs of On Site Immunity', *Journal of Investigative Dermatology*, vol. 130, no. 2, pp. 362–370, Feb. 2010.

[30] K. G. M. M. Alberti, P. Z. Zimmet, and WHO Consultation, 'Definition, diagnosis and classification of diabetes mellitus and its complications. Part 1: diagnosis and classification

of diabetes mellitus. Provisional report of a WHO Consultation', *Diabetic Medicine*, vol. 15, no. 7, pp. 539–553, Jul. 1998.

[31] World Health Organization, *Global report on diabetes*. Geneva, Switzerland, 2016.

[32] Direção-Geral da Saúde, Portugal, 'Programa nacional para a diabetes 2017'. Direção-Geral da Saúde, Portugal, 2017.

[33] N. G. Forouhi and N. J. Wareham, 'Epidemiology of diabetes', *Medicine*, vol. 42, no. 12, pp. 698–702, Dec. 2014.

[34] D. M. Maahs, N. A. West, J. M. Lawrence, and E. J. Mayer-Davis, 'Epidemiology of Type 1 Diabetes', *Endocrinology and Metabolism Clinics of North America*, vol. 39, no. 3, pp. 481–497, Sep. 2010.

[35] D. Cheng, 'Prevalence, predisposition and prevention of type II diabetes', p. 12, 2005.

[36] J. A. Bluestone, K. Herold, and G. Eisenbarth, 'Genetics, pathogenesis and clinical interventions in type 1 diabetes', *Nature*, vol. 464, no. 7293, pp. 1293–1300, Apr. 2010.

[37] American Diabetes Association, '2. Classification and Diagnosis of Diabetes: *Standards of Medical Care in Diabetes—2018*', *Diabetes Care*, vol. 41, no. Supplement 1, pp. S13–S27, Jan. 2018.

[38] World Health Organization, 'About diabetes: Types of diabetes'. [Online]. Available: http://www.who.int/diabetes/action_online/basics/en/index1.html.

[39] D. C. Klonoff, 'The Increasing Incidence of Diabetes in the 21st Century', *Journal of Diabetes Science and Technology*, vol. 3, no. 1, pp. 1–2, Jan. 2009.

[40] A. Chawla, R. Chawla, and S. Jaggi, 'Microvasular and macrovascular complications in diabetes mellitus: Distinct or continuum?', *Indian Journal of Endocrinology and Metabolism*, vol. 20, no. 4, p. 546, 2016.

[41] World Health Organization, 'About diabetes: Complications of diabetes'. [Online]. Available: http://www.who.int/diabetes/action_online/basics/en/index3.html.

[42] American Diabetes Association, 'Neuropathy (Nerve Damage)'. [Online]. Available: http://www.diabetes.org/living-with-diabetes/complications/neuropathy/.

[43] Eva L Feldman, 'Epidemiology and classification of diabetic neuropathy'. [Online]. Available: https://www.uptodate.com/contents/epidemiology-and-classification-of-diabetic-neuropathy.

[44] J. Chen, 'Diabetic Nephropathy: Scope of the Problem', in *Diabetes and Kidney Disease*, E. V. Lerma and V. Batuman, Eds. New York, NY: Springer New York, 2014, pp. 9–14.

[45] K. Boyd, 'What Is Diabetic Retinopathy?' [Online]. Available: https://www.aao.org/eye-health/diseases/what-is-diabetic-retinopathy.

[46] J. W. Y. Yau *et al.*, 'Global Prevalence and Major Risk Factors of Diabetic Retinopathy', *Diabetes Care*, vol. 35, no. 3, pp. 556–564, Mar. 2012.

[47] M. Dutra Medeiros, E. Mesquita, A. L. Papoila, V. Genro, and J. F. Raposo, 'First diabetic retinopathy prevalence study in Portugal: RETINODIAB Study—Evaluation of the screening programme for Lisbon and Tagus Valley region', *British Journal of Ophthalmology*, vol. 99, no. 10, pp. 1328–1333, Oct. 2015.

[48] S. Mangmool, T. Denkaew, W. Parichatikanond, and H. Kurose, 'β-Adrenergic Receptor and Insulin Resistance in the Heart', *Biomolecules & Therapeutics*, vol. 25, no. 1, pp. 44–56, Jan. 2017.

[49] A. R. Saltiel and C. R. Kahn, 'Insulin signalling and the regulation of glucose and lipid metabolism', *Nature*, vol. 414, no. 6865, pp. 799–806, Dec. 2001.

[50] P. Bevan, 'Insulin signalling', vol. 114, no. 8, pp. 1429–1430, 2001.

[51] G. Van den Berghe, 'How does blood glucose control with insulin save lives in intensive care?', *The Journal of clinical investigation*, vol. 114, no. 9, pp. 1187–1195, 2004.

[52] M. Björnholm and J. R. Zierath, 'Insulin signal transduction in human skeletal muscle: identifying the defects in Type II diabetes', *Biochemical Society Transactions*, vol. 33, pp. 354–357, 2005.

[53] R. A. DeFronzo, 'Pathogenesis of type 2 diabetes mellitus', *Medical Clinics of North America*, vol. 88, no. 4, pp. 787–835, Jul. 2004.

[54] E. Carvalho, P.-A. Jansson, I. Nagaev, A.-M. Wenthzel, and U. Smith, 'Insulin resistance with low cellular IRS-1 expression is also associated with low GLUT4 expression and impaired insulin-stimulated glucose transport', *The FASEB Journal*, Feb. 2001.

[55] P. Zhang, J. Lu, Y. Jing, S. Tang, D. Zhu, and Y. Bi, 'Global epidemiology of diabetic foot ulceration: a systematic review and meta-analysis', *Annals of Medicine*, vol. 49, no. 2, pp. 106–116, Feb. 2017.

[56] J. Apelqvist, 'Diagnostics and treatment of the diabetic foot', *Endocrine*, vol. 41, no. 3, pp. 384–397, Jun. 2012.

[57] N. Singh, D. G. Armstrong, and B. A. Lipsky, 'Preventing Foot Ulcers in Patients With Diabetes', *JAMA*, vol. 293, no. 2, p. 217, Jan. 2005.

[58] K. Alexiadou and J. Doupis, 'Management of Diabetic Foot Ulcers', *Diabetes Therapy*, vol. 3, no. 1, Dec. 2012.

[59] F. L. Bowling, S. T. Rashid, and A. J. M. Boulton, 'Preventing and treating foot complications associated with diabetes mellitus', *Nature Reviews Endocrinology*, vol. 11, no. 10, pp. 606–616, Oct. 2015.

[60] D. G. Armstrong, J. Wrobel, and J. M. Robbins, 'Guest Editorial: are diabetes-related wounds and amputations worse than cancer?', *International Wound Journal*, vol. 4, no. 4, pp. 286–

287, Dec. 2007.

[61] F. W. Wagner, 'The Dysvascular Foot: A System for Diagnosis and Treatment', *Foot & Ankle*, vol. 2, no. 2, pp. 64–122, Sep. 1981.

[62] M. S. Pinzur, *The Diagnosis and Treatment of Diabetic Foot Infections. In: Herscovici, Jr. D. (eds) The Surgical Management of the Diabetic Foot and Ankle*. Springer, Cham, 2016.

[63] S. Pendsey, 'Understanding diabetic foot', *International Journal of Diabetes in Developing Countries*, vol. 30, no. 2, p. 75, 2010.

[64] D. G. Armstrong, A. J. M. Boulton, and S. A. Bus, 'Diabetic Foot Ulcers and Their Recurrence', *New England Journal of Medicine*, vol. 376, no. 24, pp. 2367–2375, Jun. 2017.

[65] S. Tesfaye and D. Selvarajah, 'Advances in the epidemiology, pathogenesis and management of diabetic peripheral neuropathy: Advances in Epidemiology, Pathogenesis and Management of DPN', *Diabetes/Metabolism Research and Reviews*, vol. 28, pp. 8–14, Feb. 2012.

[66] S. Alsunousi and H. I. Marrif, 'Diabetic neuropathy and the sensory apparatus "meissner corpuscle and merkel cells"', *Frontiers in Neuroanatomy*, vol. 8, agosto 2014.

[67] American Diabetes Association, 'Peripheral Arterial Disease in People With Diabetes', *Diabetes Care :3333– 41.*, vol. 26:3333, p. 41, 2003.

[68] S. P. Marso and W. R. Hiatt, 'Peripheral Arterial Disease in Patients With Diabetes', *Journal of the American College of Cardiology*, vol. 47, no. 5, pp. 921–929, Mar. 2006.

[69] E. B. Jude, S. O. Oyibo, N. Chalmers, and A. J. M. Boulton, 'Peripheral Arterial Disease in Diabetic and Nondiabetic Patients: A comparison of severity and outcome', *Diabetes Care*, vol. 24, no. 8, pp. 1433–1437, Aug. 2001.

[70] R. G. Frykberg, 'An evidence-based approach to diabetic foot infections', *The American Journal of Surgery*, vol. 186, no. 5, pp. 44–54, Nov. 2003.

[71] B. A. Lipsky *et al.*, 'Diagnosis and Treatment of Diabetic Foot Infections', *Clinical Infectious Diseases*, pp. 885–910, 2004.

[72] C. Dunyach-Remy, C. Ngba Essebe, A. Sotto, and J.-P. Lavigne, 'Staphylococcus aureus Toxins and Diabetic Foot Ulcers: Role in Pathogenesis and Interest in Diagnosis', *Toxins*, vol. 8, no. 7, p. 209, Jul. 2016.

[73] I. Kruse, 'Evaluation and Treatment of Diabetic Foot Ulcers', *Clinical Diabetes*, vol. 24, no. 2, pp. 91–93, Apr. 2006.

[74] P. R. Cavanagh, B. A. Lipsky, A. W. Bradbury, and G. Botek, 'Treatment for diabetic foot ulcers', *The Lancet*, vol. 366, no. 9498, pp. 1725–1735, Nov. 2005.

[75] T. G. D. Pemayun, R. M. Naibaho, D. Novitasari, N. Amin, and T. T. Minuljo, 'Risk factors for lower extremity amputation in patients with diabetic foot ulcers: a hospital-based case–

control study', *Diabetic Foot & Ankle*, vol. 6, no. 1, p. 29629, Jan. 2015.

[76] T. Dinh, S. Elder, and A. Veves, 'Delayed wound healing in diabetes: considering future treatments', *Diabetes Management*, vol. 1, no. 5, pp. 509–519, Sep. 2011.

[77] S. E. Dowd, R. D. Wolcott, Y. Sun, T. McKeehan, E. Smith, and D. Rhoads, 'Polymicrobial Nature of Chronic Diabetic Foot Ulcer Biofilm Infections Determined Using Bacterial Tag Encoded FLX Amplicon Pyrosequencing (bTEFAP)', *PLoS ONE*, vol. 3, no. 10, p. e3326, Oct. 2008.

[78] R. Cornell, 'How Biofilm Affects Healing In Diabetic Foot Wounds', 2010. [Online]. Available: https://www.podiatrytoday.com/how-biofilm-affects-healing-in-diabetic-foot-wounds.

[79] D. Neut, E. J. Tijdens-Creusen, S. K. Bulstra, H. C. van der Mei, and H. J. Busscher, 'Biofilms in chronic diabetic foot ulcers—a study of 2 cases', *Acta Orthopaedica*, vol. 82, no. 3, pp. 383–385, Jun. 2011.

[80] S. P. Bennett, G. D. Griffiths, A. M. Schor, G. P. Leese, and S. L. Schor, 'Growth factors in the treatment of diabetic foot ulcers', *British Journal of Surgery*, vol. 90, no. 2, pp. 133–146, Feb. 2003.

[81] R. Eldor, I. Raz, A. Ben Yehuda, and A. J. M. Boulton, 'New and experimental approaches to treatment of diabetic foot ulcers: a comprehensive review of emerging treatment strategies', *Diabetic Medicine*, vol. 21, no. 11, pp. 1161–1173, Nov. 2004.

[82] A. Raghav, Z. A. Khan, R. K. Labala, J. Ahmad, S. Noor, and B. K. Mishra, 'Financial burden of diabetic foot ulcers to world: a progressive topic to discuss always', *Therapeutic Advances in Endocrinology and Metabolism*, vol. 9, no. 1, pp. 29–31, Jan. 2018.

[83] Diabetes UK, 'Improving footcare for people with diabetes and saving money: an economic study in England', 2017. [Online]. Available: https://diabetes-resources-production.s3-eu-west-1.amazonaws.com/diabetes-storage/migration/pdf/Improving%2520footcare%2520economic%2520study%2520%28January%25202017%29.pdf.

[84] J. B. Rice, U. Desai, A. K. G. Cummings, H. G. Birnbaum, M. Skornicki, and N. B. Parsons, 'Burden of Diabetic Foot Ulcers for Medicare and Private Insurers', *Diabetes Care*, vol. 37, no. 3, pp. 651–658, Mar. 2014.

[85] L. Prompers *et al.*, 'Resource utilisation and costs associated with the treatment of diabetic foot ulcers. Prospective data from the Eurodiale Study', *Diabetologia*, vol. 51, no. 10, pp. 1826–1834, Oct. 2008.

[86] B. K. Sun, Z. Siprashvili, and P. A. Khavari, 'Advances in skin grafting and treatment of cutaneous wounds', *Science*, vol. 346, no. 6212, pp. 941–945, Nov. 2014.

[87] T. N. Demidova-Rice, M. R. Hamblin, and I. M. Herman, 'Acute and Impaired Wound Healing: Pathophysiology and Current Methods for Drug Delivery, Part 1', *Advances in Skin & Wound Care*, vol. 25, no. 7, pp. 304–314, Jul. 2012.

[88] A. Mellott, D. Zamierowski, and B. Andrews, 'Negative Pressure Wound Therapy in Maxillofacial Applications', *Dentistry Journal*, vol. 4, no. 3, p. 30, Sep. 2016.

[89] E. Rand and A. C. Gellhorn, 'The Healing Cascade: Facilitating and Optimizing the System', *Physical Medicine and Rehabilitation Clinics of North America*, vol. 27, no. 4, pp. 765–781, Nov. 2016.

[90] W. K. Stadelmann, A. G. Digenis, and G. R. Tobin, 'Physiology and healing dynamics of chronic cutaneous wounds', *The American Journal of Surgery*, vol. 176, no. 2, pp. 26S-38S, Aug. 1998.

[91] T. Wilgus, 'Immune cells in the healing skin wound: Influential players at each stage of repair', *Pharmacological Research*, vol. 58, no. 2, pp. 112–116, Aug. 2008.

[92] N. Strbo, N. Yin, and O. Stojadinovic, 'Innate and Adaptive Immune Responses in Wound Epithelialization', *Advances in Wound Care*, vol. 3, no. 7, pp. 492–501, Jul. 2014.

[93] A. S. MacLeod and J. N. Mansbridge, 'The Innate Immune System in Acute and Chronic Wounds', *Advances in Wound Care*, vol. 5, no. 2, pp. 65–78, Feb. 2016.

[94] Y. Iwata *et al.*, 'CD19, a Response Regulator of B Lymphocytes, Regulates Wound Healing through Hyaluronan-Induced TLR4 Signaling', *The American Journal of Pathology*, vol. 175, no. 2, pp. 649–660, Aug. 2009.

[95] R. J. Snyder, J. Lantis, R. S. Kirsner, V. Shah, M. Molyneaux, and M. J. Carter, 'Macrophages: A review of their role in wound healing and their therapeutic use: Review of macrophages in wound healing', *Wound Repair and Regeneration*, vol. 24, no. 4, pp. 613–629, Jul. 2016.

[96] T. J. Koh and L. A. DiPietro, 'Inflammation and wound healing: the role of the macrophage', *expert reviews*, vol. 13, p. 12, 2011.

[97] D. A. Yanez, R. K. Lacher, A. Vidyarthi, and O. R. Colegio, 'The role of macrophages in skin homeostasis', *Pflugers Arch - Eur J Physiol*, vol. 469, no. 3–4, pp. 455–463, Apr. 2017.

[98] T. Lucas *et al.*, 'Differential Roles of Macrophages in Diverse Phases of Skin Repair', *J.I.*, vol. 184, no. 7, pp. 3964–3977, Apr. 2010.

[99] P. Krzyszczyk, R. Schloss, A. Palmer, and F. Berthiaume, 'The Role of Macrophages in Acute and Chronic Wound Healing and Interventions to Promote Pro-wound Healing Phenotypes', *Frontiers in Physiology*, vol. 9, May 2018.

[100] J. R. Mekkes, M. A. M. Loots, A. C. Van Der Wal, and J. D. Bos, 'Causes, investigation and treatment of leg ulceration', *British Journal of Dermatology*, vol. 148, no. 3, pp. 388–401, Mar. 2003.

[101] R. Diegelmann F. and M. C. Evans, 'Wound healing: an overview of acute, fibrotic and delayed healing', *Frontiers in Bioscience*, vol. 9, no. 1–3, p. 283, 2004.

[102] J. Moura, J. Rodrigues, M. Gonçalves, C. Amaral, M. Lima, and E. Carvalho, 'Impaired T-

cell differentiation in diabetic foot ulceration', *Cellular & Molecular Immunology*, vol. 14, no. 9, pp. 758–769, Sep. 2017.

[103] R. D. Galiano *et al.*, 'Topical Vascular Endothelial Growth Factor Accelerates Diabetic Wound Healing through Increased Angiogenesis and by Mobilizing and Recruiting Bone Marrow-Derived Cells', *The American Journal of Pathology*, vol. 164, no. 6, pp. 1935–1947, Jun. 2004.

[104] D. H. M. Dam, S. A. Jelsma, and A. S. Paller, 'Impaired Wound Healing in Diabetic Ulcers: Accelerated Healing Through Depletion of Ganglioside', in *Wound Healing*, K. Turksen, Ed. Hoboken, NJ, USA: John Wiley & Sons, Inc., 2017, pp. 167–175.

[105] R. G. Frykberg and J. Banks, 'Challenges in the Treatment of Chronic Wounds', *Advances in Wound Care*, vol. 4, no. 9, pp. 560–582, Sep. 2015.

[106] N. B. Menke, K. R. Ward, T. M. Witten, D. G. Bonchev, and R. F. Diegelmann, 'Impaired wound healing', *Clinics in Dermatology*, vol. 25, no. 1, pp. 19–25, Jan. 2007.

[107] M. Miao, Y. Niu, T. Xie, B. Yuan, C. Qing, and S. Lu, 'Diabetes-impaired wound healing and altered macrophage activation: A possible pathophysiologic correlation: Distinct macrophage activation in normal and diabetic wounds', *Wound Repair and Regeneration*, vol. 20, no. 2, pp. 203–213, Mar. 2012.

[108] J. Larouche, S. Sheoran, K. Maruyama, and M. M. Martino, 'Immune Regulation of Skin Wound Healing: Mechanisms and Novel Therapeutic Targets', *Advances in Wound Care*, vol. 7, no. 7, pp. 209–231, Jul. 2018.

[109] N. K. Tonks, 'Protein tyrosine phosphatases: from genes, to function, to disease', *Nature Reviews Molecular Cell Biology*, vol. 7, no. 11, pp. 833–846, Nov. 2006.

[110] N. K. Tonks, 'Protein tyrosine phosphatases - from housekeeping enzymes to master regulators of signal transduction', *FEBS Journal*, vol. 280, no. 2, pp. 346–378, Jan. 2013.

[111] T. Tiganis and A. M. Bennett, 'Protein tyrosine phosphatase function: the substrate perspective', *Biochemical Journal*, vol. 402, no. 1, pp. 1–15, Feb. 2007.

[112] N. K. Tonks, C. D. Diltz, and E. H. Fischer, 'Purification of the Major Protein-tyrosine-phosphatases of Human Placent', *Journal of Biological Chemistry*, vol. 263, no. 14, pp. 6722–6730, 1998.

[113] H. Cho, *Obesity: Chapter seventeen - Protein Tyrosine Phosphatase 1B (PTP1B) and Obesity*, First edition. Amsterdam ; Boston: Elsevier Academic Press, 2013.

[114] R. A. Bradshaw and E. A. Dennis, *Handbook of cell signaling: Chapter 45 - Structure and Mechanism of the Insulin Receptor Tyrosine Kinase*, vol. 1. Academic press, 2010.

[115] J. Zhang *et al.*, 'Protein Tyrosine Phosphatase 1B Impairs Diabetic Wound Healing Through Vascular Endothelial Growth Factor Receptor 2 Dephosphorylation', *Arteriosclerosis, Thrombosis, and Vascular Biology*, vol. 35, no. 1, pp. 163–174, Jan. 2015.

[116] M. Stuible, K. M. Doody, and M. L. Tremblay, 'PTP1B and TC-PTP: regulators of transformation and tumorigenesis', *Cancer and Metastasis Reviews*, vol. 27, no. 2, pp. 215–230, Jun. 2008.

[117] J. Zhang *et al.*, 'Protein Tyrosine Phosphatase 1B Impairs Diabetic Wound Healing Through Vascular Endothelial Growth Factor Receptor 2 Dephosphorylation', *Arteriosclerosis, Thrombosis, and Vascular Biology*, vol. 35, no. 1, pp. 163–174, Jan. 2015.

[118] Z.-Y. Zhang and S.-Y. Lee, 'PTP1B inhibitors as potential therapeutics in the treatment of Type 2 diabetes and obesity', *Expert Opin. Investig. Drugs*, p. 11, 2003.

[119] M. Elchebly, 'Increased Insulin Sensitivity and Obesity Resistance in Mice Lacking the Protein Tyrosine Phosphatase-1B Gene', *Science*, vol. 283, no. 5407, pp. 1544–1548, Mar. 1999.

[120] T. Dinh *et al.*, 'Mechanisms Involved in the Development and Healing of Diabetic Foot Ulceration', *Diabetes*, vol. 61, no. 11, pp. 2937–2947, Nov. 2012.

[121] A. Kakazu, G. Sharma, and H. E. P. Bazan, 'Association of Protein Tyrosine Phosphatases (PTPs)-1B with c-Met Receptor and Modulation of Corneal Epithelial Wound Healing', *Investigative Opthalmology & Visual Science*, vol. 49, no. 7, p. 2927, Jul. 2008.

[122] Y. Wang, F. Yan, Q. Ye, X. Wu, and F. Jiang, 'PTP1B inhibitor promotes endothelial cell motility by activating the DOCK180/Rac1 pathway', *Scientific Reports*, vol. 6, no. 1, Jul. 2016.

[123] M. B. Witte and A. Barbul, 'Role of nitric oxide in wound repair', *The American Journal of Surgery*, vol. 183, no. 4, pp. 406–412, Apr. 2002.

[124] M. Vercauteren *et al.*, 'Improvement of Peripheral Endothelial Dysfunction by Protein Tyrosine Phosphatase Inhibitors in Heart Failure', *Circulation*, vol. 114, no. 23, pp. 2498–2507, Dec. 2006.

[125] S. K. Gupta, C. Shen, S. M. Moe, L. M. Kamendulis, M. Goldman, and M. P. Dubé, 'Worsening Endothelial Function with Efavirenz Compared to Protease Inhibitors: A 12-Month Prospective Study', *PLoS ONE*, vol. 7, no. 9, p. e45716, Sep. 2012.

[126] E. Gomez *et al.*, 'Reduction of heart failure by pharmacological inhibition or gene deletion of protein tyrosine phosphatase 1B', *Journal of Molecular and Cellular Cardiology*, vol. 52, no. 6, pp. 1257–1264, Jun. 2012.

[127] D. J. Herre, J. B. Norman, R. Anderson, M. L. Tremblay, A.-C. Huby, and E. J. Belin de Chantemèle, 'Deletion of Protein Tyrosine Phosphatase 1B (PTP1B) Enhances Endothelial Cyclooxygenase 2 Expression and Protects Mice from Type 1 Diabetes-Induced Endothelial Dysfunction', *PLOS ONE*, vol. 10, no. 5, p. e0126866, May 2015.

[128] B. L. Coomber and A. I. Gotlieb, 'In vitro endothelial wound repair. Interaction of cell migration and proliferation.', *Arteriosclerosis: An Official Journal of the American Heart Association, Inc.*, vol. 10, no. 2, pp. 215–222, Mar. 1990.

[129] S. Wang, X. Li, M. Parra, E. Verdin, R. Bassel-Duby, and E. N. Olson, 'Control of endothelial cell proliferation and migration by VEGF signaling to histone deacetylase 7', *Proceedings of the National Academy of Sciences*, vol. 105, no. 22, pp. 7738–7743, Jun. 2008.

[130] T. Matsumoto and L. Claesson-Welsh, 'VEGF Receptor Signal Transduction', *Sci. Stke*, vol. 112, p. 17, 2001.

[131] Y. Nakamura *et al.*, 'Role of Protein Tyrosine Phosphatase 1B in Vascular Endothelial Growth Factor Signaling and Cell–Cell Adhesions in Endothelial Cells', *Circulation Research*, vol. 102, no. 10, pp. 1182–1191, May 2008.

[132] A. A. Lanahan *et al.*, 'PTP1b Is a Physiologic Regulator of Vascular Endothelial Growth Factor Signaling in Endothelial Cells', *Circulation*, vol. 130, no. 11, pp. 902–909, Sep. 2014.

[133] M. Besnier *et al.*, 'Enhanced angiogenesis and increased cardiac perfusion after myocardial infarction in protein tyrosine phosphatase 1B-deficient mice', *The FASEB Journal*, vol. 28, no. 8, pp. 3351–3361, Aug. 2014.

[134] D. Popov, 'Endoplasmic reticulum stress and the on site function of resident PTP1B', *Biochemical and Biophysical Research Communications*, vol. 422, no. 4, pp. 535–538, Jun. 2012.

[135] D. S. Schwarz and M. D. Blower, 'The endoplasmic reticulum: structure, function and response to cellular signaling', *Cellular and Molecular Life Sciences*, vol. 73, no. 1, pp. 79–94, Jan. 2016.

[136] C. Schürmann, I. Goren, A. Linke, J. Pfeilschifter, and S. Frank, 'Deregulated unfolded protein response in chronic wounds of diabetic ob/ob mice: A potential connection to inflammatory and angiogenic disorders in diabetes-impaired wound healing', *Biochemical and Biophysical Research Communications*, vol. 446, no. 1, pp. 195–200, Mar. 2014.

[137] M. F. Gregor and G. S. Hotamisligil, 'Adipocyte stress: the endoplasmic reticulum and metabolic disease', *Journal of Lipid Research*, vol. 48, no. 9, pp. 1905–1914, Sep. 2007.

[138] P.-A. Thiebaut *et al.*, 'Protein tyrosine phosphatase 1B regulates endothelial endoplasmic reticulum stress; role in endothelial dysfunction', *Vascular Pharmacology*, vol. 109, pp. 36–44, Oct. 2018.

[139] M. Delibegovic *et al.*, 'Liver-Specific Deletion of Protein-Tyrosine Phosphatase 1B (PTP1B) Improves Metabolic Syndrome and Attenuates Diet-Induced Endoplasmic Reticulum Stress', *Diabetes*, vol. 58, no. 3, pp. 590–599, Mar. 2009.

[140] Y.-M. Jeon *et al.*, 'Neuroprotective Effects of Protein Tyrosine Phosphatase 1B Inhibition against ER Stress-Induced Toxicity', *Molecules and Cells*, vol. 40, no. 4, pp. 280–290, Apr. 2017.

[141] F. Gu, D. T. Nguyên, M. Stuible, N. Dubé, M. L. Tremblay, and E. Chevet, 'Protein-tyrosine Phosphatase 1B Potentiates IRE1 Signaling during Endoplasmic Reticulum Stress', *Journal of Biological Chemistry*, vol. 279, no. 48, pp. 49689–49693, Nov. 2004.

[142] C. Hetz, 'The unfolded protein response: controlling cell fate decisions under ER stress and beyond', *Nature Reviews Molecular Cell Biology*, vol. 13, no. 2, pp. 89–102, Feb. 2012.

[143] N. Fujiwara and K. Kobayashi, 'Macrophages in Inflammation', *Current Drug Target - Inflammation & Allergy*, vol. 4, no. 3, pp. 281–286, Jun. 2005.

[144] J. L. Dunster, 'The macrophage and its role in inflammation and tissue repair: mathematical and systems biology approaches: Macrophage and its role in inflammation and tissue repair', *Wiley Interdisciplinary Reviews: Systems Biology and Medicine*, vol. 8, no. 1, pp. 87–99, Jan. 2016.

[145] G. A. Duque and A. Descoteaux, 'Macrophage Cytokines: Involvement in Immunity and Infectious Diseases', *Frontiers in Immunology*, vol. 5, Oct. 2014.

[146] M. Mojena *et al.*, 'Protection against gamma-radiation injury by protein tyrosine phosphatase 1B', *Redox Biology*, vol. 17, pp. 213–223, Jul. 2018.

[147] G. J. Song *et al.*, 'A novel role for protein tyrosine phosphatase 1B as a positive regulator of neuroinflammation', *Journal of Neuroinflammation*, vol. 13, no. 1, Dec. 2016.

[148] K. M. Lenz and L. H. Nelson, 'Microglia and Beyond: Innate Immune Cells As Regulators of Brain Development and Behavioral Function', *Frontiers in Immunology*, vol. 9, Apr. 2018.

[149] T. Tsunekawa *et al.*, 'Deficiency of PTP1B Attenuates Hypothalamic Inflammation via Activation of the JAK2-STAT3 Pathway in Microglia', *EBioMedicine*, vol. 16, pp. 172–183, Feb. 2017.

[150] K. A. Pike *et al.*, 'Protein Tyrosine Phosphatase 1B Is a Regulator of the Interleukin-10-Induced Transcriptional Program in Macrophages', *Science Signaling*, vol. 7, no. 324, pp. ra43–ra43, May 2014.

[151] L. Grant *et al.*, 'Myeloid-Cell Protein Tyrosine Phosphatase-1B Deficiency in Mice Protects Against High-Fat Diet and Lipopolysaccharide-Induced Inflammation, Hyperinsulinemia, and Endotoxemia Through an IL-10 STAT3-Dependent Mechanism', *Diabetes*, vol. 63, no. 2, pp. 456–470, Feb. 2014.

[152] J. Zhang *et al.*, 'Protein Tyrosine Phosphatase 1B Deficiency Ameliorates Murine Experimental Colitis via the Expansion of Myeloid-Derived Suppressor Cells', *PLoS ONE*, vol. 8, no. 8, p. e70828, Aug. 2013.

[153] J. Revuelta-Cervantes *et al.*, 'Protein Tyrosine Phosphatase 1B (PTP1B) Deficiency Accelerates Hepatic Regeneration in Mice', *The American Journal of Pathology*, vol. 178, no. 4, pp. 1591–1604, Apr. 2011.

[154] A. M. Smith, K. K. Maguire-Nguyen, T. A. Rando, M. A. Zasloff, K. B. Strange, and V. P. Yin, 'The protein tyrosine phosphatase 1B inhibitor MSI-1436 stimulates regeneration of heart and multiple other tissues', *npj Regen Med*, vol. 2, no. 1, p. 4, Dec. 2017.

[155] 'Trodusquemine'. [Online]. Available:
https://pubchem.ncbi.nlm.nih.gov/compound/Trodusquemine#section=Top.

[156] A. J. Barr, 'Protein tyrosine phosphatases as drug targets: strategies and challenges of inhibitor development', *Future Medicinal Chemistry*, vol. 2, no. 10, pp. 1563–1576, Oct. 2010.

[157] K. A. Lantz *et al.*, 'Inhibition of PTP1B by Trodusquemine (MSI-1436) Causes Fat-specific Weight Loss in Diet-induced Obese Mice', *Obesity*, vol. 18, no. 8, pp. 1516–1523, Aug. 2010.

[158] H. He *et al.*, 'Design, Synthesis and Biological Evaluation of Stilbene Derivatives as Novel Inhibitors of Protein Tyrosine Phosphatase 1B', *Molecules*, vol. 21, p. 1722, 2016.

[159] ClinicalTrials.gov, 'A Single Dose, Tolerance and Pharmacokinetic Study in Obese or Overweight Type 2 Diabetic Volunteers'. [Online]. Available: https://clinicaltrials.gov/ct2/show/study/NCT00606112.

[160] C. Proença *et al.*, 'Inhibition of protein tyrosine phosphatase 1B by flavonoids: A structure - activity relationship study', *Food and Chemical Toxicology*, vol. 111, pp. 474–481, Jan. 2018.

[161] B. Healy and A. Freedman, 'ABC of wound healing: Infections', *BMJ: British Medical Journal*, vol. 332, 2006.

[162] C. Salmi, C. Loncle, N. Vidal, M. Laget, Y. Letourneux, and J. Michel Brunel, 'Antimicrobial Activities of 3-Amino- and Polyaminosterol Analogues of Squalamine and Trodusquemine', *Journal of Enzyme Inhibition and Medicinal Chemistry*, vol. 23, no. 6, pp. 860–865, Jan. 2008.

[163] S. Guo and L. A. DiPietro, 'Factors Affecting Wound Healing', *Journal of Dental Research*, vol. 89, no. 3, pp. 219–229, Mar. 2010.

[164] A. Padilla, P. Keating, J. X. Hartmann, and F. Marí, 'Effects of α-conotoxin ImI on TNF-α, IL-8 and TGF-β expression by human macrophage-like cells derived from THP-1 pre-monocytic leukemic cells', *Sci Rep*, vol. 7, no. 1, p. 12742, Dec. 2017.

[165] C. L. Holness and D. L. Simmons, 'Molecular Cloning of CD68, a Human Macrophage Marker Related to Lysosomal Glycoproteins', *Blood*, vol. 81, p. 8, 1993.

[166] R. Landmann, B. Müller, and W. Zimmerli, 'CD14, new aspects of ligand and signal diversity', *Microbes and Infection*, vol. 2, no. 3, pp. 295–304, Mar. 2000.

[167] T. Mosmann, 'Rapid colorimetric assay for cellular growth and survival: Application to proliferation and cytotoxicity assays', *Journal of Immunological Methods*, vol. 65, no. 1–2, pp. 55–63, Dec. 1983.

[168] J. van Meerloo, G. J. L. Kaspers, and J. Cloos, 'Cell Sensitivity Assays: The MTT Assay', in *Cancer Cell Culture*, vol. 731, I. A. Cree, Ed. Totowa, NJ: Humana Press, 2011, pp. 237–245.

[169] F. Pantano *et al.*, 'The role of macrophages polarization in predicting prognosis of radically resected gastric cancer patients', *J. Cell. Mol. Med.*, vol. 17, no. 11, pp. 1415–1421, Nov.

2013.

[170] S. W. Ryter and A. M. K. Choi, 'Heme Oxygenase-1: Redox Regulation of a Stress Protein in Lung and Cell Culture Models', *Antioxidants & Redox Signaling*, vol. 7, no. 1–2, pp. 80–91, Jan. 2005.

[171] Q.-G. Ren, S.-L. Yang, J.-L. Hu, P.-D. Li, Y.-S. Chen, and Q.-S. Wang, 'Evaluation of HO-1 expression, cellular ROS production, cellular proliferation and cellular apoptosis in human esophageal squamous cell carcinoma tumors and cell lines', *Oncology Reports*, vol. 35, no. 4, pp. 2270–2276, Apr. 2016.

[172] B. Wegiel, Z. Nemeth, M. Correa-Costa, A. C. Bulmer, and L. E. Otterbein, 'Heme Oxygenase-1: A Metabolic Nike', *Antioxidants & Redox Signaling*, vol. 20, no. 11, pp. 1709–1722, Apr. 2014.

[173] M. Ozen, H. Zhao, D. B. Lewis, R. J. Wong, and D. K. Stevenson, 'Heme oxygenase and the immune system in normal and pathological pregnancies', *Front. Pharmacol.*, vol. 6, Apr. 2015.

[174] M. J. Reiniers *et al.*, 'Preparation and Practical Applications of 2′,7′-Dichlorodihydrofluorescein in Redox Assays', *Anal. Chem.*, vol. 89, no. 7, pp. 3853–3857, Apr. 2017.

[175] M. Schafer and S. Werner, 'Oxidative stress in normal and impaired wound repair', *Pharmacological Research*, vol. 58, no. 2, pp. 165–171, Aug. 2008.

[176] C. Dunnill *et al.*, 'Reactive oxygen species (ROS) and wound healing: the functional role of ROS and emerging ROS-modulating technologies for augmentation of the healing process: Reactive oxygen species and wound healing', *Int Wound J*, vol. 14, no. 1, pp. 89–96, Feb. 2017.

[177] P. K. Smith *et al.*, 'Measurement of protein using bicinchoninic acid', *Analytical Biochemistry*, vol. 150, no. 1, pp. 76–85, Oct. 1985.

[178] J. M. Walker, 'The Bicinchoninic Acid (BCA) Assay for Protein Quantitation', in *The protein protocols handbook.*, Humana Press, Totowa, NJ, 2009, pp. 11–15.

[179] J. S. Lehmann, A. Zhao, B. Sun, W. Jiang, and S. Ji, 'Multiplex Cytokine Profiling of Stimulated Mouse Splenocytes Using a Cytometric Bead-based Immunoassay Platform', *JoVE*, no. 129, p. 56440, Nov. 2017.

[180] E. C. Leal *et al.*, 'Substance P Promotes Wound Healing in Diabetes by Modulating Inflammation and Macrophage Phenotype', *The American Journal of Pathology*, vol. 185, no. 6, pp. 1638–1648, Jun. 2015.

[181] A. Akbarzadeh *et al.*, 'Induction of diabetes by Streptozotocin in rats', *Indian J Clin Biochem*, vol. 22, no. 2, pp. 60–64, Sep. 2007.

[182] C. J. Ferrante and S. J. Leibovich, 'Regulation of Macrophage Polarization and Wound Healing', *Advances in Wound Care*, vol. 1, no. 1, pp. 10–16, Feb. 2012.

[183] T. A. Wynn and K. M. Vannella, 'Macrophages in Tissue Repair, Regeneration, and Fibrosis', *Immunity*, vol. 44, no. 3, pp. 450–462, Mar. 2016.

[184] W. Chanput, J. J. Mes, and H. J. Wichers, 'THP-1 cell line: An in vitro cell model for immune modulation approach', *International Immunopharmacology*, vol. 23, no. 1, pp. 37–45, Nov. 2014.

[185] N. Krishnan *et al.*, 'PTP1B inhibition suggests a therapeutic strategy for Rett syndrome', *Journal of Clinical Investigation*, vol. 125, no. 8, pp. 3163–3177, Aug. 2015.

[186] M. Daigneault, J. A. Preston, H. M. Marriott, M. K. B. Whyte, and D. H. Dockrell, 'The Identification of Markers of Macrophage Differentiation in PMA-Stimulated THP-1 Cells and Monocyte-Derived Macrophages', *PLoS ONE*, vol. 5, no. 1, p. e8668, Jan. 2010.

[187] T. Starr, T. J. Bauler, P. Malik-Kale, and O. Steele-Mortimer, 'The phorbol 12-myristate-13-acetate differentiation protocol is critical to the interaction of THP-1 macrophages with Salmonella Typhimurium', *PLoS ONE*, vol. 13, no. 3, p. e0193601, Mar. 2018.

[188] M. B. Maeß, B. Wittig, A. Cignarella, and S. Lorkowski, 'Reduced PMA enhances the responsiveness of transfected THP-1 macrophages to polarizing stimuli', *Journal of Immunological Methods*, vol. 402, no. 1–2, pp. 76–81, Jan. 2014.

[189] V. Sampath, 'Bacterial endotoxin-lipopolysaccharide; structure, function and its role in immunity in vertebrates and invertebrates', *Agriculture and Natural Resources*, vol. 52, no. 2, pp. 115–120, Apr. 2018.

[190] K. Nishio *et al.*, 'Attenuation of lipopolysaccharide (LPS)-induced cytotoxicity by tocopherols and tocotrienols', *Redox Biology*, vol. 1, no. 1, pp. 97–103, 2013.

[191] M. Yang *et al.*, 'Dephosphorylation of Tyrosine 393 in Argonaute 2 by Protein Tyrosine Phosphatase 1B Regulates Gene Silencing in Oncogenic RAS-Induced Senescence', *Molecular Cell*, vol. 55, no. 5, pp. 782–790, Sep. 2014.

[192] N. Krishnan *et al.*, 'Targeting the disordered C terminus of PTP1B with an allosteric inhibitor', *Nat Chem Biol*, vol. 10, no. 7, pp. 558–566, Jul. 2014.

[193] C. K Tchounwou, 'D-Glucose-Induced Cytotoxic, Genotoxic, and Apoptotic Effects on Human Breast Adenocarcinoma (MCF-7) Cells', *J Cancer Sci Ther*, vol. 06, no. 05, 2014.

[194] D. Popov, M. Nemecz, M. Dumitrescu, A. Georgescu, and F. D. Böhmer, 'Long-term high glucose concentration influences Akt, ERK1/2, and PTP1B protein expression in human aortic smooth muscle cells', *Biochemical and Biophysical Research Communications*, vol. 388, no. 1, pp. 51–55, Oct. 2009.

[195] Y. Ito *et al.*, 'Protein tyrosine phosphatase 1B deficiency in podocytes mitigates hyperglycemia-induced renal injury', *Metabolism*, vol. 76, pp. 56–69, Nov. 2017.

[196] I. Torres-Castro *et al.*, 'Human monocytes and macrophages undergo M1-type inflammatory polarization in response to high levels of glucose', *Immunology Letters*, vol. 176, pp. 81–89, Aug. 2016.

[197] Y. Gonzalez *et al.*, 'High glucose concentrations induce TNF-α production through the down-regulation of CD33 in primary human monocytes', *BMC Immunol*, vol. 13, no. 1, p. 19, 2012.

[198] G. S. Ashcroft *et al.*, 'Tumor necrosis factor-alpha (TNF-α) is a therapeutic target for impaired cutaneous wound healing: TNF-α and wound healing', *Wound Repair Regen*, vol. 20, no. 1, pp. 38–49, Jan. 2012.

[199] H.-Y. Hsu and M.-H. Wen, 'Lipopolysaccharide-mediated Reactive Oxygen Species and Signal Transduction in the Regulation of Interleukin-1 Gene Expression', *J. Biol. Chem.*, vol. 277, no. 25, pp. 22131–22139, Jun. 2002.

[200] A. Nouvong, A. M. Ambrus, E. R. Zhang, L. Hultman, and H. A. Coller, 'Reactive oxygen species and bacterial biofilms in diabetic wound healing', *Physiological Genomics*, vol. 48, no. 12, pp. 889–896, Dec. 2016.

[201] P. Kumar, M. M. Swain, and A. Pal, 'Hyperglycemia-induced inflammation caused down-regulation of 8-oxoG-DNA glycosylase levels in murine macrophages is mediated by oxidative-nitrosative stress-dependent pathways', *The International Journal of Biochemistry & Cell Biology*, vol. 73, pp. 82–98, Apr. 2016.

[202] F. Felice *et al.*, 'Oxidative stress in response to high glucose levels in endothelial cells and in endothelial progenitor cellsEvidence for differential glutathione peroxidase-1 expression', *Microvascular Research*, vol. 80, no. 3, pp. 332–338, Dec. 2010.

[203] Y. Tang, J. Long, and J. Liu, 'Hyperglycemia-Associated Oxidative Stress Induces Autophagy', in *Autophagy: Cancer, Other Pathologies, Inflammation, Immunity, Infection, and Aging*, Elsevier, 2014, pp. 105–115.

[204] P. Buranasin *et al.*, 'High glucose-induced oxidative stress impairs proliferation and migration of human gingival fibroblasts', *PLoS ONE*, vol. 13, no. 8, p. e0201855, Aug. 2018.

[205] S. A. Rushworth, X.-L. Chen, N. Mackman, R. M. Ogborne, and M. A. O'Connell, 'Lipopolysaccharide-Induced Heme Oxygenase-1 Expression in Human Monocytic Cells Is Mediated via Nrf2 and Protein Kinase C', *J Immunol*, vol. 175, no. 7, pp. 4408–4415, Oct. 2005.

[206] V. Vijayan, F. A. D. T. G. Wagener, and S. Immenschuh, 'The macrophage heme-heme oxygenase-1 system and its role in inflammation', *Biochemical Pharmacology*, vol. 153, pp. 159–167, Jul. 2018.

[207] Y. Naito, T. Takagi, and Y. Higashimura, 'Heme oxygenase-1 and anti-inflammatory M2 macrophages', *Archives of Biochemistry and Biophysics*, vol. 564, pp. 83–88, Dec. 2014.

[208] H. Bosshart and M. Heinzelmann, 'THP-1 cells as a model for human monocytes', *Ann. Transl. Med.*, vol. 4, no. 21, pp. 438–438, Nov. 2016.

[209] A. Junod, A. E. Lambert, L. Orci, R. Pictet, A. E. Gonet, and A. E. Renold, 'Studies of the Diabetogenic Action of Streptozotocin.', *Experimental Biology and Medicine*, vol. 126, no. 1, pp. 201–205, Oct. 1967.

[210] K. K. Wu and Y. Huan, 'Streptozotocin-Induced Diabetic Models in Mice and Rats', *Animal Models*, p. 14, 2008.

[211] B. L. Furman, 'Streptozotocin-Induced Diabetic Models in Mice and Rats: Streptozotocin-Induced Diabetic Models', in *Current Protocols in Pharmacology*, S. J. Enna, M. Williams, R. Frechette, T. Kenakin, P. McGonigle, and B. Ruggeri, Eds. Hoboken, NJ, USA: John Wiley & Sons, Inc., 2015, pp. 5.47.1-5.47.20.

[212] B. Kunkemoeller and T. R. Kyriakides, 'Redox Signaling in Diabetic Wound Healing Regulates Extracellular Matrix Deposition', *Antioxidants & Redox Signaling*, vol. 27, no. 12, pp. 823–838, Oct. 2017.

[213] K. D. Poss and S. Tonegawa, 'Reduced stress defense in heme oxygenase 1-deficient cells', *Proceedings of the National Academy of Sciences*, vol. 94, no. 20, pp. 10925–10930, Sep. 1997.

[214] J. Dulak, A. Loboda, A. Zagórska, and A. Józkowicz, 'Complex Role of Heme Oxygenase-1 in Angiogenesis', *Antioxid. Redox Signal*, vol. 6, pp. 858–866, 2004.

[215] Q.-Y. Chen, G.-G. Wang, W. Li, Y.-X. Jiang, X.-H. Lu, and P.-P. Zhou, 'Heme Oxygenase-1 Promotes Delayed Wound Healing in Diabetic Rats', *Journal of Diabetes Research*, vol. 2016, pp. 1–10, 2016.

[216] A. Grochot-Przeczek *et al.*, 'Heme Oxygenase-1 Accelerates Cutaneous Wound Healing in Mice', *PLoS ONE*, vol. 4, no. 6, p. e5803, Jun. 2009.

[217] U. Okonkwo and L. DiPietro, 'Diabetes and Wound Angiogenesis', *IJMS*, vol. 18, no. 7, p. 1419, Jul. 2017.

[218] L. Liu and G.-P. Shi, 'CD31: beyond a marker for endothelial cells', *Cardiovascular Research*, vol. 94, no. 1, pp. 3–5, Apr. 2012.

[219] P. Lertkiatmongkol, D. Liao, H. Mei, Y. Hu, and P. J. Newman, 'Endothelial functions of platelet/endothelial cell adhesion molecule-1 (CD31)', *Current Opinion in Hematology*, vol. 23, no. 3, pp. 253–259, May 2016.

[220] Y. Zhang, Q. Li, J. Y. Youn, and H. Cai, 'Protein Phosphotyrosine Phosphatase 1B (PTP1B) in Calpain-dependent Feedback Regulation of Vascular Endothelial Growth Factor Receptor (VEGFR2) in Endothelial Cells: implications in VEGF-dependent angiogenesis and diabetic wound healing', *Journal of Biological Chemistry*, vol. 292, no. 2, pp. 407–416, Jan. 2017.

[221] X. Sun and P. D. Kaufman, 'Ki-67: more than a proliferation marker', *Chromosoma*, vol. 127, no. 2, pp. 175–186, Jun. 2018.

[222] L. M. Jaacks, K. R. Siegel, U. P. Gujral, and K. M. V. Narayan, 'Type 2 diabetes: A 21st century epidemic', *Best Practice & Research Clinical Endocrinology & Metabolism*, vol. 30, no. 3, pp. 331–343, Jun. 2016.

[223] R. O. Bonow and M. Gheorghiade, 'The diabetes epidemic: a national and global crisis',

The American Journal of Medicine, vol. 116, no. 5, pp. 2–10, Mar. 2004.

[224] P. Zimmet, K. G. M. M. Alberti, and J. Shaw, 'Global and societal implications of the diabetes epidemic', *Nature*, vol. 414, no. 6865, pp. 782–787, Dec. 2001.

[225] International Diabetes Federation, *IDF diabetes atlas*. Brussels: International Diabetes Federation, 2015.

[226] J. Montalibet and B. P. Kennedy, 'Therapeutic strategies for targeting PTP1B in diabetes', *Drug Discovery Today: Therapeutic Strategies*, vol. 2, no. 2, pp. 129–135, Jun. 2005.

[227] A. K. Tamrakar, C. K. Maurya, and A. K. Rai, 'PTP1B inhibitors for type 2 diabetes treatment: a patent review (2011 – 2014)', *Expert Opinion on Therapeutic Patents*, vol. 24, no. 10, pp. 1101–1115, Oct. 2014.

[228] D. Thompson *et al.*, 'Pharmacological inhibition of protein tyrosine phosphatase 1B protects against atherosclerotic plaque formation in the LDLR $^{-/-}$ mouse model of atherosclerosis', *Clinical Science*, vol. 131, no. 20, pp. 2489–2501, Oct. 2017.

[229] 'Genaera Corporation Presents Preliminary Phase 1b Data for Trodusquemine (MSI-1436)', 2009. [Online]. Available: https://www.biospace.com/article/releases/genaera-corporation-presents-preliminary-phase-1b-data-for-trodusquemine-msi-1436-/.

[230] Y.-W. Lin, B. Lee, P.-S. Liu, and L.-N. Wei, 'Receptor-Interacting Protein 140 Orchestrates the Dynamics of Macrophage M1/M2 Polarization', *J Innate Immun*, vol. 8, no. 1, pp. 97–107, 2016.

[231] X. Xu *et al.*, 'Punicalagin, a PTP1B inhibitor, induces M2c phenotype polarization via up-regulation of HO-1 in murine macrophages', *Free Radical Biology and Medicine*, vol. 110, pp. 408–420, Sep. 2017.

[232] X. Xu *et al.*, 'Inhibition of PTP1B Promotes M2 Polarization via MicroRNA-26a/MKP1 Signaling Pathway in Murine Macrophages', *Frontiers in Immunology*, vol. 10, p. 11, 2019.

[233] N. Dubé and M. L. Tremblay, 'Beyond the Metabolic Function of PTP1B', *Cell Cycle*, vol. 3, no. 5, pp. 548–551, May 2004.

[234] M. A. Mobasher *et al.*, 'Protein tyrosine phosphatase 1B modulates GSK3β/Nrf2 and IGFIR signaling pathways in acetaminophen-induced hepatotoxicity', *Cell Death Dis*, vol. 4, no. 5, pp. 626–626, May 2013.

[235] G. Mohammad, H. P. Pandey, and K. Tripathi, 'Diabetic wound healing and its angiogenesis with special reference to nanoparticles', *Digest Journal of Nanomaterials and Biostructures*, vol. 3, no. 4, pp. 203–208, 2008.

[236] H. Maamoun, T. Benameur, G. Pintus, S. Munusamy, and A. Agouni, 'Crosstalk Between Oxidative Stress and Endoplasmic Reticulum (ER) Stress in Endothelial Dysfunction and Aberrant Angiogenesis Associated With Diabetes: A Focus on the Protective Roles of Heme Oxygenase (HO)-1', *Front. Physiol.*, vol. 10, p. 70, Feb. 2019.

[237] A. Yachie *et al.*, 'Oxidative stress causes enhanced endothelial cell injury in human heme oxygenase-1 deficiency', *J. Clin. Invest.*, vol. 103, no. 1, pp. 129–135, 1998.

[238] P. A. Dennery, 'Heme Oxygenase in Neonatal Lung Injury and Repair', *Antioxidants & Redox Signaling*, vol. 21, no. 13, pp. 1881–1892, Nov. 2014.

[239] A. Jozkowicz, H. Was, and J. Dulak, 'Heme Oxygenase-1 in Tumors: Is It a False Friend?', *Antioxidants & Redox Signaling*, vol. 9, no. 12, pp. 2099–2118, Dec. 2007.

[240] D.-S. Lee *et al.*, 'PTP1B Inhibitory and Anti-Inflammatory Effects of Secondary Metabolites Isolated from the Marine-Derived Fungus Penicillium sp. JF-55', *Marine Drugs*, vol. 11, no. 4, pp. 1409–1426, Apr. 2013.